ABSTRACT

Title of Thesis:	**QUANTIFYING THE ECOSYSTEM METABOLISM OF A TIDAL ESTUARY AS A CONSEQUENCE OF AERATION**
	Zachary Gotthardt, Master of Science , Environmental Science, 2019
Thesis Directed By:	Lora Harris, Associate Professor, Marine, Estuarine, and Environmental Sciences

As anthropogenic activity affects shallow estuaries it is imperative to quantify how these systems respond to changing conditions. Ecosystem metabolism is an integrative, metric to measure how ecosystems change, and can act as the focus of comparative experiments. We leveraged an aeration system, to examine the ecosystem metabolism of the estuary through comparative experiments. The aeration system allows us to study a normoxic, eutrophic ecosystem. Chapter 1 explains the causes and effects of eutrophication, with an emphasis on the connection between hypoxia and eutrophication.

In chapter 2, we describe an experiment focused on quantifying the ecosystem metabolism in a tidal, eutrophic estuary where engineered aeration has been operational since the 1980s. The aeration system provides an ideal site for addressing some of the difficulties inherent to studying eutrophication. In our experiments, we observed evidence of chemoautotrophy when the aerators were operational. Bottle methods and open water methods provided conflicting results.

TITLE OF THESIS: QUANTIFYING THE ECOSYSTEM METABOLISM OF A TIDAL

ESTUARY AS A CONSEQUENCE OF AERATION

By

Zachary Evan Gotthardt

Dissertation submitted to the Faculty of the Graduate School of the
University of Maryland, College Park, in partial fulfillment of the
requirements for the degree of
Environmental Science
2019

Advisory Committee:

Associate Professor Lora Harris, Chair

Jeremy Testa

Greg Silsbe

PREFACE

Chapter 1 is an introduction to the significance of ecosystem metabolism as a comprehensive measurement in tidal estuaries, and establishes the framework for Chapter Two. Chapter Two is a standalone manuscript, which will be submitted to *Estuaries and Coasts* with co-authors Dr. Lora Harris, Dr. Jeremy Testa, Laura Lapham, Melinda Forsyth, and Casey Hodgkins. Additional authors may be added prior to publication.

To my grandfather, William Meyers

ACKNOWLEDGEMENTS

TABLE OF CONTENTS

LIST OF TABLES

LIST OF FIGURES

CHAPTER 1: INTRODUCTION AND BACKGROUND

ABSTRACT

Eutrophication is a widespread problem in both the Chesapeake Bay and globally. Understanding the causes, effects, and nuances of eutrophication is of critical importance to decision-makers and those that interact with coastal estuaries. Hypoxia is one common symptom of eutrophication, where low dissolved oxygen develops through some combination of decomposing organic material and hydrodynamic conditions that reduce water column mixing. This connection has the consequence of creating feedbacks between eutrophication and hypoxia that are discussed at length here. A solution to understanding the complexity of eutrophication, and its high tendency to beget hypoxia, is to use a metric that inherently incorporates the processes influencing production and consumption. The concept of ecosystem metabolism, the net result of biotic processes that produce and consume energy within an ecosystem, is discussed in this chapter as a useful metric for unraveling the complexities of these feedbacks. We also discuss the knowledge gap in the role of oxygen in eutrophic estuaries and propose relevant research solutions.

Eutrophication: Causes and Consequences

Eutrophic aquatic systems are characterized by an increased rate of production and import of organic material (Nixon 1995). When this material is autochthonous, eutrophication can lead to a surplus of producer biomass (i.e. phytoplankton) that is not completely restored by the ecosystem of interest. Because this phytoplankton-based organic material is labile and plentiful in eutrophic ecosystems, decomposition readily occurs and creates a high biological oxygen demand in the water column. Therefore, eutrophic systems typically exhibit hypoxia or anoxia (Nixon 1998, Howarth et al 2011).

Anoxic and hypoxic waterways, defined as having less than 0.5 $mg*L^{-1}$ and 2.0 $mg*L^{-1}$ of dissolved oxygen concentrations, respectively (Kemp et al, 2009), have been documented to have vastly different biogeochemistry than normoxic waterways (e.g. Conley et al, 2007, Kemp et al, 2009, Howarth et al, 2011, Testa and Kemp, 2012, Harris et al, 2015). Under normoxic conditions, ammonia is converted to nitrite through nitrification, a microbially mediated process. Nitrite is then further oxidized into nitrate. Within sediments, nitrification is coupled to denitrification, which occurs in deeper, oxygen-poor sediments. The result of this chemical pathway is production of N_2 gas, which outgases to the atmosphere and is removed from the system. However, nitrification is oxygen dependent, and is inhibited under anoxia or hypoxia. Consequently, ammonia accumulation is common in hypoxic systems (Testa and Kemp, 2012, Middelburg and Levin, 2009). This condition is exacerbated in stratified systems, where atmospheric oxygen cannot penetrate below the pycnocline and bottom waters experience higher hypoxic volumes (Hagy et al, 2004). Due to the strong association between eutrophication and hypoxia, eutrophic systems commonly experience ammonia accumulation (Kemp et al, 2005, Eyre and Ferguson, 2009).

The hypoxia associated with eutrophication can lead to higher rates of nitrogen (N) and phosphorous (P) recycling (Conley et al, 2007, Vahtera et al, 2007, Kemp et al, 2009). Labile species of N and P more readily flux from the sediment under hypoxic conditions. In nutrient limited systems, this recycling of N or P acts to encourage primary productivity and, in turn, strengthen eutrophication. These interactions establish a positive feedback loop between eutrophication and hypoxia that ensures the perpetuation of the hypoxic and eutrophic states. Typically, this feedback is initially created due to a large input of allocthonous nutrients, from atmospheric deposition, fertilizer runoff, or wastewater from treatment plants or septic systems (Spokes and Jickells, 2005, Howarth and Ramakrrshra, 2005).

Due to the presence of the feedback loop between hypoxia and eutrophication (referred to here as the hypoxic-eutrophic feedback and depicted in Figure 1), eutrophic systems can be highly resilient in the face of nutrient reductions (e.g. Duarte et al 2009); they resist changes that would otherwise alter their state (Holling 1973, Scheffer et al 2001). Furthermore, these systems sometimes exhibit hysteresis, an apparent lag between a stimulus and the ecosystem response. In hypoxic and eutrophic systems, this phenomenon is due to the relatively high efficiency of nutrient recycling. Restoration efforts have been complicated by these factors; the resilience of the eutrophic state requires considerable resources to mediate change while hysteresis makes observing these changes difficult (Scheffer et al 2001). In particular, observation of the effects of oxygen in eutrophic, hypoxic waterways is complicated by the high biological oxygen demand immediately consuming any oxygen that enters the system. Understanding the intricacies and consequences of the hypoxic-eutrophic feedback is critical in ecosystem management of estuaries and coastal waters, especially those affected by human activity (Scheffer et al 2001, Howarth et al 2011) and in systems where management seeks insights on restoration trajectories.

Eutrophication and its biogeochemical consequences create management problems both locally in the Chesapeake Bay and globally (Diaz and Rosenberg 2008, Gilbert et al 2009) (See Figure 2). Aside from the overall decrease in ecosystem health, eutrophic systems experience decreased water clarity due to increased phytoplankton biomass, sulfur smells due to sulfide accumulation, and fish kills due to lower oxygen concentrations (Corrales and Maclean 1995, Scheffer et al, 1993. These problems add recreational and living concerns to the slough of consequences associated with eutrophication, exacerbating the need for proper management and research.

An appropriate experimental design to examine the hypoxic-eutrophic feedback would include measuring the difference between a hypoxic, eutrophic state and a normoxic, eutrophic state, ideally within the same system under the same physical conditions (e.g., temperature, salinity). However, the association between eutrophication and hypoxia make their occurrence in isolation unlikely in many estuaries where freshwater inputs set up conditions that encourage stratification and low oxygen bottom water.

Net Ecosystem Metabolism: Purpose and Applications

Ecosystems can be categorized by their metabolic state; if respiration (R) is greater than gross primary productivity (GPP), the system is considered heterotrophic. If GPP is greater than R, the system is considered autotrophic. Similarly, we can determine the metabolic state by examining the ratio between GPP and R, with GPP:R ratios greater than 1 suggesting autotrophy while GPP:R ratios lower than 1 suggesting heterotrophy. The balance between production and consumption (i.e. GPP-R) in an ecosystem is referred to as the net ecosystem metabolism (NEM) of that system. NEM inherently encompasses the processes that influence production and respiration (Giordano et al 2012). NEM determines whether a system is a source (autotrophic) or

a sink (heterotrophic) of carbon. Quantifying the metabolism of the water column microbial community reveals how much energy is available for higher trophic levels or is exported to adjacent systems (Fisher and Likens 1973, Eyre et al 2009) and determines the ecosystem's trophic status (Odum 1956). The magnitude of NEM determines the amount of organic matter available to higher trophic levels and if the system is a net source (autotrophic) or sink (heterotrophic) or carbon. Shifts in NEM can indicate the net effects of factors than control primary productivity (e.g. example, a shift from autotrophy to heterotrophy may be proximately explained by changing nutrient dynamics). This integrative tool is particularly useful in coastal systems that experience large quantities of nutrient inputs and allochthonous carbon, such as the Chesapeake Bay and its tributaries.

NEM can be quantified with a multitude of techniques by changing the biogeochemical constituent used as a metric. In estuarine studies, these metrics are typically either dissolved oxygen (DO) and dissolved inorganic carbon (DIC) in the form of CO_2. These constituents are suitable metrics for NEM because they are involved in metabolic energy related processes, namely, the coupled processes of photosynthesis and respiration. Therefore, changes in DO and DIC can be considered analogous to NEM.

When properly quantified, changes in NEM can be compared based on changing conditions within an ecosystem. Caffrey (2004) examined diel changes in DO over seasonal and annual timeframes to discern how NEM changes over time in 22 coastal systems on the east coast. Crosswell et al (2017) calculated NEM using diel changes in DIC to constrain changes in carbon balance at several locations within the New River Estuary. In both cases, NEM quantification enables comparisons and provides insight to answer the authors' questions. The balance of heterotrophy and autotrophy in coastal systems has been disturbed by anthropogenic

increases in nutrient loads and organic loads (Schlesinger 1997, Smith and Hollibaugh 1993, Boynton et al 1996). Studies and efforts that examine NEM can capture and describe these changes as they occur. These relatively recent shifts place higher importance on monitoring changes in NEM for ecosystem management.

The concepts of hysteresis and resilience can be applied to NEM once it is properly constrained. The recovery of hypoxic, eutrophic estuaries is poorly understood, but critical in establishing appropriate management action (Howarth et. al. 2011). Studies of NEM (Caffrey 2004) and eutrophication recovery trajectories (Howarth et al 2011) in shallow, coastal systems are presently lacking. The Clean Water Act provides the policy to support restoration of estuarine systems experiencing eutrophic conditions. However, the Total Maximum Daily Loads currently used as a mechanism to carry out this restoration largely focuses on reductions of pollutant inputs and the resulting symptoms associated with impaired water quality (USEPA 1972). A rate measurement, such as NEM, that can be examined over space, time, and changing conditions, provides more mechanistic insight, as it is a more direct measure of the metabolic processes influencing eutrophication. Furthermore, the hypoxic-eutrophic feedback can be more appropriately examined when one of its processes (such as NEM) is quantified.

Figures
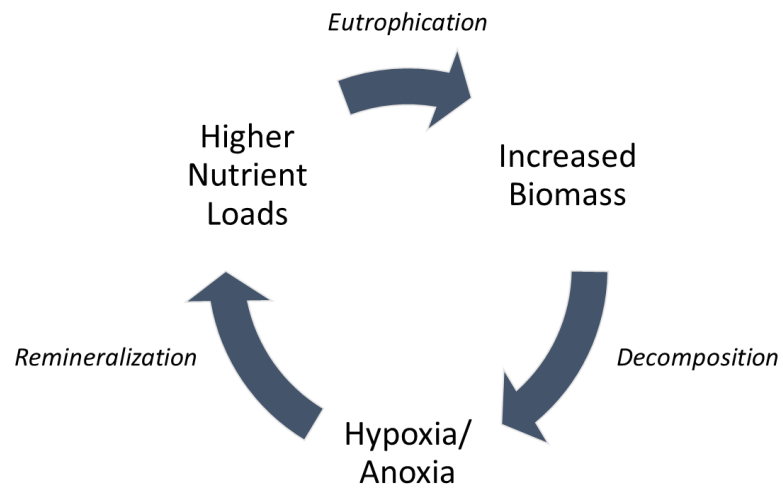
Figure 1: Conceptual visualization of the hypoxic eutrophic feedback. The cycle is typically initiated by an introduction of nutrients into the system
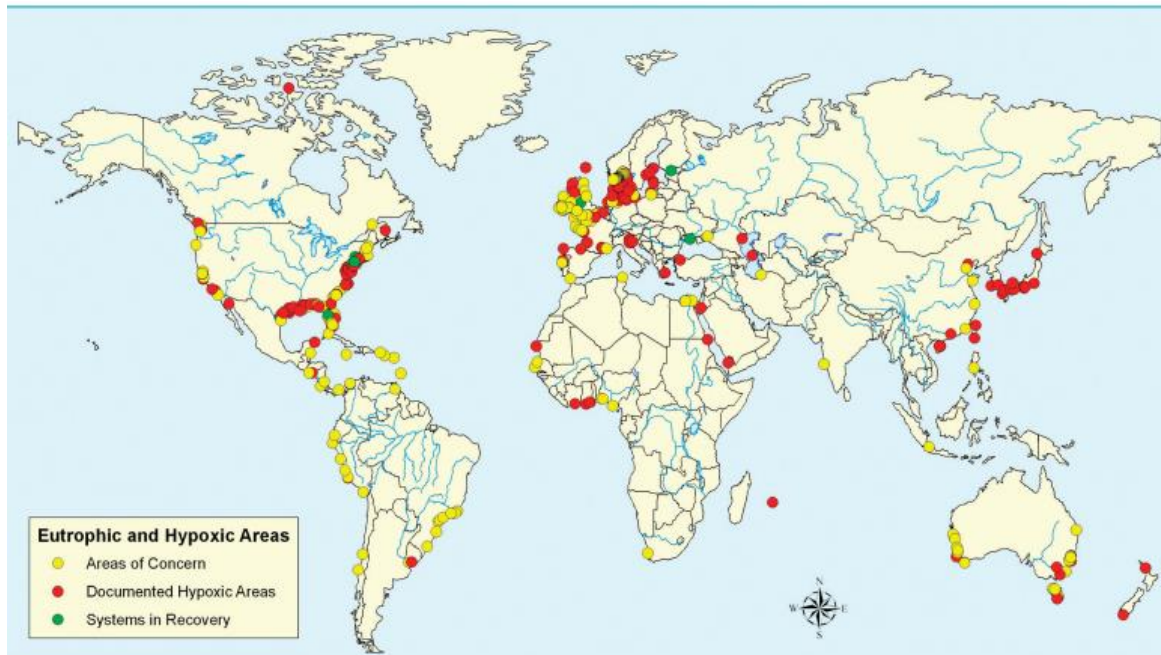
Figure 2: Map of global hypoxic and eutrophic coastal areas worldwide from Diaz et al (2017). Each circle represents a eutrophic system and red circle represents a hypoxic system. Of the 415 coastal systems examined, Diaz et al (2017) identified 169 that were both eutrophic and hypoxic.

CHAPTER 2: RESPONSE OF ECOSYSTEM METABOLISM TO ENGINEERED DESTRATIFICATION

ABSTRACT

Eutrophication and hypoxia are widespread problems globally and within the Chesapeake Bay. There is a growing need to understand the effects and consequences of eutrophication and hypoxia, but research is complicated by the inability to decouple these linked phenomena. Net ecosystem metabolism (NEM) was quantified in a tidal, eutrophic estuary using two methods; an open water method examining changes in dissolved inorganic carbon (DIC) and dissolved oxygen (DO), and a bottle method examining changes in DO during incubations. Whole-ecosystem experiments were performed by controlling the operation of an aeration system installed within the Rock Creek, MD estuary, allowing us to examine the NEM of a eutrophic estuary with contrasting oxygen conditions. Results from the open water method and the bottle method were conflicting. Open water results using DIC as a metabolite suggested chemoautotrophy occurred in 2017 when the aerators were on at all stations. Open water results using DO as a metabolite suggested a shift towards heterotrophy when the aerators were off at all stations in both 2017 and 2018. Our analyses emphasize the importance of the aerators controlling the physics of the water column as a controller of NEM in Rock Creek.

INTRODUCTION

Eutrophication, defined as an increased rate in organic matter supply to an ecosystem (Nixon 1995), is a pervasive problem globally and within the Chesapeake Bay (Diaz and Rosenberg 2008, Gilbert et al 2009). A common consequence of this increased organic matter is hypoxia or anoxia caused by oxygen consumption during the rapid decomposition of organic matter. The hypoxia associated with eutrophication presents a multitude of concerns for ecosystems managers and those who rely upon estuaries, such as fish kills, sulfur smells, and overall inhibition of ecosystem health (Corrales and Maclean 1995, Scheffer et al, 1993, Bricker et al, 2007).

A common cause of eutrophication is increased nutrient loading that increases phytoplankton growth rates in estuarine systems where N or P are limiting (Nixon et al 1986). Nutrient inputs are typically attributable to human activity such as fertilizer runoff, wastewater from treatment plants or septic systems, and atmospheric deposition as a result of fossil fuel combustion. Today, many estuaries are undergoing restoration and the trajectory of ecosystem recovery is of great interest to those managing and investing in these efforts (Duarte et al 2009).

Net ecosystem metabolism (NEM) provides an integrative measurement of the balance of metabolic processes within an ecosystem and its overall metabolic state (i.e. net heterotrophy or net autotrophy). Measurements of NEM consider all factors that affect metabolic processes (Giordano et al 2012), including those that contribute to eutrophication (e.g., primary production and respiration). While many monitoring programs track reductions in nutrient inputs and whether restoration is having the desired impacts on dissolved oxygen, water clarity, or submerged aquatic vegetation, fewer programs attempt to more directly document oligotrophication (Nixon et al 1996), which requires a rate process such as NEM to determine

whether overall organic matter is increasing, decreasing, or staying the same. Mathematically, we can compute shifts in the metabolic state by examining the change to the ratio between gross primary productivity (GPP) and respiration (R). When GPP is greater than R (GPP:R>1) the system is considered autotrophic and when R is greater than GPP (GPP:R<1) the system is considered heterotrophic. . The consequences of autotrophic NEM include, for example, increased organic matter and higher turbidity, while consequences of heterotrophic NEM include decreased oxygen supply and higher nutrient recycling.

Accumulation of nutrients, namely NH_4 and PO_4, is higher under hypoxic conditions (Kemp et al 1990, 2005, Jordan et al, 2008), which are common in stratified estuaries. Ammonium accumulates due to the inhibition of nitrification under hypoxia (Middelburg and Levin 2009). Phosphate accumulates when it is released by iron oxides, which readily occurs under hypoxic conditions. (Jordan et al 2008, Middelburg and Levin 2009). These compounds encourage productivity in surface waters. Phytoplankton can remain in the euphotic zone in a stratified system, and their biomass sinks below the pycnocline and decomposes, further decreasing oxygen concentrations. The connection between these processes establishes a feedback loop, referred to here as the hypoxic-eutrophic feedback. The intrinsic connection between hypoxia and eutrophication makes studying oxygen in eutrophic estuaries difficult, as normoxia and eutrophication are rarely concurrent.

In 1988, a whole estuary aeration system was installed in Rock Creek of Anne Arundel County, MD. The system was designed to destratify the water column and encourage oxygen penetration through increased air-sea exchange by pumping 15,574 liters of atmospheric air into the water column per minute. The small tidal estuary receives a high annual nutrient load and is considered eutrophic (Dames and Moore 1988). Rock Creek had experienced many of the

consequences associated with eutrophication, including fish kills, decreased water clarity, and sulfur smells. Harris et al (2015) leveraged the same system for experiments that showed oxygen concentration drastically increases when the aeration system is operational, but rapidly decreases when it is turned off. Despite the relatively small area occupied by the aeration system, oxygen concentrations declined in regions of Rock Creek well-beyond the footprint of the aerators (Harris et al. 2015). The engineered conditions in Rock Creek permit whole ecosystem experiments that support manipulation of the dissolved oxygen conditions to test a number of research questions associated with the hypoxic-eutrophic feedback.

The engineering approach implemented in Rock Creek focused on destratification of the water column. It is important to note that other aeration technologies manipulate dissolved oxygen using different techniques, such as fine-bubble aeration (Shammas 2007). In the case of engineered destratification, the process affects the NEM of the estuary through both chemical and physical mechanisms. Engineered destratification homogenizes surface and bottom waters as conceptualized in Figure 1. Theoretically, the pycnocline disappears or is shifted lower in the water column. Oxygen rich surface waters can mix to depth while hypoxic bottom waters are exposed to the atmosphere, decreasing overall hypoxic volume. Meanwhile, phytoplankton, which aggregate in surface waters, are also pushed to depth. The overall time they spend in the euphotic zone is reduced, and their productivity is inhibited by restricting their access to sunlight, akin to Sverdrup's (1953) critical depth hypothesis. The rapid decomposition inherent to the hypoxic-eutrophic feedback is inhibited, as there is less biomass available. Additionally, the nitrogen cycle is no longer inhibited, preventing NH_4 accumulation, and iron oxides retain their orthophosphate, preventing PO_4 accumulation (conditions (Kemp et al 1990, 2005, Jordan et al, 2008).

Based on the framework established above, we propose that a system subjected to engineered destratification will be more net autotrophic compared to a stratified system, assuming all other biotic and abiotic factors are equal. Phytoplankton production will be inhibited by the aerators mixing them below the compensation depth and the subsequent decrease in organic material will cause a decrease in respiration. Overall, the trophic state of the ecosystem will shift towards autotrophy as the respiration decreases. Conveniently, this hypothesis is testable in Rock Creek. We predict that the NEM of Rock Creek will shift towards heterotrophy when the aeration system is turned off. We would also like to emphasize that Rock Creek and its aerators are ideal for studying the dilemma presented by the hypoxic-eutrophic feedback, that few similar sites exist, and, of those that do exist, fewer have been properly leveraged for study.

Research questions and approaches

Here, we seek to answer the following questions; 1) What is the ecosystem response of a eutrophic estuary to aeration with regards to NEM? 2) What portions of NEM in Rock Creek are due to anaerobic and aerobic processes?

METHODS AND ANALYSES

This thesis will examine the NEM of Rock Creek through various methods and metrics. In this thesis, we focus on measurements of DO and DIC through various measurement techniques. We also examined the response of these chemical constituents to changing aeration condition (i.e. on or off).

Study site

Rock Creek is a 353-hectare tributary of the Patapsco River in Anne Arundel County, MD. The reported volume in the tributary is 9.6 x 10^6 m^3 (Cronin and Pritchard, 1975) The average depth is 2.9 m with a maximum reported depth of 5.7 m and a tidal range of 0.3 m. Water residence times range from 13 to 32 days. The surrounding watershed encompasses an area of 1041 hectares, resulting in a land to water ratio of 2.9. Within this area, approximately 80% of land use is residential and urban developments, 20% is forested area, and 0.2% is agricultural based on 2010 Maryland Department of Planning data. It is considered an "upside-down" estuary (Dimillia et al 2011), where the largest percent of its nutrient input originates from the adjoining, larger estuary (in this case, the Patapsco River).

The whole-tributary aeration system was installed in 1988 in response to complaints of fish kills and sulfur smells resulting from anoxic conditions. The system uses 276 on-land compressors to pump approximately 15,574 liters of atmospheric air into the water column per minute. The aerated portion of the creek has an area of about 22 acres and 2700 linear feet of piping. The system is active during the spring and summer months and, barring equipment error or our experiments, operates continuously during this time.

According to Harris et al (2015), a substantial increase in oxygen is observed when the aeration system is operational. This increase in oxygen is observed in both the aerated portion and the main stem of the estuary extending towards the mouth of Rock Creek. When the aeration system is turned off, a rapid (i.e. one day) return to hypoxia is observed in all portions of the estuary (Harris et al 2015). Based upon these observations, the aeration system can shift Rock Creek between a normoxic state and a hypoxic state within a short enough timeframe to allow experimental manipulation. These conditions create an ideal framework for testing our research questions through comparative experimentation.

Figure 3 shows the location of each of our stations. Stations 1, 2, and 4 are located within the aerated portion of the creek and station 7 is located along the main-stem of the creek outside the aerated portion and closer to the Patapsco. The station naming convention is based on over five years of monitoring in the system, where some stations have been dropped from sampling over time. For quality control purposes we retained the historical numbering conventions.

When the aerators were operational, collection cruises were performed in pairs; the first cruise was performed when the aerators were on and the second was performed when the aerators were off. The duration between paired cruises varied with the year of sampling; in 2017 cruises took place 3 days apart and in 2018, cruises took place 1 week apart. In 2017, the "aerators on" collection cruises took place on 9/28/2017 and 9/29/2017 and the "aerators off" cruises took place on 10/2/2017 and 10/3/2017. In 2018, the "aerators on" cruises took place on 7/9/2018 and 7/10/2018 and the "aerators off" cruises took place on 7/16/2018 and 7/17/2018. Cruises were designed to capture diurnal changes, with sample collection occurring at dawn, dusk, and the following dawn for open water method samples. A noon sampling time was included in 2017. In 2017, photosynthetron experiments were not performed for stations 2 and 4.

No metabolic data was collected for station 4 in 2018. Sampling dates are summarized in Table 1 and a list of when metabolic data was collected for each method is summarized on Table 2.

Nutrient and Chlorophyll-a Sampling

During each cruise, surface and bottom whole water grab samples were taken at each station and chilled until further analysis. Sample water was analyzed for ammonium (NH_4), nitrate-nitrite (NO_3-NO_2), nitrite (NO_2), total dissolved nitrogen (TDN), particulate nitrogen (Part-N), orthophosphate (PO_4), total dissolved phosphorous (TDP), and particulate phosphate (Part-P) following techniques established by Grasshoff (1976) and D' Elia et al. (1977). Active chlorophyll-a and pheophytin concentrations were fluorometrically measured with a Trilogy fluorometer by Turner Designs following EPA method 445.0, SM 10200H.3. To determine nutrient limitation, we calculated the ratio between dissolved nitrogen species and orthophosphate. The molar mass of N in NH_4 and NO_{23} together was divided by the molar mass of P in PO_4 to determine the N to P ratio (N:P). N:P values above 16 suggest P limitation and values below 16 suggest N limitation, as per Redfield (1963).

Rate measurements: Productivity and respiration

The chemical constituent used as a metric to quantify NEM reveals unique insight about the ecosystem. DO and DIC are convenient metrics for measuring NEM, as they are components of the reactions of photosynthesis and aerobic respiration. For DO, decreases represent respiration while increases represent photosynthesis. The opposite is true for DIC, where decreases represent photosynthesis (due to carbon fixation) while increases represent respiration. However, DIC is utilized in additional metabolic processes. DIC is a byproduct of both aerobic and anaerobic respiration processes (Smith et al 1991), while DO is only used in aerobic

respiration. For this reason, DIC, as a metric, provides unique information into NEM that DO alone cannot. Because aerobic respiration also produces CO_2 at a molar ratio equivalent to DO consumed, we can easily convert aerobic respiration into carbon units by measuring only DO changes. By taking the difference between DIC and DO measurements, we can isolate the aerobic and anaerobic components of metabolism and answer question 2. These assumptions establish the framework on which our methods are analyzed.

Our first method, the photosynthetron method, utilized a modified version of Smith and Kemp's (2001) light and dark bottle method. Surface and bottom water samples were decanted into 60ml glass Biological Oxygen Demand (BOD) bottles and their oxygen concentration was measured with a handheld YSI Professional Series ProBOD probe attached to a YSI Digital Professional Series data logger. Samples were then incubated in a photosynthetron, a temperature-controlled water chamber with several cells subjected to known light levels. Light levels were generated by full spectrum photosynthetically active radiation (PAR) 400-watt metal halide bulbs. A gradient was established in the photosynthetron by dampening the light with selective placement of mesh fabric. The photosynthetron was divided into cells of varying light levels (See Figure 4). Each cell was subjected to an irradiance between 0 and 1500 µmol photons$*$m$^{-2}*$s^{-1}. Irradiance of each cell was measured with a LI-COR underwater light sensor attached to a LI-COR 1400 data logger. Between 15 and 18 surface samples were incubated in light. Locations within the photosynthetron were chosen to ensure each station was subjected to a gradient. Several surface and bottom samples (n=3) were incubated in darkness for the duration. Incubations lasted until a 0.5 mg$*$L^{-1} change was observed as adapted to ProBOD detection limits and recommendations from Carignan et al. (1998). Incubations typically lasted between 4 and 6 hours. Temperatures within the photosynthetron were chosen to emulate *in situ* collection

temperatures as closely as possible (within 1.5 degrees). Following the incubation, the DO concentration of each bottle was collected and recorded. We assumed that DO changes in light are indicative of NPP while changes in darkness are indicative of respiration.

Our second method examined changes in DIC and DO *in situ*. While the photosynthetron method is efficient in capturing microbial activity, it was performed under controlled conditions. *In situ* examinations of changes are more representative of the ecosystem, as it inherently captures all factors that influence production and respiration, even if they are not directly measured (e.g. sediment chemistry). The concentrations of DO and DIC were recorded at dawn, dusk, and the following dawn. In 2017, concentrations were also measured at noon for additional resolution. Changes in concentration during daylight hours were assumed to represent NEM while changes at night represent R, which is analogous to the photosynthetron experiments. Our results were corrected for air-water exchange, as gas exchange between the water and atmosphere can affect the concentrations and only metabolic processes were of interest. This method was used to constrain NEM from a different perspective compared to the previous method and differences between DO and DIC results were used to determine aerobic and anaerobic components of metabolism in Rock Creek.

Analysis and Calculations

For each station, the relationship between PAR (in μmol photons$*m^{-2}*s^{-1}$) and NPP (in DO$*L^{-1}*hr^{-1}$) was plotted, with each bottle treated as an individual point. The relationship between irradiance and NPP was described with one of two model fits using the R-package *Phytotools* (Silsbe and Malkin 2015) and a P-I curve was generated when possible. Two fitted models were used: 1) Jassby and Platt (1976) and 2) Eilers and Peeters (1988). The Eilers and

Peeters (1988) model was used only when photoinhibition was observed in the P-I curve and the

Jassby and Platt (1976) model was used in all other scenarios. The Jassby and Platt model has the

following equation:

$$1) \quad y = \alpha \times E_k \times \tanh\left(\frac{Iz}{E_k}\right)$$

Where α (initial slope) and E_k (Optimal Light) are parameters given by the phytotools fit, I_z is the

irradiance, and y is NPP in mg DO*L^{-1}*hr^{-1}. The Eilers and Peeters (1988) model has the

following equation:

$$2) \quad y = \frac{Iz}{I^2*\left(\frac{1}{\alpha*E_{opt}^2}\right)+\left(\frac{Iz}{PS}\right)-\left(\frac{2Iz}{\alpha*E_{opt}}\right)+\left(\frac{1}{\alpha}\right)}$$

Where α (initial slope), E_{opt} (light of highest production) and Ps (Dimensionless parameter of

photoinhibition) are parameters given by the fit in *phytotools,* I_z is the irradiance, and y is the

NPP in mM DO/hr. For both models, NPP values were converted to molar units and then

converted to carbon units with a photosynthetic quotient of 1.3 (Redfield 1963). The values of

parameters for each model fit used in proceeding calculations can be found in Appendix B.

The relationship between depth and *in situ* light at each station was described using

Beer's law. At each station, a light profile was taken using a LI-COR underwater PAR sensor

attached to a LI-1400 of LI-1500 LI-COR light sensor logger. Simultaneously, incident light was

measured on deck with a quantum light sensor attached to the same logger. The relationship

between depth and percentage of incident light reaching that depth was graphed and a log-based

equation was fit to the relationship. The light-attenuation (k_d) coefficient was determined via the

following fit:

$$3) \quad \frac{I_z}{I_0} = e^{-k_d * z}$$

Where I_z is the light at depth, I_0 is incident light, and z is the depth at which Iz was measured.

Then, the kd value was used to find the euphotic depth, defined here as the maximum depth of

the water column that receives at least 1% of incident light ($I_z/I_o = .01$). The euphotic depth for

each station was calculated using the following equations:

$$4) \quad .01 = e^{-k_d * z_E}$$

$$5) \quad z_E = \ln(.01) / -k_d$$

Where z_E is the euphotic depth and ln represents the natural logarithm. If the euphotic depth was

larger than the mid-tide depth, the mid-tide depth was substituted. Then, the Beer-lambert law

was rearranged to compute light at any given depth.

$$6) \quad I_z = \frac{e^{-k_d * z}}{I_0}$$

An equation was generated to solve for NPP at any depth by inserting equation 6 into the NPP

model fit for the corresponding station:

$$7a) \quad NPP = \alpha \times ek \times \tanh\left(\frac{\frac{e^{-kd*z}}{Io}}{ek}\right)$$

$$7b) \quad NPP = \frac{\frac{e^{-kd*z}}{Io}}{\frac{e^{-kd*z}}{Io}*\left(\frac{1}{\alpha*Eopt^2}\right)+\left(\frac{\frac{e^{-kd*z}}{Io}}{Ps}\right)-\left(2\frac{\frac{e^{-kd*z}}{Io}}{\alpha*Eopt}\right)+\left(\frac{1}{\alpha}\right)}$$

This equation was integrated over the euphotic depth.

$$8) \quad NPP_{depth} = \int_0^{Z_E} NPP * dz$$

Where NPP$_{depth}$ is the depth integrated NPP. This equation was repeated using incoming radiation PAR values measured at the Jug Bay Sanctuary at 15-minute intervals for 24 hours starting from sunrise on the date of collection as a substitute for Io. Each integral was divided by 4 to correct for time units and all integrals for one day were summed together to calculate daily depth-integrated NPP.

$$9)\ NPP_{daily} = \sum_{t=1}^{tmax} \frac{NPP_{depth,t}}{4}$$

Where t is the 15-minute time interval from which Io was taken, NPP$_{depth,t}$ is the NPP of that time interval, and tmax is the total number of time intervals on the given day.

Daily R values were calculated by up-scaling photosynthetron R values to the whole water column. The water column was divided into 2 layers, surface and bottom. Total depths of each station used were the mid-tide depth and remained constant for all dates. Table 4 lists all depths used in calculations. The euphotic depth was the dividing point between surface and bottom layers.

Average hourly rates from the photosynthetron R measurements were multiplied by the volume of water in 1 square meter (based on the station depth) to generate hourly surface and bottom respiration values. These values were then summed and multiplied by 24 to generate daily respiration values for one square meter of water column. When the euphotic depth was higher than the total depth of the water column, the average between surface and bottom values were used to calculate depth-integrated respiration. Respiration rates were then converted to carbon units with a respiratory quotient of 1 (Hopkinson and Smith, 2005).

Daily GPP was calculated using the following equations:

$$10)\ NPP = GPP - R$$

$$11)\ GPP = NPP + R$$

The calculations for quantifying NPP and GPP as measured by the photosynthetron results were performed using MATLAB and code is included in Appendix A.

Rate measurements: Carbon-based estimate of NEM

To determine the net effects of all ecosystem processes on NEM, we examined in-situ concentrations of DIC and DO to generate daily production and respiration rates at each station. Sampling times were chosen to calculate diel rates of R, GPP, and, ultimately, NEM. By sampling DO and DIC concurrently, we can calculate both aerobic and anaerobic portions of respiration. This method relies on the following assumptions: 1) changes of DO or DIC in daylight hours are indicative of the sum of gross primary productivity and respiration and changes at night are indicative of respiration, 2) nighttime changes in DIC are indicative of both aerobic and anaerobic respiration while nighttime changes in DO are indicative of only aerobic respiration 3) oxidative processes (annamox, sulfide oxidation, etc) that might decrease water column DO are ignored, 4) productivity completely ceases between dusk and dawn, 5) photosynthesis produces an amount of moles of oxygen equivalent to 1.3 times the amount of moles of carbon dioxide it fixes (i.e. a photosynthetic quotient of 1.3 as per Redfield 1963), 6) respiration produces an amount of moles of carbon dioxide equivalent to the amount of moles of oxygen it consumes (i.e. a commonly used respiratory quotient of 1, e.g. Hopkinson and Smith 2005), and 7) changes in DIC and DO are controlled only by air-sea exchange and metabolic processes 8) changes in DIC due to calcification and dissolution are ignored.

At each station and sampling time, surface and bottom DO concentrations were measured using a YSI probe. In addition, salinity, temperature, specific conductivity, and % DO saturation were taken concurrently. *In situ* DO was measured using either a YSI 660 multiparameter sonde or a YSI EXO-2 multiparameter sonde. DO measurements were calibrated by using 100% air saturation while salinity and conductivity measurements were calibrated using Ricca 10,000 $\mu S*cm^{-1}$ potassium chloride (KCl) conductivity standard. Duplicate surface and bottom samples were pumped with no headspace into 10ml hungate tubes pre-filled with 10uL of HgCl2 as a preservative. These samples were analyzed on a DIC analyzer, an automated digital pump, a mass flow controller, and an infrared CO_2 detector by LI-COR as originally described by Cai and Wang (1988). Samples were refrigerated and stored in darkness until analysis. DIC samples were analyzed within 1 month of collection.

To complement the DIC analysis, alkalinity was also measured. Duplicate surface and bottom water samples were filtered and decanted into 150 mL plastic bottles with minimal headspace. Samples were filtered with a 110 mL 0.2-micron capsule filter (Millipore) and refrigerated in darkness until titration. Samples were titrated with 0.1 N HCl with an open titration method as described by Dickson (1981). All samples were analyzed within 3 months of collection. Results of titrations were used to calculate total alkalinity. The pH of these samples was measured using a Mettler Toledo FE20 pH probe calibrated using Ricca 4, 7, and 10 pH buffer reference standards.

Partial pressure of carbon dioxide (pCO_2) in the water column was calculated using the Matlab code CO2sys (Lewis et al 1998) using alkalinity and pH as inputs for the carbonate system. *In situ* temperature, salinity, and pressure were required inputs to the CO2sys code (Lewis et al. 1998). Phosphate and silica concentrations were optional and entered when

available. Partial pressure of carbon dioxide in the atmosphere was measured by analyzing gas

samples taken from the site in 140mL gas tight syringes at every station and every time

point. As soon as possible, carbon dioxide concentrations were measured on a cavity ring down

spectrometer (Picarro 2201i) according to theory presented in Crosson (2008). Concentrations

were checked using a calibration of certified CO_2 standards (Airgas 360ppm +/-4%).

To properly constrain metabolism, changes due to air-sea exchange were calculated. For

DO, air-sea exchange was calculated using the following equation:

$$12) \ \Delta DO_{g,t} = k_r * (C_s - [DO])$$

Where k_r is the volumetric reaeration coefficient as described by Caffrey (2014), C_s is the DO

saturation concentration as specified by Benson and Krause (1984), [DO] is the measured

dissolved oxygen concentration. k_r was calculated with the following equation:

$$13) \ k_r = \frac{e^{1.09+0.249*U_{10}}}{10}$$

Where U_{10} is the wind speed at 10 meters above the water surface. Cs was calculated using the

following equation:

$$14) \ Cs = e^{\wedge}(A1 + \frac{A2}{T} + \frac{A3}{T^2} + \frac{A4}{T^3} + \frac{A5}{T^4} - (s * B1 + \frac{B2}{T} + \frac{B3}{T^2}))$$

Where T is the measured temperature in degrees Kelvin, s is the salinity, and A1, A2, A3, A4,

A5, B1, B2, and B3 are constants specified by Benson and Krause (1984) The exact values for

these constants are shown in Table 3 These calculations were performed automatically in the

NEPcalc R code. For DIC, air-sea exchange was calculated from equations from Crosswell et al

(2017):

$$15)\ \Delta DIC_{g,t} = k_0 * k_{600} * \Delta pCO2 * \left(\frac{Sc}{600}\right)^{-0.5}$$

Where k_0 is the solubility coefficient as specified by Weiss (1974), k_{600} is the gas exchange coefficient as specified by Jiang et al (2008), ΔpCO_2 is the difference between the pCO_2 of the water column and the atmosphere, and Sc is the Schmidt number as specified by Wanninkhof (1992). This calculation was only performed on the surface layer, as air-sea exchange is not possible with bottom water samples. The dividing point between surface and bottom layers was the pycnocline and was calculated via a method proposed by DNR.

For both DO and DIC calculations, wind speeds were taken from data provided by a NOAA monitoring station located at the Francis Scott Key Bridge, located in the main stem of the Patapsco River in six-minute intervals (https://tidesandcurrents.noaa.gov/ports/ports.html?id=8574728). In equations 12 and 15, t refers to one of these six minute intervals. The wind speeds were normalized to a height of 10 m using equation 16 from Marino and Howarth (1993):

$$16)\ U_{10} = \frac{U}{0.097*\log(H/10)+1}$$

Where U is the wind speed measured at the Francis Scott Key Bridge and H is the height of the monitoring station above the water level, 6.61 m. All other *in situ* data necessary for calculations were interpolated using linear regressions between measured points to generate values parallel to the wind speeds measured every six minutes. The gas exchange equations were performed on each of these six-minute time intervals and summed together to calculate the total gas exchange between our measured time points.

$$17)\Delta DIC = \sum_{t=1}^{tmax}\left(\Delta DIC_{g,t}\right)$$

$$18) \; \Delta DO = \sum_{t=1}^{tmax} \left(\Delta DO_{g,t} \right)$$

Where t is the six-minute time interval and tmax is the total amount of intervals between measure points.

Destratification Model

A simple model was constructed to quantify the effect of engineered destratification on air sea exchange (DIC_g and DO_g). The aeration system, on average, pumps approximately 174 liters of atmospheric air per minute per square meter into the water column. This value is normalized to the aerated portion of the creek (in this manuscript, stations 1 and 2). The system is designed to expose a larger volume of water to the atmosphere, thereby encouraging higher air-sea exchange. The model constructed assumes 1) the volume of water displaced by aeration is equal to the volume of water pumped into the water column, 2) air-sea exchange occurs only with the topmost portion of the water column, 3) exchange between pumped air and the water column is ignored.

We calculated the time it takes for one square meter of water column to be completely overturned due to the aeration system, or the time it takes for the aeration system to pump a volume of air equivalent to the volume of the water column. The turnover time, τ, was calculated as:

$$19) \; \tau = \left(\frac{V}{a} \right) * A$$

Where a is the airflow rate from the aerators (174 L*m^{-2}*min^{-1}), A is the area of 1 square meter of water column, and V is the volume of one square meter of water column (L*m^{-2}). We then calculated how many complete displacement (δ) would occur in one hour as expressed in equation 20):

$$20) \; \delta = 1/(\tau * 60)$$

For each hour of our model run, our air-sea exchange calculation (see equation 17) was repeated a number of times equal to δ. The contribution of each turnover to air-sea exchange was summed together to calculate the increased rate due to destratification (D):

$$21) \; D_{DIC} = \sum_{\tau=1}^{\delta} \Delta DIC_{g,\tau}$$

$$22) D_{DO} = \sum_{\tau=1}^{\delta} \Delta DO_{g,\tau}$$

When the aerators were off, or the station was not directly in the aerated zone (stations 4 and 7), δ is equal to 1.

Daily NEM was calculated using assumptions from Crosswell et al (2017). Changes in DO and DIC were assumed to be caused by metabolism. Therefore, the metabolic flux, F, was calculated as the difference between the total change and the air-sea exchange rate.

$$23) \; F_{DO} = \Delta DO_{Total} - D_{DO}$$

$$24) \; F_{DIC} = \Delta DIC_{Total} - D_{DIC}$$

Where ΔDO_{Total} and ΔDIC_{Total} are the observed differences between DO and DIC, respectively, between the two time intervals of interest. This equation was performed on daytime (F_1) and nighttime (F_2) intervals. Daily respiration was calculated by multiplying the hourly nighttime rate by 24.

$$25)\ R = F_2 * 24$$

Daily gross primary productivity was calculated by multiplying the difference between daytime and nighttime hourly rates by the number of daylight hours.

$$26)\ GPP = (F_1 - F_2) * h_1$$

Where h_1 is the hours of daylight. Finally, Daily NEM was calculated as the difference between GPP and R.

$$27)\ NEM = GPP + R$$

Using the results of these computations, we calculated the contribution to metabolism due to aerobic respiration and anaerobic respiration individually. We assumed that R observed in our DO changes are representative of aerobic respiration and R observed in DIC changes are representative of both aerobic and anaerobic respiration.

$$28)\ R_{DO} = R_A$$

$$29)\ R_{DIC} = R_A + R_{AN}$$

Where R_A is the aerobic component of respiration and R_{AN} is the anaerobic component of respiration. Changes in DIC due to calcification and dissolution were considered negligible and were ignored. By extension, the anaerobic component of R was calculated by substituting R_A for R_{DO} and rearranging the previous equations accordingly.

$$30) \; R_{AN} = R_{DIC} - R_{DO}$$

These results were compared spatially (i.e. by station), temporally, and by aerator status (i.e. on and off).

Statistical Analyses

Linear model tests were performed to determine significance of correlations between metabolic data (i.e. NEM/NPP, GPP, and R) and measured variables that may affect metabolism. Metabolic data were tested for correlations with temperature, salinity, light extinction coefficient (kd), active chlorophyll, pheophytin, NH_4, NO_{23}, PO_4, DOC, TDN, TDP, Part-N, Part-P, and the N to P ratio. As productivity in shallow, stratified estuaries such as Rock Creek is concentrated in surface waters, only surface concentrations were used for these tests. Linear model tests were performed using R.

RESULTS

Station Abiotic Data

Water temperatures ranged between 19.43 degrees Celsius at station 4 on the dawn of October 2nd, 2017 to 29.03 degrees Celsius at station 7 on the dawn of July 16th, 2018. 2017 was colder on average with a mean temperature of 22.08 ± 2.08 while 2018 had a mean temperature of 27.33 ± 0.57. There was no significant difference between surface and bottom temperatures at the same station and time (paired t-test, p>.05). Final dawn temperature values can be found on Table 4.

Salinity values ranged between 4.89 at station 1 on July 9th, 2018 at dusk in surface waters to 15.14 at station 7 on October 3rd, 2017 at dawn in surface waters. 2017 was considerably more saline than 2018, with an average value of 11.51 ± 1.68 in 2017 versus 5.37 ± 0.28 in 2018. Part of the difference in salinity between years can possibly be described by high precipitation prior to sampling in 2018. There was a significant difference between simultaneous surface and bottom salinities (paired t-test, p<.0001) suggesting a propensity towards stratification in Rock Creek. Final dawn salinity values can be found on Table 4.

Daylight hours ranged between 11 hrs, 41 minutes on October 3rd, 2017 to 14 hours, 45 minutes on July 9th, 2018. Daylight hours were shorter in 2017 than 2018 (11 hrs, 47.25 minutes on average versus 14 hours. 41.5 minutes on average, respectively) due to seasonality. Daylight hours and surface irradiance values used in calculations can be found on Table 4.

Light attenuation coefficient values are shown on Table 4 and plotted in Figure 6. A consistent trend between the on and off state was not observed; We observed decreases at

stations 1 and 7 in 2017 and at stations 1 and 2 in 2018 and observed increases at all other stations.

There was no pycnocline observed at stations 1 and 2 in both 2017 and 2018 when the aerators were on, presumably due to the aerators themselves. Furthermore, the remaining stations had deep pycnoclines (> 2.5) when the aerators were on. All stations saw the pycnocline move upwards when the aerators were turned off. Additionally, the most common pycnocline depth when the aerators were off was 0.75 m, which is the shallowest pycnocline we can calculate by our method (See Table 4) These results show that Rock Creek heavily stratifies without the aerators.

Nutrient Data

Water column nutrient concentrations are reported in Table 5. NH_4 values ranged between 0.29 µM at station 7 on July 10th, 2018 in surface waters and 11.71 µM at station 1 on September 29th, 2017 in bottom waters. 2017 saw higher NH_4 concentrations on average (6.37 ± 3.47 µM in 2017 versus 3.30 ± 2.57 µM in 2018). In both 2017 and 2018, bottom waters had higher concentrations than surface waters on average. When aerators were turned off, we observed increases in NH_4 concentrations in surface waters at station 7 in 2017 and 2018 and increases in bottom waters of station 4 in 2017 and station 7 in 2018. Conversely, we observed decreases in surface waters of station 1, 2, and 4 in 2017 and station 1 and 2 in 2018 and decreases in bottom waters at stations 1, 2, and 7 in 2017 and stations 1 and 2 in 2018.

We observed NO_{23} concentrations between 0.478 µM at station 7 on 7/10/2018 in surface waters and 13.71 µM at station 1 on 9/29/2018 in bottom waters. 2017 had higher concentrations on average ($8.93 + 3.36$ µM versus 5.29 ± 4.00 µM). On average, bottom waters had higher

concentrations in 2017, while surface waters had higher concentrations in 2018. When the aerators were turned off, we observed increases in surface waters of stations 4 and 7 in 2017 and station 7 in 2018 and in bottom waters of station 2, 4, and 7 in 2017 and station 7 in 2018. We observed decreases in surface waters of stations 1 and 2 in 2017 and at station2 in 2018. Concentrations decreased in bottom waters at station 1 in 2017 and stations 1 and 2 in 2018.

In our data, we observed an average TDN concentration of 68.72 ± 29.78 µM in 2017 and an average concentration of 32.66 ± 7.72 µM in 2018.The highest concentration observed was found at station 1 on 10/3/2017 in surface waters at a value of 132.08 µM. The lowest concentration was 23.56 µM at 2 stations: station 7 on 7/10/2018 in surface waters and station 2 on 7/16/2018 in surface waters. In 2017 when aerators were turned off, we observed increases in surface waters at station 1 and in bottom waters at station 4. All other stations and layers saw decreases in TDN concentrations. In 2018, stations 1 and 2 saw increases in both surface and bottom waters when the aerators were turned off while station 7 saw increases in surface and bottom waters.

Part-N values peaked at 177.77 µM at station 1 on 10/3/2017 in surface waters and were lowest at station 2 on 7/16/2018 in surface waters at a value of 10.42 µM. 2017 had higher concentrations on average, with a value of $79.19 + 47.35$ µM compared to 21.97 ± 6.85 µM in 2018. When the aerators were turned off, we observed increases in surface waters at stations 1 and 2 in 2017 and station 1 in 2018. We observed decreases in surface waters at stations 4 and 7 in 2017 and stations 2 and 7 in 2018. All stations saw decreases in bottom water concentrations in response to the aerators being turned off in both 2017 and 2018.

PO_4 concentrations ranged from 0.052 µM at station 2 on 7/17/2018 in surface waters to 6.89 µM at station 1 on 10/3/2017. On average, 2017 had higher PO_4 concentrations than 2018

(1.87 $\pm$ 1.79 µM in 2017 versus 0.43 + 0.70 µM in 2018). When aerators were turned off, we observed increases in PO_4 concentrations in surface waters at stations 1, 2, and 7 in 2017 and at stations 1 and 7 in 2018. Bottom water concentrations increased at stations 4 and 7 in 2017 and stations 1 and 2 in 2018. Conversely, concentrations decreased in surface waters at station 4 in 2017 and station 2 in 2018. Concentrations decreased in bottom waters at station 1 and 2 in 2017 and at station 7 in 2018.

TDP concentrations ranged from 0.29 µM at station 2 on 7/9/2018 in bottom waters to 12.00 µM on 10/3/2017 in surface waters. In 2017 when aerators were turned off, we observed increases in TDP in surface waters at stations 1, 2, and 7 and increases in bottom waters at station 4. Conversely, we observed decreases in surface waters at station 4 and decreases in bottom waters at stations 1 and 2. In 2018, we observed increases in surface waters at stations 1 and 7 and in bottom waters at stations 1 and 2. Conversely, we observed decreases surface waters at station 2 and in bottom waters at station 7. 2017 saw higher concentrations on average (4.09 + 3.32 µM vs 0.80 + 0.74 µM).

Part-P values peaked at 8.72 µM at station 1 in surface waters on 10/3/2017 and were lowest at a value of 1.26 µM at station 7 in surface waters on 7/17/2018. In 2017, when the aerators were turned off, increases in surface water concentrations were observed at stations 1, 2, and 4, and a decrease was observed in surface waters of station 7. In bottom waters, decreases were observed at stations 1 and 4 and increases were observed at stations 2 and 7. In 2018, we observed an increase in Part-P concentrations in surface waters at station 2 when the aerators were turned off. All other stations and depth saw decreases in concentrations. 2017 saw higher Part-P concentrations than 2018 on average (4.34 + 1.99 µM vs 1.83 + 0.63 µM, respectively).

N to P ratios are summarized on Table 6. In 2017, N limitation was more common. Surface waters did not shift their state of nutrient limitation when the aerators were turned on, but bottom waters at stations 1 and 2 shifted from N limitation to P limitation. In 2017, the aerated stations (1,2, and 4) showed N limitation more frequently than station 7. In 2018, P limitation was present in surface water at all stations except for station 7 when the aerators were on. Bottom waters at stations 1 and 2 shifted to N limitation when the aerators were turned on. The highest N to P ratio was observed at Station 1 in surface waters on 7/10/2018 with a value of 113.33. The lowest value was 1.51 and was observed at station 1 in surface waters on 10/3/2017.

Carbon-Based Water Quality Data

DOC concentrations ranged between 0.24 mM at station 7 on 7/17/2018 in bottom waters and 0.97 mM at station 1 on 10/3/2017 in surface waters and are reported in Table 7. Both 2017 and 2018 saw higher concentrations in surface waters than in bottom waters, with average values of 0.48 mM and 0.26 mM, respectively. When the aerators were turned off, all stations saw decreases in bottom water DOC concentrations. In surface waters, concentrations increased at station 1 in 2017, increased at stations 1 and 7 in 2018 and decreased at all other stations. DOC concentrations are shown in Table 8.

Average active chlorophyll values are summarized in Table 8A. We observed average active chlorophyll values ranging between 7.08 $\pm$ 1.02 µg/L at station 1 in bottom waters on 7/16/2018 and 300.50 $\pm$ 173.33 µg/L at station 1 in surface waters on 9/28/2017. In 2017, all stations and depths saw decreases in chlorophyll concentrations when the aerators were turned off. In 2018, all surface waters saw increases in concentrations when the aerators were turned

off. Stations 1 and 2 saw increases in bottom waters while station 7 saw a decrease in concentrations in bottom waters.

Pheophytin concentrations are summarized on Table 8B. The highest concentration observed was found at station 1 in surface waters on 9/28/2017 at a value of 88.11 ± 55.17 µg/L. The lowest concentration was found at station 1 in surface waters on 7/16/2018 at a value of 4.17 ± 1.08 µg/L. In both 2017 and 2018, we observed consistent decreases in both surface and bottom waters in the aerated portion of the creek when the aerators were turned off.

In 2017, pCO_2 values ranged from 251.3 uatm at station 2 at dusk on 10/2/2018 to 6219.24 uatm at station 1 at noon on 9/28/2017. In 2018, pCO_2 values ranged between 279.72 at station 7 at dusk of 7/16/2018 to 4238.98 at station 2 at dawn of 7/17/2018. pCO_2 in surface was saturated with respect to the atmosphere at all but 6 time points out of the 50 surface measurements we made. An example of diel changes in pCO_2 can be found in Figure 11.

Metabolism Results

Open Water DIC Metabolism

Metabolism as measured by changes in DIC in the open water method are detailed in Table 9A. When measured using changes in open water DIC concentrations, NEM ranged between 1336.43 ± 17.87 mM C/m2/day at station 4 in 2017 when the aerators were on and -86.74 ± 9.66 mM C/m2/day at station 7 in 2018 when the aerators were on. Net carbon fixation was observed at all stations when the aerators were on in both 2017 and 2018, except for station 7 in 2018, suggesting a net release of carbon into the system. When the aerators were turned off, all stations experienced a decrease in NEM (i.e. less carbon fixation) in 2017 and 2018 except for station 7 in 2018. NEM values are plotted in Figures 14 and 15.

We observed positive GPP values at stations 2 ,4, and 7 2017 when the aerators were on,

contradicting our assumptions regarding DIC metabolism. At the remaining stations, we

observed higher GPP rates when the aerators were turned off at all stations. As calculated, GPP

values ranged from -764.80 $\pm$ 12.76 mM C/m2/day at station 4 in 2017 when the aerators were

on to 689.75 $\pm$ 4.99 mM C/m2/day at station 7 in 2018 when the aerators were on. GPP values

are plotted in Figures 16 and 17.

In 2017, we observed nighttime decreases in DIC when the aerators were on at all

stations (Figure 13) and, subsequently, nonsensical R rates in these cases, suggesting net carbon

fixation and contradicting our assumptions on DIC metabolism. This observation made

interpreting respiration values, and all calculations that rely on respiration, in 2017 difficult. As

calculated, respiration values ranged between -2101.23 $\pm$ 30.63 mM C/m2/day at station 4 in

2017 when the aerators were on to   -764.05 $\pm$ 5.18 mM C/m2/day at station 7 in 2017 when the

aerators were off. In 2017, all respiration rates changed from suggesting carbon fixation to net

carbon release when the aerators were turned off, and rates were not contradictory to our

hypotheses following the aerators being turned off. In 2018, we observed increases in the

magnitude of respiration rates at all stations (Figure 19). All respiration rates followed our

hypotheses in 2018.

Because metabolic rates did not always follow assumptions used for calculations (e.g.

DIC uptake during the day and release at night), GPP:R values are difficult to interpret for the

open water DIC method. Despite this, we show the values of GPP:R in Table 10.

Open water DO Metabolism

Metabolic rates using open water DO are summarized on Table 9B and Figures 14-19. As measured with in situ DO changes, NEM values ranged between 306.45 mM C/m^2/day at station 7 in 2017 when the aerators were on to -712.02 mM C/m^2/day at station 2 when the aerators were off in 2018. All stations experienced a decrease in NEM in 2017 and 2018 when the aerators were turned off. This trend mirrors the trends observed in NEM when measured using DIC, but with different scales. These results suggest a general trend towards more carbon release when the aerators were turned off. NEM values are plotted alongside NEM/NPP measurements from other methods in Figures 14 and 15.

Unlike our DIC metabolism analysis, GPP as measured using DO changes did not contradict our assumptions. When the aerators were turned off, we observed increases in GPP rates at stations 2, 4, and 7 in 2017 and at station 7 in 2018. Conversely, we observed decreases in GPP rates at station 1 in 2017 and at stations 1 and 2 in 2018. The highest GPP rate observed was at station 4 in 2017 with the aerators off with a value of 1535.71 mM C/m^2/day The lowest GPP value was observed at station 1 in 2018 when the aerators were off with a value of 12.73 mM C/m^2/day. Daily GPP values are plotted on Figures 16 and 17.

Like GPP, DO-based respiration values adhered to our hypotheses regarding the impact of aeration on metabolic rates. Respiration rates ranged between 2035.09 mM C/m2/day at station 4 in 2017 when the aerators were off to 241.19 mM C/m2/day at station 1 in 2018 when the aerators were off. The magnitude of respiration increased at most stations when the aerators were turned off. Respiration rates increased at all stations except for station 1 in 2017 and station 1 in 2018, suggesting a general trend towards less carbon release at night. Daily R values are plotted on Figures 18 and 19.

GPP:R ratios are summarized on Table 10 and represented graphically in Figure 15. When examining GPP:R to evaluate the balance of production and respiration, we observed a shift towards heterotrophy at all stations in both 2017 and 2018 when the aerators were turned off (i.e., GPP:R decreased). Furthermore, nearly all stations were either autotrophic (GPP:R >1) or nearly auototrophic when the aerators were on, and all stations were heterotrophic when the aeration system was off. The highest GPP:R value was measured at station 7 in 2018 when the aerators were on (1.98) and the lowest value was measured at station 1 in 2018 when the aerators were off (0.053).

Photosynthetron Metabolism-DO

We were unable to fit a P-I curve model (equations 1 or 2 to station 1 in 2017 when the aerators were off as the points did not exhibit the typical shape of a PI curve (See Appendix B). Individual bottle rates at this station were relatively high at 2.57 mgO_2/L/hr on average. All other stations were successfully fit to either the Jassby and Platt (1976) model of the Eilers and Peeters (1988) model. The PI curve for Station 2 in 2018 when the aerators were on was fit using the Jassby and Platt (1976) model. All other stations were fit with the Eilers and Peeters (1988) Model. A sample PI curve is shown in Figure 5. Model fits and equation parameters can be found in Appendix B.

The highest water column NPP rate observed in the photosynthetron method was 223.60 $\pm$ 33.46 mM C/m^2/day at station 7 in 2017 with the aerators off. The lowest NPP rate observed was -303.38 $\pm$ 29.39 mM C/m^2/day at station 7 in 2017 with the aerators on. NPP increased when the aerators were turned off at all stations in both years except for station 1 in 2018. We cannot comment on the change to NEM at station 1 in 2017 due to the lack of an appropriate PI curve when the aerators were off.

The highest GPP observed was 527.83 mmol C/m^2/day at station 7 in 2017 with the aerators on. The lowest rate observed was found at station 1 in 2018 when the aerators on with a value of 35.30 mmol C/m^2/day. Similar to NEM, we cannot comment on the magnitude of GPP at station 1 in 2017 when the aerators were off nor can we comment on its response to aeration, as GPP is derived from NPP. Otherwise, we observed increases in GPP at stations 1 and 2 in 2018 and decreases in GPP at station 7 in both 2017 and 2018.

Respiration values ranged between 9.16 mmol C/m^2/day at station 1 in 2017 with the aerators on to 1080.57 mmol C/m^2/day at station 7 in 2017 with the aerators on. In response to the aeration system being turned off, respiration rates increased in magnitude at station 1 in 2017 and 2018. Respiration rates decreased in magnitude at stations 2 and 7 in both 2017 and 2018. Values can be found in Table 9C and are represented in Figures 18 and 19.

According to GPP to R ratios, we observed an autotrophic shift at all stations where we could observe changes in the photosynthetron method. The water column was autotrophic (GPP:R>1) at station 7 in 2017 when the aerators were on and station 2 in 2018 when the aerators were off. The water column was heterotrophic (GPP:R<1) at all other stations. GPP:R values ranged from 0.33 at station 7 in 2018 when the aerators were on to 8.97 at station 1 in 2017 when the aerators were on. We cannot comment on the GPP:R ratio of station 1 in 2017 when the aerators were off due to the lack of a PI curve fit.

Figure 16 shows the relationship between DOC and R from our three methods and the strengths of these relationships are shown in Table 11. While we observed the expected increases in the magnitude of R in our methods (See Table 9 and Figures 18 and 19), these changes are not consistently accompanied by an increase in organic matter as we would anticipate. In many

cases, DOC actually decreased when the aerators were turned off, and all stations in 2018 saw

virtually no changes between the on and off states.

While originally measured as a means of constraining pCO_2, alkalinity results were

plotted against salinity values at the same time on Figure 10. This relationship was plotted

alongside an equation describing the relationship between alkalinity and salinity in the

Chesapeake Bay originally presented by Cai et al (2017). Our data appears to fit this relationship,

suggesting that alkalinity values in Rock Creek are typical for the Chesapeake Bay. Moreover,

alkalinity values do not change much by the aerator condition, suggesting salinity and/or

seasonality are more immediate influencers of alkalinity.

Statistical Analysis

At a 95% confidence interval, NEM as measured with DIC significantly correlated with

Active Chlorophyll, Pheophytin, and NH_4 (Table 11). Interestingly, we do not see significant

correlations between these analytes and planktonic activity. Instead, R as measured with DIC

significantly correlated with chlorophyll, pheophytin, and NH_4. It is important to note these

relationships exist despite the nonsensical points observed in 2018. Moreover, these are the only

analytes that correlate with metabolic activity. Overall, it is likely that nutrients do not exert a

very significant control on DIC metabolism in Rock Creek.

GPP as measured in the photosynthetron significantly correlated with salinity at a 95%

confidence interval, but with no other analyte. It is possible that this relationship is a result of the

large difference in salinity between 2017 and 2018. Furthermore, respiration measured in the

open water methods did not correlate with salinity. Otherwise, no metabolic data measured in the

photosynthetron correlated with any metric. Again, nutrients do not appear to control the

metabolism of the water column in Rock Creek.

Metabolic States

While GPP:R ratios in the open water DIC method are difficult to interpret, we can still comment on metabolic states by examining the NEM values, as they are representative of the overall change in DIC on a daily scale. At all stations in both 2017 and 2018, we observed a decrease in NEM when the aerators were turned off. NEM values were considerably lower in the summer of 2018 compared to the fall of 2017 (Table 9A). Station 7, located furthest from the aerators, in 2018 was the only scenario where we observed a negative NEM rate when the aerators were on and the only scenario where NEM values did not decrease in response to the aerators. While it is difficult to attribute the NEM shifts to changes in R or the changes in GPP (due to the nonsensical values of GPP and R in 2017), these changes are still consistent with our understanding of how the estuary should respond to aeration; heterotrophic shifts were observed in most cases.

Our observations of aerobic metabolism (i.e. Changes in DO) were also consistent with our understanding of ecosystem response to aeration; heterotrophic shifts were observed at all stations when aerators were turned off based on GPP:R values (Table 11). Presumably, this is due to the decomposition of excess phytoplankton biomass produced when phytoplankton are no longer mixed below the compensation depth, as we observed higher respiration rates at all but two stations in response to the aerators being turned off. Interestingly, the aerators also appear to control whether Rock Creek is heterotrophic or autotrophic in general, as all but two stations shifted from net autotrophy to net heterotrophy when the aerators were turned off. Again, this is consistent with our understanding of estuarine metabolism and the tidal nature of the system, as

the buildup of autochthonous carbon will encourage net heterotrophy through increased

respiration combined with previous evidence that aeration affects large spatial areas of Rock

Creek (Harris et al 2015). Furthermore, the activation energies of autotrophs are roughly half that

of heterotrophs (Harris et al 2006). Therefore, it is reasonable to conclude that it is easier to

suppress respiration (and decomposition, in this case) than it is to suppress primary production,

possibly explaining our results.

It is important to note that our results from the photosynthetron method measurements are

not representative of NEM and only indicate the metabolic activity of water column plankton

(which we call NPP here). Changes in NPP were consistent, showing increases at all stations and

dates that a PI curve could be fit. However, whether the water column was a net source or sink of

carbon was inconsistent. Planktonic activity (GPP) showed increases in the aerated portion of the

estuary when comparisons were possible, and decreases in the unaerated portion. GPP:R values

were consistent, suggesting a net autotrophic shift at all stations where comparisons were

possible, but did not match our hypotheses. While this data set is small, it meets some

expectations; we anticipated the increases in GPP:R when the aerators were off. Higher

phytoplankton activity is expected when the system stratifies and benthic nutrient cycling when

bottom water oxygen becomes low is hypothesized to increase remineralization of N and P.

We can examine our open water production rates compared to the trophic state

definitions proposed by Nixon (1995). If scaled to annual rates of carbon production, our

phytoplankton production rates suggest that virtually all stations are hypertrophic (carbon

production > 500 g m^{-2} yr^{-1}). While this is likely an overestimate, as daily summer rates would

likely be higher than other seasons, this exercise can still serve to place our stations, and Rock

Creek as a whole, into a trophic status. Rock Creek is likely eutrophic (at a minimum) on an annual basis.

Comparisons between methods

Net ecosystem metabolism considers production and consumption of organic material by all components of the system (water column, sediments, adjacent wetlands, benthic microalgae, submerged aquatic vegetation, etc). When comparing results between the open water DO method and the photosynthetron method, results were inconsistent. Water column production values (i.e., the photosynthetron measurements) suggested net autotrophy in all cases examined and suggested shifts towards autotrophy when the aerators were turned off more frequently than towards heterotrophy. In contrast, there was a clear, consistent shift towards heterotrophy when examining results in the open water DO method (Table 10), which captures NEM. Respiration values were not consistent between the two methods in terms of value and response to the aeration system. Direct comparison between the two methods is not entirely appropriate, as the open water method is a representation of NEM and is influenced by benthic (mostly bare sediment in Rock Creek) metabolism. However, both the open water measurements capture planktonic activity in the water column, so the difference between the two methods is (theoretically) due to benthic activity. It is unlikely that the sediment metabolism would account for the differences we observed between the open water method and the water column measurements. Differences between the two methods are often greater than a factor of 10, and previously measured sediment oxygen demand values (Testa, et al, unpublished) in Rock Creek are far smaller (Table 12).

Discrepancies in these observations are not unprecedented. Giordano et al (2012) reported divergent results when comparing open water metabolism measurements to a summation of individual components (plankton, SAV, benthic microalgae). In their analysis, Giordano et al (2012) attributed the differences to hydrodynamics and physics (which bottle measurements do not capture) and to the spatial and temporal scale differences between the methods. Gazeau et al (2005) observed higher estimates of net heterotrophy using an open water method compared to a bottle method, which is consistent with our observations (Table 10). Our methods are equally susceptible to these analytical issues. For this reason, it is likely that comparisons within one method (open water DIC vs open water DO) are appropriate, while comparisons between methods (open water DIC/DO vs photosynthetron DO) are inappropriate. While not performed here, it is worth noting that comparisons between DIC and DO changes in bottle methods are possible (e.g. Stokes 1996).

While the general trends in shifts in NEM in the open water methods (DO and DIC) are consistent, the magnitude of these changes are not. Both of these observations are to be expected; the metrics of DO and DIC capture different processes (e.g. DIC constrains all organic oxidation while DO does not constrain anaerobic processes as per Smith et al 1991)and exchange differently with the atmosphere, but the shift in NEM is observable in both cases. It is also noteworthy that these changes are independent of the distance to the aerators, confirming the ecosystem-wide influence of the aeration system observed by Harris et al (2015).

Open Water DIC Method; Evidence of Chemoautotrophy

In 2017 we observed nighttime decreases in DIC concentrations when the aerators were on at all stations. This observation initially contradicted our assumptions of how estuarine

metabolism functions; photosynthesis should not occur between dusk and dawn, when no sunlight is available, and only increases in DIC would be expected at night, analogous to respiration and production. However, Casamayor et al (2012) proposed that nighttime decreases in DIC concentration are possible within estuaries and indicative of chemoautotrophy, where inorganic carbon is fixed by metabolic processes not dependent upon sunlight. The occurrence of chemoautotrophy complicates our analysis as originally proposed.

Because chemoautotrophy does not depend upon sunlight, it readily occurs regardless of time of day. While a net decrease of DIC at night is indicative of chemoautotrophy, an increase in DIC at night is not indicative of a lack of chemoautotrophy. We can adapt our NEM equation to incorporate chemoautotrophy as follows:

$$27') \; NEM = GPP - R + CA$$

Where CA is chemoautotrophy, and all other variables mimic those found in the original equation 27. Our original methods depend upon nighttime changes indicating R and only R as a means to isolate this rate processes. Because chemoautotrophy affects DIC concentrations and can be coincident with photosynthesis and respiration, we cannot isolate R or chemoautotrophy using our open water methods. Instead, we can only confirm its presence in specific circumstances (i.e. when we observe carbon fixation at night), because the effects of R and chemoautotrophy on the DIC pool occur in opposing directions on the overall rate change. It is not appropriate to call the nighttime decrease we observed a chemoautotrophy rate, as respiration could also be occurring. In Rock Creek, it is unlikely that respiration rates would ever be zero considering the system's high organic loading and eutrophication (Caffrey 2004). Furthermore, we cannot accurately constrain photosynthesis or respiration if we have reason to believe chemoautotrophy is occurring, as there is no way to isolate either process with our open water

method alone. Constraining chemoautotrophy rates requires controlled bottle experiments that measure uptake of isotope labeled carbon with controls that inhibit photosynthesis (e.g. Lee et al 2015).

While we cannot ascribe a numeric rate to chemoautotrophy in 2017 when the aerators are on, we can reasonably assume that the rate is higher compared to when the aerators are off based on the magnitude of nighttime decreases observed. Therefore, it is possible that chemoautotrophy can be connected to the aerator status, as shown by the nonsensical values in Table 9A. In a study examining chemoautotrophy in the Chesapeake Bay, Lee et al (2015) observed the highest rates at the water column oxic/anoxic interface around the estuarine turbidity maximum. Chemoautotrophy is known to be encouraged by the simultaneous presence of oxidized and reduced compounds (Sorokin et al 1995, Casamayor 2010, Casamayor et al, 2012).

The primary goal of Rock Creek's aeration system is destratification. Therefore, it is possible that the aeration system homogenizes the water column in such a way that encourages interaction between oxidized and reduced compounds. It is also possible that chemoautotrophy is present in Rock Creek when the aeration system is off, but our collection techniques did not sample the oxic/anoxic interface, where rates would be highest. In Rock Creek, nitrification is a likely candidate for a prevalent chemoautotrophic process. Nitrification also relies on the simultaneous presence of various compounds and occurs at an oxic/hypoxic interface (Kemp et al 1990), and we would anticipate higher nitrification rates when the aerators are on. Should this chemoautotrophy represent higher rates of nitrification in the water column, there are impacts on the nitrogen cycle that would likely affect the hypoxic-eutrophic feedbacks in Rock Creek.

Because of our observations of chemoautotrophy and how it interferes with constraining individual components of NEM, we are reluctant to comment on the anaerobic respiration versus aerobic respiration of Rock Creek. Our inability to isolate any one process restricts our capability to accurately quantify all of them, similar to the problems with constraining chemoautotrophy mentioned above. Instead we can reasonably conclude that chemoautotrophy is a potential component of NEM in Rock Creek and should be considered in future experiments.

Estuarine Carbon Balance: Air-Sea Exchange

pCO_2 values suggest that Rock Creek is supersaturated at nearly every time point, regardless of aeration, and that there is a net flux of CO_2 from the water to the atmosphere (e.g. Figure 11). The calculations proposed by Crosswell et al (2017) were developed for an open water method but were not designed with engineered destratification in mind. It is outside the scope of this thesis to develop a comprehensive model for air-sea exchange under engineered destratification, and the model we propose rests on many simplifying assumptions. However, the scale of our measurements and estimates permits some interpretations in this regard. Regardless of the aerators, the chemistry of the water is such that there is a net flux from the water to the atmosphere. Furthermore, engineered destratification only acts to encourage air-sea exchange, which we have established to be directed out of the water in nearly every scenario. Therefore, while we are likely underestimating the magnitude of air-sea exchange of CO_2, we can have confidence in its directionality. From a carbon balance perspective, we can confirm that Rock Creek is a source of CO_2 to the atmosphere and this propensity is not altered by the aerators; only the magnitude of this exchange will change. While we would expect the carbon pool to eventually deplete and slowly become not super-saturated with respect to the atmosphere, our measurements still showed super saturation. This is only sustainable if there is a perpetual source

48

of allochthonous carbon to the system. The observation of super saturation is consistent with the global trend that estuaries significantly contribute to atmospheric CO_2 (Borges and Abril, 2011, Cai 2011). Furthermore, it is unlikely that any errors in the air-sea exchange under engineered destratification model we propose would change the general trends we observe in DIC-based metabolic measurements. Air sea exchange has been shown to be small in comparison to the overall changes in DIC observed in previous carbon balance analyses (Crosswell et al 2017).

NEM/NPP Insights: Chlorophyll

Table 13 shows metabolic rates normalized to surface chlorophyll values. This calculation was designed to unveil any potential connection between metabolic rates and standing stock phytoplankton biomass. However, these results are inconclusive. While NEM as measured with DIC significantly correlates with Active Chlorophyll (Table 11), the relationship is not strong (R^2=0.34). Furthermore, the significant relationship exists with GPP, but the correlation is negative and the relationship is not strong (R^2=0.33) the more accurate measurement of planktonic activity. A significant correlation does exist with R, but this relationship is also weak (R^2=0.35). When examining our other two methods, chlorophyll does not significantly correlate with any metabolic rate. We can reasonably conclude that chlorophyll levels do not have any significant causal relationship with metabolic data in Rock Creek during our sampling. Because we did not measure grazing by zooplankton, it is likely that our measurements missed a key aspect of the ecosystem that also contributes to standing stock biomass and has unknown relationships with the aerator conditions.

Chlorophyll values themselves showed a mix response to the aerators. We would expect to see higher surface chlorophyll values when the aerators were turned off, as stratification

allows phytoplankton to congregate in surface layers and prevents circulation below the critical zone depth. However, we did not observe this in 2017. Time series plots in 2017 when on (See Appendix C) suggest a bloom around noon time at all stations, which skew the standard deviations of chlorophyll values accordingly. This bloom occurs during a period of N limitation, but a similar bloom is not observed when the aerators are turned off and surface waters remain N limited. Furthermore, the time of this bloom is not coincident in time to our nutrient sampling. While we cannot pinpoint an exact reason for this bloom, the fact that it occurred when the aerators were on (the opposite of our expectations) it is reasonable to assume that the aerators are not responsible. Furthermore, we did not observe consistent shift in light attenuation coefficients in 2017(Figure 7), so it is unlikely to explain the bloom either. While the aeration system appears to impact the metabolism of Rock Creek, it does not appear to impact chlorophyll concentrations in a similar manner.

Proximate Causes of Metabolic Shifts: Nutrients and Physics

The N:P ratios at all stations and dates suggest N limitation (N:P<16) in surface waters in the aerated portion of the estuary in fall 2017 (Table 6 and Figure 10). In summer 2018, P limitation (N:P>16) was more common in the aerated portion of the estuary. Salinity values in Summer 2018 were lower, which often coincides with a shift to P limitation. The summer 2018 data contradicts the historical precedent that coastal systems are generally N limited (Nixon, 1995, Paerl et al, 1999, Howarth and Marino 2006). However, this tendency is only true when considering chemistry and physics along the estuarine gradient and does not consider how human activity can influence the ratios (Dortch and Whitledge 1992, Conley 2000, Sylvan et al 2006). Considering the high land development of the Rock Creek watershed (Maryland Department of Planning, 2010) and the estuary's downstream location from Baltimore, MD, this

is possibility the case here. Moreover, the aerator status does not appear to consistently effect N:P values (Table 6). Surface values in the aerated portion of the estuary maintain their nutrient limitation when the aerators are turned off, but bottom concentrations change variably.

The dual nutrient dependency of the Chesapeake Bay (Paerl et al 2004, Paerl 2009) suggests that both N and P species can influence the phytoplankton activity in the Bay. However, neither N species nor P species significantly correlate with NEM/NPP or GPP in our metabolism analyses (the exception being NH_4 in the open water DIC NEM rate, but the relationship is not strong, $r^2 = 0.41$). Similarly, contrasting particulate forms (Part-N and Part-P) and dissolved forms (TDN and TDP) does not provide insights (Table 11). However, as previously mentioned, we observed a consistent response to the aerators towards autotrophy. Phytoplankton productivity is susceptible to multiple limitation factors, including physical parameters (Boynton et al 1982, Heip et al 1995). The aerators alter the light climate of phytoplankton in Rock Creek through destratification, but not by changing the light attenuation, as we did not observe consistent changes in kd values (Figure 7). While it is likely that nutrients are affecting metabolism in Rock Creek, the effects are either unknowingly synergistic, nonlinear, and/or masked by the effects of the aerators. Liebig's law of the minimum suggests that the most limiting resource ultimately controls a rate process like primary productivity. The lack of correlation between metabolism and nutrient correlations may also be due to nutrient saturation. Dissolved nitrogen concentrations above 10 μM (which we observed at all stations and dates-see Table 5) are super-saturating and effectively force P limitation (Malone et al, 1996). This occurrence would make observing linear relationships between nutrients and metabolic rates difficult. High concentrations of NH_4 can also suppress metabolism above certain thresholds (Daganais – Bellfeuille and Morse 2013).

Resilience of the Hypoxic-Eutrophic Feedback

Figure 4 shows how water column oxygen concentrations decrease when the aerators are turned off. This ecosystem wide trend towards hypoxia is accompanied by a consistent heterotrophic shift when metabolism is measured using changes in DO (Table 10). This trend speaks to the strong resilience of the hypoxic eutrophic feedback and the intrinsic link between eutrophication and hypoxia (Nixon 1998, Howarth et al 2011). While oxygen concentrations changed in response to the aerators, Rock Creek was perpetually eutrophic during our sampling. The resilience of eutrophication is well documented (Duarte et al 2009). This tendency is perhaps most striking when considering the dates on which we sampled in 2017; Anne Arundel County turns off the aeration system at the beginning of October each year, and it is turned back on in the following April. The only time the aerators are turned off otherwise are for our sampling, so the time between April and October on any year represents the longest period of time that the aerators are operational. Despite six months of near continuous operation, the system returns to a heterotrophic and hypoxic state in only 3 days (Table 10 and Figure 4).

CONCLUSIONS

Our measurements provide meaningful insight to how engineered destratification influences metabolism in shallow estuaries. When the aerators were turned off, measurements of NPP and NEM adhered to expectations in most cases. Respiration rates increased in magnitude at most stations using the open water methods. The expected shift towards heterotrophy in response to the aerators was observed at all stations. We observed divergence in results between methods, a result that is not without precedent. Nutrient limitation varied by station and year, and nutrients did not exhibit meaningful relationships with metabolic rates. Overall, our experiments reaffirm the ecosystem-wide effects of aeration established in Harris et al (2015). Secondly, we have reaffirmed the notion that DIC based measurements are more comprehensive (Smith et al 1991), and have unveiled chemoautotrophy in Rock Creek. Thirdly, we have shown just how strong the resilience of eutrophication (Duarte et al 2009) and its effect on the hypoxic-eutrophic feedback is through comparative experimentation within the same system. Our results suggest that the physics associated with the aeration system itself have a larger influence on metabolism compared to nutrients in this highly enriched system.

Future work should strive to expand upon the initial findings of this thesis. Dedicated experiments to constrain chemoautotrophy would provide concrete evidence of its existence regardless of NEM, and provide numeric rates on which statistical analysis could be performed. Increased resolution of DIC measurements, particularly in the oxycline, would constrain chemoautotrophy regardless of aerator status. While cumbersome to develop and implement, an appropriate air-sea exchange model that accounts for aeration would provide more accurate NEM measurements. Diel nutrient measurements, parallel to metabolic data, may establish a relationship between nutrients and NEM not seen in this thesis.

Tables

Table 1: Dates on which collection cruises took place. Sampling started and ended on dawn of their respective days.

Year	Aerators On Dates		Aerators Off Dates	
	Start	End	Start	End
2017	September 28, 2017	September 29, 2017	October 2, 2017	October 3, 2017
2018	July 9, 2018	July 10, 2018	July 16, 2019	July 17, 2019

Table 2: Checklist of when metabolic sampling occurred in 2017 and 2018. A check indicates that sampling took place while an X indicates sampling did not take place.

Station	In Situ DIC	In Situ DO	Photosynthetron
		2017	
1	✓	✓	✓
2	✓	✓	X
4	✓	✓	X
7	✓	✓	✓
		2018	
1	✓	✓	✓
2	✓	✓	✓
4	X	X	X
7	✓	✓	✓

Table 3: Coefficient values used in Equation 14 as per Bensen and Krause's (1984) DO air-sea exchange calculation. All values are unitless.

Coefficient	Value
A1	-135.3
A2	1.572288E+05
A3	-6.637149E+07
A4	1.243678E+10
A5	8.621061E+11
B1	0.020573
B2	-12.142
B3	2363.1

Table 4: Physical Data at each station in 2017 and 2018. Temperature and salinity values listed here were taken from the second dawn of each sampling day.

Station	Temperature (°C)				Salinity				kd		Average Daylight PAR (uE/m2/sec)		Daylight Hours (hr)		Pycnocline Depth (m)		Total Depth (m)
	Aerators On		Aerators Off		Aerators On		Aerators Off		Aerators On	Aerators Off	Aerators On	Aerators Off	Aerators On	Aerators Off	Aerators On	Aerators Off	
	Surface	Bottom	Surface	Bottom	Surface	Bottom	Surface	Bottom									
2017																	
1	23.63	23.53	20.39	20.91	9.65	9.57	12.24	14.15	5.5	3.73	911.44	869.7	11.85	11.85	None	0.75	2.8
2	24.08	24.05	19.86	20.87	10.02	10.01	12.25	14.21	3.28	4	911.44	869.7	11.85	11.85	None	0.75	3.2
4	24.14	24.27	20.12	20.83	10.11	10.2	12.57	14.27	3.23	4.39	911.44	869.7	11.85	11.85	2.75	1	4
7	23.88	23.86	19.94	21.29	10.41	10.41	12.42	15.14	2.19	2.14	911.44	869.7	11.85	11.85	3.25	0.75	3.5
1	23.63	27.1	20.39	26.77	5.01	5.06	5.21	5.72	5.9	2.22	1090.6	688.09	14.75	14.6	None	0.75	2.8
2	27.1	27.2	27.33	27	5.13	5.16	5.09	5.71	4.23	2.05	1090.6	688.09	14.75	14.6	None	0.75	3.2
7	27.4	26.9	27.77	26.91	5.31	5.33	5.6	5.83	1.76	3.74	1090.6	688.09	14.75	14.6	2.5	1.75	3.5

Table 5: Nutrient Data for all stations in 2017 and 2018. Table 4A shows all nitrogen data while Table 4B shows all Phosphorus data. N.D. represents no data available.

A

Station	NH4 (µmol) On Surface	NH4 On Bottom	NH4 Off Surface	NH4 Off Bottom	NO23 (µmol) On Surface	NO23 On Bottom	NO23 Off Surface	NO23 Off Bottom	TDN (µmol) On Surface	TDN On Bottom	TDN Off Surface	TDN Off Bottom	Part-N (µmol) On Surface	Part-N On Bottom	Part-N Off Surface	Part-N Off Bottom
2017																
1	10.35	11.71	2.14	9.85	13.71	13.99	8.28	10.71	81.39	85.67	132.08	54.97	105.66	114.94	177.77	54.97
2	10.14	10.78	4.00	0.92	11.99	9.85	9.42	10.92	103.52	76.39	94.95	46.41	122.80	92.10	130.65	33.56
4	5.07	5.43	3.78	8.07	6.79	5.11	9.35	10.42	115.66	42.84	65.68	44.98	139.22	41.41	95.67	22.92
7	2.21	8.78	2.57	6.14	2.13	2.19	8.42	9.50	40.69	34.27	37.84	42.12	41.19	33.70	28.13	32.27
2018																
1	4.64	7.35	0.43	7.28	12.92	11.35	8.35	4.23	43.55	48.55	34.27	32.13	21.28	24.70	35.41	14.85
2	2.21	4.07	0.43	3.93	8.50	6.53	3.06	0.97	37.84	37.84	23.56	29.27	27.77	22.92	10.42	11.28
7	0.29	2.36	0.43	6.14	0.48	1.46	3.31	2.30	23.56	24.99	25.70	30.70	27.49	24.27	23.20	19.99

B

Station	PO4 (µmol) On Surface	PO4 On Bottom	PO4 Off Surface	PO4 Off Bottom	TDP (µmol) On Surface	TDP On Bottom	TDP Off Surface	TDP Off Bottom	Part-P (µmol) On Surface	Part-P On Bottom	Part-P Off Surface	Part-P Off Bottom
2017												
1	2.34	2.26	6.89	0.97	5.28	5.69	12.00	2.53	5.17	6.33	8.72	4.16
2	3.29	1.96	3.97	0.56	6.88	4.47	7.99	1.42	4.39	3.91	5.94	2.81
4	3.34	0.28	2.33	0.51	8.13	1.18	5.25	1.24	4.91	2.86	7.43	3.49
7	0.13	0.13	0.33	0.71	0.56	0.50	1.18	1.10	1.76	1.91	1.36	4.36
2018												
1	0.15	0.20	0.29	2.44	0.53	0.60	0.88	2.96	1.48	3.52	1.29	2.52
2	0.13	0.12	0.05	1.36	0.60	0.54	0.29	1.66	1.67	1.89	1.94	1.34
7	0.05	0.12	0.15	0.08	0.38	0.37	0.47	0.28	1.31	2.06	1.26	1.69

Table 6: Molar N to P ratios at each station and depth. Values were calculated by dividing the summation of molar N in NH_4 and NO_{23} by the molar P in PO_4. N-limited waters are indicated in green and P-limited waters are indicated in white.

Station	On		Off	
	Surface	Bottom	Surface	Bottom
2017				
1	10.29	11.39	1.51	21.30
2	6.72	10.55	3.38	36.05
4	3.55	37.95	5.64	36.25
7	32.79	82.90	33.06	22.01
2018				
1	113.33	91.96	30.56	4.72
2	85.05	91.16	67.39	3.59
7	13.91	31.13	24.65	104.57

Table 7: DOC data from each station in 2017 and 2018. N.D. represents no data available.

Station	DOC (mmol)			
	On		Off	
	Surface	Bottom	Surface	Bottom
2017				
1	5.39E-01	5.67E-01	9.72E-01	3.30E-01
2	6.46E-01	5.00E-01	6.30E-01	2.71E-01
4	8.53E-01	2.72E-01	4.50E-01	2.71E-01
7	3.24E-01	3.41E-01	3.03E-01	N.D.
2018				
1	2.56E-01	2.63E-01	2.87E-01	2.43E-01
2	2.79E-01	2.65E-01	2.56E-01	2.48E-01
7	2.73E-01	2.56E-01	2.79E-01	2.38E-01

Table 8: Average Chlorophyll and Pheophytin data for surface and bottom waters in 2017 and 2018 at each station. Values represent an average of all values measured at that station and depth over the sampling day. Time series plots of chlorophyll and pheophytin can be found in Appendix C.

A

	Active Chlorophyll (µg/L)			
	On		Off	
Station	Surface	Bottom	Surface	Bottom
	2017			
1	300.50 ± 173.33	187.81 ± 72.85	143.95 ± 62.01	68.85 ± 21.49
2	206.13 ± 124.04	142.73 ± 28.41	109.04 ± 71.55	68.64 ± 30.81
4	132.67 ± 39.16	77.79 ± 40.12	73.41 ± 40.36	46.07 ± 4.40
7	61.29 ± 7.83	46.92 ± 3.65	31.74 ± 2.75	31.07 ± 9.64
	2018			
1	30.46 ± 18.04	37.4 ± 20.07	122.84 ± 88.41	7.08 ± 1.02
2	32.50 ± 20.12	79.64 ± 42.51	78.23 ± 46.64	33.90 ± 38.45
7	16.13 ± 2.46	31.09 ± 13.16	51.16 ± 31.59	50.45 ± 9.64

B

	Pheophytin (µg/L)			
	On		Off	
Station	Surface	Bottom	Surface	Bottom
	2017			
1	88.11 ± 55.17	82.38 ± 18.07	71.41 ± 28.24	48.8 ± 7.92
2	81.75 ± 38.89	67.67 ± 22.69	49.06 ± 23.45	49.68 ± 15.29
4	56.83 ± 14.44	51.63 ± 25.60	40.27 ± 16.04	43.35 ± 4.31
7	27.64 ± 3.49	24.85 ± 6.48	25.34 ± 8.49	42.84 ± 11.12
	2018			
1	17.66 ± 7.41	20.63 ± 2.57	4.17 ± 1.08	8.90 ± 3.15
2	18.89 ± 5.35	18.65 ± 4.14	7.09 ± 1.36	10.12 ± 1.71
7	8.65 ± 1.11	10.07 ± 1.52	17.57 ± 10.10	12.30 ± 3.83

Table 9: Summary table of metabolic data. Table 6A shows metabolic data as measured by DIC in the open water method. Table 6B shows metabolic data as measured by DO in the open water method. Table 6C shows metabolic data as measured by the bottle method in the photosynthetron. N.D. represents no data available. No fit indicates that the data taken could not be appropriately fit to a model.

A

	Open Water DIC					
	NEM (mmol C/m2/day)		GPP (mmol C/m2/day)		R (mmol C/m2/day)	
Station	Aerators On	Aerators Off	Aerators On	Aerators Off	Aerators On	Aerators Off
Fall 2017						
1	683.66 ± 47.36	-43.01 ± 13.31	156.59 ± 15.59	365.25 ± 66.13	527.06 ± 62.94*	-408.26 ± 52.81
2	936.62 ± 0.94	-13.08 ± 10.43	-237.90 ± 2.99*	303.00 ± 22.91	1174.52 ± 3.92*	-316.08 ± 12.48
4	1336.43 ± 17.87	-10.17 ± 5.61	-764.80 ± 12.76*	405.73 ± 34.68	2101.23 ± 30.63*	-415.91 ± 29.08
7	763.39 ± 36.15	47.35 ± 24.51	-90.45 ± 26.05*	160.77 ± 25.50	853.83 ± 62.20*	-113.42 ± 50.00
Summer 2018						
1	3.96 ± 4.35	-23.92 ± 8.76	202.06 ± 0.66	218.29 ± 0.57	-198.1 ± 3.69	-242.21 ± 8.19
2	40.96 ± 11.29	-60.99 ± 3.66	341.72 ± 35.10	486.45 ± 18.45	-300.75 ± 46.38	-547.44 ± 22.11
7	-86.74 ± 9.66	-74.3 ± 0.19	483.59 ± 9.40	689.75 ± 4.99	-570.33 ± 0.26	-764.05 ± 5.18

B

	Open Water DO					
	NEM (mmol C/m2/day)		GPP (mmol C/m2/day)		R (mmol C/m2/day)	
Station	Aerators On	Aerators Off	Aerators On	Aerators Off	Aerators On	Aerators Off
Fall 2017						
1	-37.22	-151.68	728.74	182.74	-765.96	-334.42
2	-27.55	-374.36	600.58	1093.80	-628.13	-1468.17
4	102.11	-499.37	635.06	1535.71	-532.95	-2035.09
7	306.45	-158.81	717.26	819.62	-410.81	-978.43
Summer 2018						
1	94.50	-228.46	485.59	12.73	-391.09	-241.19
2	73.38	-712.02	639.49	306.19	-566.11	-1018.21
7	305.94	-232.97	617.78	697.30	-311.84	-930.27

C

	Photosynthetron-DO					
	NPP (mmol C/m2/day)		GPP (mmol C/m2/day)		R (mmol C/m2/day)	
Station	Aerators On	Aerators Off	Aerators On	Aerators Off	Aerators On	Aerators Off
Fall 2017						
1	75.17 ± 32.51	No fit	82.22	No fit	9.16	310.62
2	NA	NA	N.A.	N.A.	N.A.	N.A.
4	NA	NA	N.A.	N.A.	N.A.	N.A.
7	-303.38 ± 29.39	223.60 ± 33.46	527.83	343.80	1080.57	156.25
Summer 2018						
1	-34.19 ± 4.31	-47.64 ± 11.18	35.30	77.40	90.34	162.54
2	-29.73 ± 8.47	119.43 ± 9.33	81.33	164.82	144.38	59.01
7	-231.74 ± 17.567	-44.91 ± 8.49	177.91	65.92	532.53	144.07

Table 10: Ratios between planktonic production (GPP) and respiration as measured by our three methods. Asterisks indicate values that were calculated with results that contradicted expectations (See results and Table 8). N.D. Indicates no data available.

| Station | GPP:R | | | | | |
| | In Situ DIC | | In Situ DO | | Photosynthetron DO | |
	Aerators On	Aerators Off	Aerators On	Aerators Off	Aerators On	Aerators Off
Fall 2017						
1	0.3*	0.89	0.95	0.55	8.97	N.D.
2	0.02*	0.96	0.96	0.75	N.D.	N.D.
4	0.36*	0.98	1.19	0.75	N.D.	N.D.
7	0.1*	1.42	1.75	0.84	0.49	2.20
Summer 2018						
1	1.02	0.90	1.24	0.05	0.39	0.48
2	1.14	0.89	1.13	0.30	0.56	2.79
7	0.85	0.90	1.98	0.75	0.33	0.46

Table 11: Correlation coefficients for relationships between metabolic data and abiotic and biotic factors. Significant results at a 95% confidence level are indicated in yellow. Plots for correlations can be found in Appendix D.

	Temperature		Salinity		kd	
	Coeffiecient	R-Squared	Coeffiecient	R-Squared	Coeffiecient	R-Squared
NEM-DIC	8.37	0.00	43.80	0.09	7.88	0.00
GPP-DIC	19.54	0.03	-37.05	0.11	11.83	0.00
R-DIC	-11.18	0.00	80.86	0.10	-3.94	0.00
NEM-DO	23.43	0.06	-10.71	0.01	-0.09	0.00
GPP-DO	-25.95	0.04	60.79	0.28	79.33	0.08
R-DO	49.37	0.01	-71.50	0.14	-79.42	-0.04
NPP-Photosynthetron	-16.51	0.09	12.48	0.05	18.07	0.03
GPP-Photosynthetron	-13.68	0.07	39.73	0.50	-57.82	0.32
R-Photosynthetron	-1.08	0.00	-28.55	0.08	96.92	0.21

	Active Chl-a		Pheophytin		DOC	
	Coeffiecient	R-Squared	Coeffiecient	R-Squared	Coeffiecient	R-Squared
NEM-DIC	6.21	0.34	12.92	0.40	913.90	0.22
GPP-DIC	-4.74	0.33	-9.25	0.34	-742.10	0.24
R-DIC	10.95	0.35	22.17	0.39	1656.00	0.24
NEM-DO	-0.65	0.01	1.88	0.02	10.03	0.00
GPP-DO	-3.50	0.17	0.84	0.00	-7.60	0.00
R-DO	2.85	-0.02	1.04	-0.08	17.63	-0.08
NPP-Photosynthetron	1.25	0.05	1.58	0.02	304.60	0.03
GPP-Photosynthetron	-0.11	0.00	3.31	0.07	6.20	0.00
R-Photosynthetron	0.66	0.01	-1.29	0.01	-6.89	0.00

Table 11-Continued: Correlation coefficients for relationships between metabolic data and abiotic and biotic factors. Significant results at a 95% confidence level are indicated in yellow Plots for correlations can be found in Appendix D.

	NH4		NO23		TDN		Part-N	
	Coeffiecient	R-Squared	Coeffiecient	R-Squared	Coeffiecient	R-Squared	Coeffiecient	R-Squared
NEM-DIC	91.72	0.41	19.48	0.03	6.27	0.25	3.59	0.18
GPP-DIC	-56.93	0.26	-20.80	0.05	-5.09	0.27	-2.75	0.18
R-DIC	148.65	0.36	40.28	0.04	11.37	0.27	6.34	0.19
NEM-DO	13.98	0.02	-6.60	0.01	0.12	0.00	-0.21	0.00
GPP-DO	27.53	0.06	10.81	0.01	0.67	0.00	0.98	0.02
R-DO	-13.55	-0.07	-17.41	-0.06	-0.55	-0.08	-1.19	-0.06
NPP-Photosynthetron	13.30	0.07	17.29	0.25	1.91	0.04	0.34	0.00
GPP-Photosynthetron	-7.67	0.02	-15.36	0.20	-0.82	0.01	-0.24	0.00
R-Photosynthetron	27.43	0.07	41.62	0.34	0.48	0.00	-0.06	0.00

	PO4		TDP		Part-P		N:P	
	Coeffiecient	R-Squared	Coeffiecient	R-Squared	Coeffiecient	R-Squared	Coeffiecient	R-Squared
NEM-DIC	52.68	0.06	40.50	0.11	30.68	0.03	-4.37	0.10
GPP-DIC	-44.28	0.07	-33.20	0.13	-20.61	0.02	2.26	0.05
R-DIC	96.97	0.06	73.71	0.13	51.29	0.03	-6.63	0.08
NEM-DO	-18.58	0.02	-8.87	0.01	-31.34	0.08	0.54	0.00
GPP-DO	8.18	0.00	10.73	0.01	46.00	0.10	-3.02	0.08
R-DO	-26.76	-0.07	-19.60	-0.06	-77.34	0.09	3.56	-0.02
NPP-Photosynthetron	66.37	0.09	32.32	0.10	31.81	0.06	0.67	0.02
GPP-Photosynthetron	-43.23	0.04	-17.12	0.03	-18.73	0.02	-1.33	0.08
R-Photosynthetron	8.06	0.00	6.58	0.01	9.77	0.01	1.33	0.08

Table 12: The highest sediment oxygen demands measured by Testa et al (unpublished) from 2016 to 2018 at all stations in Rock Creek. While the measurements were originally made in terms of oxygen concentrations, they were converted to carbon units with a photosynthetic quotient of 1 to be comparable to our results.

Station	Rate (mM C/m2/day)	Date	Aerators
1	-56.56 ± 6.41	7/12/2016	On
2	-41.75 ± 22.57	7/10/2018	On
4	-52.66 ± 6.88	7/12/2016	On
7	-21.88 ± 2.81	7/12/2016	On

Table 13: Chlorophyll normalized values of NEM/NPP and GPP for our three methods. Table 14A shows values for our Open water DIC method, Table 14B shows values for our open water DO method, and Table 14C shows values for our Photosynthetron method. Values were calculated by dividing the metabolic data found in Table 10 by the average surface chlorophyll values found in table 9.

A

Station	Open Water DIC			
	NEM (mmol C/m2/day/µg Chl-a/L)		GPP (mmol C/m2/day/µg Chl-a/L)	
	Aerators On	Aerators Off	Aerators On	Aerators Off
Fall 2017				
1	2.28	-0.30	0.52	2.54
2	4.54	-0.12	-1.15	2.78
4	10.07	-0.14	-5.76	5.53
7	12.46	1.49	-1.48	5.07
Summer 2018				
1	0.13	-0.19	6.63	1.78
2	1.26	-0.78	10.51	6.22
7	-5.38	-1.45	29.98	13.48

B

Station	Open Water DO			
	NEM (mmol C/m2/day/µg Chl-a/L)		GPP (mmol C/m2/day/µg Chl-a/L)	
	Aerators On	Aerators Off	Aerators On	Aerators Off
Fall 2017				
1	-0.12	-1.05	2.43	1.27
2	-0.13	-3.43	2.91	10.03
4	0.77	-6.80	4.79	20.92
7	5.00	-5.00	11.70	25.82
Summer 2018				
1	3.10	-1.86	15.94	0.10
2	2.26	-9.10	19.68	3.91
7	18.97	-4.55	38.30	13.63

C

Station	Photosynthetron-DO			
	NPP (mmol C/m2/day/µg Chl-a/L)		GPP (mmol C/m2/day/µg Chl-a/L)	
	Aerators On	Aerators Off	Aerators On	Aerators Off
Fall 2017				
1	0.25	N.D.	0.27	N.D.
2	N.D.	N.D.	N.D.	N.D.
4	N.D.	N.D.	N.D.	N.D.
7	-4.95	7.04	8.61	10.83
Summer 2018				
1	-1.12	-0.39	1.16	0.63
2	-0.91	1.53	2.50	2.11
7	-14.37	-0.88	11.03	1.29

Table 14: Air Sea Exchange values of each time interval. In 2017, dawn-noon and noon-dusk intervals were averaged together to generate the Dawn-Dusk interval values. Values are reported in mmol C/m2. Positive values indicate gas fluxes directed out of the water column.

	2017							
	Station 1		Station 2		Station 4		Station 7	
	Dawn-Dusk	Dusk-Dawn	Dawn-Dusk	Dusk-Dawn	Dawn-Dusk	Dusk-Dawn	Dawn-Dusk	Dusk-Dawn
Aerators On	46.31	93.21	16.62	20.78	3.69	5.03	1.95	1.87
Aerators Off	0.86	2.42	0.51	2.64	0.80	2.76	0.42	1.71
	2018							
	Station 1		Station 2		Station 4		Station 7	
	Dawn-Dusk	Dusk-Dawn	Dawn-Dusk	Dusk-Dawn	Dawn-Dusk	Dusk-Dawn	Dawn-Dusk	Dusk-Dawn
Aerators On	18.18	18.87	15.25	11.44	N.D.	N.D.	-0.14	0.33
Aerators Off	3.86	3.51	4.21	4.80	N.D.	N.D.	1.61	1.18

Figures
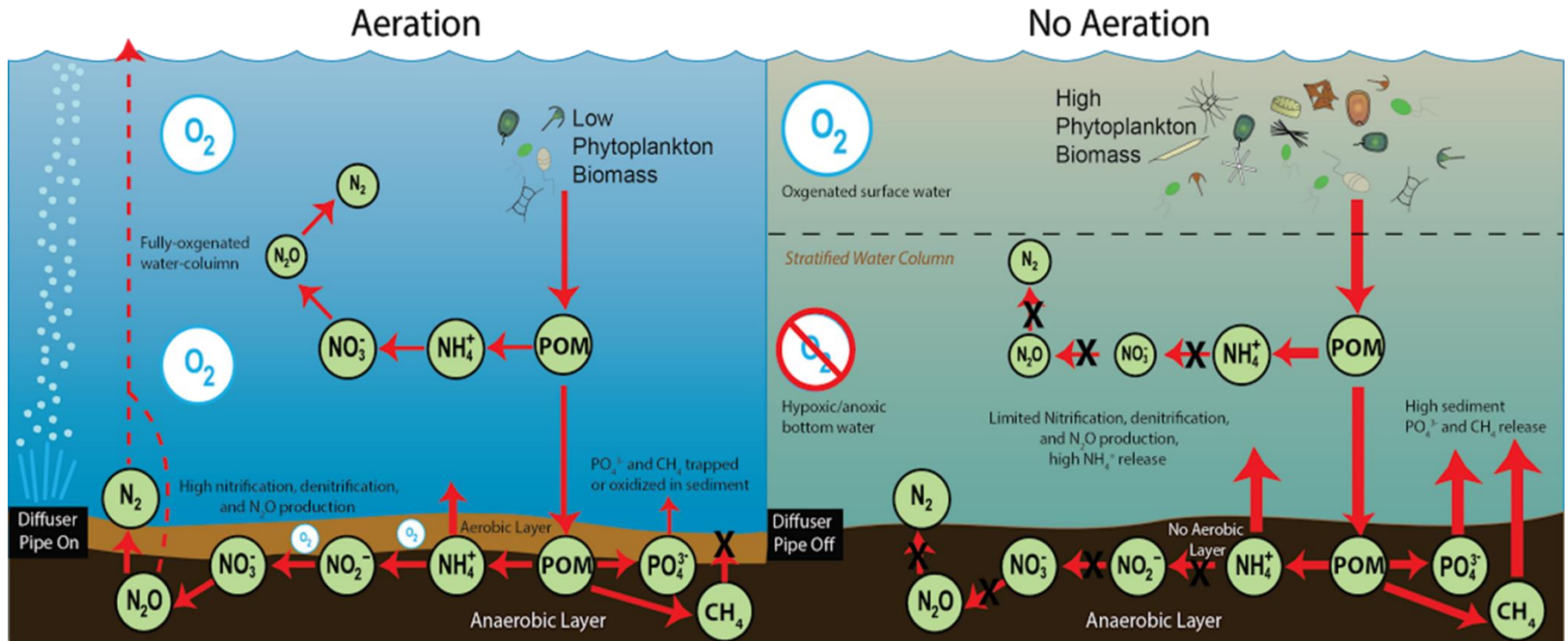
Figure 1: Theoretical effects of aeration in Rock Creek. When on, the water column is destratified, the phytoplankton biomass in the euphotic zone decreases, and the oxygen concentration in the water column increases. When off, the water column stratifies, phytoplankton biomass increases, and decomposition increases hypoxic volumes. Created by Dr. Laura Lapham.
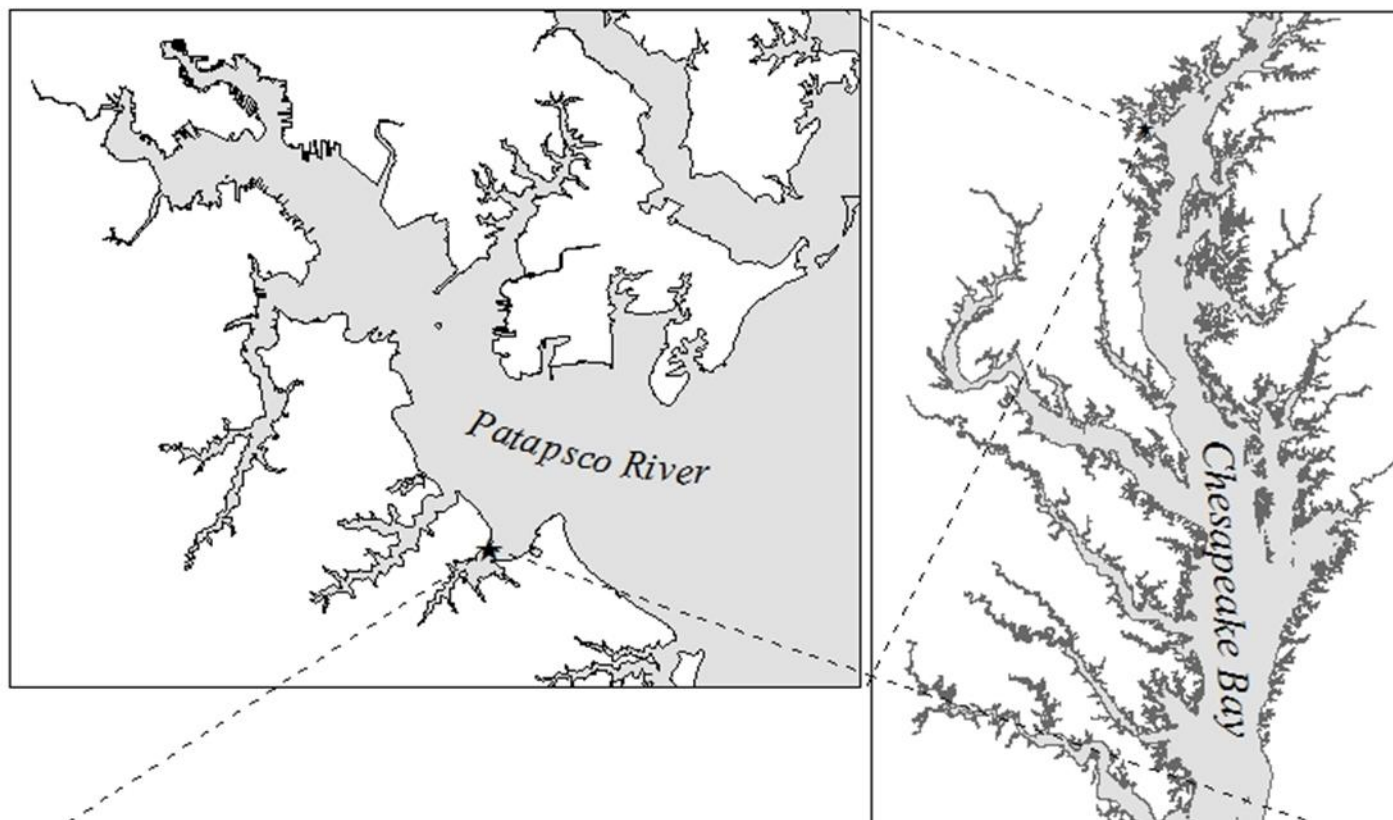
Figure 2: Map of Rock Creek within the Chesapeake Bay, denoted by the star.
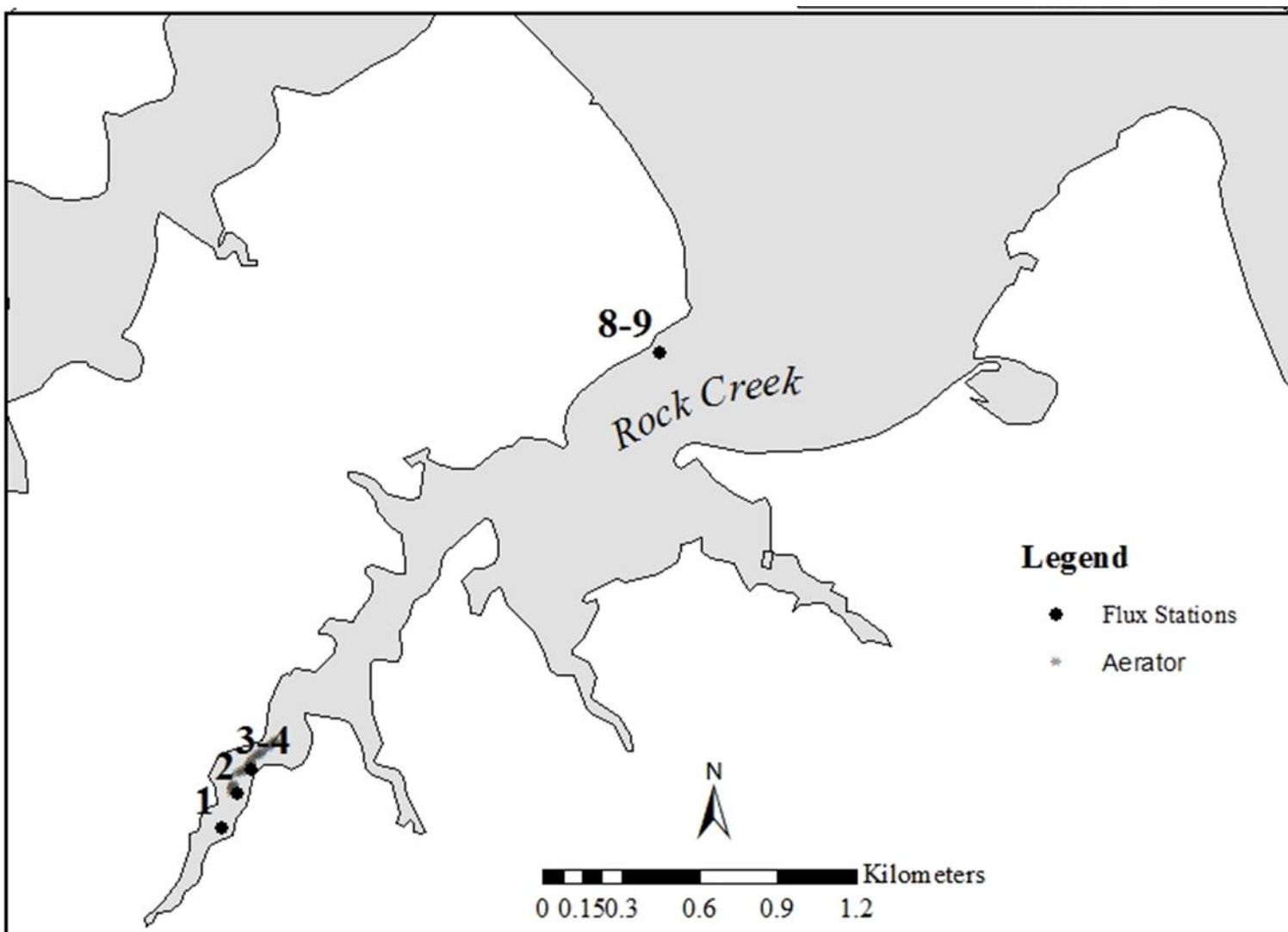
Figure 3: Map of sampling stations and aerators within Rock Creek
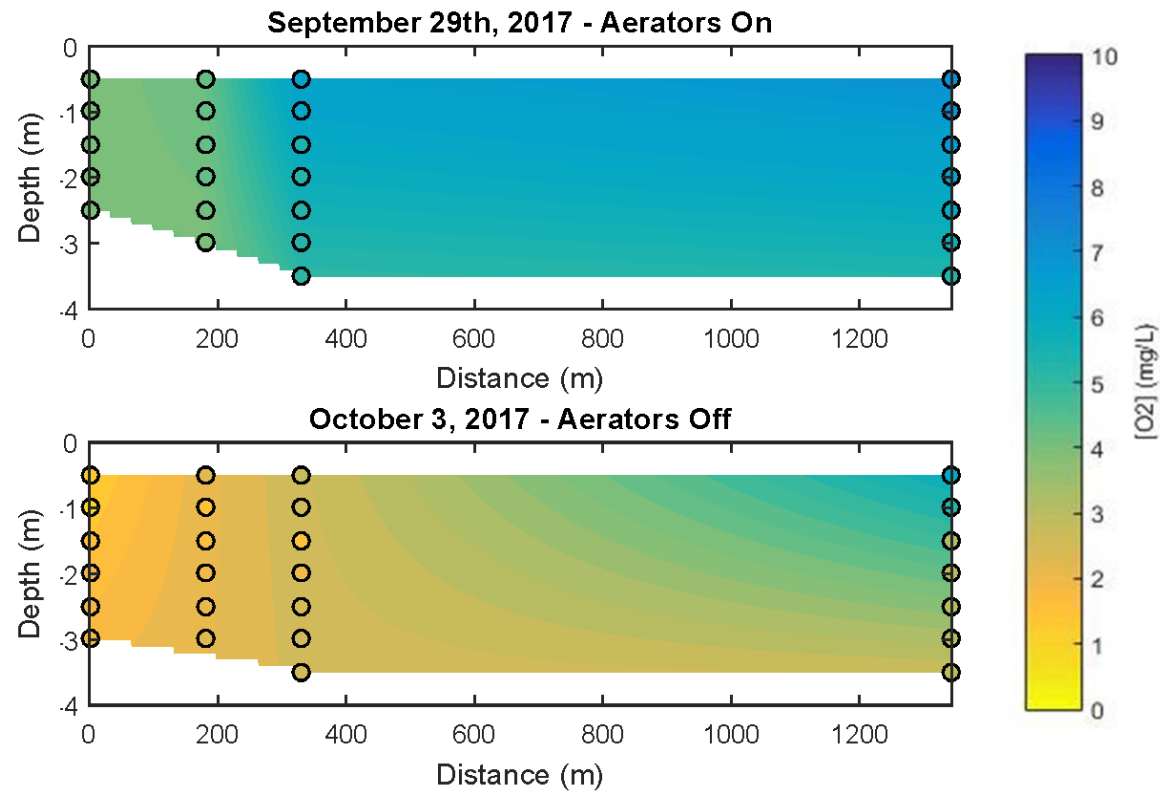
Figure 4: Sample oxygen profiles in Rock Creek in 2017 when the aerators were on and off interpolated between station measurements. When the aerators are turned off, oxygen decreases throughout the entire system. Station 1 is considered position 0 and all other stations are plotted according to their relative distance from station 1.
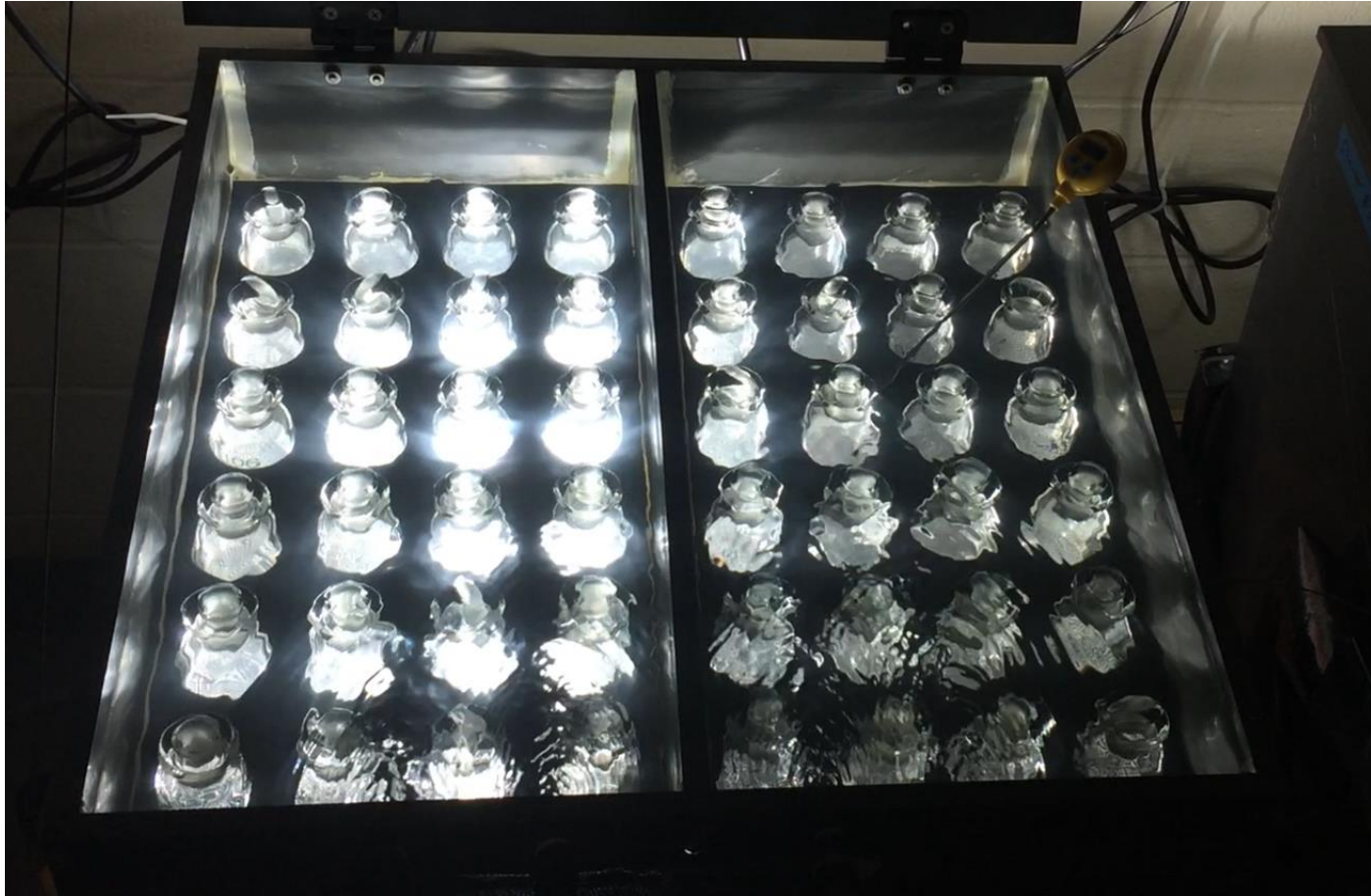
Figure 5: Picture of an operational photosynthetron. Each bottle is subjected to a different light level and cells were chosen to ensure each station was subjected to a gradient of light.
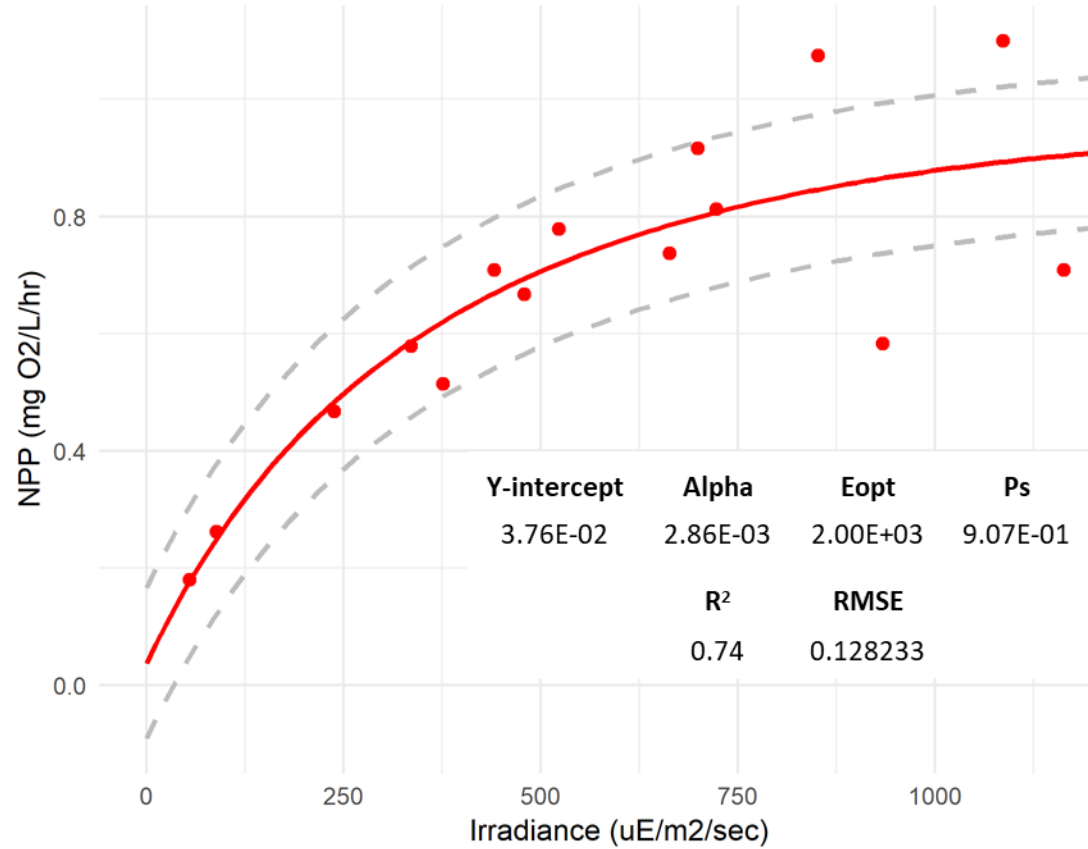
Figure 6: Sample P-I curve with equation parameters used for calculations. This particular curve was taken from station 7 in 2017 when the aerators were on and was fit using the Eilers and Peeters (1988) equation. The red dots represent the change in oxygen measured in the photosynthetron, the red line represents the equation of the model fit, and the dotted gray lines represent the RMSE of the model fit. All P-I curves can be found in Appendix B.
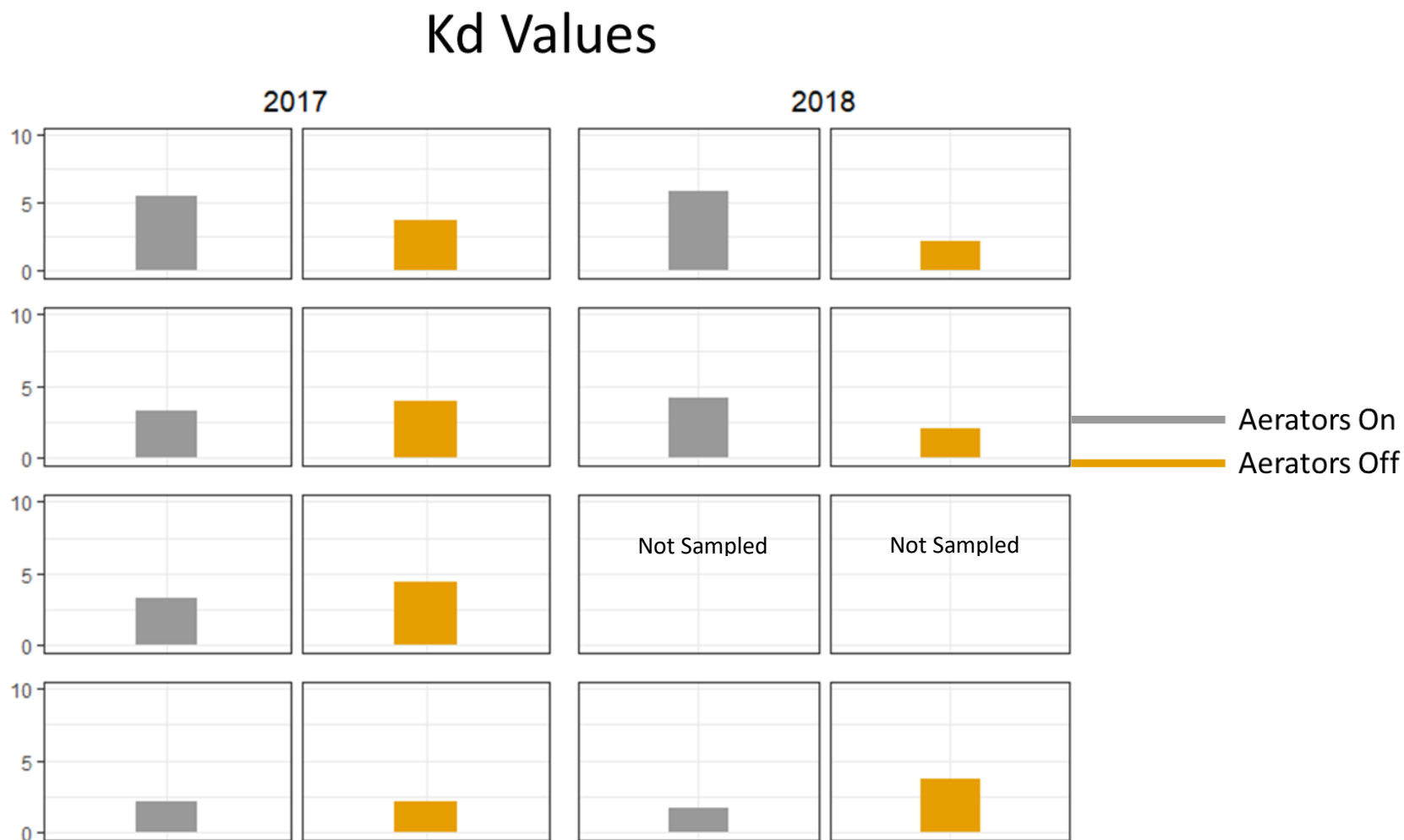
Figure 7: Light attenuation coefficient (kd) values at all stations in 2017 and 2018. No consistent change was observed when aerators were turned off in either year. Station 4 was not sampled in 2018. Kd values are in units of m^{-1}.
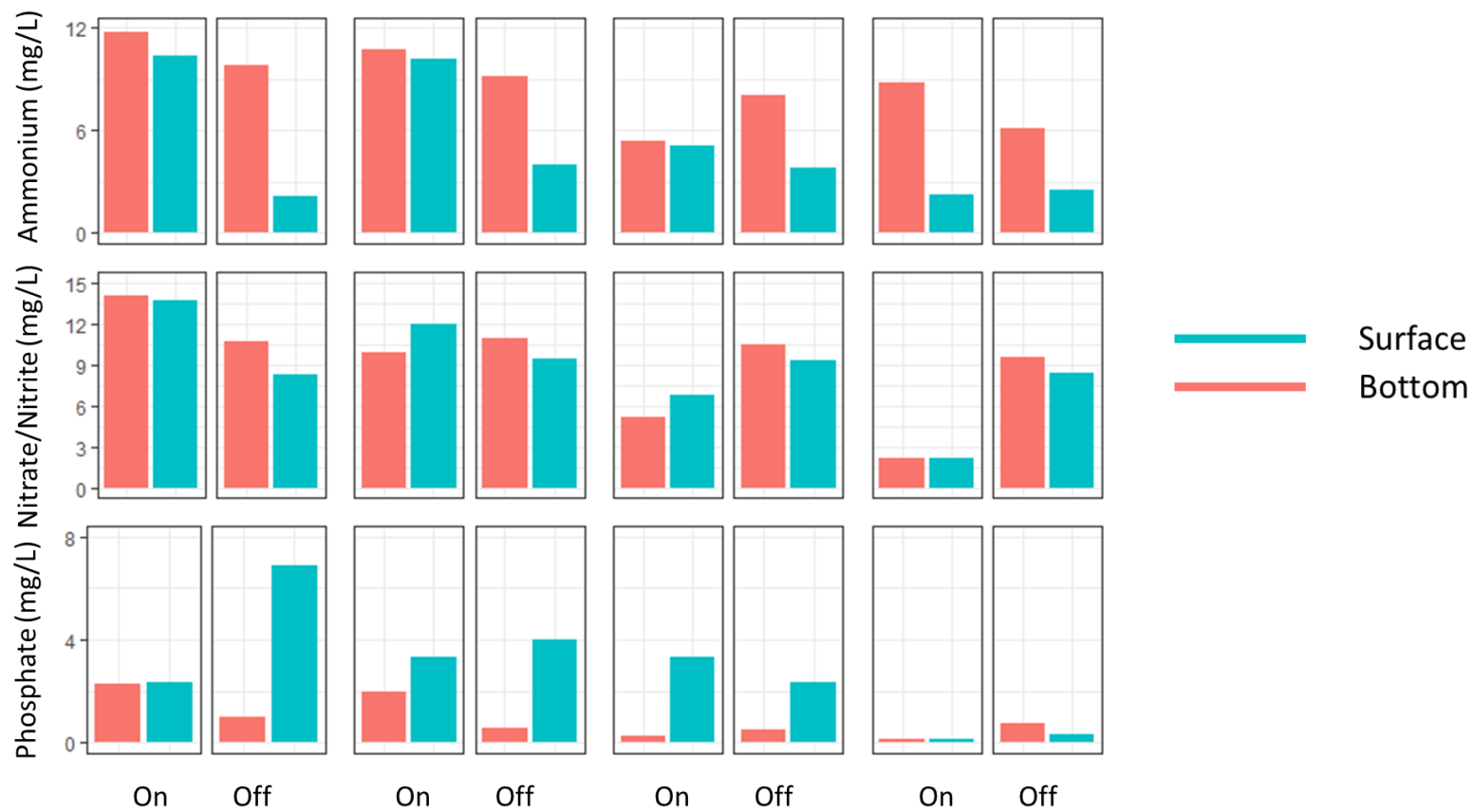
Figure 8:   Ammonium, Nitrate/Nitrite, and Orthophosphate values in 2017 at each station in the surface and bottom layers.
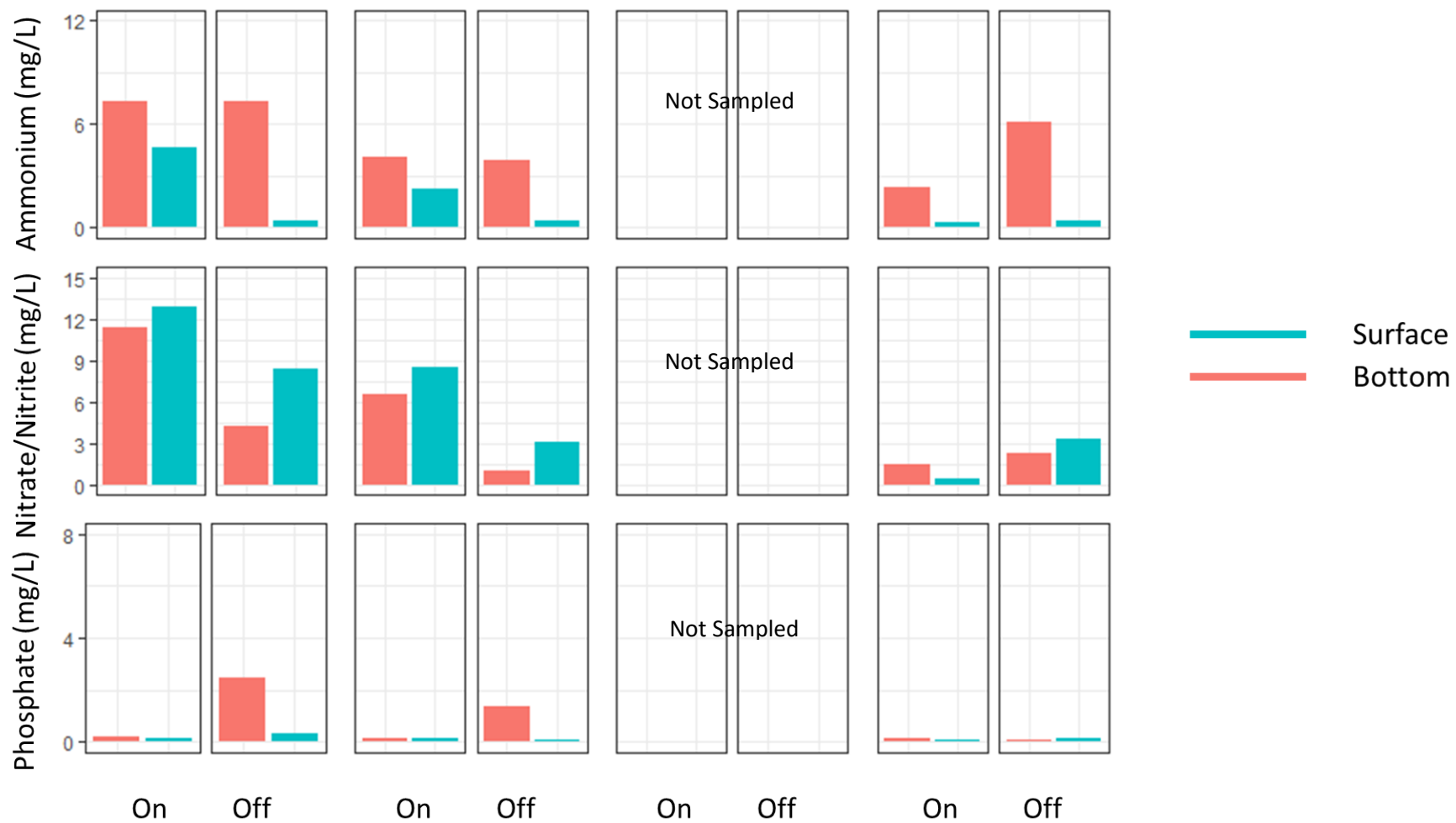
Figure 9: Ammonium, Nitrate/Nitrite, and Orthophosphate values in 2018 at each station in the surface and bottom layers. Station 4 was not sampled in 2018.

Figure 10: The ratio between molar N and P at all stations in surface and bottom waters in 2017 and 2018.
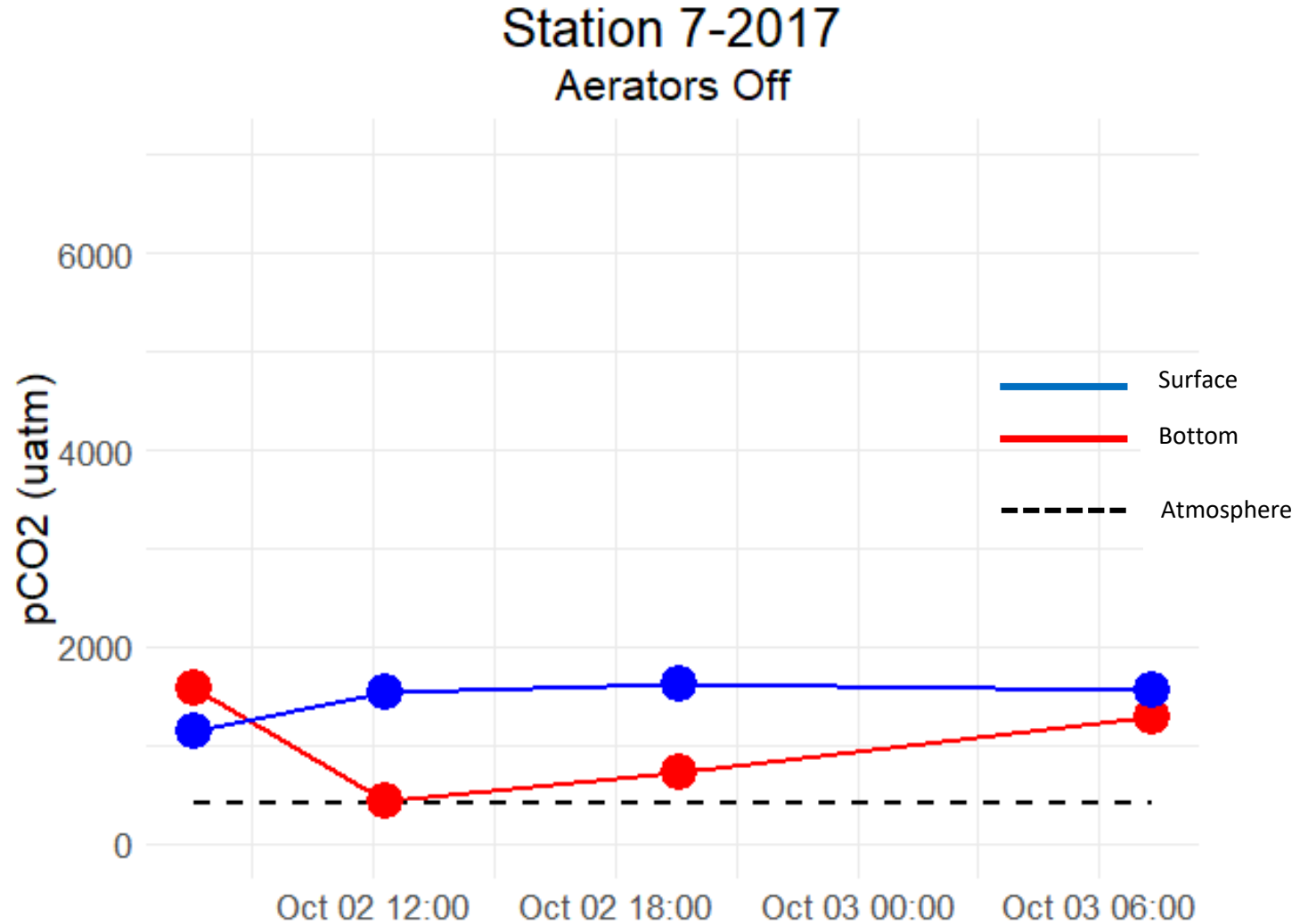
Figure 11:   Example pCO₂
concentrations, showing saturation of DIC in surface waters with respect to atmospheric pCO_2 (represented by the dotted line). Only 6 time points had lower pCO_2 than the atmosphere at the same time. This particular plot was taken from Station 7 in 2017 when the aerators were off, but all plots show the same saturation tendency. All time series plots of pCO_2 can be found in Appendix C.

Figure   12: Plot of
alkalinity versus salinity at all stations in 2017 and 2018. While there is a clear separation between 2017 and 2018 in terms of both alkalinity and salinity, results from both years appear to agree with previously established values in the Chesapeake Bay by Cai et al (2017). The equation presented in Cai et al (2017) is expressed as y=34.676x+1082.7, where y is alkalinity in umol/kg and x is salinity.
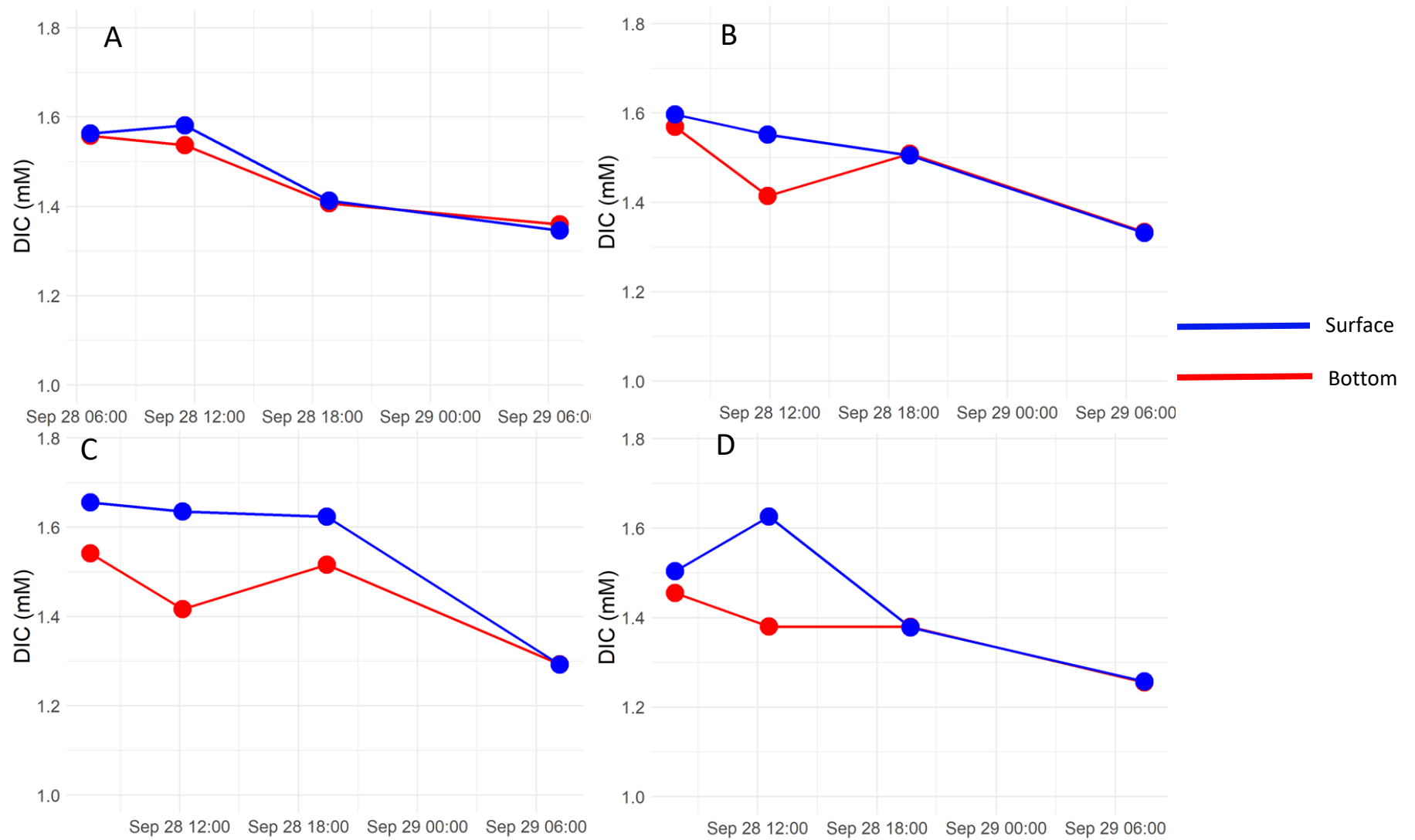
Figure 13: DIC concentrations at station 1 (A), 2 (B), 4 (C) and 7 (D) at dawn, noon, dusk, and the following dawn in 2017 when the aerators were on. A decrease in DIC was observed at all stations at night (the third point to the fourth point), suggesting chemoautotrophy. All time series for DIC can be found in Appendix C.
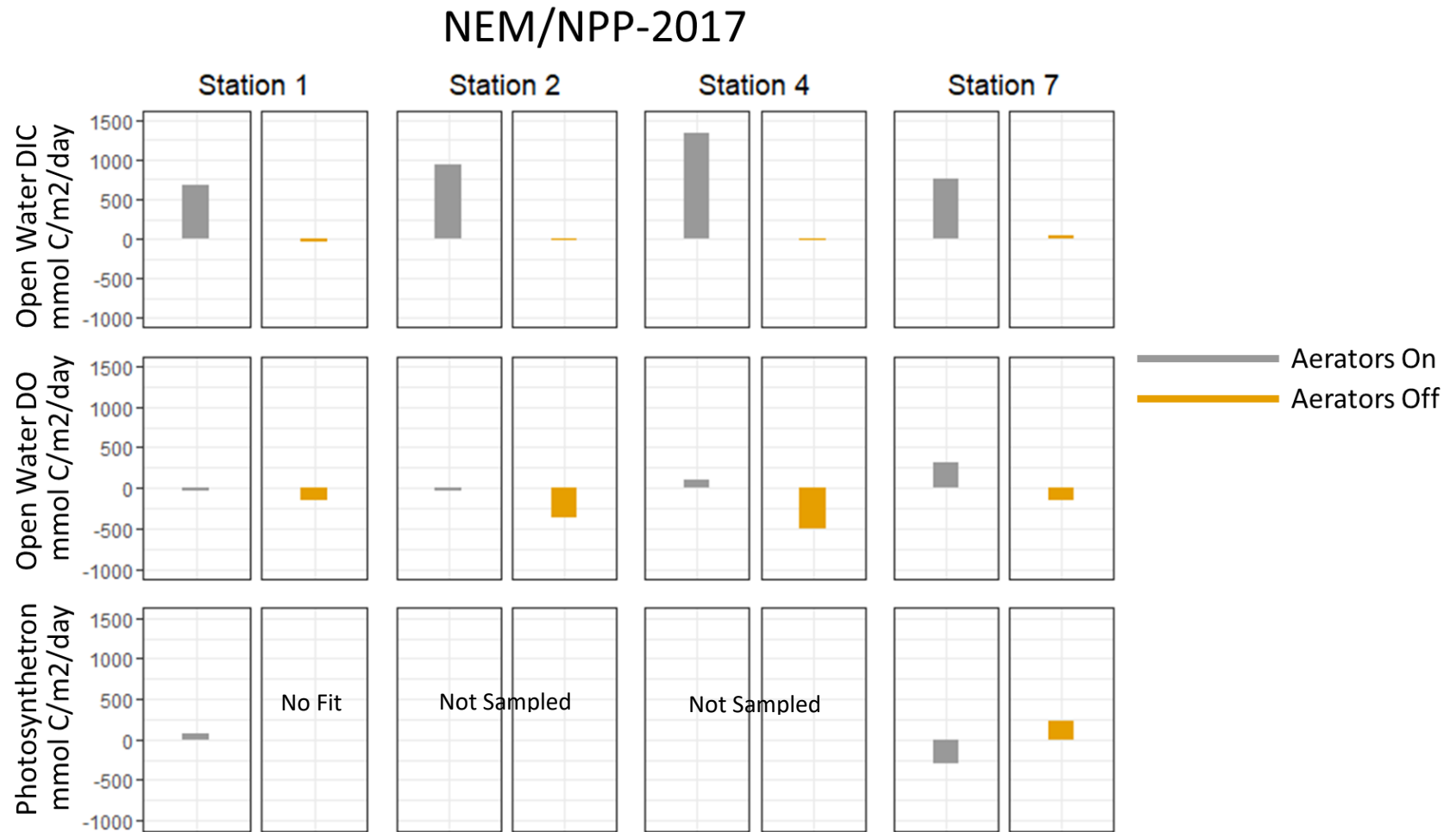
Figure 14: NEM/NPP values for 2017 at all stations using our three methods. It is inappropriate to call results from our photosynthetron NEM, as it only captures the net effect of phytoplankton activity and is more appropriately called NPP. No model could be fit to the data for station 1 when the aerators were off. Not sampled means that metabolism was not measured with that method at that station (See Table 2).
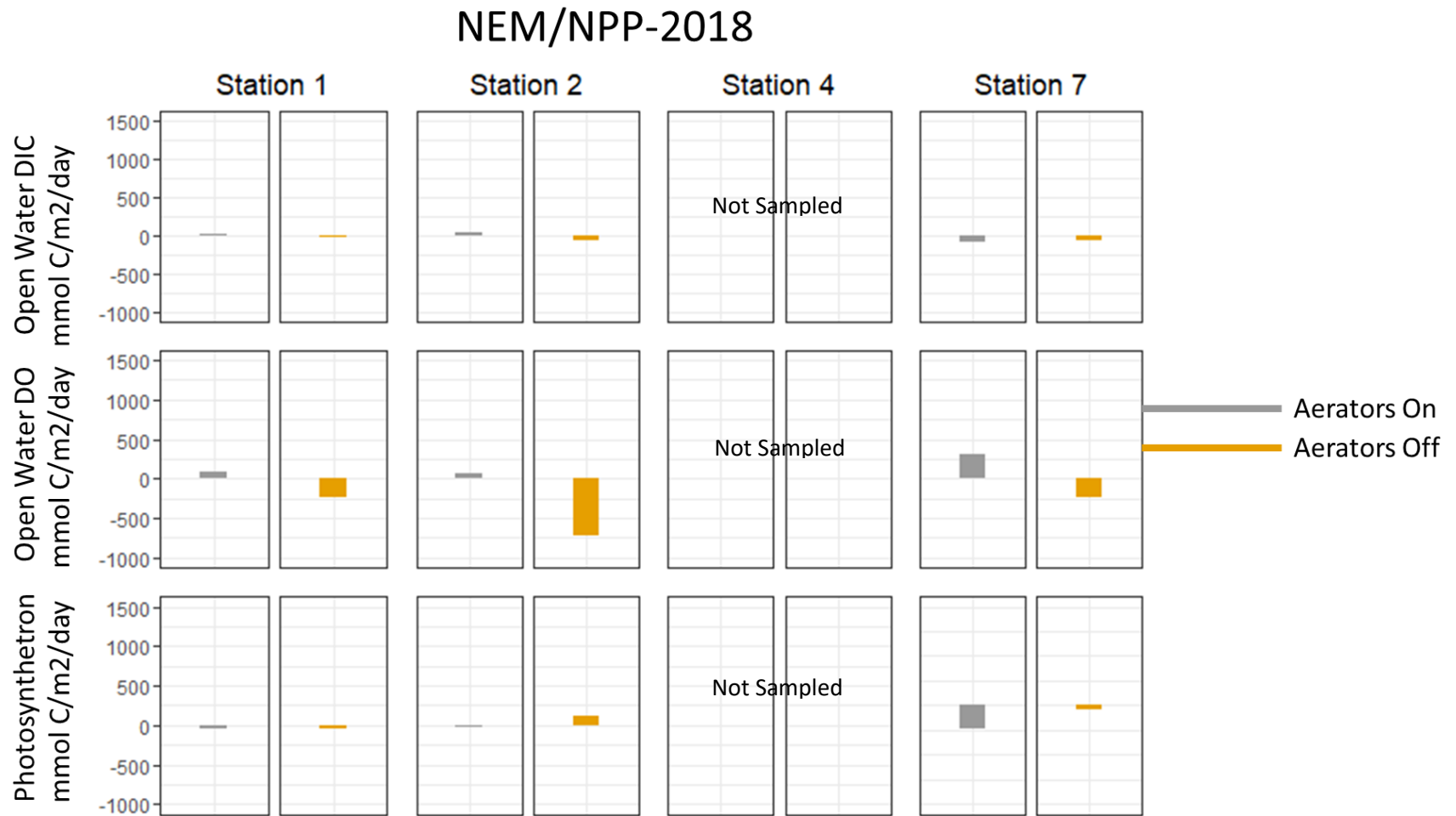
Figure 15: NEM/NPP values for and 2018 at all stations using our three methods. It is inappropriate to call results from our photosynthetron NEM, as it only captures the net effect of phytoplankton activity and is more appropriately called NPP. Not sampled means that metabolism was not measured with that method at that station (See Table 2).
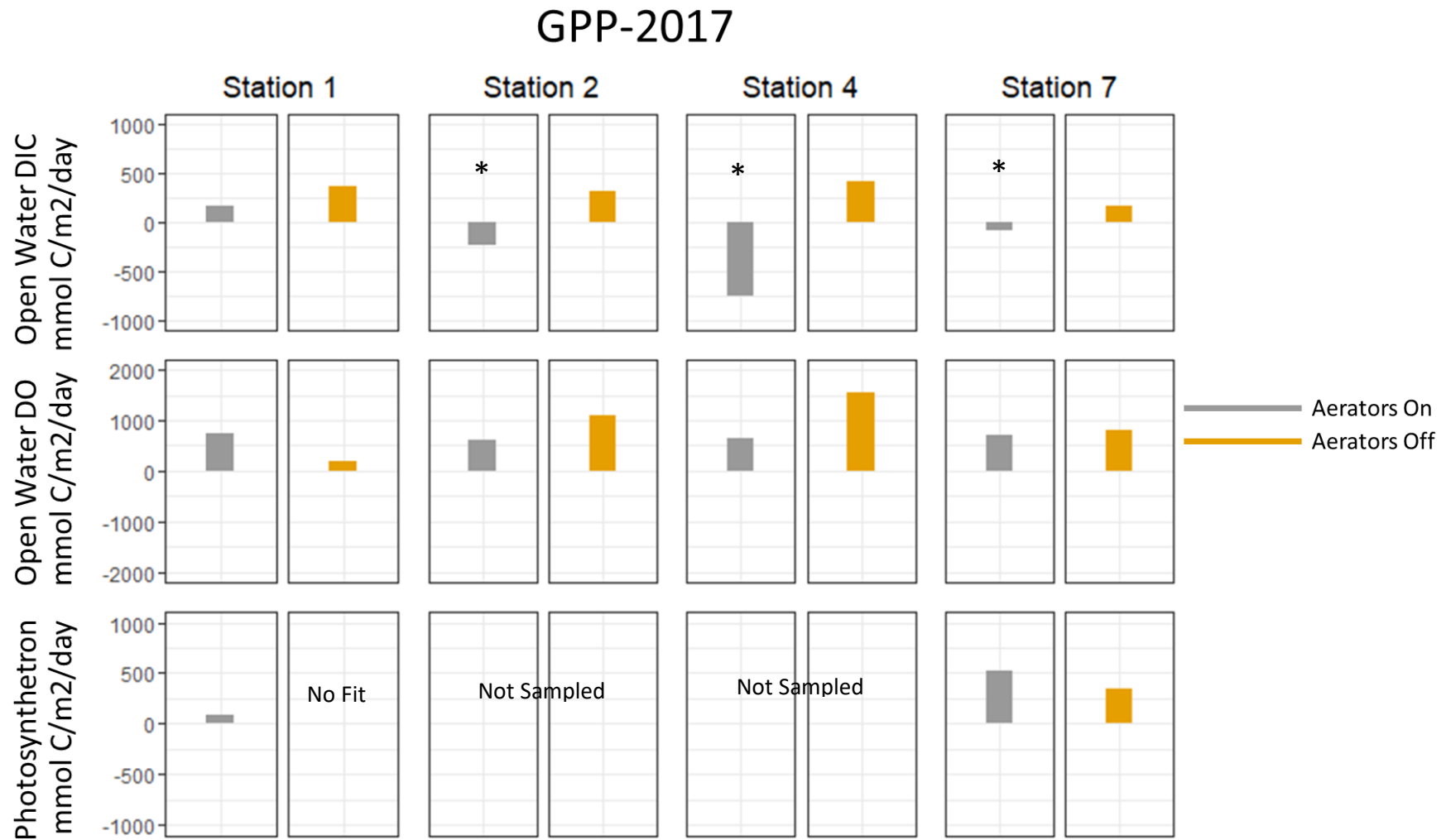
Figure 16: GPP values at all stations in 2017 as measured with our three methods. Asterisks indicate values that contradict our assumptions (See Table 8 and results). No model could be fit to station 1 when the aerators were off. Not sampled means that the GPP was not measured with that method at that station (See Table 2).

GPP-2018
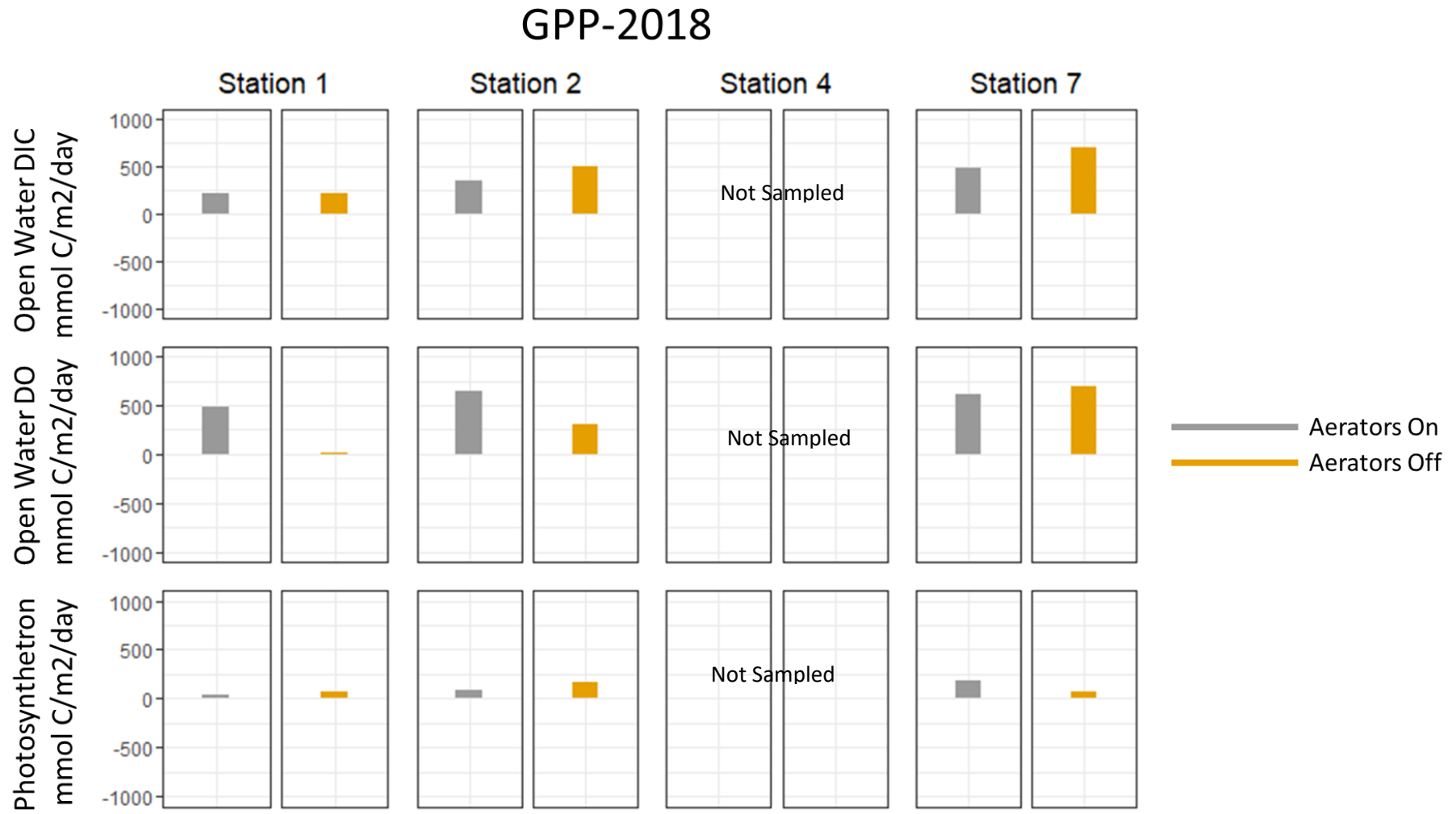
Figure 17: GPP values at all stations in 2017 as measured with our three methods. Asterisks indicate values that contradict our assumptions (See Table 8 and results). No model could be fit to station 1 when the aerators were off. Not sampled means that the GPP was not measured with that method at that station (See Table 2).
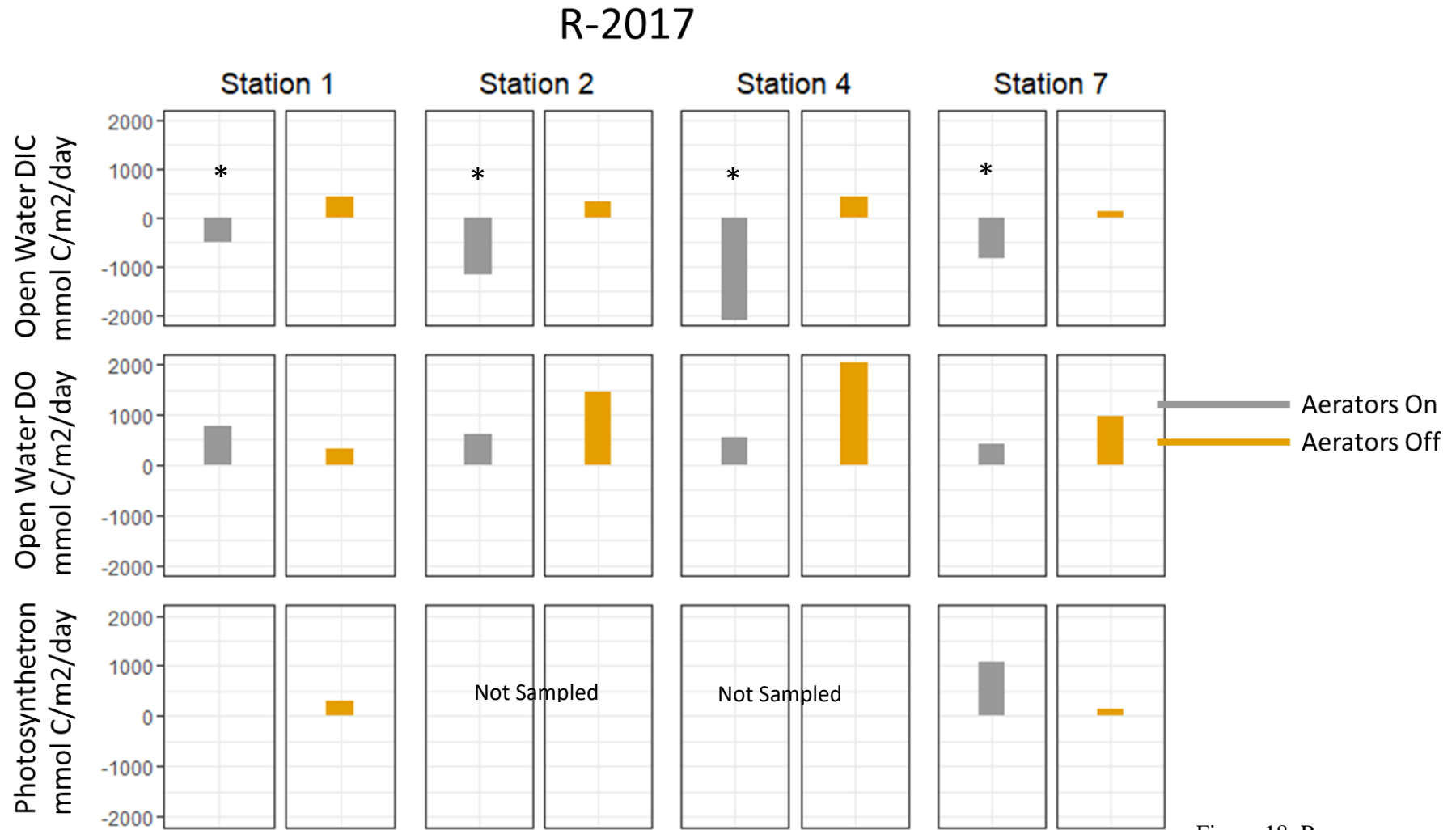
Figure 18: R values at all stations in 2017 and as measured with our three methods. Asterisks indicate values that contradict our assumptions (See Table 8 and results). Not sampled means that the NEM was not measured with that method at that station (See Table 2). The value of Station 1 when the aerators are on using the photosynthetron method (9.16 mmol/m2/day) is not visible at this resolution.
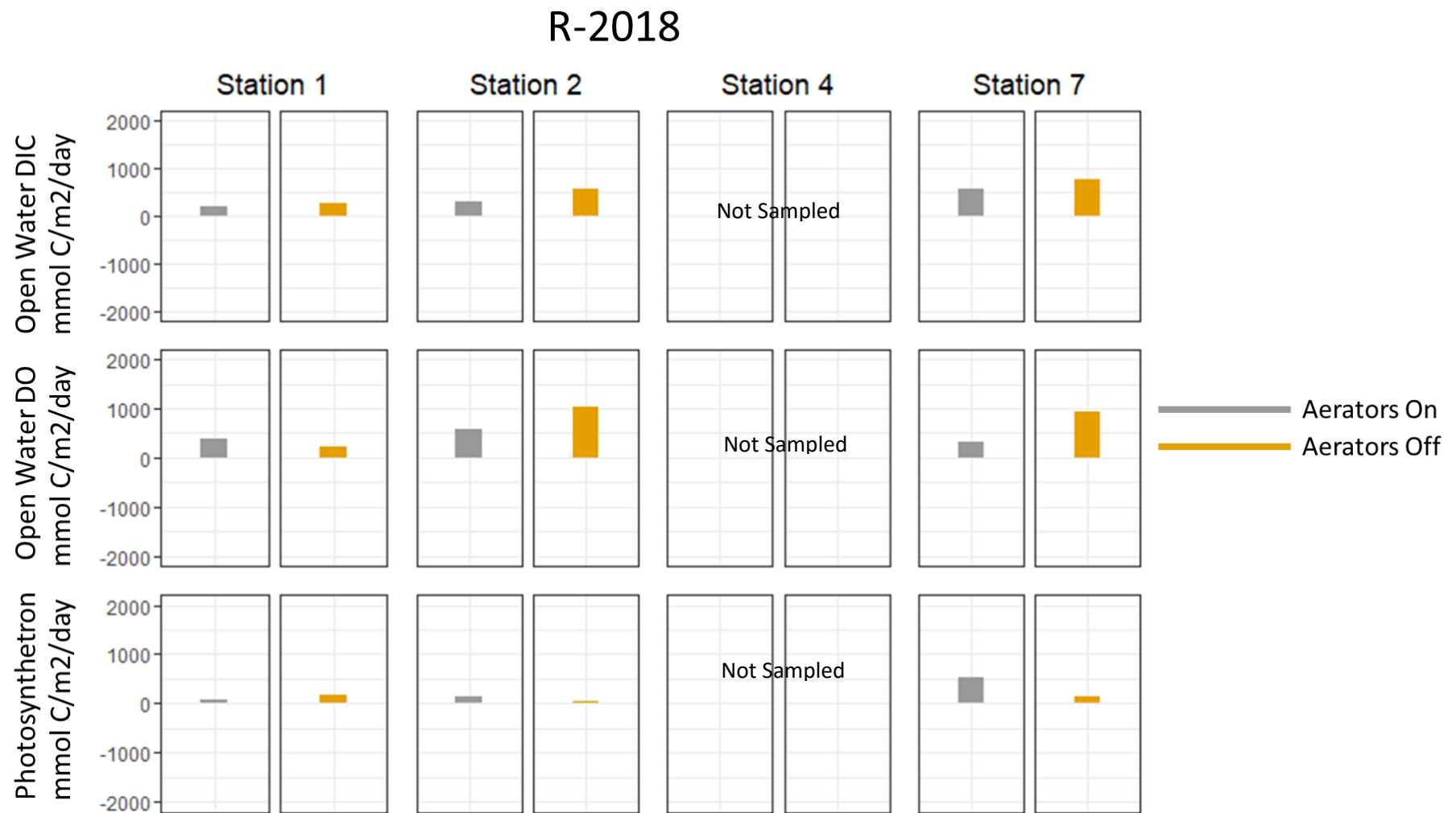
Figure 19: R values at all stations in 2018 and as measured with our three methods. Asterisks indicate values that contradict our assumptions (See Table 8 and results). Not sampled means that the NEM was not measured with that method at that station (See Table 2).

GPP:R-2017

Figure 20: GPP to R ratios as measured by our three methods in 2017. A consistent shift towards heterotrophy (GPP:R<1) was observed at all stations when the aerators were turned off when measured using Open water DO. Asterisks indicate scenarios where metabolic data contradicts our assumptions (See Table 8 and Results). Not sampled means that the metabolism was not measured with that method at that station (See Table 2).
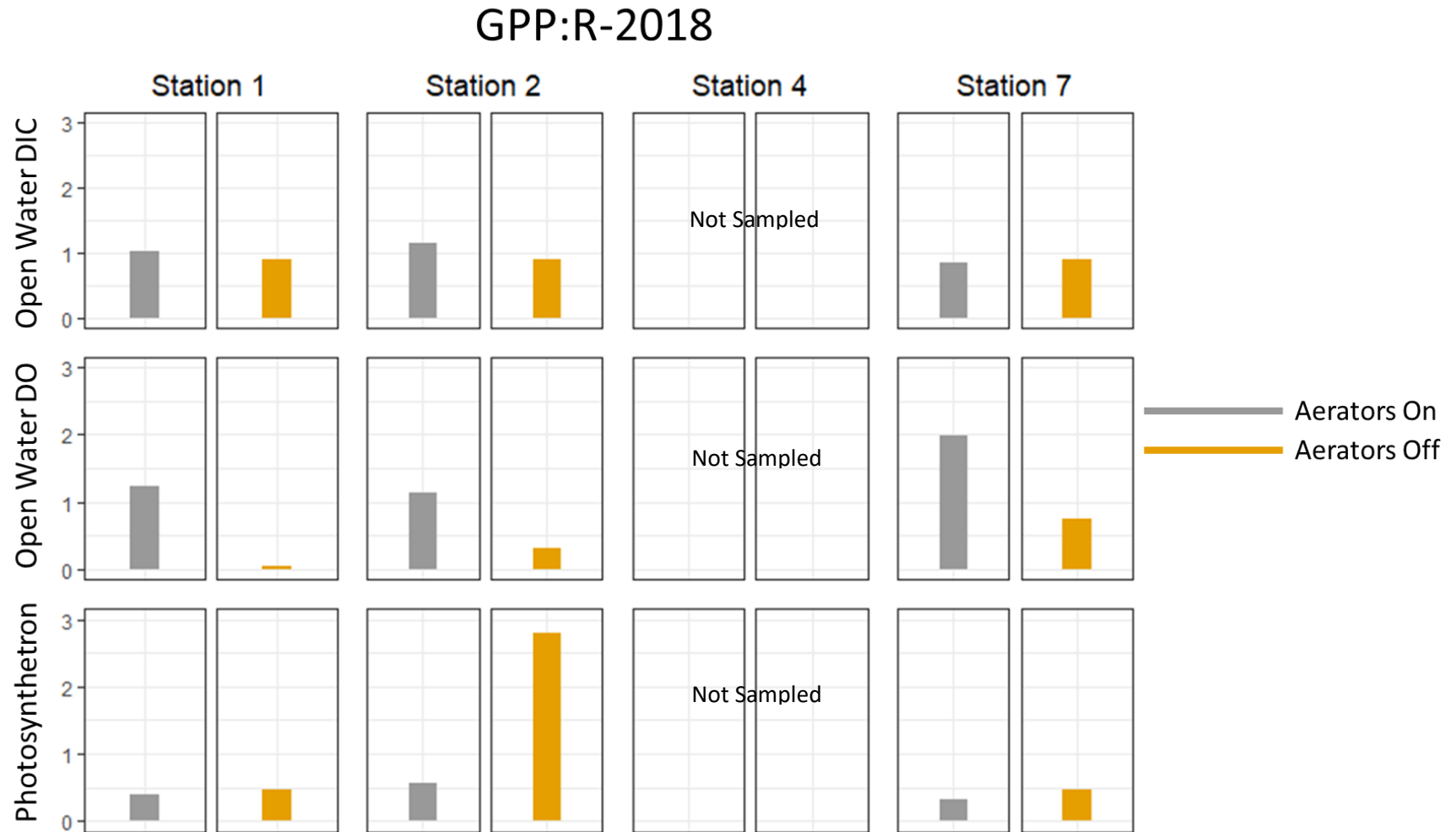
Figure 21: GPP to R ratios as measured by our three methods in 2017. A consistent shift towards heterotrophy (GPP:R<1) was observed at all stations when the aerators were turned off when measured using Open water DO. Asterisks indicate scenarios where metabolic data contradicts our assumptions (See Table 8 and Results). Not sampled means that the metabolism was not measured with that method at that station (See Table 2).

DOC vs R
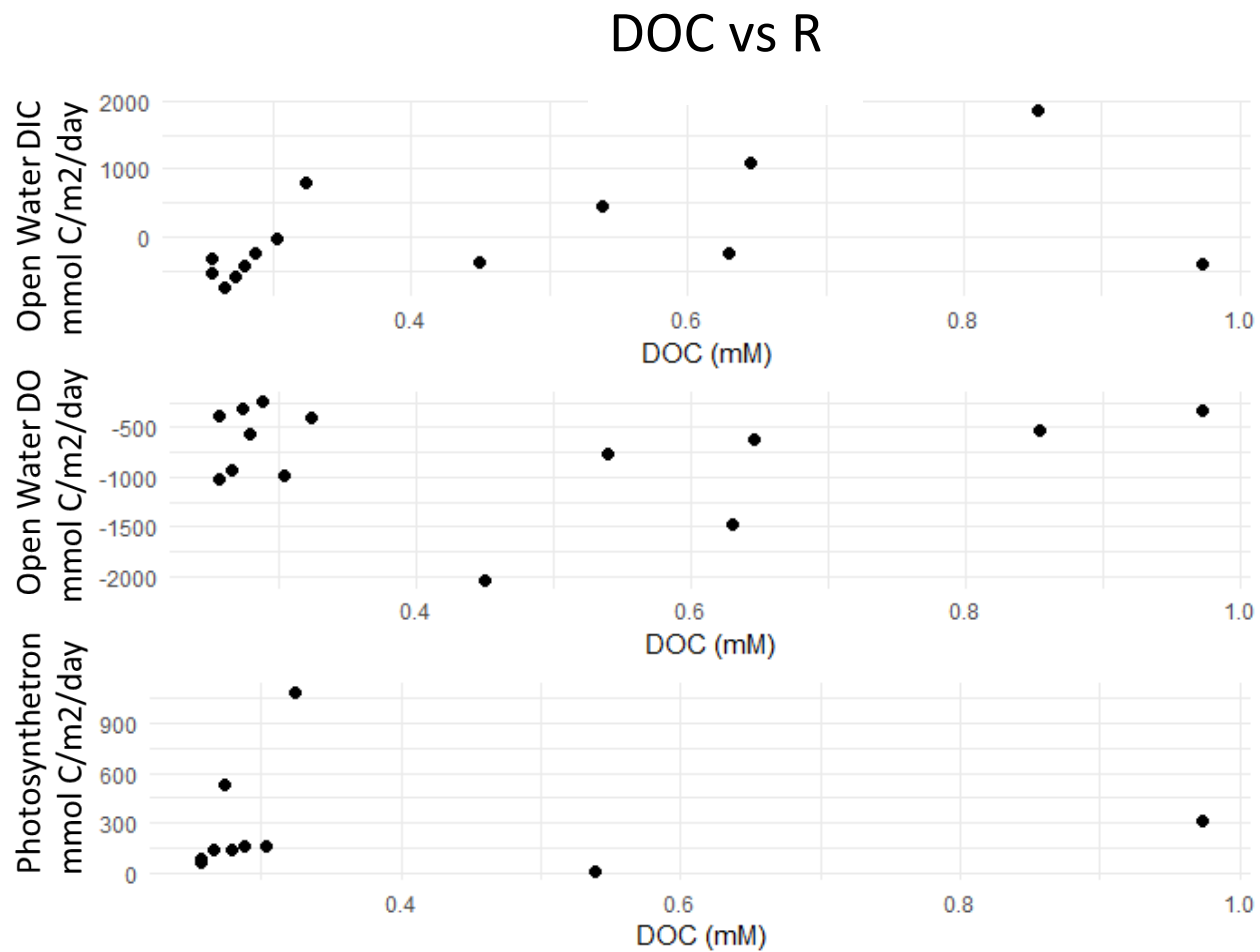
Figure 22: DOC concentrations plotted against respiration as measured by all three methods. No significant correlation was noted in any relationship presented above (See Table 10).

APPENDICES

Appendix A: Mathematical Coding

This appendix contains the code used to fit the Jassby and Platt (1976) model and the Eilers and Peeters (1988) model to the photosynthetron data and the depth integration code to calculate daily NPP, GPP and R. Section 1 contains the R studio code for the curve fitting, and Section 2 contains the MATLAB code used for daily rates.

Section 1: Photosynthetron PI Curve Fitting

```
PPdata$NPP<-as.numeric(as.character(PPdata$NPP))

attach(PPdata)
names(PPdata)
head(PPdata)

library(purrr)
library(ggplot2)

#library(phytotools)
source("fit with intercepts.R")


#JP-

Station=NULL
Alpha=NULL
AlphaSE=NULL
AlphaP=NULL
Ek=NULL
EkSE=NULL
EkP=NULL
Rsquared=NULL
RMSE=NULL
Yintercept=NULL
YinterceptSE=NULL
YinterceptP=NULL
SSE=NULL



for (k in unique(PPdata$Station.ID)){

subdata <- subset(PPdata, Station.ID == k)

 Par=subdata$Light
 Pc=subdata$NPP


 myfit=fitJP(Par,Pc)

 alpha<-myfit$alpha
 ek<-myfit$ek
 yintercept<-myfit$yintercept
 E <- seq(0,1500,by=1)
```

```r
q<-function(x) {yintercept[1]+alpha[1]*(ek[1])*tanh(x/(ek[1]))}

###Standard Error calculation
for (j in 1:length(subdata$Light)){
  subdata$Predicted[j]=q(subdata$Light[j])
}

SSE[k]=sqrt((sum((subdata$NPP-subdata$Predicted)^2))/length(subdata$NPP))
r<-function(x) {yintercept[1]+SSE[k]+alpha[1]*(ek[1])*tanh(x/(ek[1]))}
s<-function(x) {yintercept[1]-SSE[k]+alpha[1]*(ek[1])*tanh(x/(ek[1]))}

a<-data.frame(Par, Pc)


print(ggplot(data.frame(x = c(0, 1200)), aes(x))+
    stat_function(fun=q, size=1, color="red")+
    stat_function(fun=r, size=1, color="gray", linetype=2)+
    stat_function(fun=s, size=1, color="gray", linetype=2)+
    geom_point(data=a, aes(x=Par, y=Pc), size=2, color="red") +
    ggtitle(k,"-JP")+
    theme_light()+
    theme(plot.title = element_text(hjust = 0.5))+
    xlab("Irradiance (uE/m2/sec)")+ylab("NPP (mg O2/L/hr)"))
ggsave(k, plot=last_plot(), device="png", path=NULL, width=6, height=5, units="in")

Station[k]=k
Alpha[k]=alpha[1]
AlphaSE[k]=alpha[2]
AlphaP[k]=alpha[4]
Ek[k]=ek[1]
EkSE[k]=ek[2]
EkP[k]=ek[4]
Yintercept[k]=myfit$yintercept[1]
YinterceptSE[k]=yintercept[2]
YinterceptP[k]=yintercept[4]

residuals<-myfit$residuals

SSR=sum(residuals^2)

Pcsquared=Pc*Pc

SST=sum(Pcsquared)-((sum(Pc)^2/length(Pc)))

Rsquared[k]=1-(SSR/SST)
RMSE[k]=sqrt((sum(residuals*residuals))/length(residuals))



}

Station<-data.frame(as.vector(Station))
Alpha<-data.frame(as.vector(Alpha))
AlphaSE<-data.frame(as.vector(AlphaSE))
```

```r
AlphaP<-data.frame(as.vector(AlphaP))
Ek<-data.frame(as.vector(Ek))
EkSE<-data.frame(as.vector(EkSE))
EkP<-data.frame(as.vector(EkP))
Rsquared<-data.frame(as.vector(Rsquared))
RMSE<-data.frame(as.vector(RMSE))
Yintercept<-data.frame(as.vector(Yintercept))
YinterceptSE<-data.frame(as.vector(YinterceptSE))
YinterceptP<-data.frame(as.vector(YinterceptP))
SSE<-data.frame(as.vector(SSE))

JP=NULL

JP$Station<-Station
JP$Yintercept=Yintercept
JP$YinterceptSE=YinterceptSE
JP$YinterceptP=YinterceptP
JP$Alpha<-Alpha
JP$AlphaSE<-AlphaSE
JP$AlphaP<-AlphaP
JP$Ek<-Ek
JP$EkSE<-EkSE
JP$EkP<-EkP
JP$Rsquared<-Rsquared
JP$RMSE<-RMSE
JP$SSE<-SSE

write.csv(JP,file="JP.csv")

#EP

Station=NULL
Alpha=NULL
AlphaSE=NULL
AlphaP=NULL
Eopt=NULL
EoptSE=NULL
EoptP=NULL
Ps=NULL
PsSE=NULL
PsP=NULL
Rsquared=NULL
RMSE=NULL
Yintercept=NULL
YinterceptSE=NULL
YinterceptP=NULL
SSE=NULL

for (k in unique(PPdata$Station.ID)){
  subdata <- subset(PPdata, Station.ID == k)

  Par=subdata$Light
  Pc=subdata$NPP


  myfit <- fitEP(Par, Pc)
```

```
#Plot input data

#Add model fit
E <- seq(0,1500,by=1)


myfit
alpha<-myfit$alpha
eopt<-myfit$eopt
ps<-myfit$ps
yintercept<-myfit$yintercept

E <- seq(0,1500,by=1)



q<-function(x) {yintercept[1]+(x/((1/(alpha[1]*eopt[1]^2))*x^2+(1/ps[1]-2/(alpha[1]*eopt[1]))*x+(1/alpha[1])))}
for (j in 1:length(subdata$Light)){
  subdata$Predicted[j]=q(subdata$Light[j])
}


SSE[k]=sqrt((((sum((subdata$NPP-subdata$Predicted)^2)))/length(subdata$NPP))

r<-function(x) {yintercept[1]+SSE[k]+(x/((1/(alpha[1]*eopt[1]^2))*x^2+(1/ps[1]-
2/(alpha[1]*eopt[1]))*x+(1/alpha[1])))}
s<-function(x) {yintercept[1]-SSE[k]+(x/((1/(alpha[1]*eopt[1]^2))*x^2+(1/ps[1]-
2/(alpha[1]*eopt[1]))*x+(1/alpha[1])))}

a<-data.frame(Par, Pc)



print(ggplot(data.frame(x = c(0, 1200)), aes(x))+
      stat_function(fun=q, size=1, color="red")+
      stat_function(fun=r, size=1, color="gray", linetype=2)+
      stat_function(fun=s, size=1, color="gray", linetype=2)+
      geom_point(data=a, aes(x=Par, y=Pc), size=2, color="red") +
      ggtitle(k,"-EP")+
      theme(plot.title = element_text(hjust = 0.5))+
      theme_light()+
      xlab("Irradiance (uE/m2/sec)")+ylab("NPP (mg O2/L/hr)"))
ggsave(k, plot=last_plot(), device="png", path=NULL, width=6, height=5, units="in")


Station[k]=k
Alpha[k]=alpha[1]
AlphaSE[k]=alpha[2]
AlphaP[k]=alpha[4]
Eopt[k]=eopt[1]
EoptSE[k]=eopt[2]
EoptP[k]=eopt[4]
Ps[k]=ps[1]
PsSE[k]=ps[2]
PsP[k]=ps[4]
Yintercept[k]=myfit$yintercept[1]
YinterceptSE[k]=yintercept[2]
```

```
YinterceptP[k]=yintercept[4]

residuals<-myfit$residuals

SSR=sum(residuals^2)

Pcsquared=Pc*Pc

SST=sum(Pcsquared)-((sum(Pc)^2/length(Pc)))

Rsquared[k]=1-(SSR/SST)
RMSE[k]=sqrt((sum(residuals*residuals))/length(residuals))


}

Station<-data.frame(as.vector(Station))
Alpha<-data.frame(as.vector(Alpha))
AlphaSE<-data.frame(as.vector(AlphaSE))
AlphaP<-data.frame(as.vector(AlphaP))
Eopt<-data.frame(as.vector(Eopt))
EoptSE<-data.frame(as.vector(EoptSE))
EoptP<-data.frame(as.vector(EoptP))
Ps<-data.frame(as.vector(Ps))
PsSE<-data.frame(as.vector(PsSE))
PsP<-data.frame(as.vector(PsP))
Rsquared<-data.frame(as.vector(Rsquared))
RMSE<-data.frame(as.vector(RMSE))
Yintercept<-data.frame(as.vector(Yintercept))
YinterceptSE<-data.frame(as.vector(YinterceptSE))
YinterceptP<-data.frame(as.vector(YinterceptP))
SSE<-data.frame(as.vector(SSE))

EP=NULL

EP$Station<-Station
EP$Yintercept<-Yintercept
EP$YinterceptSE<-YinterceptSE
EP$YinterceptP<-YinterceptP
EP$Alpha<-Alpha
EP$AlphaSE<-AlphaSE
EP$AlphaP<-AlphaP

EP$Eopt<-Eopt
EP$EoptSE<-EoptSE
EP$EoptP<-EoptP

EP$Ps<-Ps
EP$PsSE<-PsSE
EP$PsP<-PsP


EP$Rsquared<-Rsquared
EP$RMSE<-RMSE
EP$SSE<-SSE
```

```
write.csv(EP,file="EP.csv")
```

Section 2: MATLAB Depth Integration Code

```
%Read PAR file

[~, ~, raw, dateNums] = xlsread("C:\Users\Lora\Desktop\Zack's PC\Grad School\Thesis\Jug Bay
PAR.xlsx",'Sheet1','A2:M5000',",@convertSpreadsheetDates);

raw(cellfun(@(x) ~isempty(x) && isnumeric(x) && isnan(x),raw)) = {"};
cellVectors = raw(:,[1,6,10,11,12]);
raw = raw(:,[2,3,4,5,7,8,9,13]);
dateNums = dateNums(:,[2,3,4,5,7,8,9,13]);

% Replace date strings by MATLAB serial date numbers (datenum)
R = ~cellfun(@isequalwithequalnans,dateNums,raw) & cellfun('isclass',raw,'char'); % Find spreadsheet dates
raw(R) = dateNums(R);

% Replace non-numeric cells with NaN
R = cellfun(@(x) ~isnumeric(x) && ~islogical(x),raw); % Find non-numeric cells
raw(R) = {NaN}; % Replace non-numeric cells

% Create output variable
data = reshape([raw{:}],size(raw));

% Allocate imported array to column variable names


Station    = cellVectors(:,1);

PARDate    = data(:,1);


format long g
PARTime    = data(:,2);
PAR  = data(:,3);

%Correct PAR Units
PAR=PAR*1.111;

%%Read paramter file from phytotools

[~,~,Dates]=xlsread("C:\Users\Lora\Desktop\Zack's PC\Thesis Final Data sets\New Phytotools Package\Diel
Production Graphs-NPP\Parameters.xlsx",'EP','A1:M52');
parameters=xlsread("C:\Users\Lora\Desktop\Zack's PC\Thesis Final Data sets\New Phytotools Package\Diel
Production Graphs-NPP\Parameters.xlsx",'EP','A1:M52');

%Establish variable names
Date= Dates(:,3);
Station1= Dates(:,2);
Yintercept=parameters(:,4);
Alpha=parameters(:,5);
Eopt=parameters(:,6);
Ps=parameters(:,7);
Depth=parameters(:,10)
Kd=parameters(:,11);
```

```matlab
SurfR=parameters(:,12);
BotR=parameters(:,13);
RMSE=parameters(:,9);
%%


%1 loop is for 1 station
for l=1:(length(Yintercept))

    clear DepthProd
    clear f1

%Specify kd
kd=Kd(l,1);

%specify euphotic depth
zmax(l)=log(.01)/-kd;

if zmax (l) > Depth(l);
    zmax (l)=Depth(1);
else
    zmax(l)=zmax(l);
end


%Specify date

date=(Date(l+1));
n=datenum(date);

%Find all PAR values with same date
in = find(PARDate==n);


    % 1 loops is one 15 minute interval starting at sunrise on specified date
for i=1:1:length(in)
    Io=PAR(in(i));

    %Create function of Beer-Lambert Law
    fun = @(x) Io*exp(-kd*x);

    %Specify parameter values for this station
    alpha=Alpha(l);
    eopt=Eopt(l);
    ps=Ps(l);
    yintercept=Yintercept(l);

    %generate function according to phytotools
    f1 = @(x) yintercept + (fun(x)./((1/(alpha*eopt^2))*fun(x).^2+(1/ps-2/(alpha*eopt))*fun(x)+(1/alpha)));



    %Integrate function over the euphotic depth
    %Normalized to 1 m2
    DepthProd(i)=integral(f1,0,zmax(l))/.001;
```

97

```
end

for i=1:1:length(DepthProd)
   if PAR(in(i))==0
      DepthProd(i)=0
   else
      DepthProd(i)=DepthProd(i)
   end
end

%Time=Time-Time(1);

%Correct time units


%GPP
  for i=1:1:length(DepthProd)
  if PAR(in(i))==0;
     SurfGPP(i)=0;

  elseif zmax(l) == Depth(l);
     SurfGPP(i)=DepthProd(i)+(SurfR(l)*zmax(l)*1000);

  else
     SurfGPP(i)=DepthProd(i)+((SurfR(l)+BotR(l)/2)*zmax(l)*1000);
  end
  end


SurfGPP=SurfGPP*.25
GPP(l)=sum(SurfGPP)
DepthProd=DepthProd*.25;
EuphoticNPP(l)=sum(DepthProd)

end

GPP=transpose(GPP)
EuphoticNPP=transpose(EuphoticNPP)

%%
%%
%Respiration
for i=1:1:length(SurfR)
   if zmax (i) > Depth(i);
      Resp(i)=(SurfR(i)+BotR(i)/2)*1000*Depth(i)*24

   else
      Resp(i)=((SurfR(i)*zmax(i)*1000)+(BotR(i)*Depth(i)*zmax(i)*1000))*24
   end
end
Resp=transpose(Resp)
WaterNPP=GPP-Resp;
%% Upper Limit
%1 loop is for 1 station
for l=1:(length(Yintercept))
```

```matlab
    clear DepthProd
    clear f1

%Specify kd
kd=Kd(l,1);

%specify euphotic depth
zmax(l)=log(.01)/-kd;

if zmax (l) > Depth(l);
    zmax (l)=Depth(1);
else
    zmax(l)=zmax(l);
end


%Specify date

date=(Date(l+1));
n=datenum(date);

%Find all PAR values with same date
in = find(PARDate==n);


    % 1 loops is one 15 minute interval starting at sunrise on specified date
for i=1:1:length(in)
    Io=PAR(in(i));

    %Create function of Beer-Lambert Law
    fun = @(x) Io*exp(-kd*x);

    %Specify parameter values for this station
    alpha=Alpha(l);
    eopt=Eopt(l);
    ps=Ps(l);
    yintercept=Yintercept(l);
    rmse=RMSE(l)
    %generate function according to phytotools
  f1 = @(x) yintercept + rmse + (fun(x)./((1/(alpha*eopt^2))*fun(x).^2+(1/ps-2/(alpha*eopt))*fun(x)+(1/alpha)));



    %Integrate function over the euphotic depth
    %Normalized to 1 m2
    UpperDepthProd(i)=integral(f1,0,zmax(l))/.001;

end

for i=1:1:length(UpperDepthProd)
    if PAR(in(i))==0
        UpperDepthProd(i)=0
    else
        UpperDepthProd(i)=UpperDepthProd(i)
```

```
      end
end

%Time=Time-Time(1);

%Correct time units


%GPP
  for i=1:1:length(UpperDepthProd)
   if PAR(in(i))==0;
      SurfGPP(i)=0;

   elseif zmax(l) == Depth(l);
      SurfGPP(i)=UpperDepthProd(i)+(SurfR(l)*zmax(l)*1000);

   else
      SurfGPP(i)=UpperDepthProd(i)+((SurfR(l)+BotR(l)/2)*zmax(l)*1000);
   end
  end


UpperSurfGPP=SurfGPP*.25
UpperGPP(l)=transpose(sum(UpperSurfGPP))
UpperDepthProd=UpperDepthProd*.25;
UpperEuphoticNPP(l)=sum(UpperDepthProd)

end


UpperEuphoticNPP=transpose(UpperEuphoticNPP)


%%
%%
%Respiration
for i=1:1:length(SurfR)
   if zmax (i) > Depth(i);
      Resp(i)=(SurfR(i)+BotR(i)/2)*1000*Depth(i)*24

   else
      Resp(i)=((SurfR(i)*zmax(i)*1000)+(BotR(i)*Depth(i)*zmax(i)*1000))*24
   end
end
Resp=transpose(Resp)
UpperWaterNPP=UpperGPP-Resp;
%%
%%Lower Limit
%1 loop is for 1 station
for l=1:(length(Yintercept))

   clear DepthProd
   clear f1

%Specify kd
kd=Kd(l,1);
```

```matlab
%specify euphotic depth
zmax(l)=log(.01)/-kd;

if zmax (l) > Depth(l);
    zmax (l)=Depth(1);
else
    zmax(l)=zmax(l);
end


%Specify date

date=(Date(l+1));
n=datenum(date);

%Find all PAR values with same date
in = find(PARDate==n);


    % 1 loops is one 15 minute interval starting at sunrise on specified date
for i=1:1:length(in)
    Io=PAR(in(i));

    %Create function of Beer-Lambert Law
    fun = @(x) Io*exp(-kd*x);

    %Specify parameter values for this station
    alpha=Alpha(l);
    eopt=Eopt(l);
    ps=Ps(l);
    yintercept=Yintercept(l);
    rmse=RMSE(l)
    %generate function according to phytotools
    f1 = @(x) yintercept - rmse + (fun(x)./((1/(alpha*eopt^2))*fun(x).^2+(1/ps-2/(alpha*eopt))*fun(x)+(1/alpha)));



    %Integrate function over the euphotic depth
    %Normalized to 1 m2
    LowerDepthProd(i)=integral(f1,0,zmax(l))/.001;

end

for i=1:1:length(LowerDepthProd)
    if PAR(in(i))==0
        LowerDepthProd(i)=0
    else
        LowerDepthProd(i)=LowerDepthProd(i)
    end
end

%Time=Time-Time(1);

%Correct time units
```

```
%GPP
  for i=1:1:length(LowerDepthProd)
   if PAR(in(i))==0;
     SurfGPP(i)=0;

   elseif zmax(l) == Depth(l);
     SurfGPP(i)=LowerDepthProd(i)+(SurfR(l)*zmax(l)*1000);

   else
     SurfGPP(i)=LowerDepthProd(i)+((SurfR(l)+BotR(l)/2)*zmax(l)*1000);
   end
  end


LowerSurfGPP=SurfGPP*.25
LowerGPP(l)=transpose(sum(LowerSurfGPP))
LowerDepthProd=LowerDepthProd*.25;
LowerEuphoticNPP(l)=sum(LowerDepthProd)

end


LowerEuphoticNPP=transpose(LowerEuphoticNPP)


%%
%%
%Respiration
for i=1:1:length(SurfR)
   if zmax (i) > Depth(i);
     Resp(i)=(SurfR(i)+BotR(i)/2)*1000*Depth(i)*24

   else
     Resp(i)=((SurfR(i)*zmax(i)*1000)+(BotR(i)*Depth(i)*zmax(i)*1000))*24
   end
end

LowerWaterNPP=LowerGPP-Resp;

%Jassby and Platt Model

%Read PAR file

[~, ~, raw, dateNums] = xlsread("C:\Users\Lora\Desktop\Zack's PC\Grad School\Thesis\Jug Bay
PAR.xlsx",'Sheet1','A2:M5000',",@convertSpreadsheetDates);

raw(cellfun(@(x) ~isempty(x) && isnumeric(x) && isnan(x),raw)) = {"};
cellVectors = raw(:,[1,6,10,11,12]);
raw = raw(:,[2,3,4,5,7,8,9,13]);
dateNums = dateNums(:,[2,3,4,5,7,8,9,13]);

% Replace date strings by MATLAB serial date numbers (datenum)
R = ~cellfun(@isequalwithequalnans,dateNums,raw) & cellfun('isclass',raw,'char'); % Find spreadsheet dates
raw(R) = dateNums(R);
```

```
% Replace non-numeric cells with NaN
R = cellfun(@(x) ~isnumeric(x) && ~islogical(x),raw); % Find non-numeric cells
raw(R) = {NaN}; % Replace non-numeric cells

% Create output variable
data = reshape([raw{:}],size(raw));

% Allocate imported array to column variable names


Station    = cellVectors(:,1);

PARDate    = data(:,1);


format long g
PARTime    = data(:,2);
PAR  = data(:,3);

%Correct units of PAR data
PAR=PAR*1.111;
%Read paramter file
%Parameters generated from phytotools
[~,~,Dates]=xlsread("C:\Users\Lora\Desktop\Zack's PC\Thesis Final Data sets\New Phytotools Package\Diel
Production Graphs-NPP\Parameters.xlsx",'JP','A1:M52');
parameters=xlsread("C:\Users\Lora\Desktop\Zack's PC\Thesis Final Data sets\New Phytotools Package\Diel
Production Graphs-NPP\Parameters.xlsx",'JP','A1:M52');

%Establish Variable Names
Date= Dates(:,3);
Station1= Dates(:,2);
Yintercept=parameters(:,4);
Alpha=parameters(:,5);
Ek=parameters(:,6);
Depth=parameters(:,9);
Kd=parameters(:,10);
SurfR=parameters(:,11);
BotR=parameters(:,12);
RMSE=parameters(:,8);
%%

% 1 loop is for 1 station
for l=1:(length(Yintercept))
    clear DepthProd
    clear f1
    %specify kd value
kd=Kd(l,1)

%find euphotic depth
%if euphotic depth is greater than total depth, use total depth
zmax(l)=log(.01)/-kd

if zmax (l) > Depth(l)
    zmax (l)=Depth(1)
else
```

```matlab
    zmax(l)=zmax(l)
end


%Specify date
date=(Date(l+1))
n=datenum(date);


%Find All PAR values with the same date
in = find(PARDate==n);


% 1 loop is a 15 minute time interval starting at sunrise on specified date
for i=1:1:length(in)
    Io=PAR(in(i));
    %Create function of Beer-Lambert Law
    fun = @(x) Io*exp(-kd*x);

    %Call variable according to Phytotools fit
    alpha=Alpha(l);
    ek=Ek(l);
    yintercept=Yintercept(l);
    %Generate according to phytotools
    f1 = @(x) yintercept+((alpha)*(ek)*tanh(fun(x)/(ek)));



    %integrate over the depth of the euphotic zone
    %calculation normalized to 1 m2 (.001 is unit correction)
    DepthProd(i)=integral(f1,0,zmax(l))/.001;

end

for i=1:1:length(DepthProd)
    if PAR(in(i))==0
        DepthProd(i)=0;
    else
        DepthProd(i)=DepthProd(i);
    end
end

for i=1:1:length(DepthProd)
    if PAR(in(i))==0;
        SurfGPP(i)=0;

    elseif zmax(l) == Depth(l);
        SurfGPP(i)=DepthProd(i)+(SurfR(l)*zmax(l)*1000);

    else
        SurfGPP(i)=DepthProd(i)+((SurfR(l)+BotR(l)/2)*zmax(l)*1000);
    end
end
%Correct time units (each interval is 15 minutes, so divide results by 4)

SurfGPP=SurfGPP*.25
```

```matlab
GPP(l)=sum(SurfGPP);
DepthProd=DepthProd*.25;
EuphoticNPP(l)=sum(DepthProd);

end


GPP=transpose(GPP)
EuphoticNPP=transpose(EuphoticNPP)
%%
%Respiration
for i=1:1:length(SurfR)
    if zmax (i) > Depth(i);
        Resp(i)=(SurfR(i)+BotR(i)/2)*1000*Depth(i)*24;

    else
        Resp(i)=((SurfR(i)*zmax(i)*1000)+(BotR(i)*Depth(i)*zmax(i)*1000))*24;
    end
end

%%
Resp=transpose(Resp)
WaterNPP=GPP-Resp;

%%
%%

% 1 loop is for 1 station
for l=1:(length(Yintercept))
    clear DepthProd
    clear f1
    %specify kd value
kd=Kd(l,1)

%find euphotic depth
%if euphotic depth is greater than total depth, use total depth
zmax(l)=log(.01)/-kd

if zmax (l) > Depth(l)
    zmax (l)=Depth(1)
else
    zmax(l)=zmax(l)
end


%Specify date
date=(Date(l+1))
n=datenum(date);


%Find All PAR values with the same date
in = find(PARDate==n);


% 1 loop is a 15 minute time interval starting at sunrise on specified date
for i=1:1:length(in)
```

```
   Io=PAR(in(i));
   %Create function of Beer-Lambert Law
   fun = @(x) Io*exp(-kd*x);


   %Call variable according to Phytotools fit
   alpha=Alpha(l);
   ek=Ek(l);
   yintercept=Yintercept(l);
   rmse=RMSE(l);
   %Generate according to phytotools
  f1 = @(x) yintercept + rmse +((alpha)*(ek)*tanh(fun(x)/(ek)));




   %integrate over the depth of the euphotic zone
   %calculation normalized to 1 m2 (.001 is unit correction)
   UpperDepthProd(i)=integral(f1,0,zmax(l))/.001;

end

for i=1:1:length(UpperDepthProd)
   if PAR(in(i))==0
      UpperDepthProd(i)=0;
   else
      UpperDepthProd(i)=UpperDepthProd(i);
   end
end

for i=1:1:length(UpperDepthProd)
   if PAR(in(i))==0;
      UpperSurfGPP(i)=0;

   elseif zmax(l) == Depth(l);
      UpperSurfGPP(i)=UpperDepthProd(i)+(SurfR(l)*zmax(l)*1000);

   else
      UpperSurfGPP(i)=UpperDepthProd(i)+((SurfR(l)+BotR(l)/2)*zmax(l)*1000);
   end
end
%Correct time units (each interval is 15 minutes, so divide results by 4)

UpperSurfGPP=UpperSurfGPP*.25
UpperGPP(l)=sum(UpperSurfGPP);
UpperDepthProd=UpperDepthProd*.25;
UpperEuphoticNPP(l)=sum(UpperDepthProd);

end


UpperGPP=transpose(UpperGPP)
UpperEuphoticNPP=transpose(UpperEuphoticNPP)
%%
%Respiration
for i=1:1:length(SurfR)
   if zmax (i) > Depth(i);
      Resp(i)=(SurfR(i)+BotR(i)/2)*1000*Depth(i)*24;
```

```matlab
    else
        Resp(i)=((SurfR(i)*zmax(i)*1000)+(BotR(i)*Depth(i)*zmax(i)*1000))*24;
    end
end

%%

UpperWaterNPP=UpperGPP-Resp;

%%
% 1 loop is for 1 station
for l=1:(length(Yintercept))
    clear DepthProd
    clear f1
    %specify kd value
kd=Kd(l,1)

%find euphotic depth
%if euphotic depth is greater than total depth, use total depth
zmax(l)=log(.01)/-kd

if zmax (l) > Depth(l)
    zmax (l)=Depth(1)
else
    zmax(l)=zmax(l)
end


%Specify date
date=(Date(l+1))
n=datenum(date);


%Find All PAR values with the same date
in = find(PARDate==n);


% 1 loop is a 15 minute time interval starting at sunrise on specified date
for i=1:1:length(in)
    Io=PAR(in(i));
    %Create function of Beer-Lambert Law
    fun = @(x) Io*exp(-kd*x);

    %Call variable according to Phytotools fit
    alpha=Alpha(l);
    ek=Ek(l);
    yintercept=Yintercept(l);
    rmse=RMSE(l);
    %Generate according to phytotools
    f1 = @(x) yintercept - rmse +((alpha)*(ek)*tanh(fun(x)/(ek)));



    %integrate over the depth of the euphotic zone
    %calculation normalized to 1 m2 (.001 is unit correction)
```

```matlab
    LowerDepthProd(i)=integral(f1,0,zmax(l))/.001;

end

for i=1:1:length(LowerDepthProd)
    if PAR(in(i))==0
        LowerDepthProd(i)=0;
    else
        LowerDepthProd(i)=LowerDepthProd(i);
    end
end

for i=1:1:length(LowerDepthProd)
    if PAR(in(i))==0;
        LowerSurfGPP(i)=0;

    elseif zmax(l) == Depth(l);
        LowerSurfGPP(i)=LowerDepthProd(i)+(SurfR(l)*zmax(l)*1000);

    else
        LowerSurfGPP(i)=LowerDepthProd(i)+((SurfR(l)+BotR(l)/2)*zmax(l)*1000);
    end
end
%Correct time units (each interval is 15 minutes, so divide results by 4)

LowerSurfGPP=LowerSurfGPP*.25
LowerGPP(l)=sum(LowerSurfGPP);
LowerDepthProd=LowerDepthProd*.25;
LowerEuphoticNPP(l)=sum(LowerDepthProd);

end


LowerGPP=transpose(LowerGPP)
LowerEuphoticNPP=transpose(LowerEuphoticNPP)
%%
%Respiration
for i=1:1:length(SurfR)
    if zmax (i) > Depth(i);
        Resp(i)=(SurfR(i)+BotR(i)/2)*1000*Depth(i)*24;

    else
        Resp(i)=((SurfR(i)*zmax(i)*1000)+(BotR(i)*Depth(i)*zmax(i)*1000))*24;
    end
end

%%

LowerWaterNPP=LowerGPP-Resp;
```

Appendix B-Photosynthetron PI Curves and Model Fits:

This appendix shows the PI curves generated from the code in Appendix A. Model fits were taken from either the Jassby and Platt (1976) model or the Eilers and Peeters (1988) model. Red points represent the points from the photosynthetron incubations, the red line represents the model fit, and the dotted gray lines represent the root mean square error.

Station 1-2017- Aerators Off
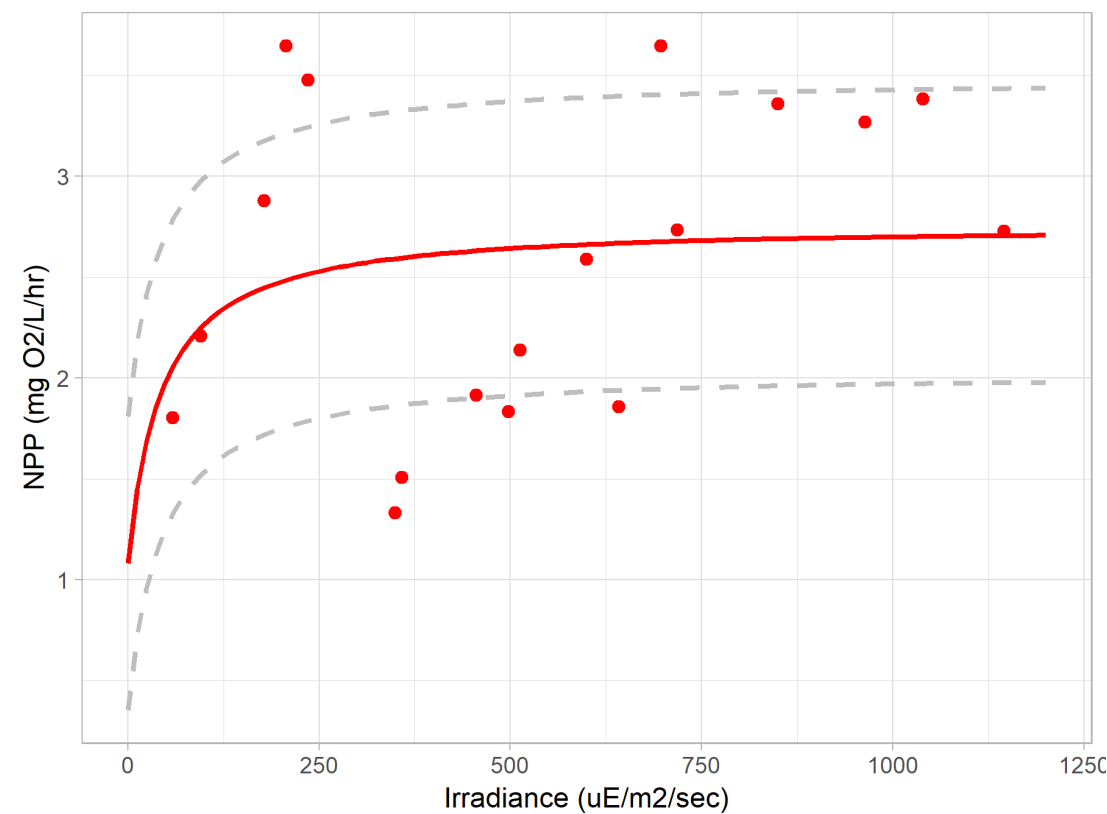
Best Fit-Eilers and Peeters (1988)

Y intercept	Alpha	Eopt	Ps	R-squared	RMSE
1.08189	0.03865	1974.81007	1.63363	0.05368	0.72927

110

Station 7-2017- Aerators On
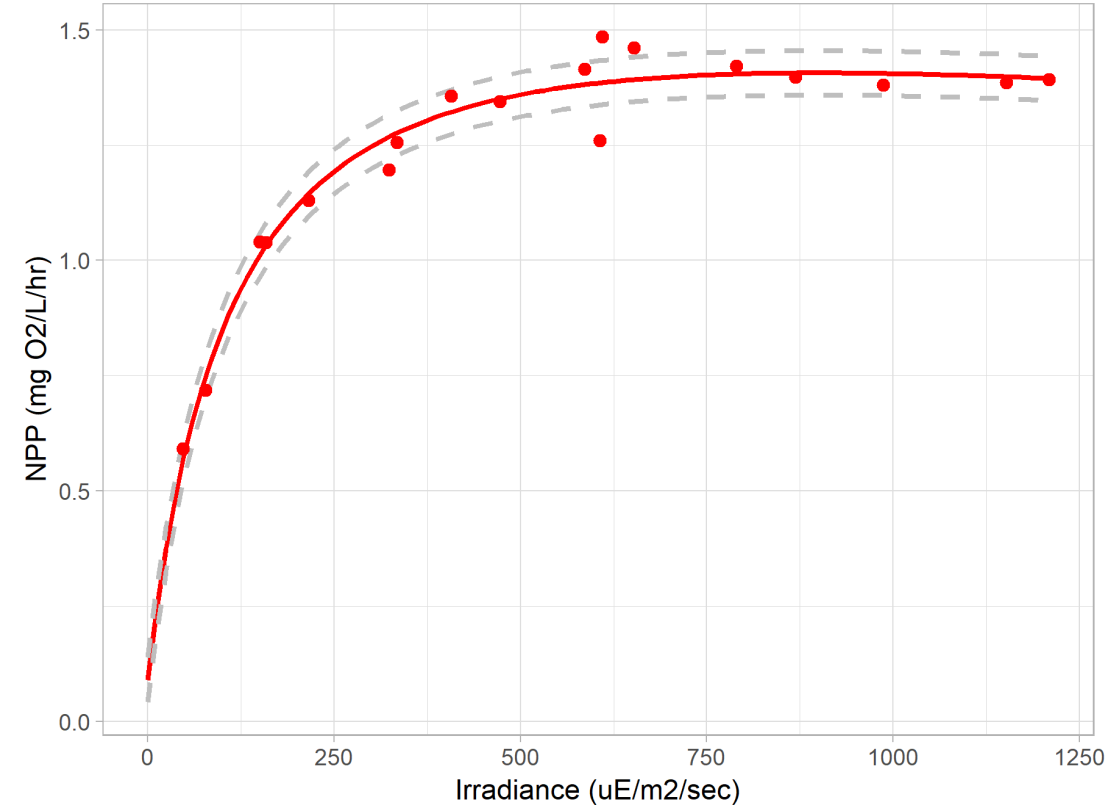
Fit-Eilers and Peeters (1988)

Y intercept	Alpha	Eopt	Ps	R-squared	RMSE
0.09030	0.01418	900.49000	1.31612	0.96105	0.04821

Station 7-2017- Aerators Off
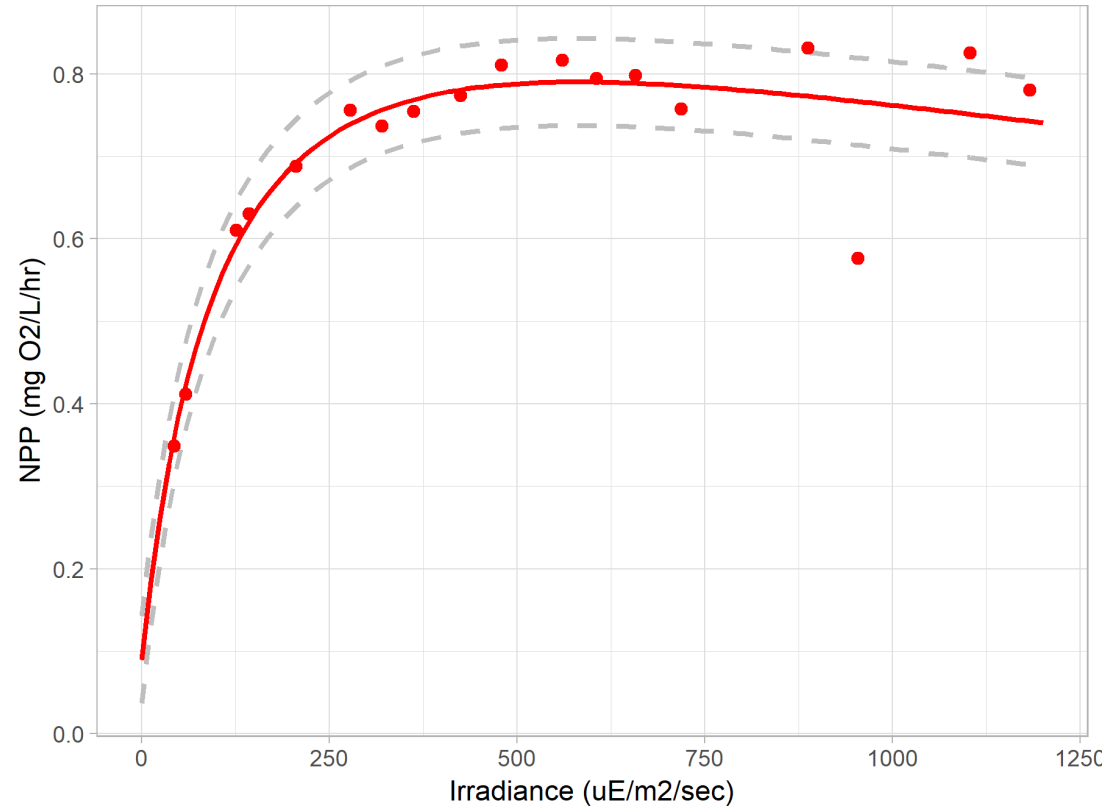
Fit-Eilers and Peeters (1988)

Y intercept	Alpha	Eopt	Ps	R-squared	RMSE
0.08985	0.00875	580.50865	0.70035	0.84923	0.05291

Station 1-2018- Aerators On
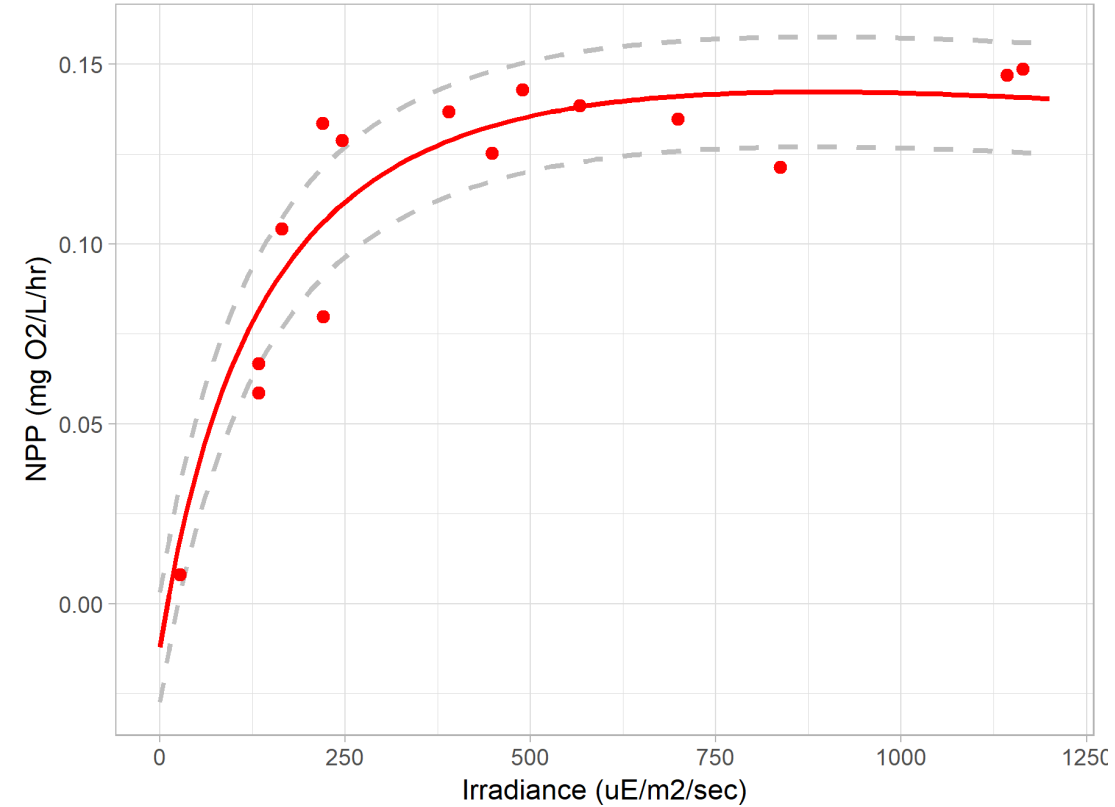
Fit-Eilers and Peeters (1988)

Y intercept	Alpha	Eopt	Ps	R-squared	RMSE
-0.01211	0.00129	886.57142	0.15442	0.84811	0.01531

Station 1-2018- Aerators Off
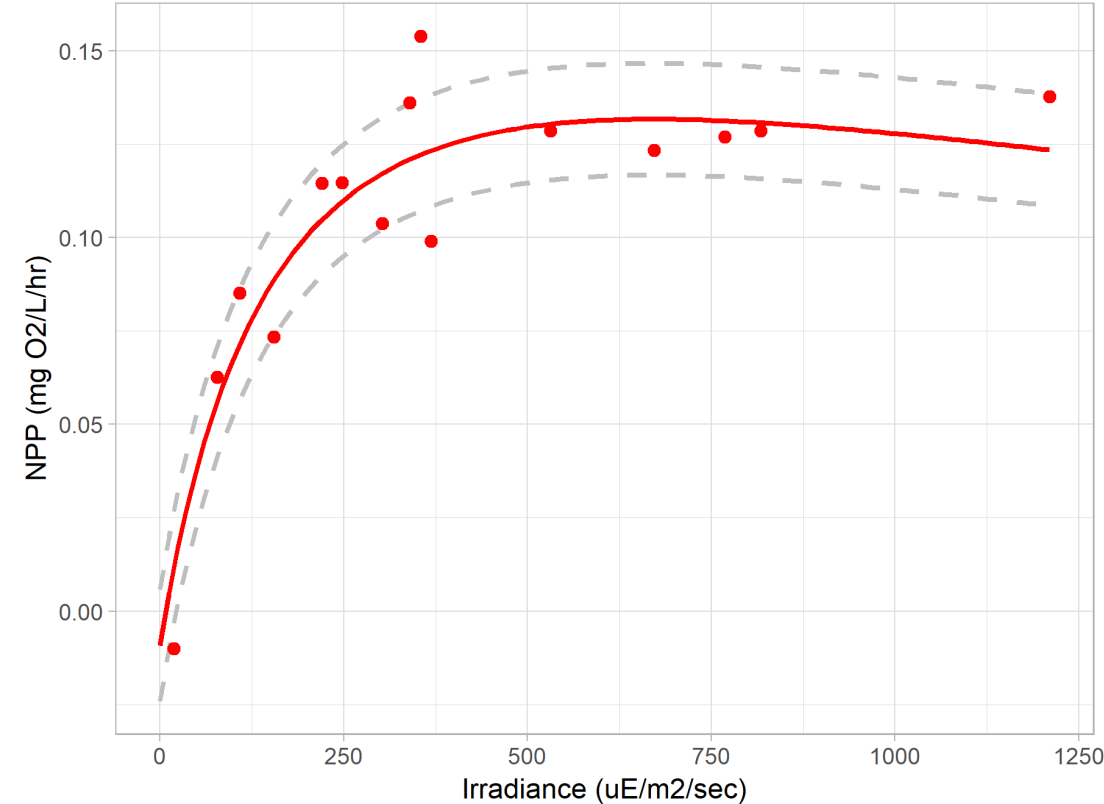
Fit-Eilers and Peeters (1988)

Y intercept	Alpha	Eopt	Ps	R-squared	RMSE
-0.00914	0.00122	670.26612	0.14086	0.85398	0.01497

114

Station 2-2018- Aerators On
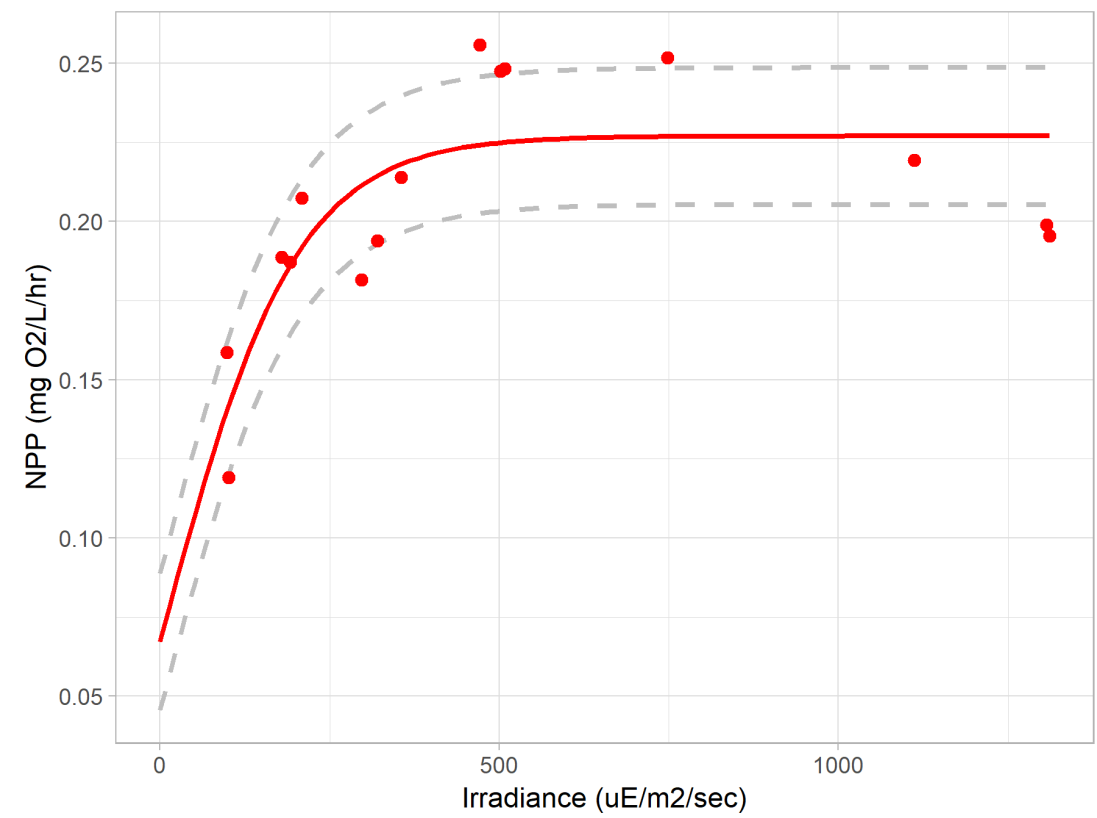
Fit-Jassby and Platt (1976)

Y intercept	Alpha	Ek	R-Squared	RMSE
0.0671885	0.0007995	199.8503137	0.6437539	0.0216091

Station 2-2018- Aerators Off
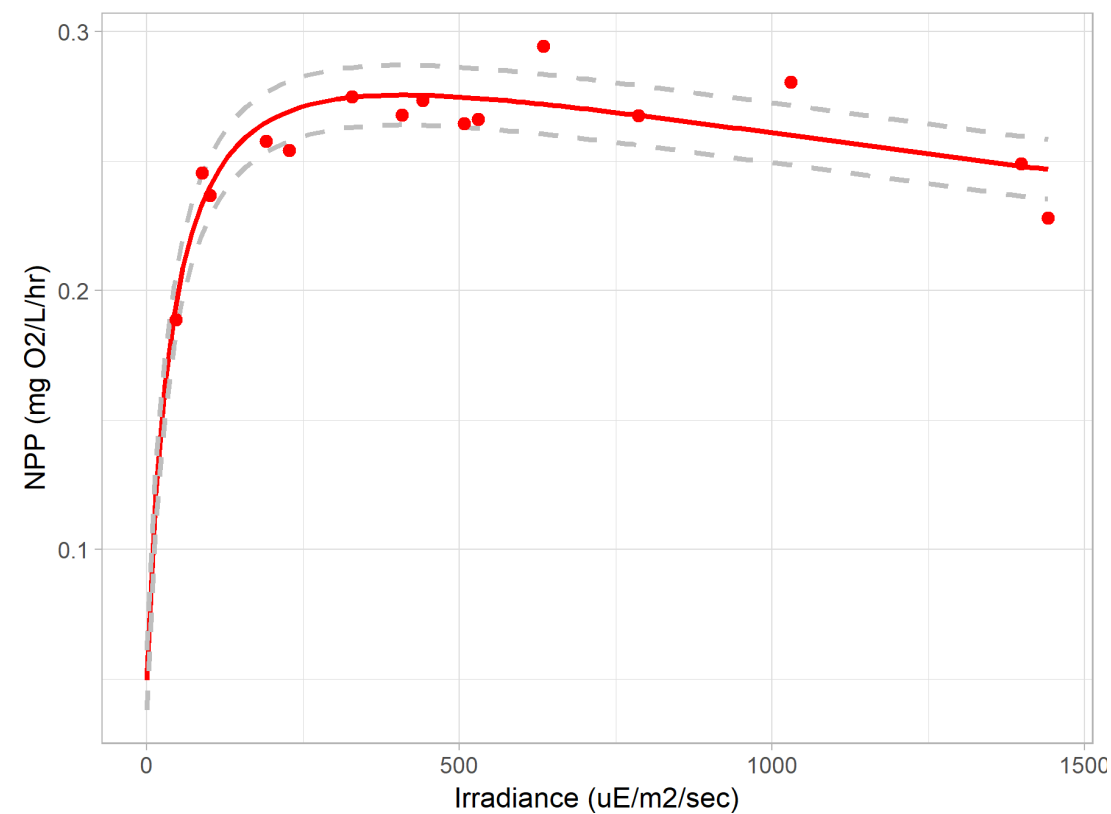
Fit-Eilers and Peeters (1988)

Y intercept	Alpha	Eopt	Ps	R-squared	RMSE
0.04942	0.00690	408.29903	0.22603	0.77887	0.01154

Station 7-2018- Aerators On
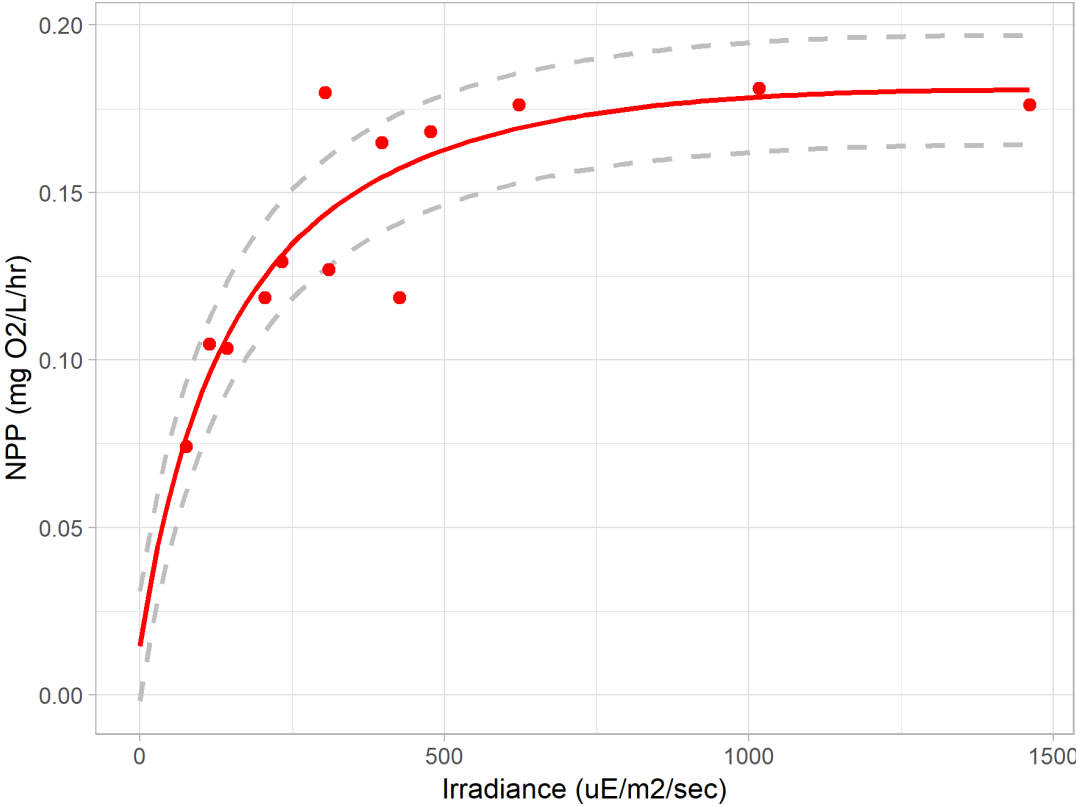
Fit-Eilers and Peeters (1988)

Y intercept	Alpha	Eopt	Ps	R-squared	RMSE
0.01454	0.00119	1445.11381	0.16595	0.77397	0.01638

117

Station 7-2018- Aerators Off
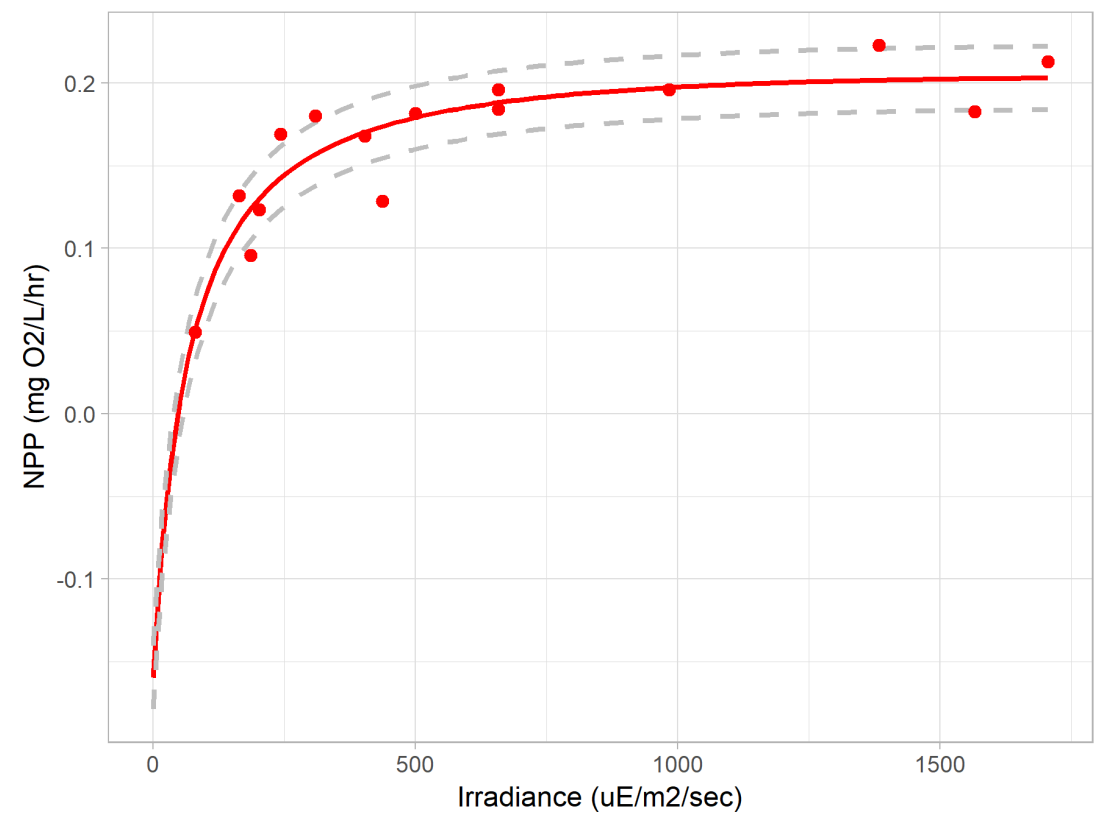
Fit-Eilers and Peeters (1988)

Y intercept	Alpha	Eopt	Ps	R-squared	RMSE
-0.15966	0.00573	1999.99162	0.36282	0.82285	0.01913

118

Station 1-2017- Aerators On
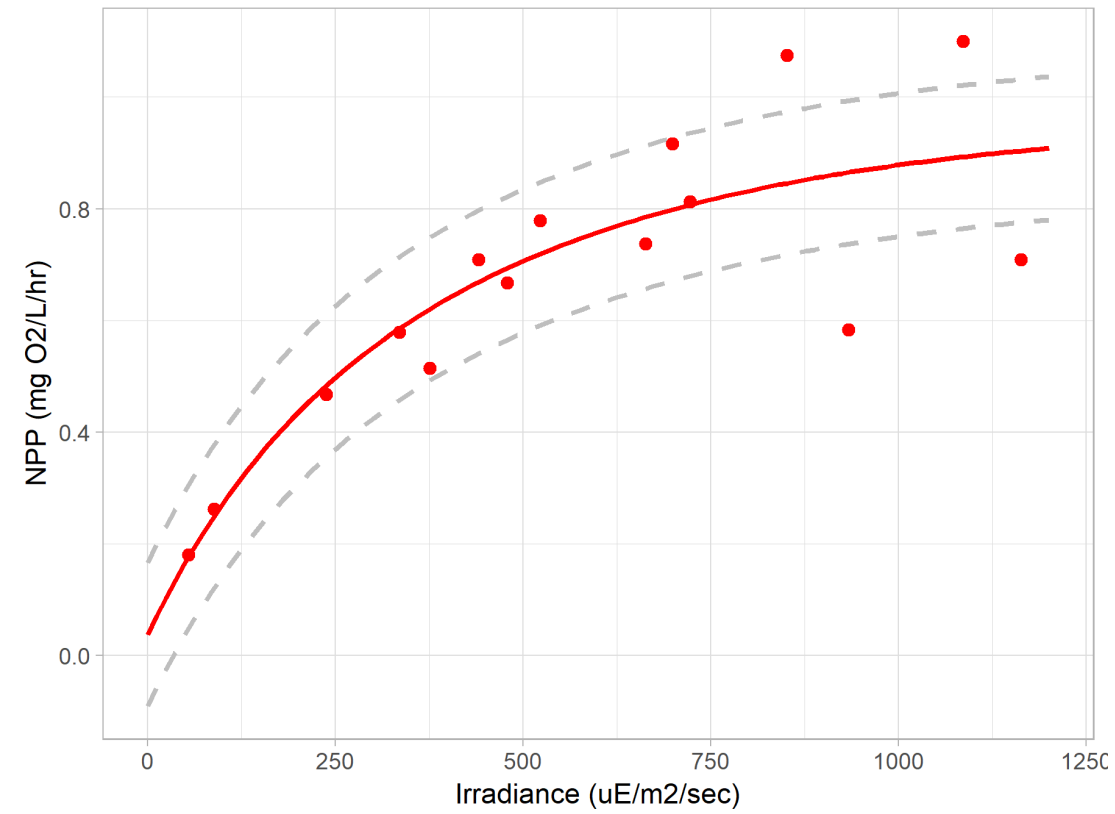
Fit-Eilers and Peeters (1988)

Y intercept	Alpha	Eopt	Ps	R-squared	RMSE
0.03757	0.00286	1999.48748	0.90743	0.73670	0.12823

Appendix C: Time Series Plots

This appendix contains the time series plots for DO, DIC, pCO_2, Active Chlorophyll, and Pheophytin. Blue points and lines denote surface values and red points and lines denote bottom values. For pCO_2 plots, the dotted black line denotes the pCO_2 of the atmosphere.
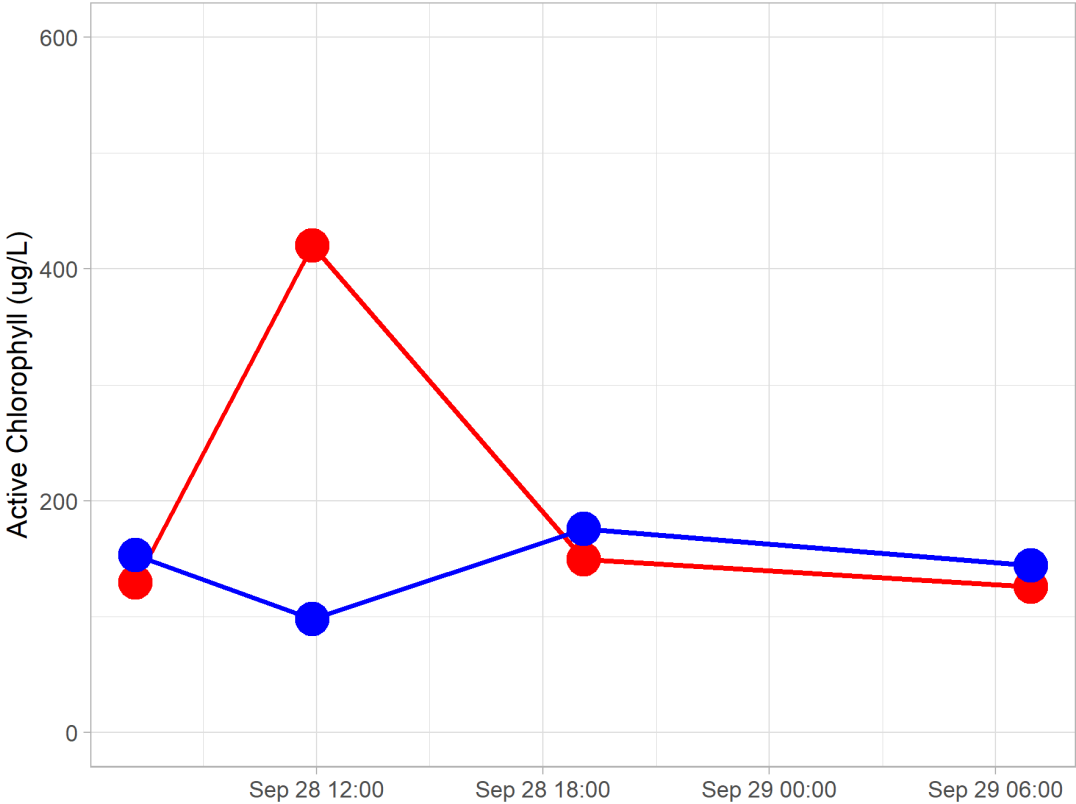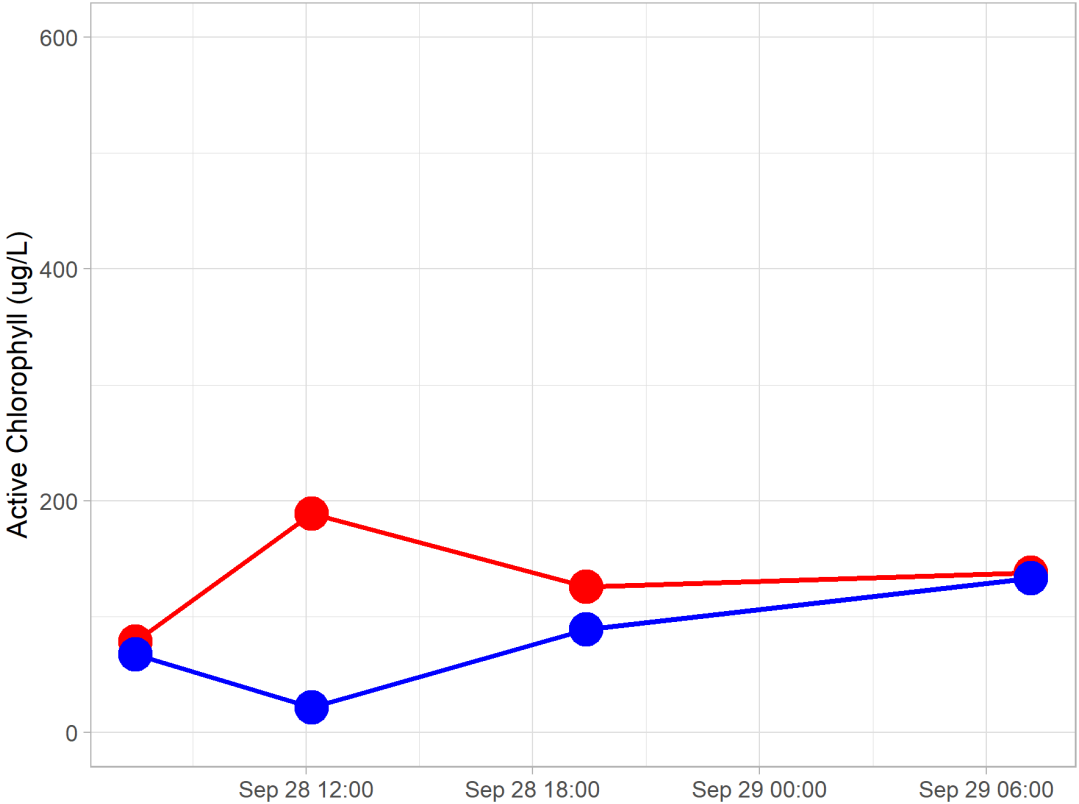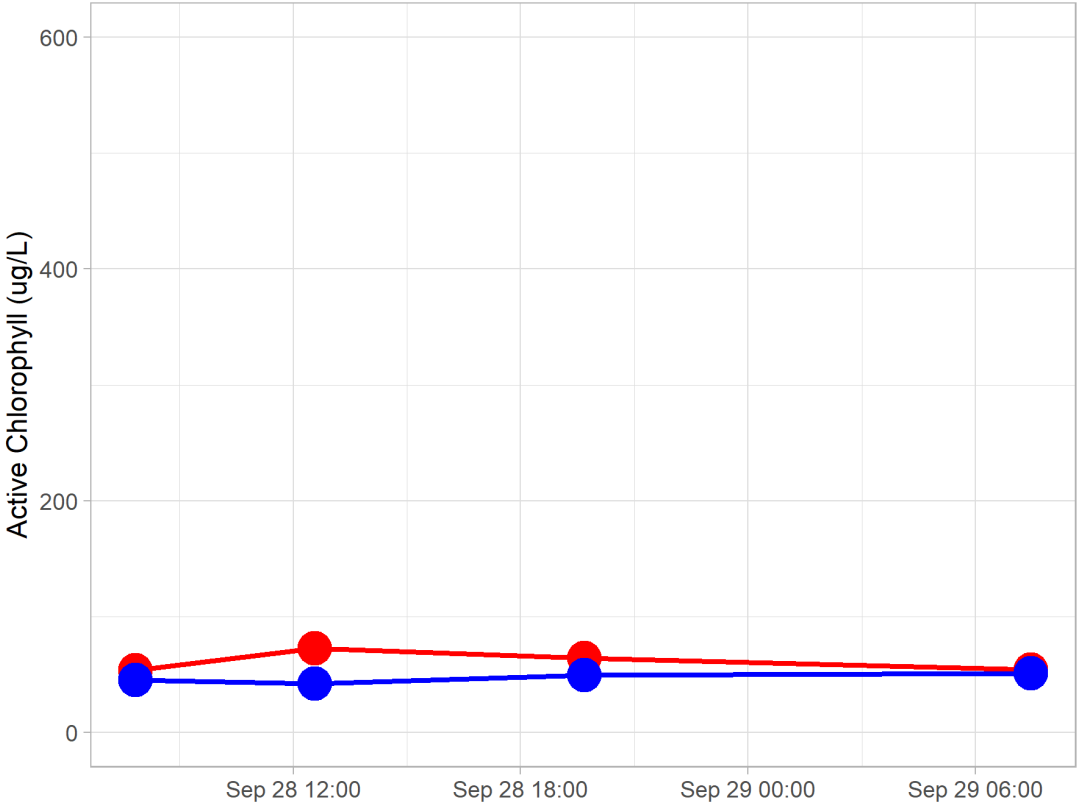
Station 1-2017
Aerators On

Station 2-2017
Aerators On

Station 4-2017
Aerators On

Station 7-2017
Aerators On

Station 1-2017
Aerators Off

125

Station 2-2017
Aerators Off

Station 4-2017
Aerators Off

Station 7-2017
Aerators Off

Station 1-2018
Aerators On

Station 2-2018
Aerators On

Station 7-2018
Aerators On

Station 1-2018
Aerators Off

Station 2-2018
Aerators Off

133

Station 7-2018
Aerators Off
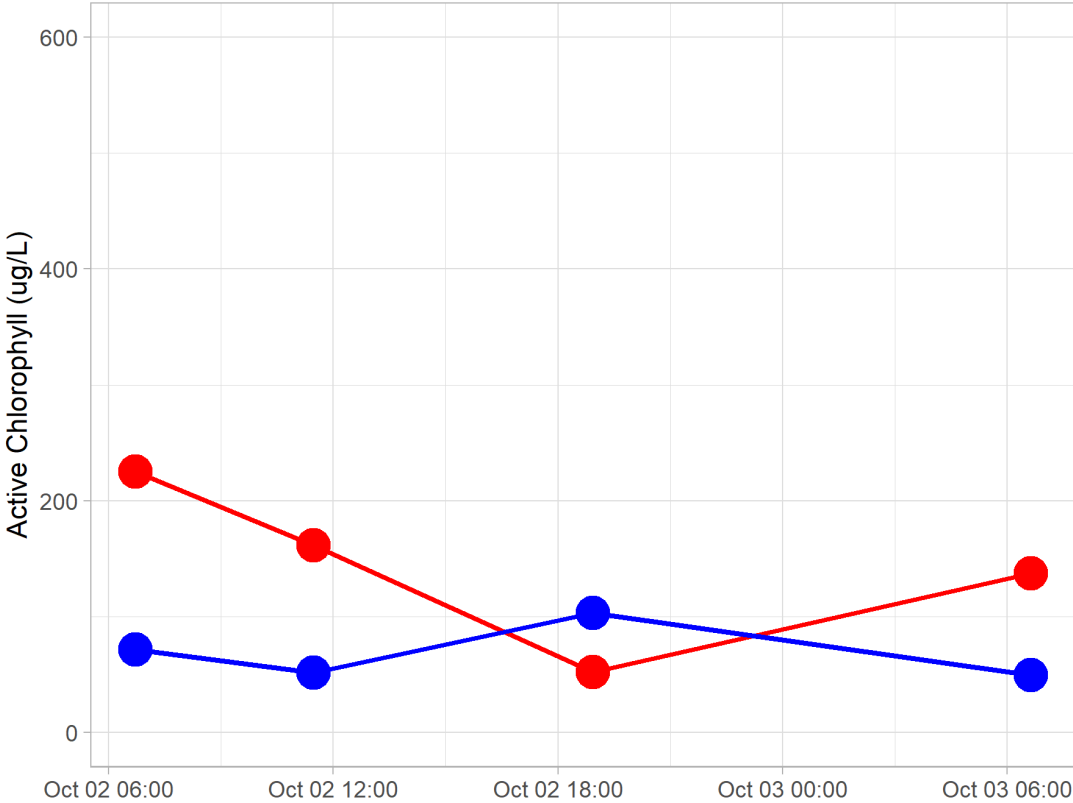
Station 1-2017
Aerators On
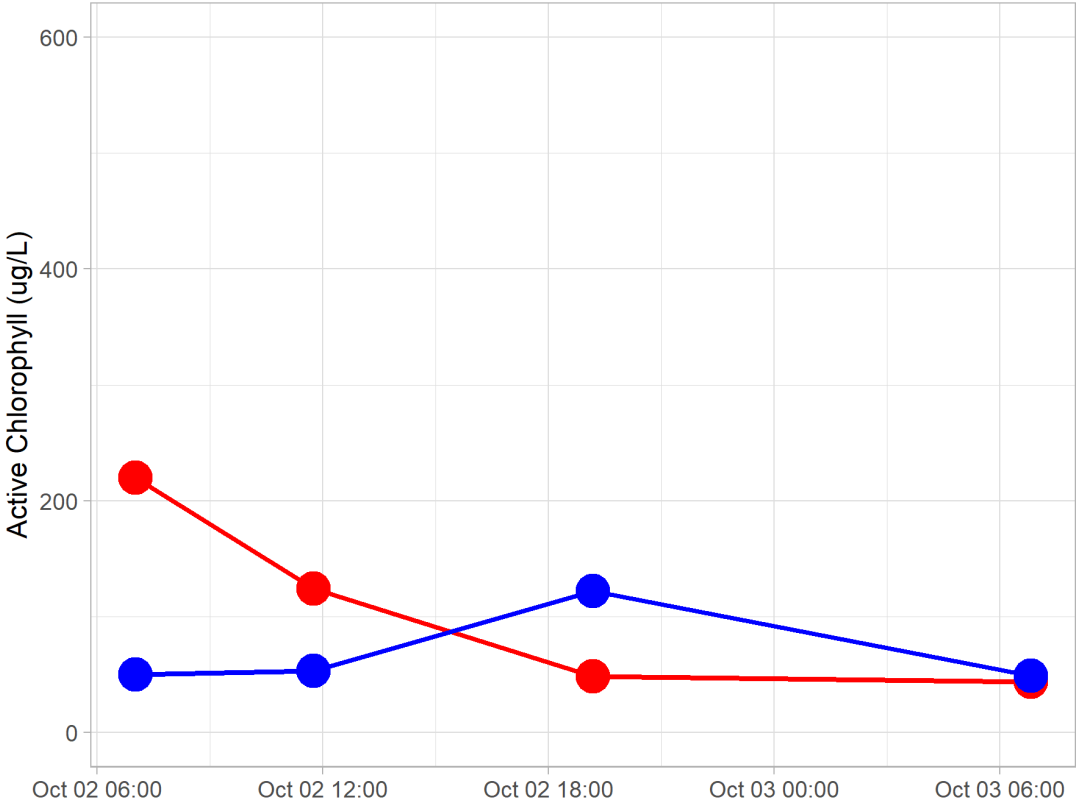
Station 2-2017

Aerators On

Station 4-2017
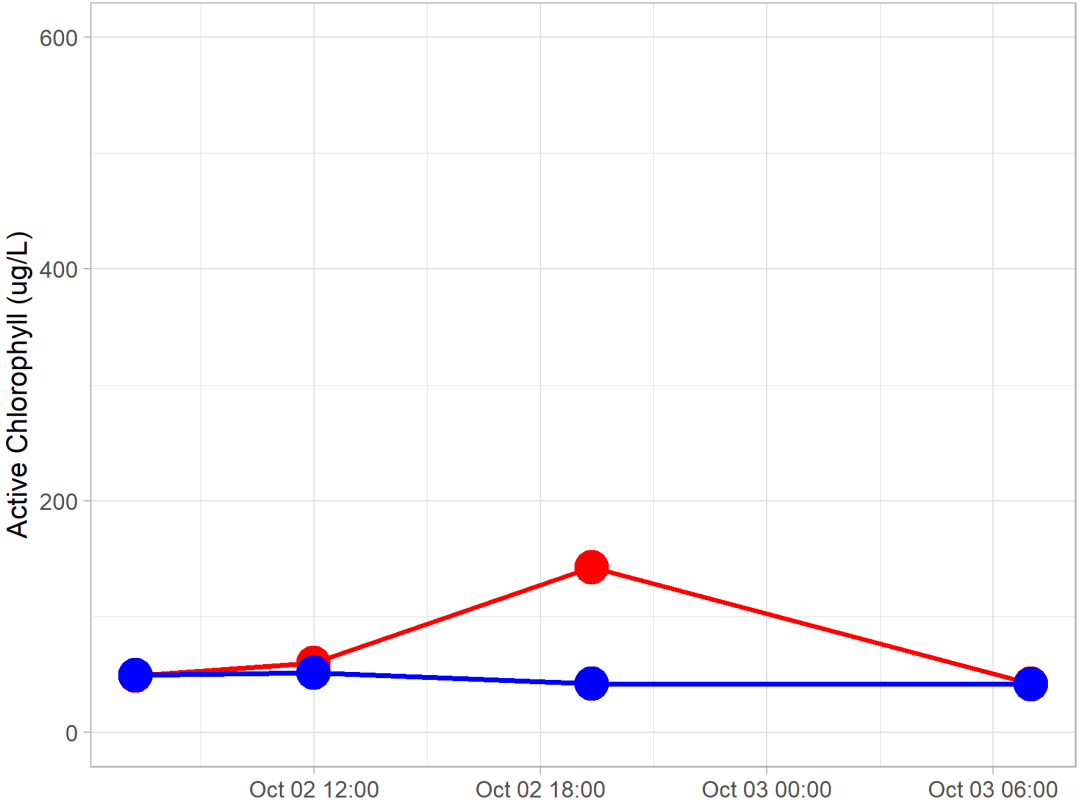Aerators On
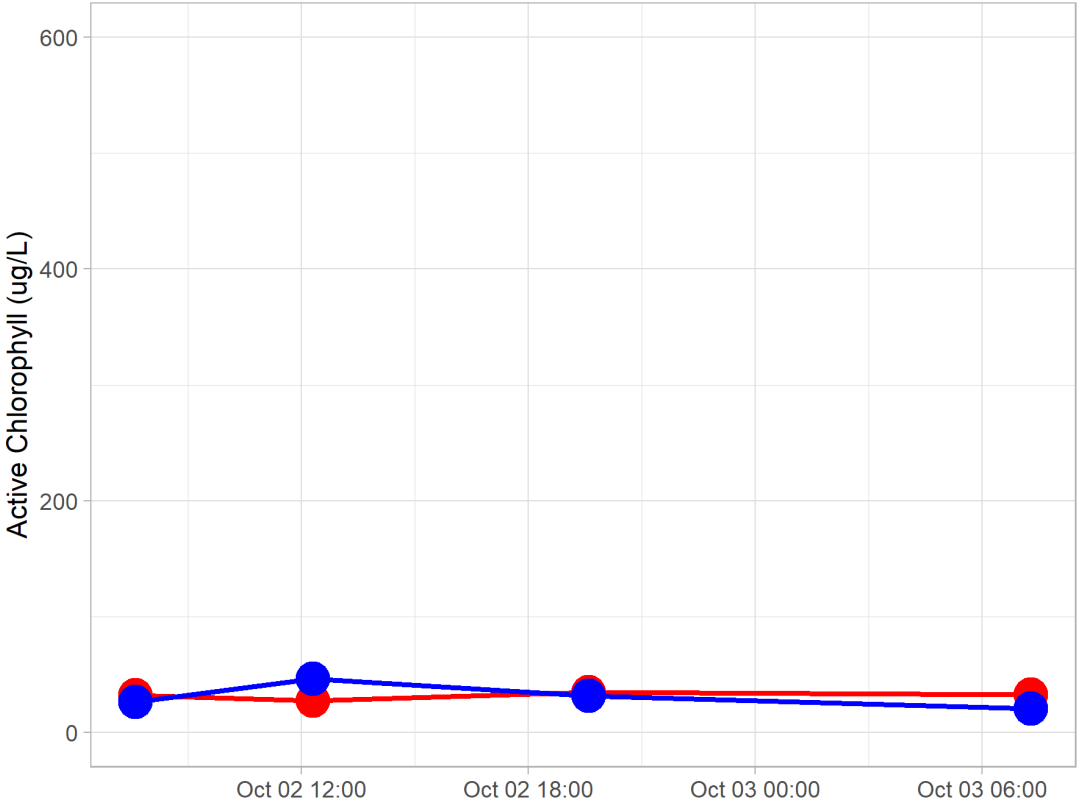
Station 7-2017
Aerators On

Station 1-2017

Aerators Off

Station 2-2017

Aerators Off

Station 4-2017

Aerators Off

Station 1-2018

Aerators On

Station 2-2018

Aerators On

Station 7-2018
Aerators On

Station 1-2018

Aerators Off

Station 2-2018

Aerators Off

Station 7-2018

Aerators Off

148

Station 1-2017
Aerators On

Station 2-2017
Aerators On

Station 4-2017
Aerators On

Station 7-2017
Aerators On

Station 1-2017

Aerators Off

Station 2-2017

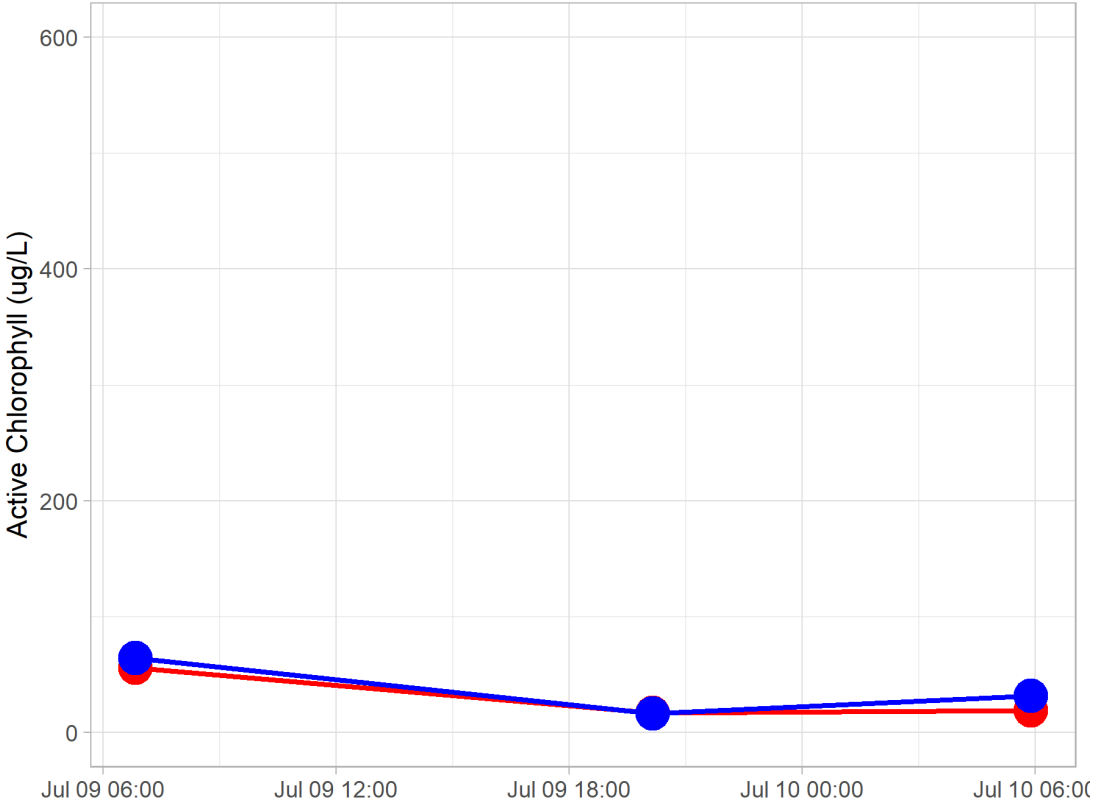Aerators Off

Station 4-2017

Aerators Off
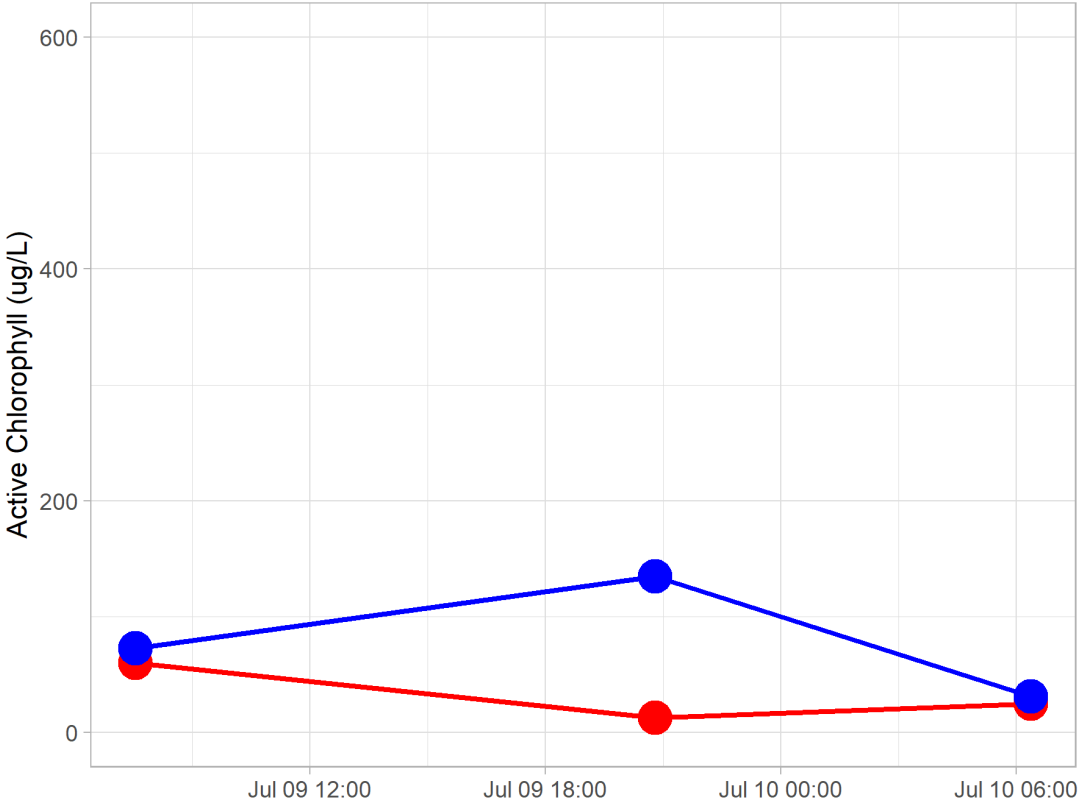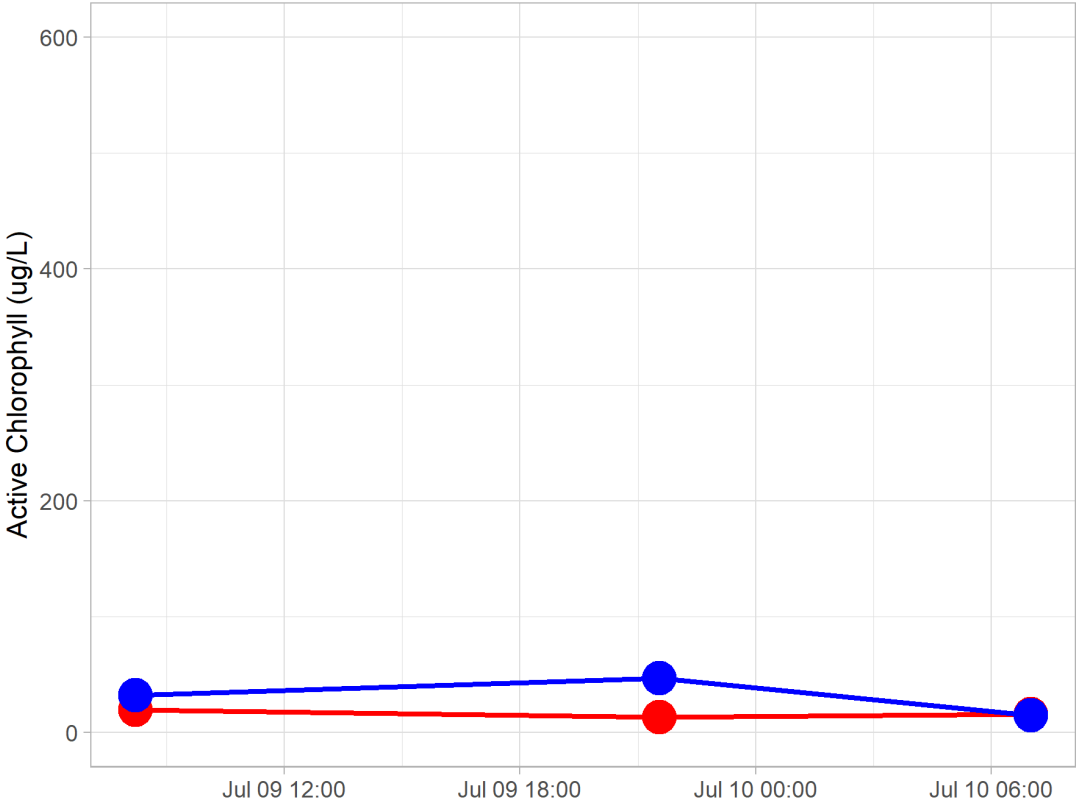
Station 7-2017
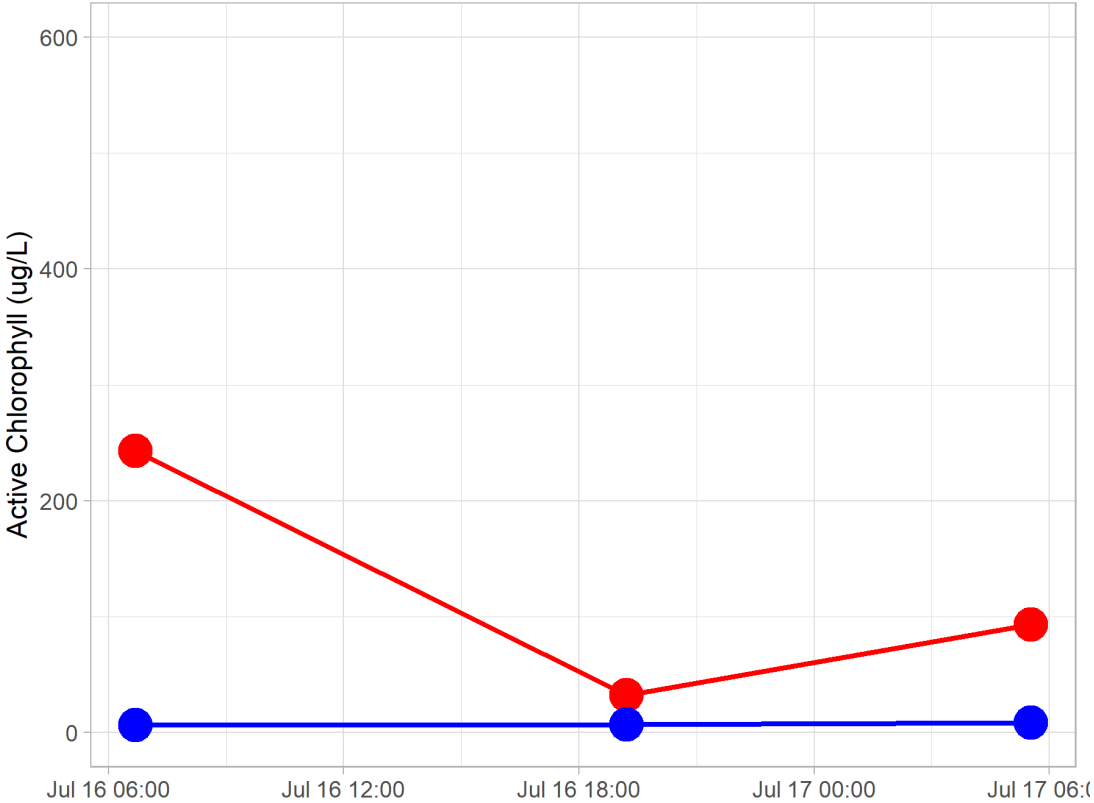
Aerators Off

156

Station 1-2018
Aerators On

Station 2-2018
Aerators On

Station 7-2018
Aerators On

Station 1-2018

Aerators Off

Station 2-2018
Aerators Off

Station 7-2018
Aerators Off

Station 1-2017

Aerators On

Station 2-2017

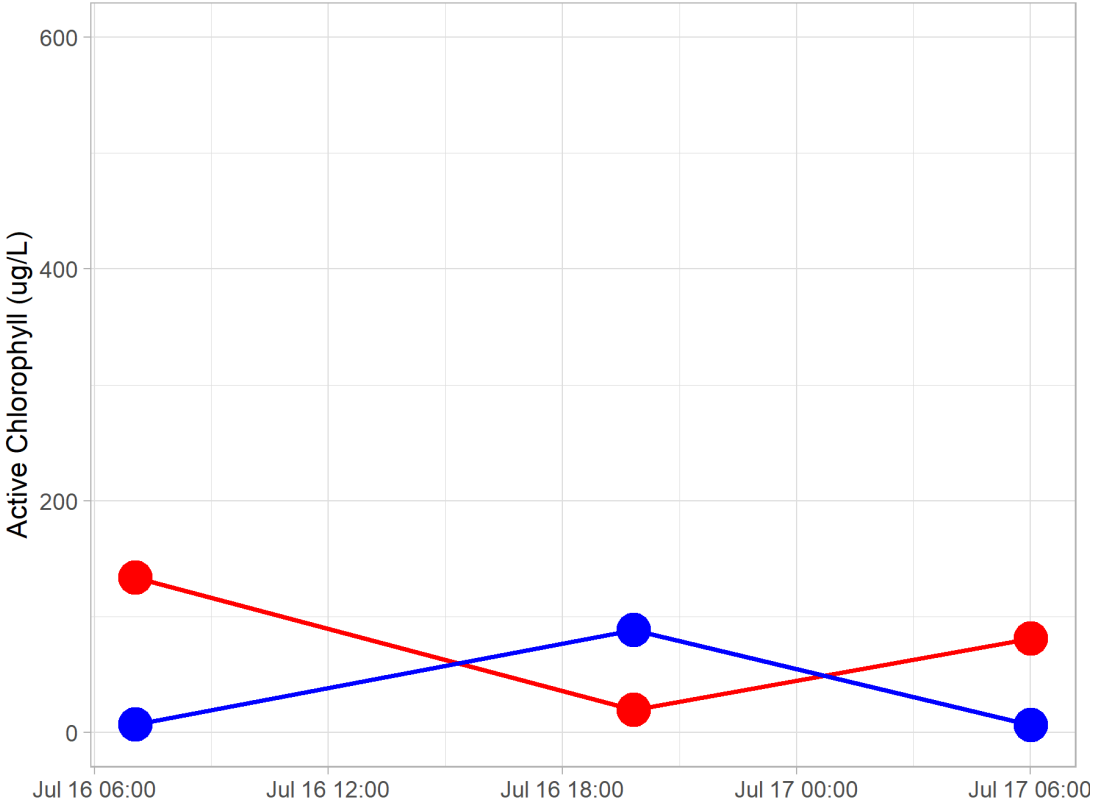Aerators On

Station 4-2017

Aerators On

Station 7-2017

Aerators On

Station 1-2017

Aerators Off

Station 2-2017

Aerators Off

Station 4-2017

Aerators Off

Station 7-2017

Aerators Off

Active Chlorophyll (ug/L)

600

400

200

0

Oct 02 12:00   Oct 02 18:00   Oct 03 00:00   Oct 03 06:00

170

Station 1-2018

Aerators On

Station 2-2018

Aerators On

172

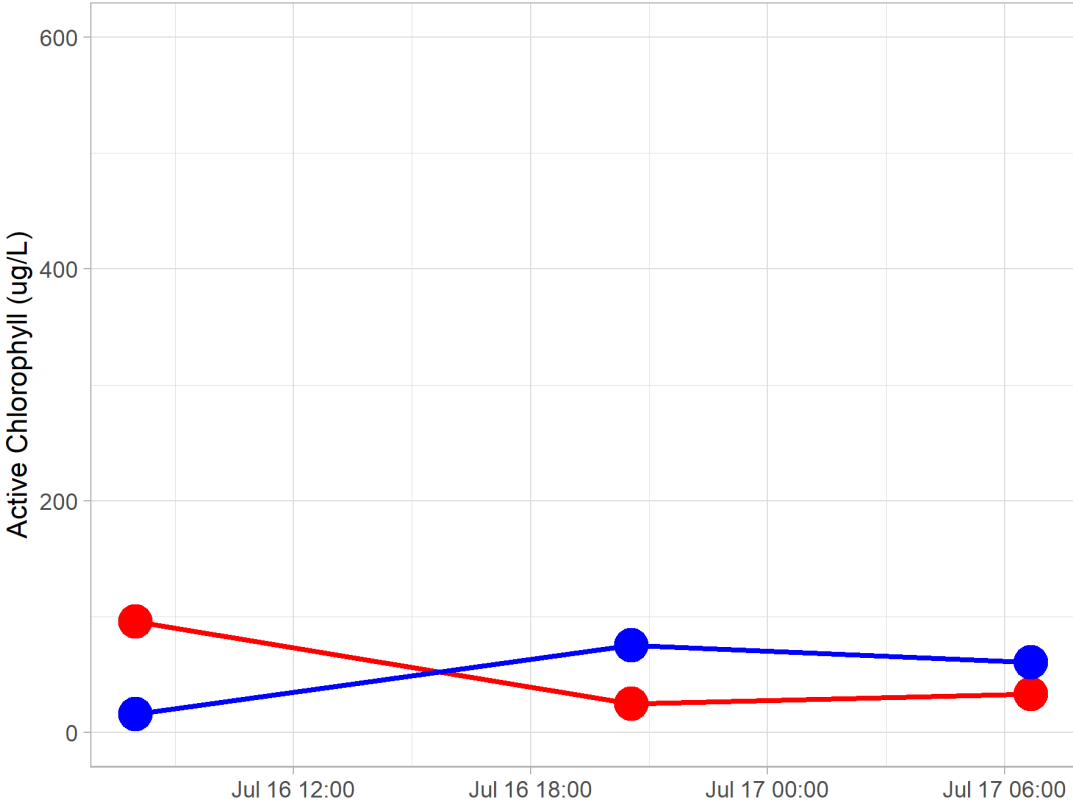Station 7-2018

Aerators On

173

Station 1-2018

Aerators Off

174

Station 2-2018

Aerators Off

Station 7-2018

Aerators Off

Station 1-2017

Aerators On

Station 2-2017

Aerators On

Station 4-2017

Aerators On

Station 7-2017

Aerators On

Station 1-2017

Aerators Off

181

Station 2-2017

Aerators Off

Station 7-2017

Aerators Off

Station 1-2018

Aerators On

Station 2-2018

Aerators On

Station 7-2018
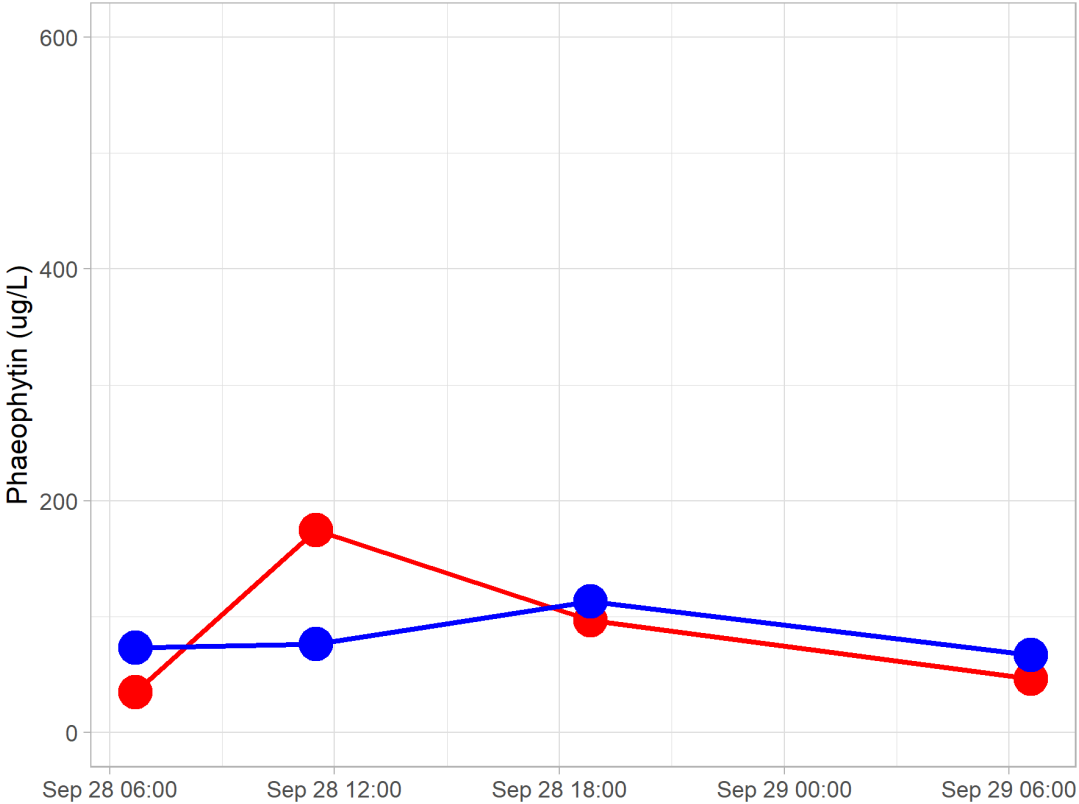
Aerators On

Station 1-2018

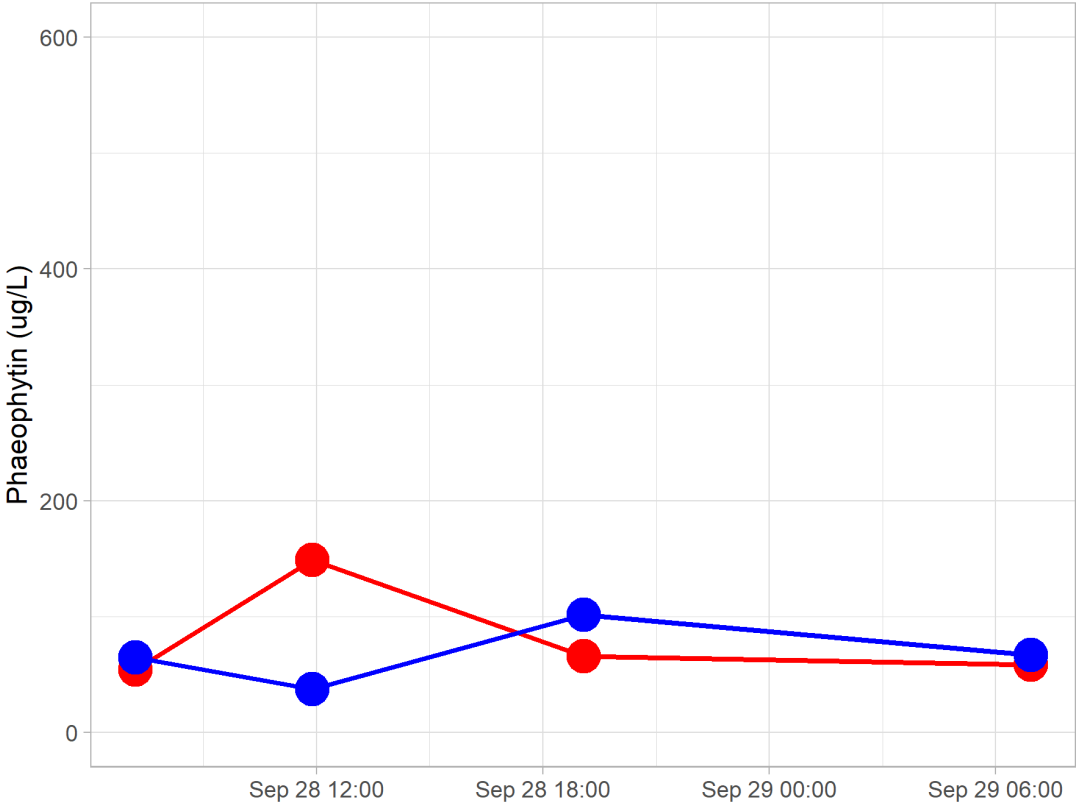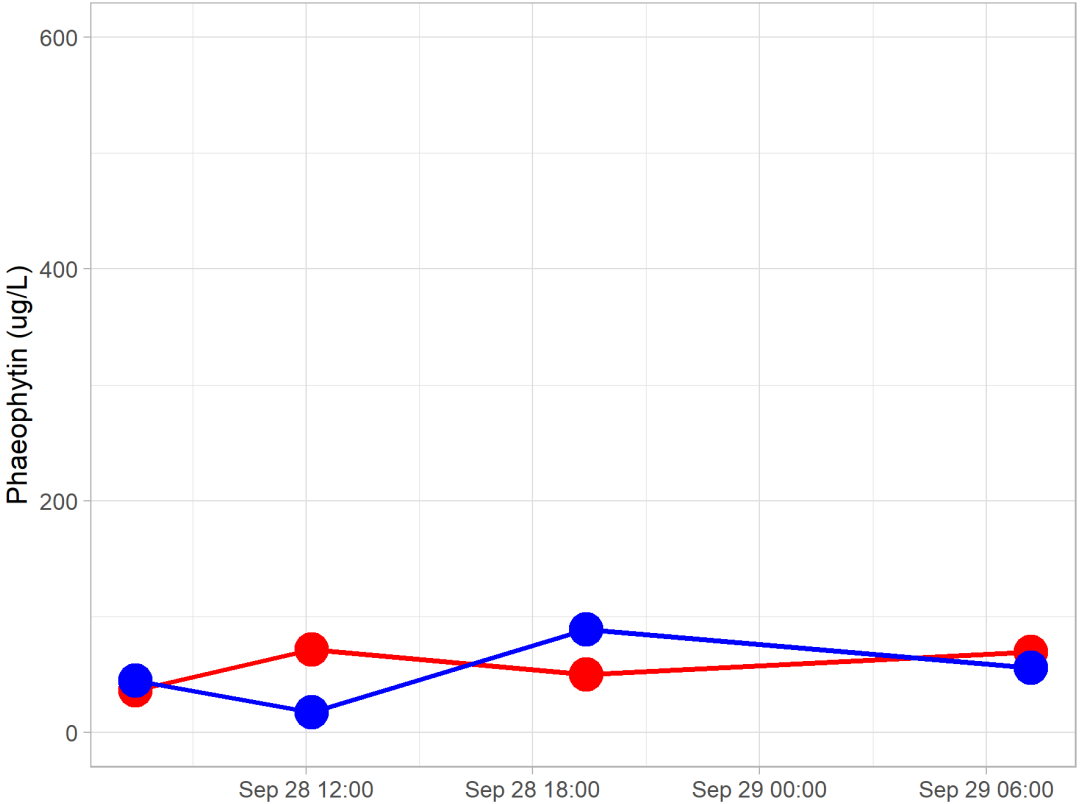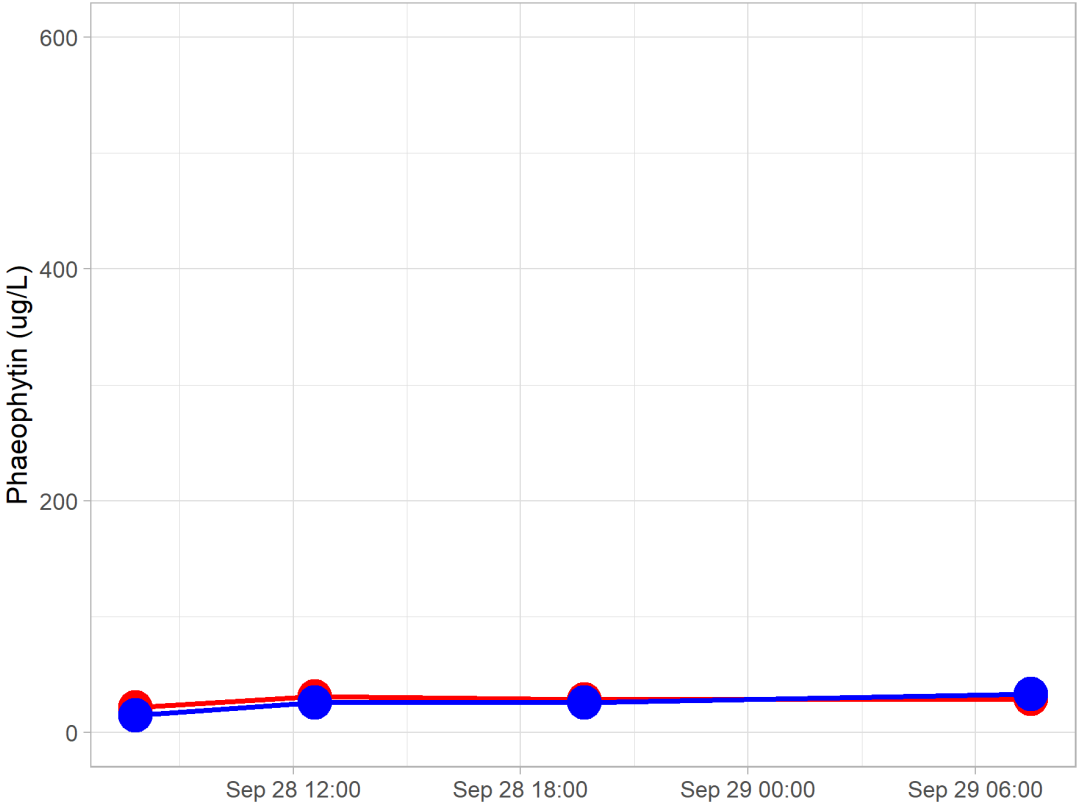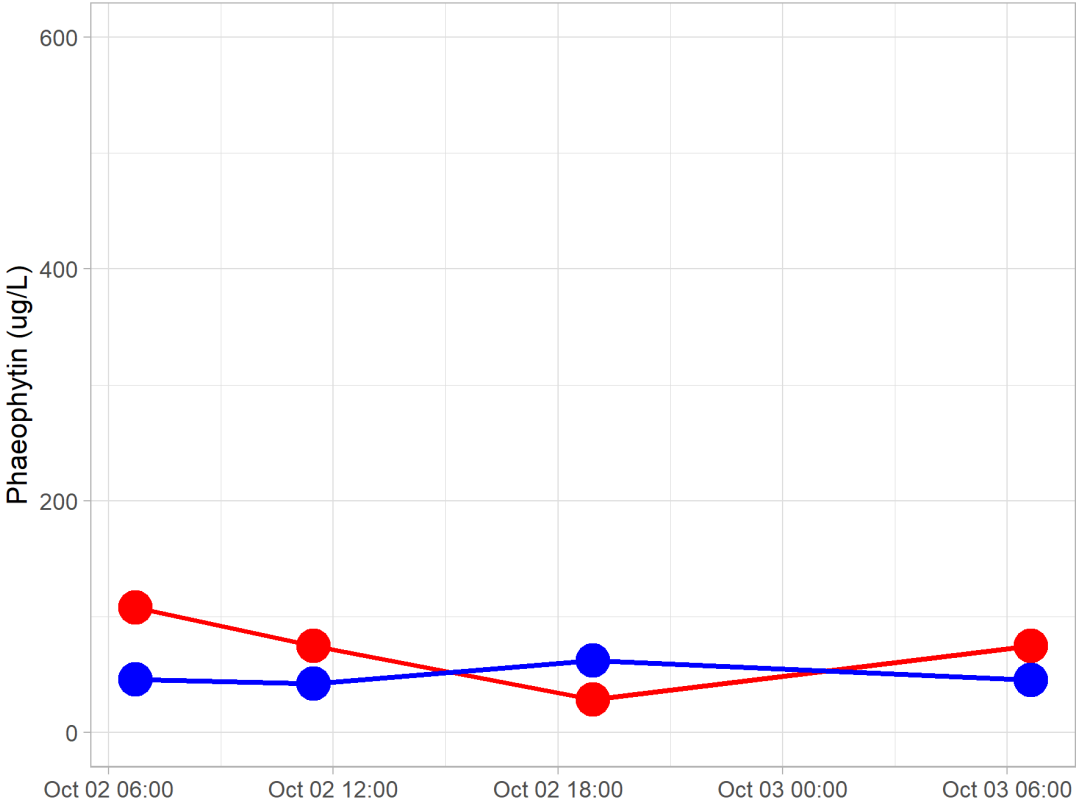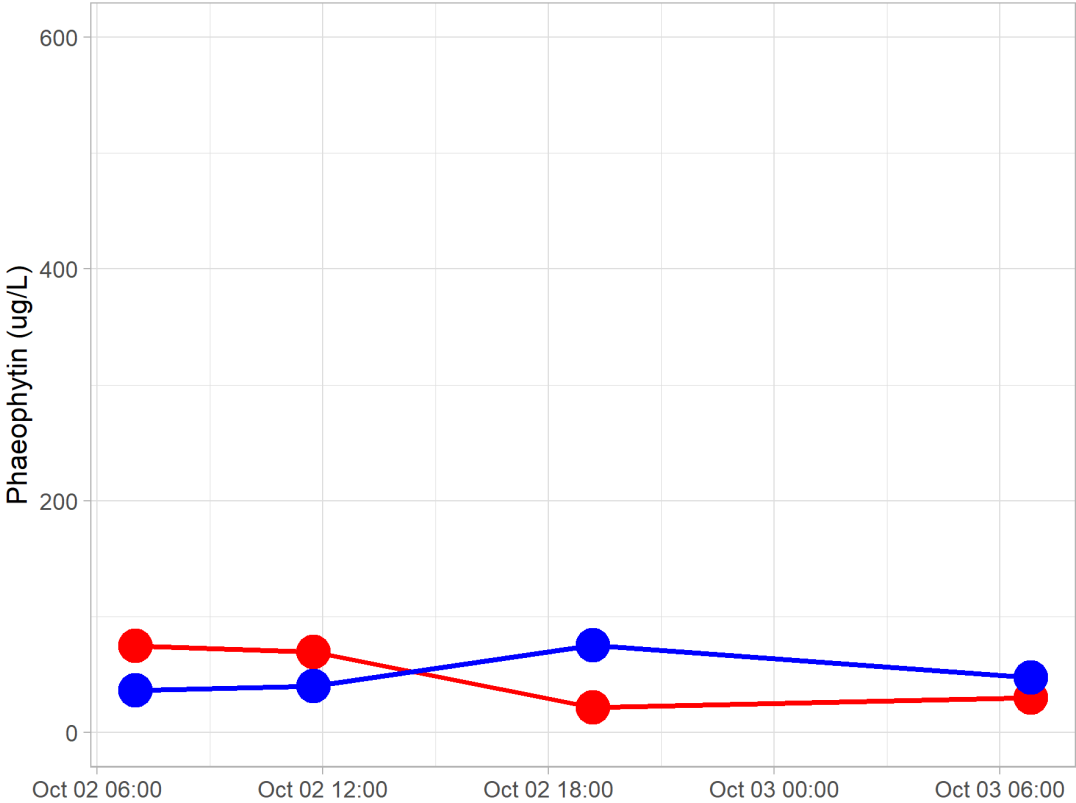Aerators Off

Station 2-2018

Aerators Off

Station 7-2018

Aerators Off

Appendix D: Linear Model Fits

This appendix contains the linear model fits and test results for the data represented on Table 12 in Chapter 2. Section 1 contains the model fits from metabolic data as measured in the open water DIC method, Section 2 contains the model fits from metabolic data as measured in the open water DO method, and Section 3 contains the model fits as measured in the photosynthetron method. Circles represent data points from 2017 and triangles represent data points from 2018. Blue points represent data points from when the aerators were on and orange points represent data from when the aerators were off. The black line in each graph denotes the linear model itself. Significance was evaluated at a 95% confidence interval.

DIC Metabolism Correlation
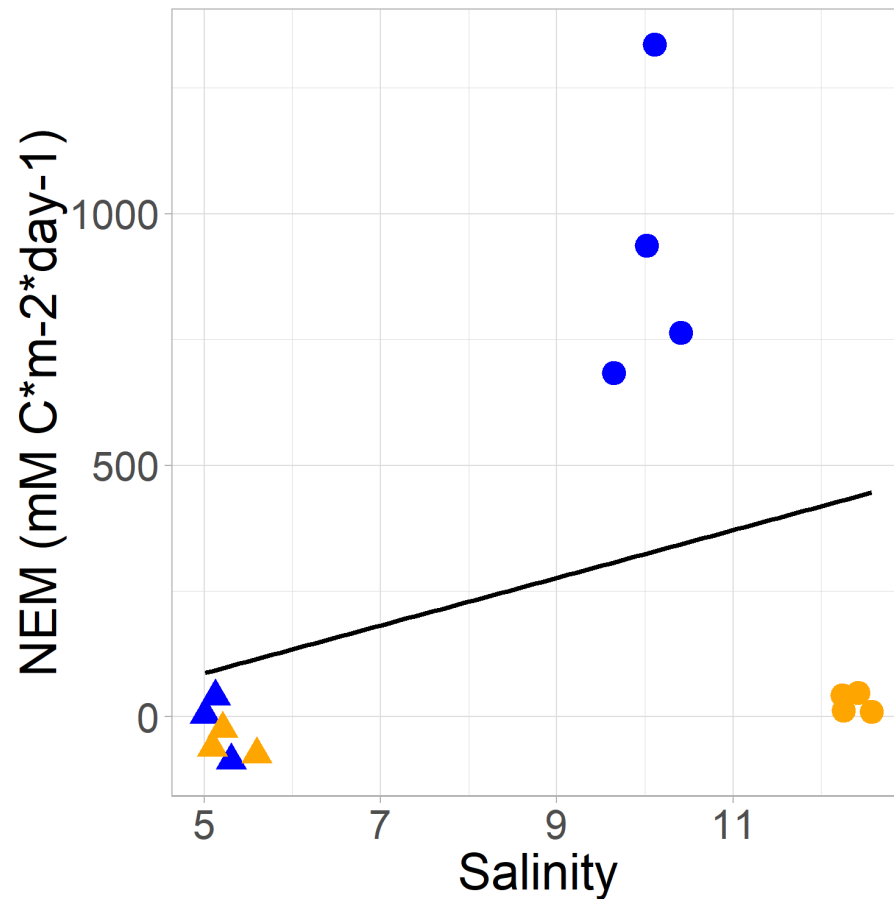
Residuals:

Min	1Q	Median	3Q	Max
-450.5	-323.8	-139.4	278.4	1022.2

Coefficients:

	Estimate	Std. Error	t value	Pr(>|t|)
(Intercept)	-128.65	369.33	-0.348	0.734
data$Salinity	43.80	40.22	1.089	0.298

Residual standard error: 465.9 on 12 degrees of freedom

Multiple R-squared: 0.08994, Adjusted R-squared: 0.0141

F-statistic: 1.186 on 1 and 12 DF, p-value: 0.2975
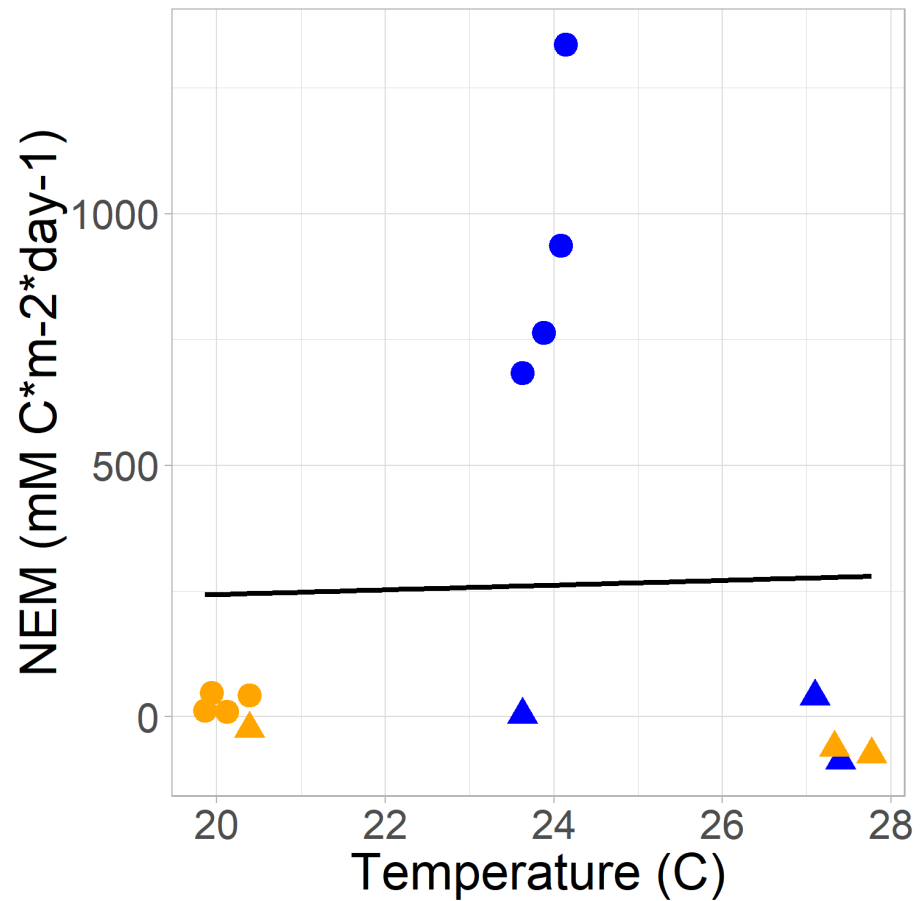
Residuals:

    Min   1Q Median   3Q   Max

-369.0 -261.8 -235.5 281.6 1081.5

Coefficients:

                    Estimate Std. Error t value Pr(>|t|)

(Intercept)   52.970   1062.140 0.050   0.961

data$Temperature..C.   8.368   44.766 0.187   0.855

Residual standard error: 487.6 on 12 degrees of freedom

Multiple R-squared: 0.002903,   Adjusted R-squared: -0.08019

F-statistic: 0.03494 on 1 and 12 DF, p-value: 0.8548
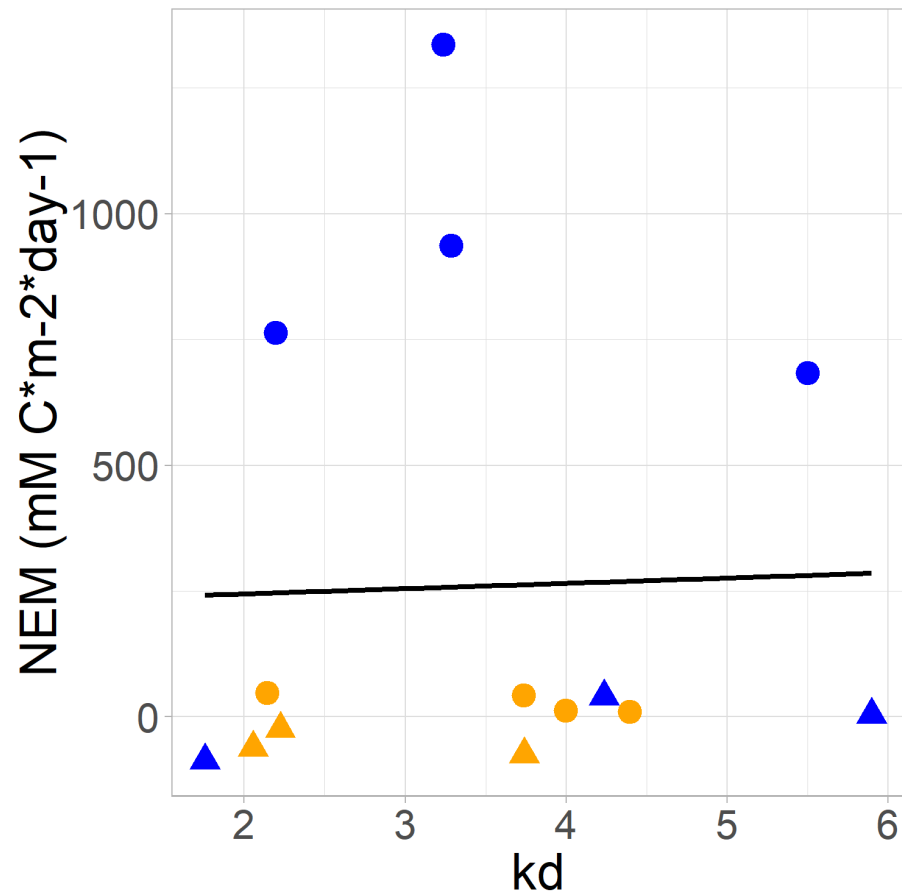
Residuals:

Min	1Q	Median	3Q	Max
-326.5	-288.3	-264.8	265.1	1088.2

Coefficients:

	Estimate	Std. Error	t value	Pr(>|t|)
(Intercept)	222.757	384.082	0.580	0.573
data$kd	7.884	104.502	0.075	0.941

Residual standard error: 488.2 on 12 degrees of freedom

Multiple R-squared: 0.0004741, Adjusted R-squared: -0.08282

F-statistic: 0.005692 on 1 and 12 DF, p-value: 0.9411
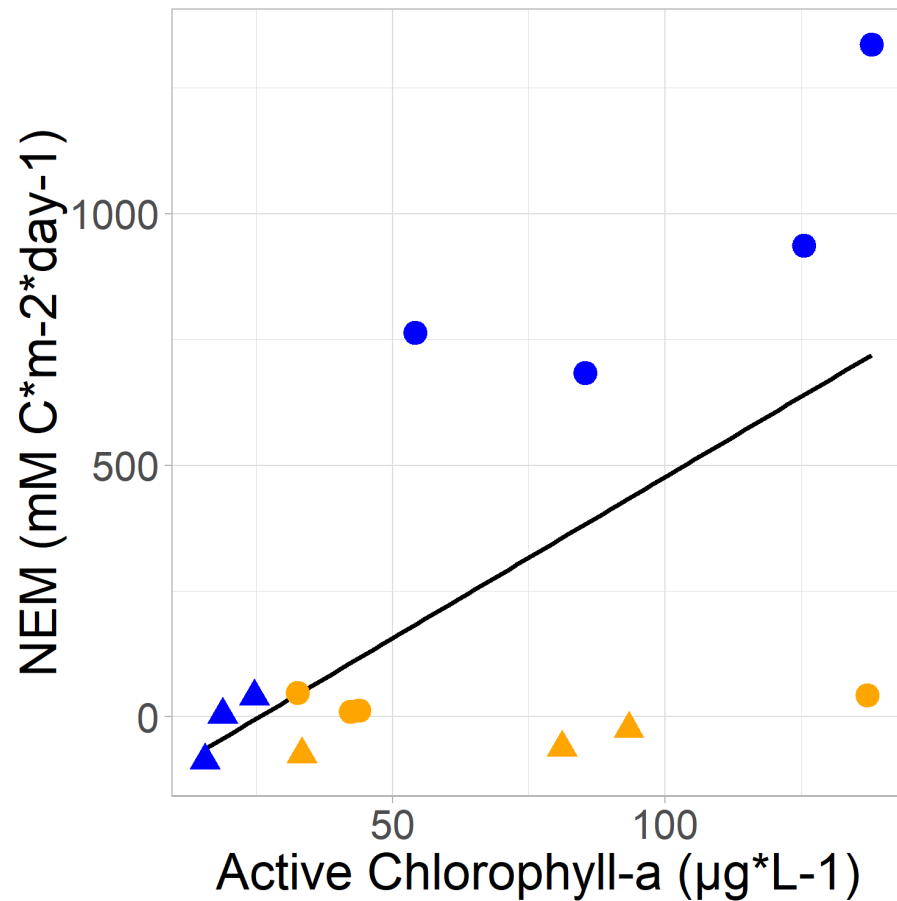
Residuals:

Min	1Q	Median	3Q	Max
-733.2	-124.0	-9.0	247.7	641.1

Coefficients:

	Estimate	Std. Error	t value
(Intercept)	-160.345	197.698	-0.811
data$Active.Chlorophyll.a..ug.L.	6.206	2.520	2.463

	Pr(>|t|)
(Intercept)	0.4331
data$Active.Chlorophyll.a..ug.L.	0.0299 *

Signif. codes: 0 '***' 0.001 '**' 0.01 '*' 0.05 '.' 0.1 ' ' 1

Residual standard error: 398 on 12 degrees of freedom

Multiple R-squared: 0.3357,   Adjusted R-squared: 0.2803

F-statistic: 6.064 on 1 and 12 DF, p-value: 0.0299
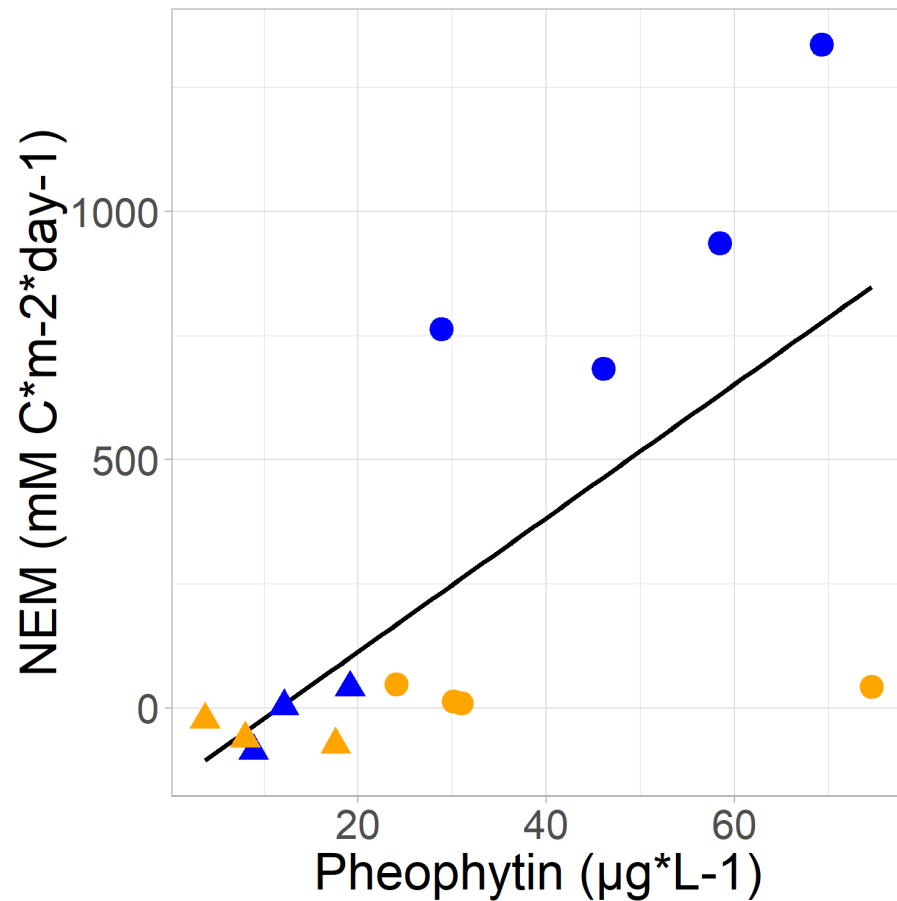
Residuals:

Min	1Q	Median	3Q	Max
-857.69	-143.85	-34.38	197.07	590.32

Coefficients:

	Estimate	Std. Error	t value	Pr(>|t|)
(Intercept)	-148.616	173.908	-0.855	0.4095
data$Pheophytin..ug.L.	12.915	4.581	2.819	0.0155 *

Signif. codes: 0 '***' 0.001 '**' 0.01 '*' 0.05 '.' 0.1 ' ' 1

Residual standard error: 378.8 on 12 degrees of freedom

Multiple R-squared: 0.3984,   Adjusted R-squared: 0.3483

F-statistic: 7.947 on 1 and 12 DF, p-value: 0.01549
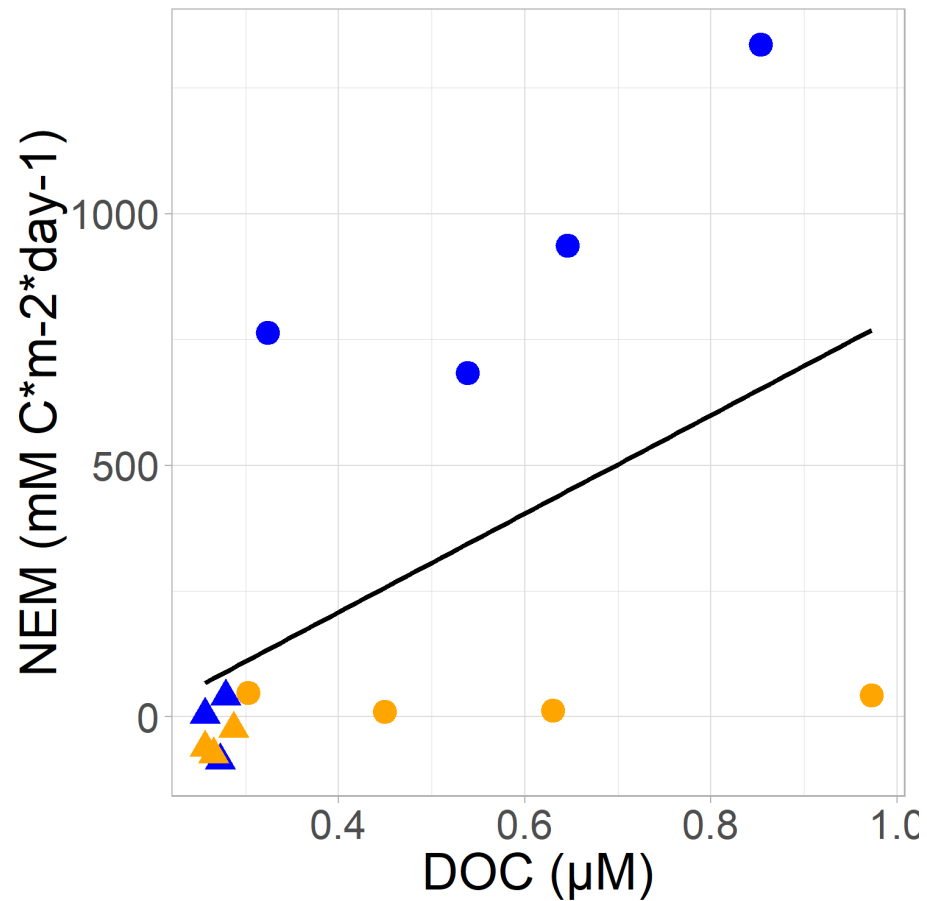
Residuals:

Min	1Q	Median	3Q	Max
-768.21	-167.95	-94.87	253.57	720.04

Coefficients:

	Estimate	Std. Error	t value	Pr(>|t|)	
(Intercept)	-163.5	253.7	-0.645	0.5313	
data$DOC	913.9	499.3	1.831	0.0921	.

Signif. codes: 0 '***' 0.001 '**' 0.01 '*' 0.05 '.' 0.1 ' ' 1

Residual standard error: 431.8 on 12 degrees of freedom

Multiple R-squared: 0.2183,   Adjusted R-squared: 0.1531

F-statistic: 3.351 on 1 and 12 DF, p-value: 0.0921
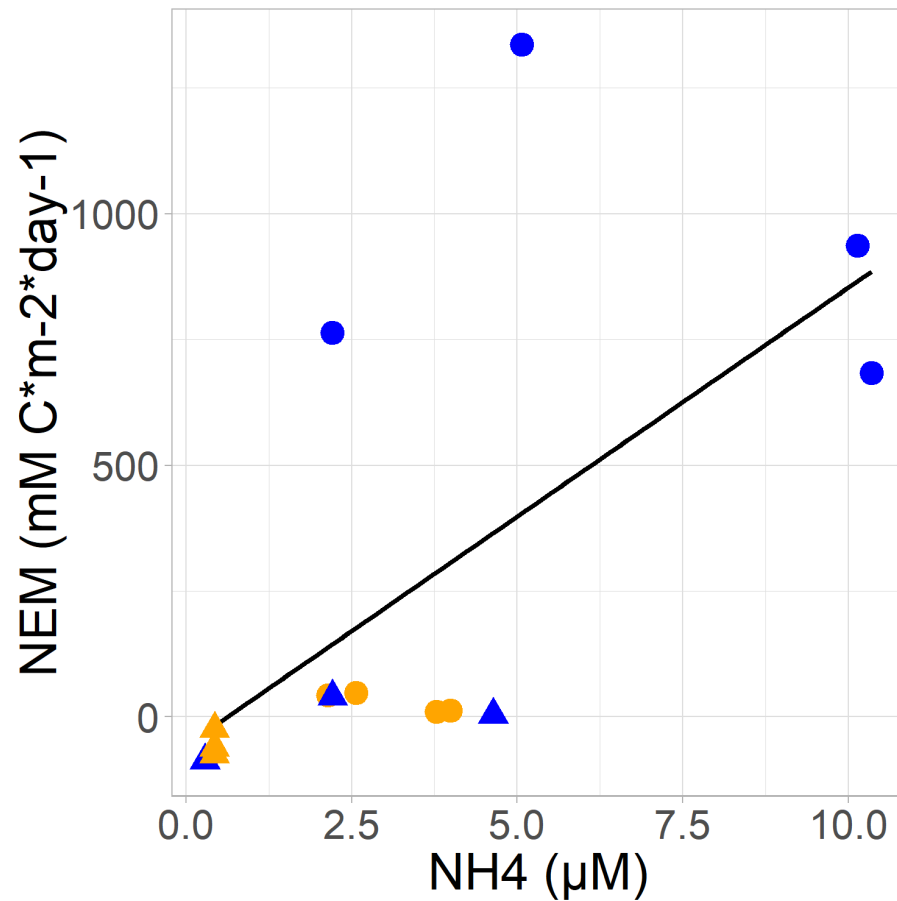
Residuals:

   Min   1Q Median   3Q   Max

-352.69 -190.25 -68.83 -3.50 940.49

Coefficients:

        Estimate Std. Error t value Pr(>|t|)

(Intercept) -68.98   148.99 -0.463 0.6517

data$NH4   91.72   31.71 2.893 0.0135 *

Signif. codes: 0 '***' 0.001 '**' 0.01 '*' 0.05 '.' 0.1 ' ' 1

Residual standard error: 374.8 on 12 degrees of freedom

Multiple R-squared: 0.4108,   Adjusted R-squared: 0.3617

F-statistic: 8.367 on 1 and 12 DF, p-value: 0.01351

Residuals:

Min	1Q	Median	3Q	Max
-349.3	-292.4	-224.1	186.9	1102.7

Coefficients:

	Estimate	Std. Error	t value	Pr(>|t|)
(Intercept)	101.55	281.80	0.360	0.725
data$NO23	19.48	32.89	0.592	0.565

Residual standard error: 481.4 on 12 degrees of freedom

Multiple R-squared: 0.02839,   Adjusted R-squared: -0.05258

F-statistic: 0.3507 on 1 and 12 DF, p-value: 0.5647

199
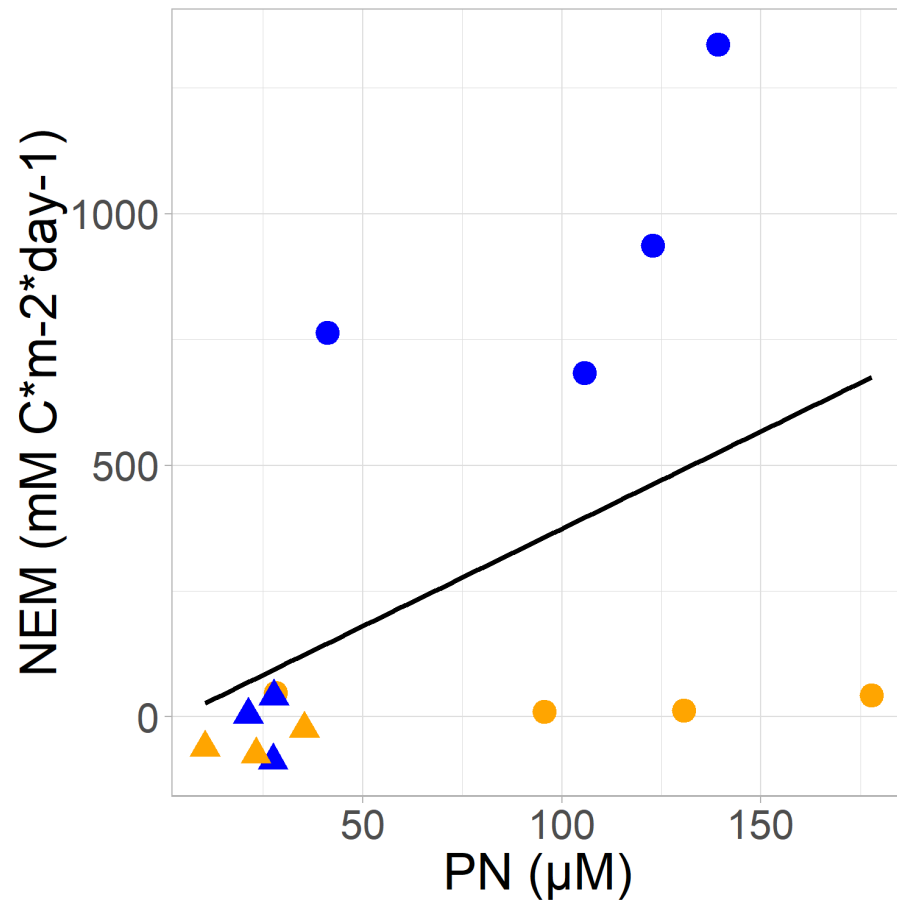
Residuals:

Min	1Q	Median	3Q	Max
-678.47	-175.36	-82.28	217.80	839.47

Coefficients:

	Estimate	Std. Error	t value	Pr(>|t|)
(Intercept)	-3.169	194.944	-0.016	0.987
data$PN	3.592	2.201	1.632	0.129

Residual standard error: 441.8 on 12 degrees of freedom

Multiple R-squared: 0.1817, Adjusted R-squared: 0.1135

F-statistic: 2.664 on 1 and 12 DF, p-value: 0.1286
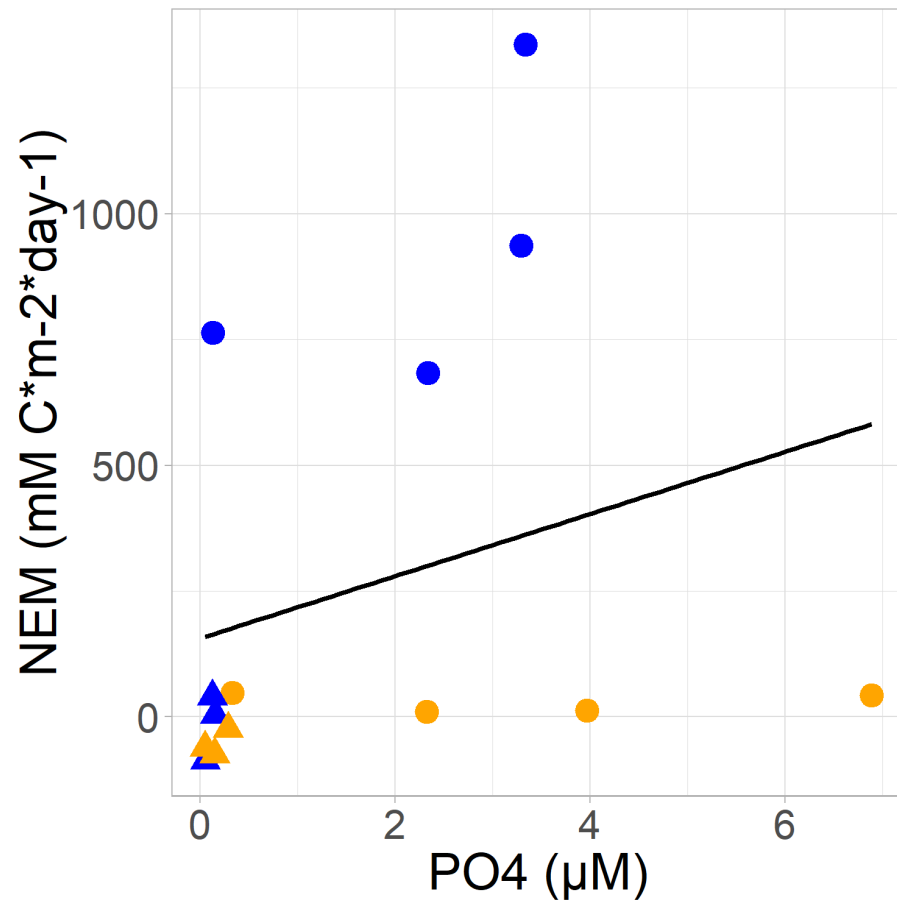
Residuals:

Min	1Q	Median	3Q	Max
-567.6	-249.6	-183.4	267.2	998.8

Coefficients:

	Estimate	Std. Error	t value	Pr(>|t|)
(Intercept)	161.79	164.81	0.982	0.346
data$PO4	52.68	62.82	0.839	0.418

Residual standard error: 474.6 on 12 degrees of freedom

Multiple R-squared: 0.05535, Adjusted R-squared: -0.02337

F-statistic: 0.7031 on 1 and 12 DF, p-value: 0.4181
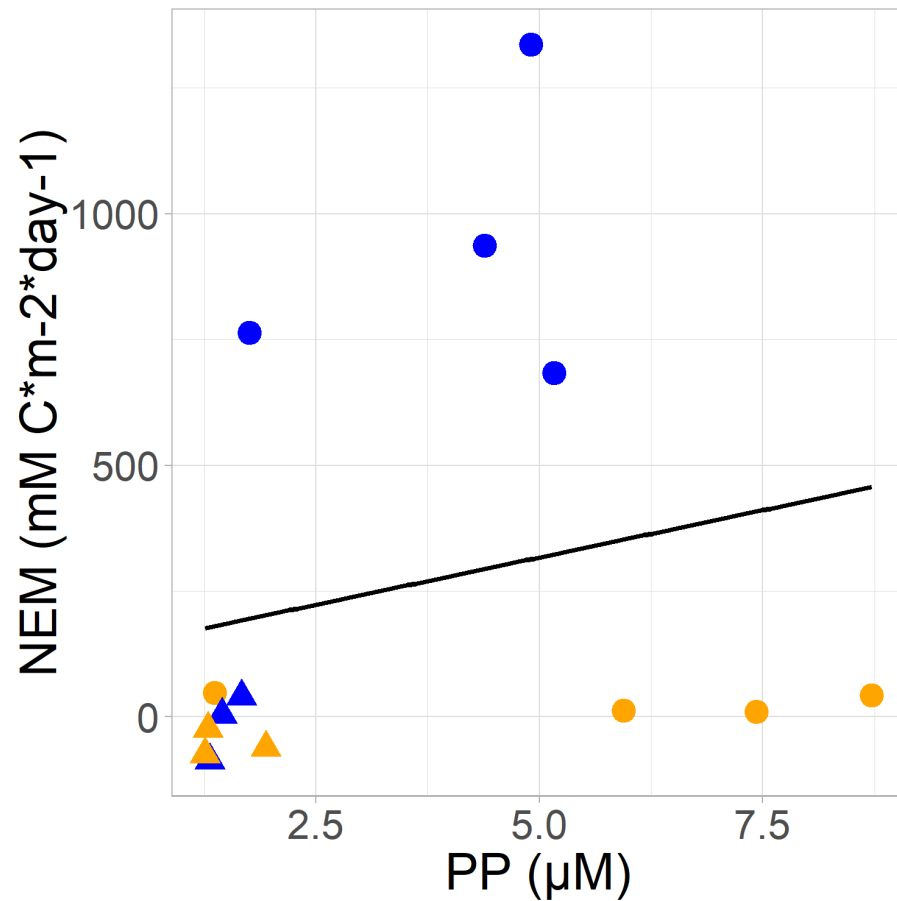
Residuals:

Min	1Q	Median	3Q	Max
-453.9	-268.9	-195.6	251.7	1042.4

Coefficients:

	Estimate	Std. Error	t value	Pr(>|t|)
(Intercept)	143.52	221.09	0.649	0.528
data$PP	30.68	51.80	0.592	0.565

Residual standard error: 481.4 on 12 degrees of freedom

Multiple R-squared: 0.0284, Adjusted R-squared: -0.05257

F-statistic: 0.3507 on 1 and 12 DF, p-value: 0.5647
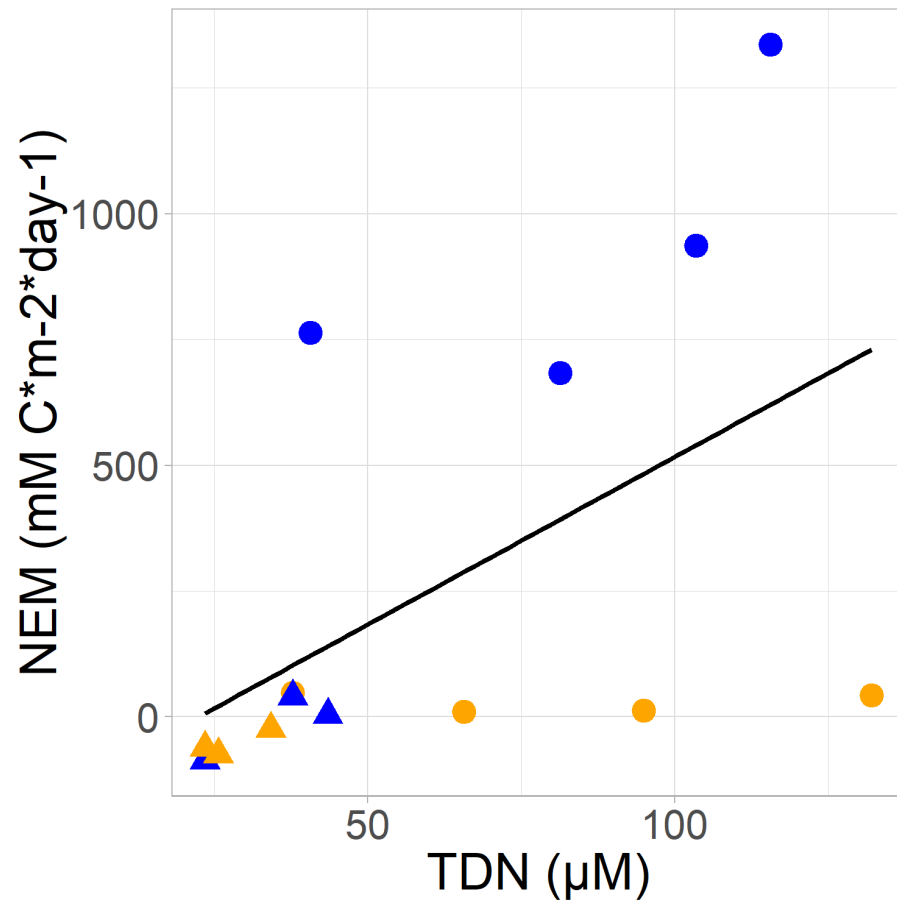
Residuals:

Min	1Q	Median	3Q	Max
-736.16	-126.16	-86.15	217.78	746.31

Coefficients:

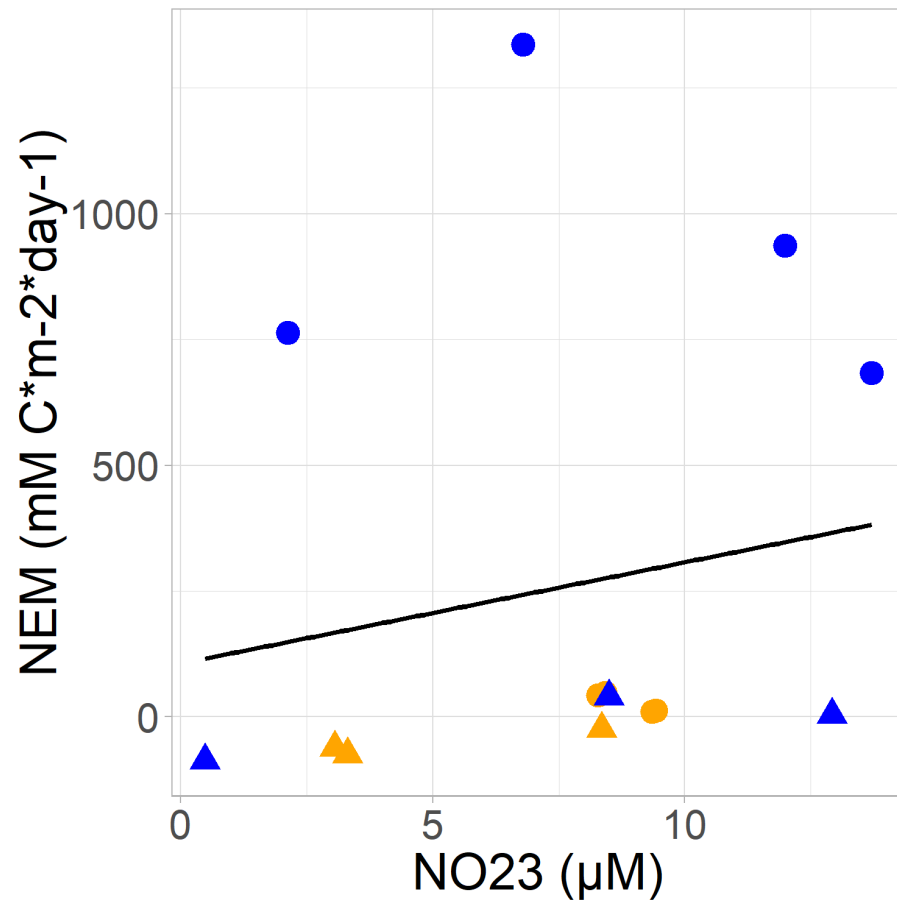|	Estimate	Std. Error	t value	Pr(>|t|)
(Intercept)	-135.534	224.703	-0.603	0.5576
data$TDN	6.274	3.159	1.986	0.0703 .

Signif. codes: 0 '***' 0.001 '**' 0.01 '*' 0.05 '.' 0.1 ' ' 1

Residual standard error: 423.6 on 12 degrees of freedom

Multiple R-squared: 0.2474,   Adjusted R-squared: 0.1847

F-statistic: 3.946 on 1 and 12 DF, p-value: 0.07031

Residuals:

Min	1Q	Median	3Q	Max
-633.1	-204.2	-142.7	252.3	903.1

Coefficients:

	Estimate	Std. Error	t value	Pr(>|t|)
(Intercept)	104.14	170.00	0.613	0.552
data$TDP	40.50	32.62	1.242	0.238

Residual standard error: 459.7 on 12 degrees of freedom

Multiple R-squared: 0.1138, Adjusted R-squared: 0.03999

F-statistic: 1.541 on 1 and 12 DF, p-value: 0.2381
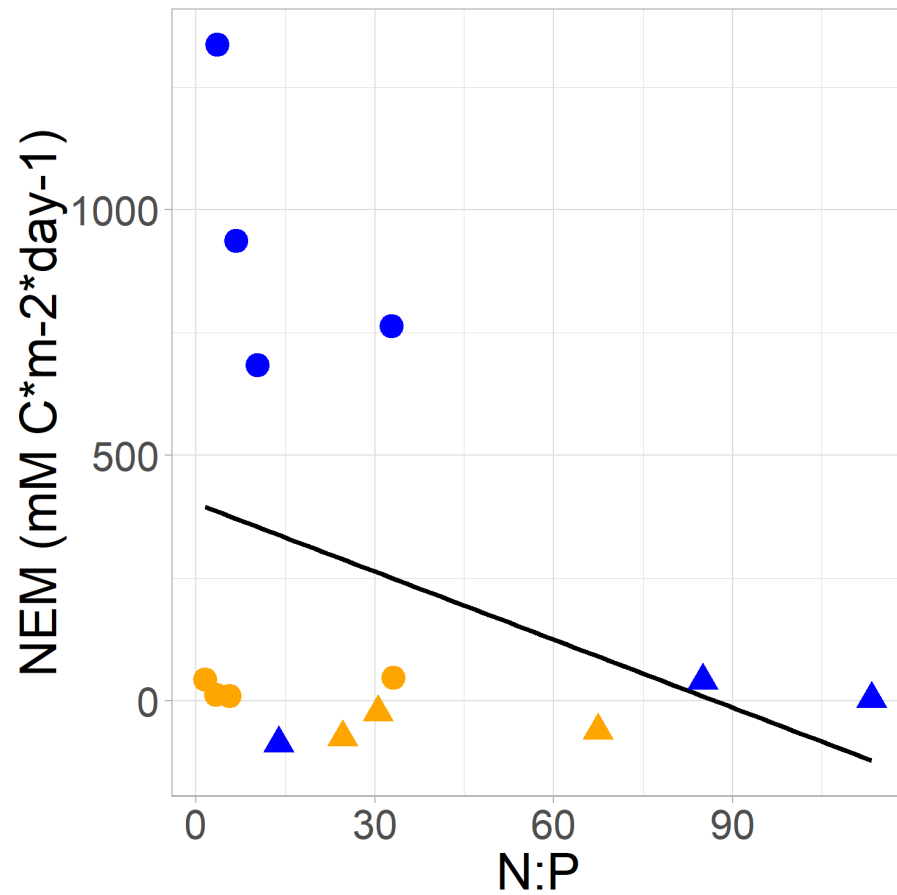
Residuals:

Min   1Q Median   3Q   Max

-421.4 -365.7 -172.0 286.5 967.0

Coefficients:

            Estimate Std. Error t value Pr(>|t|)

(Intercept) 384.958   168.781   2.281   0.0416 *

data$N.P   -4.374   3.725 -1.174   0.2631

Signif. codes: 0 '***' 0.001 '**' 0.01 '*' 0.05 '.' 0.1 ' ' 1

Residual standard error: 462.5 on 12 degrees of freedom

Multiple R-squared: 0.1031,   Adjusted R-squared: 0.02831

F-statistic: 1.379 on 1 and 12 DF, p-value: 0.2631

Residuals:

Min	1Q	Median	3Q	Max
-904.80	-120.99	61.78	223.34	382.65

Coefficients:

	Estimate	Std. Error	t value	Pr(>|t|)
(Intercept)	514.59	282.97	1.819	0.094 .
data$Salinity	-37.05	30.82	-1.202	0.252

Signif. codes: 0 '***' 0.001 '**' 0.01 '*' 0.05 '.' 0.1 ' ' 1

Residual standard error: 356.9 on 12 degrees of freedom

Multiple R-squared: 0.1075,   Adjusted R-squared: 0.03313

F-statistic: 1.445 on 1 and 12 DF, p-value: 0.2525
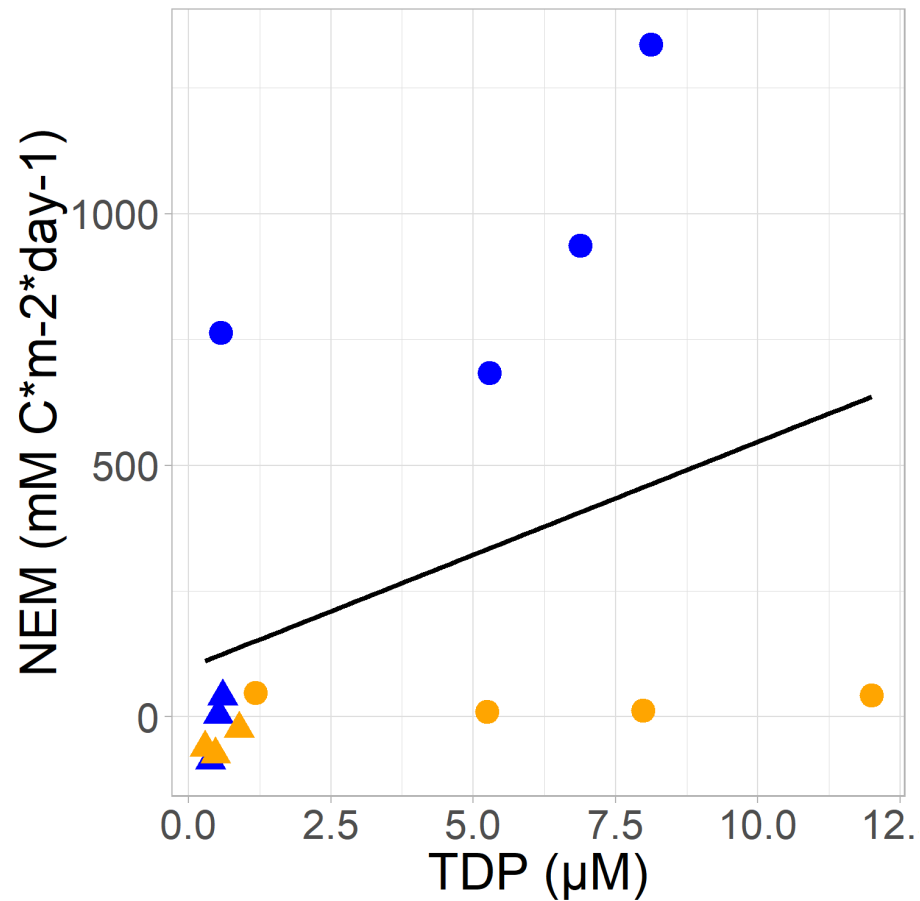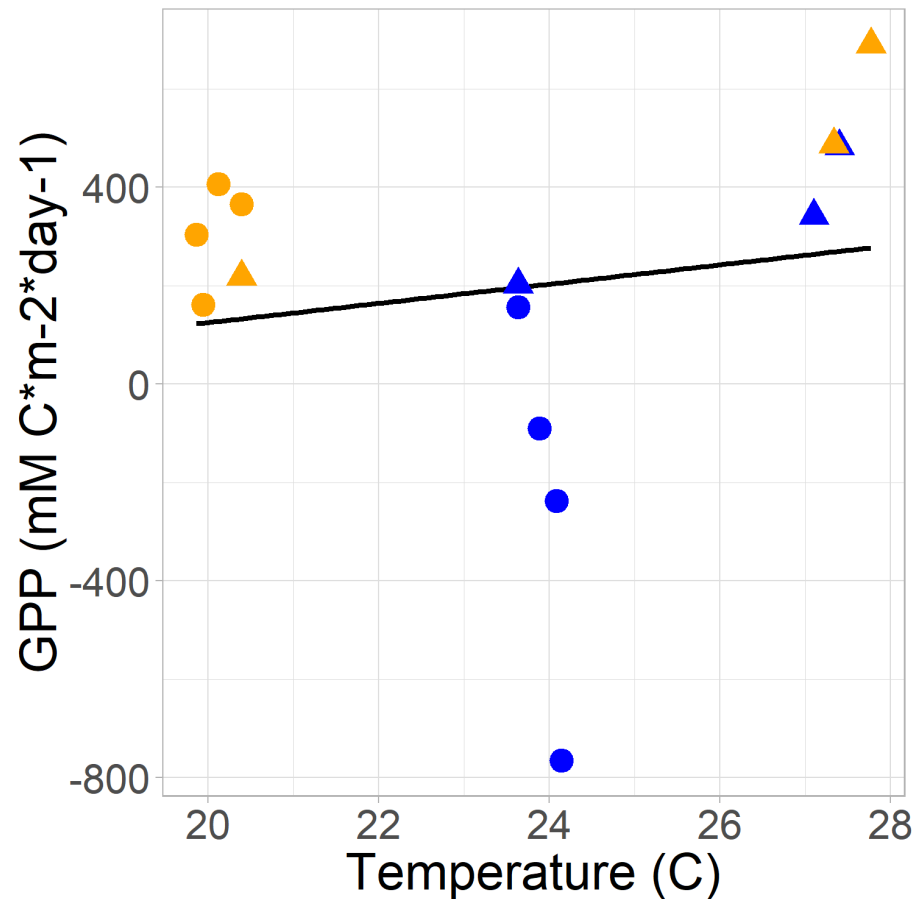
Residuals:

Min	1Q	Median	3Q	Max
-970.69	-27.97	81.83	217.16	412.92

Coefficients:

	Estimate	Std. Error	t value	Pr(>|t|)
(Intercept)	-265.84	811.99	-0.327	0.749
data$Temperature..C.	19.54	34.22	0.571	0.579

Residual standard error: 372.8 on 12 degrees of freedom

Multiple R-squared: 0.02645,   Adjusted R-squared: -0.05468

F-statistic: 0.326 on 1 and 12 DF, p-value: 0.5785
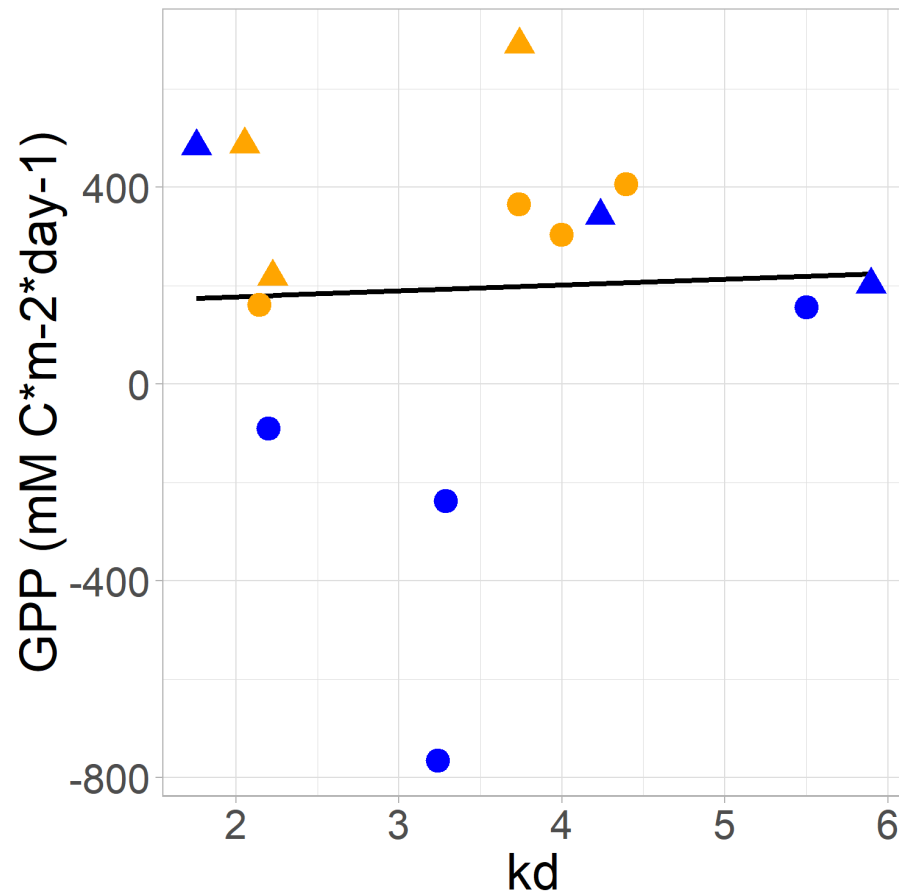
Residuals:

Min	1Q	Median	3Q	Max
-956.50	-51.69	70.56	192.17	492.09

Coefficients:

	Estimate	Std. Error	t value	Pr(>|t|)
(Intercept)	153.42	296.96	0.517	0.615
data$kd	11.83	80.80	0.146	0.886

Residual standard error: 377.5 on 12 degrees of freedom

Multiple R-squared: 0.001783, Adjusted R-squared: -0.0814

F-statistic: 0.02143 on 1 and 12 DF, p-value: 0.886
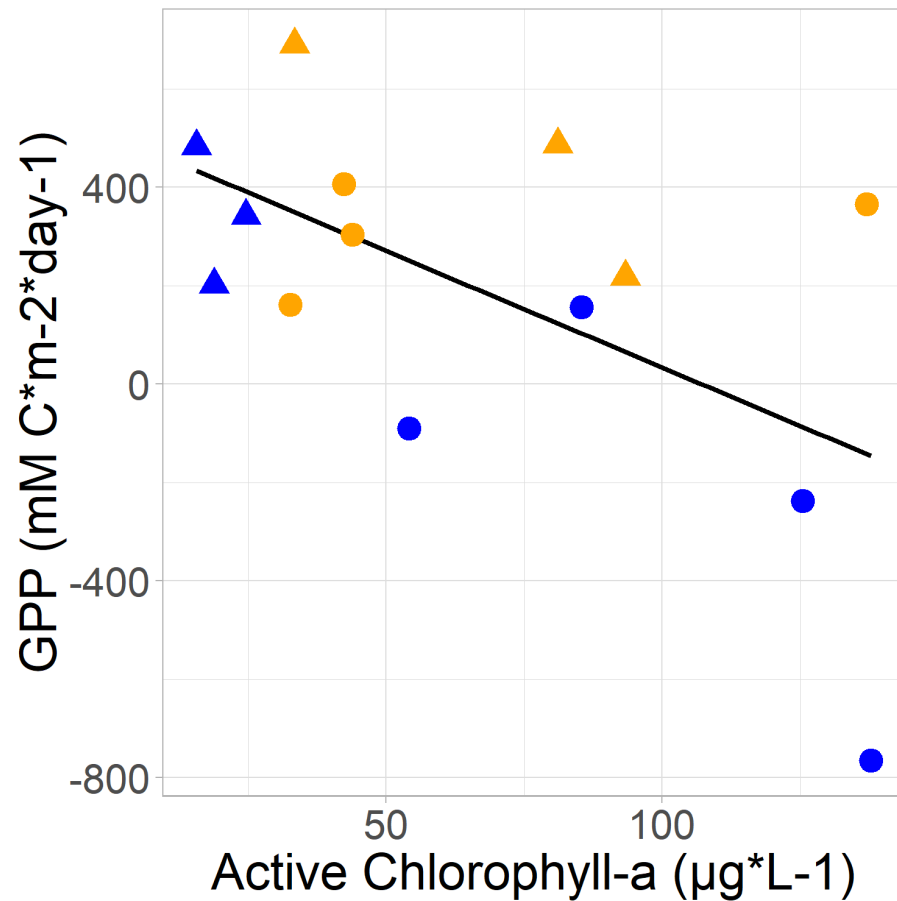
Residuals:

Min   1Q Median   3Q   Max

-618.84 -182.06   26.58 139.46 507.32

Coefficients:

	Estimate	Std. Error	t value
(Intercept)	507.872	153.898	3.300
data$Active.Chlorophyll.a..ug.L.	-4.742	1.962	-2.417

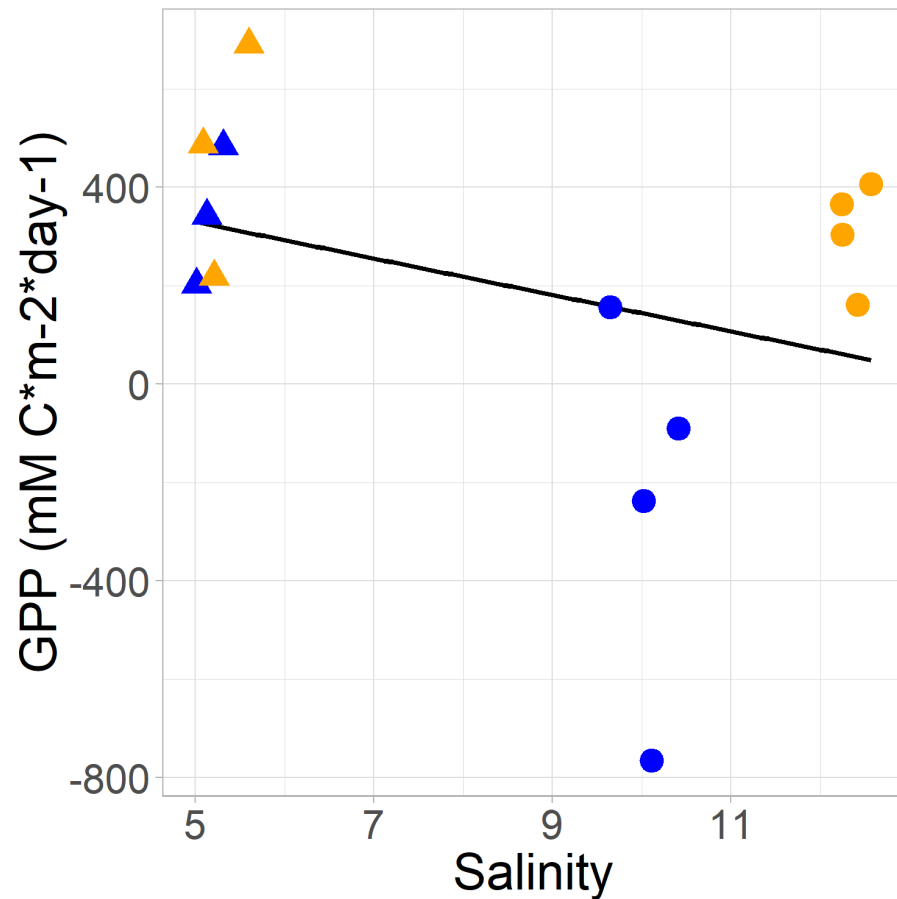|	Pr(>|t|)
(Intercept)	0.00634 **
data$Active.Chlorophyll.a..ug.L.	0.03248 *

Signif. codes: 0 '***' 0.001 '**' 0.01 '*' 0.05 '.' 0.1 ' ' 1

Residual standard error: 309.8 on 12 degrees of freedom

Multiple R-squared: 0.3275,   Adjusted R-squared: 0.2714

F-statistic: 5.843 on 1 and 12 DF, p-value: 0.03248
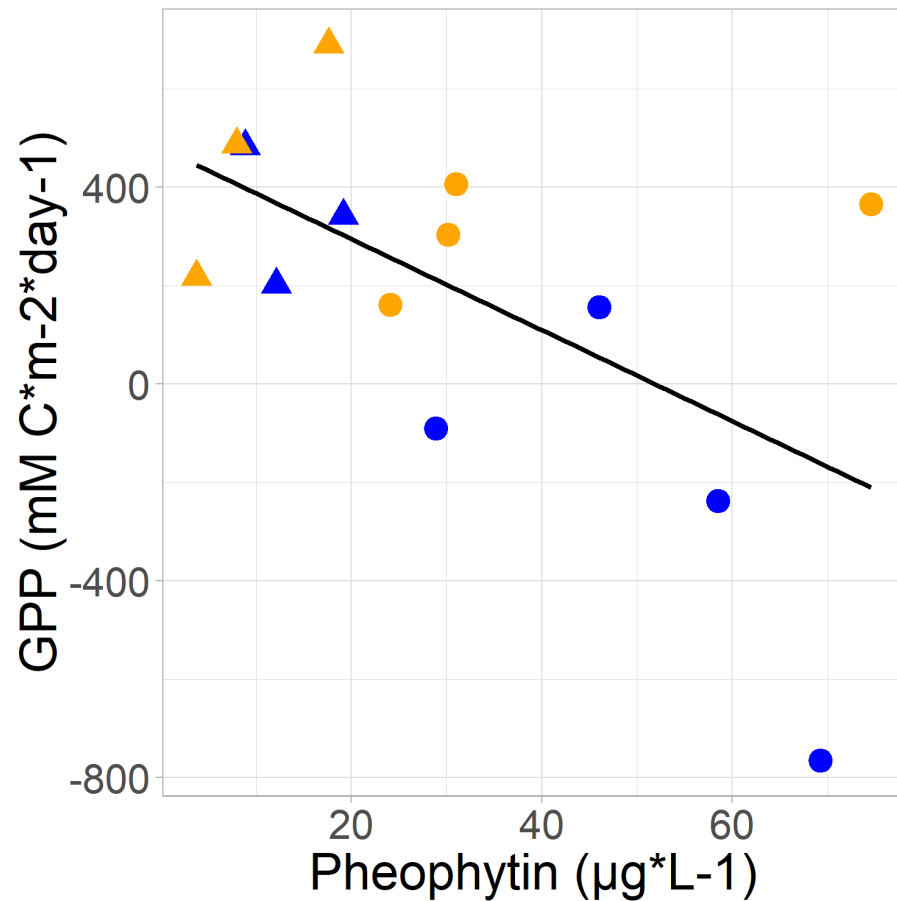
Residuals:

Min	1Q	Median	3Q	Max
-603.64	-173.85	59.95	102.81	575.55

Coefficients:

	Estimate	Std. Error	t value	Pr(>|t|)	
(Intercept)	479.935	140.744	3.410	0.00517	**
data$Pheophytin..ug.L.	-9.254	3.708	-2.496	0.02813	*

---

Signif. codes: 0 '***' 0.001 '**' 0.01 '*' 0.05 '.' 0.1 ' ' 1

Residual standard error: 306.5 on 12 degrees of freedom

Multiple R-squared: 0.3417,   Adjusted R-squared: 0.2869

F-statistic: 6.229 on 1 and 12 DF, p-value: 0.02813

Residuals:

   Min   1Q Median   3Q   Max
-661.62 -142.77   22.41 195.98 556.78

Coefficients:

          Estimate Std. Error t value Pr(>|t|)
(Intercept)   530.1   193.5   2.740   0.0179 *
data$DOC   -742.1   380.8 -1.949   0.0751 .

Signif. codes: 0 '***' 0.001 '**' 0.01 '*' 0.05 '.' 0.1 ' ' 1

Residual standard error: 329.3 on 12 degrees of freedom

Multiple R-squared: 0.2404,   Adjusted R-squared: 0.1771

F-statistic: 3.798 on 1 and 12 DF, p-value: 0.07506

Residuals:

Min	1Q	Median	3Q	Max
-868.53	-77.18	85.15	133.55	353.62

Coefficients:

	Estimate	Std. Error	t value	Pr(>|t|)	
(Intercept)	392.30	128.80	3.046	0.0102	*
data$NH4	-56.93	27.41	-2.077	0.0600	.

Signif. codes: 0 '***' 0.001 '**' 0.01 '*' 0.05 '.' 0.1 ' ' 1

Residual standard error: 324 on 12 degrees of freedom

Multiple R-squared: 0.2644,　　　Adjusted R-squared: 0.2031

F-statistic: 4.313 on 1 and 12 DF, p-value: 0.05995

Residuals:

Min	1Q	Median	3Q	Max
-976.44	-2.85	129.33	179.88	405.77

Coefficients:

	Estimate	Std. Error	t value	Pr(>|t|)
(Intercept)	352.90	215.11	1.641	0.127
data$NO23	-20.80	25.11	-0.829	0.423

Residual standard error: 367.5 on 12 degrees of freedom

Multiple R-squared: 0.05412, Adjusted R-squared: -0.0247

F-statistic: 0.6866 on 1 and 12 DF, p-value: 0.4235
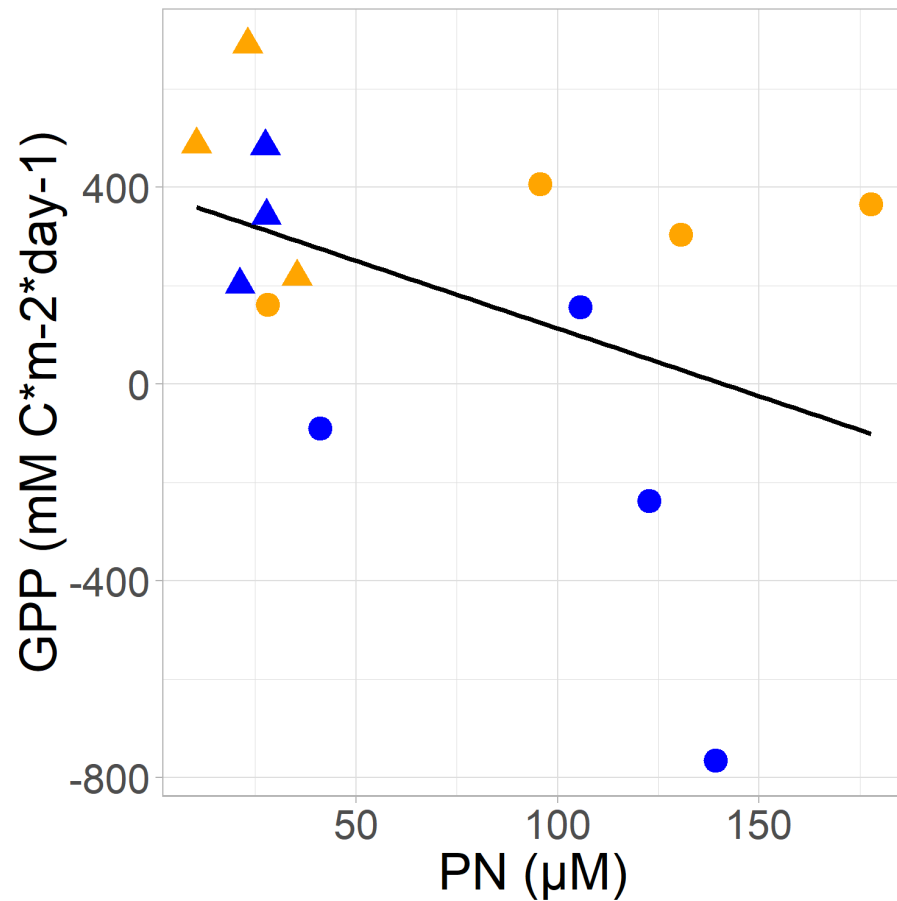
Residuals:

    Min   1Q Median   3Q   Max
-770.01 -144.42   44.51 248.61 466.09

Coefficients:

          Estimate Std. Error t value Pr(>|t|)
(Intercept) 388.172   151.165   2.568   0.0246 *
data$PN   -2.751   1.707 -1.612   0.1330

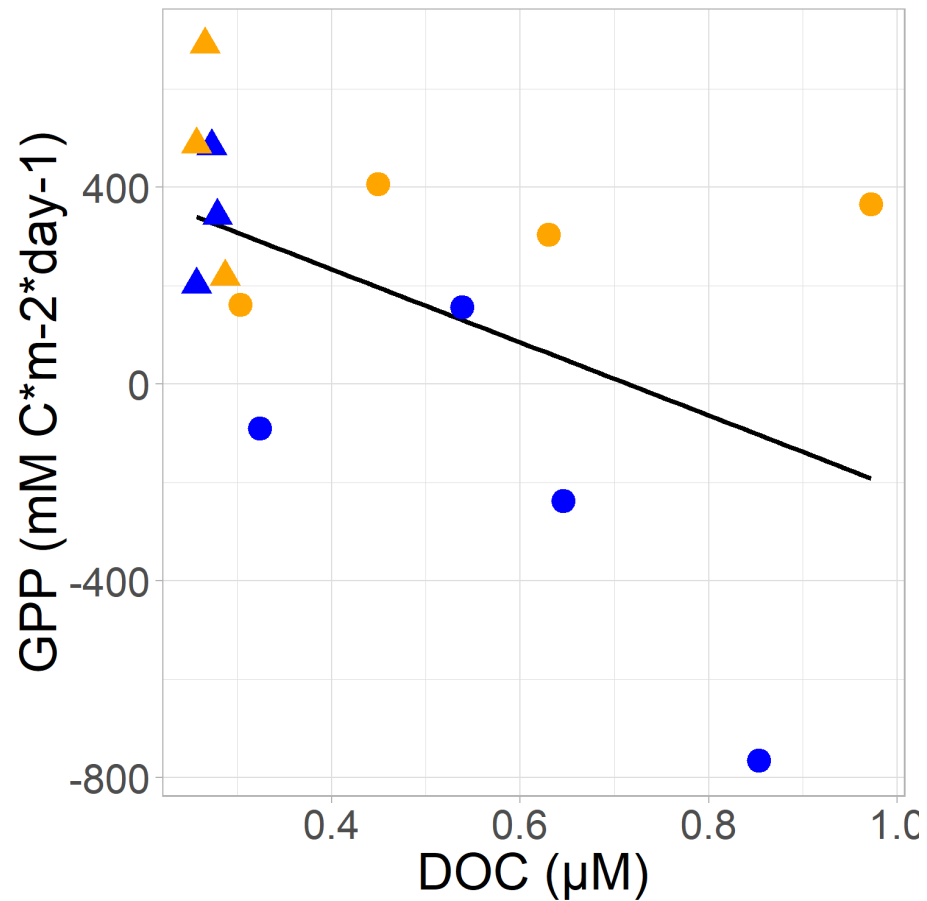
Signif. codes: 0 '***' 0.001 '**' 0.01 '*' 0.05 '.' 0.1 ' ' 1

Residual standard error: 342.6 on 12 degrees of freedom

Multiple R-squared: 0.1779,   Adjusted R-squared: 0.1094

F-statistic: 2.598 on 1 and 12 DF, p-value: 0.133

Residuals:

Min	1Q	Median	3Q	Max
-885.45	-84.61	35.23	219.60	428.01

Coefficients:

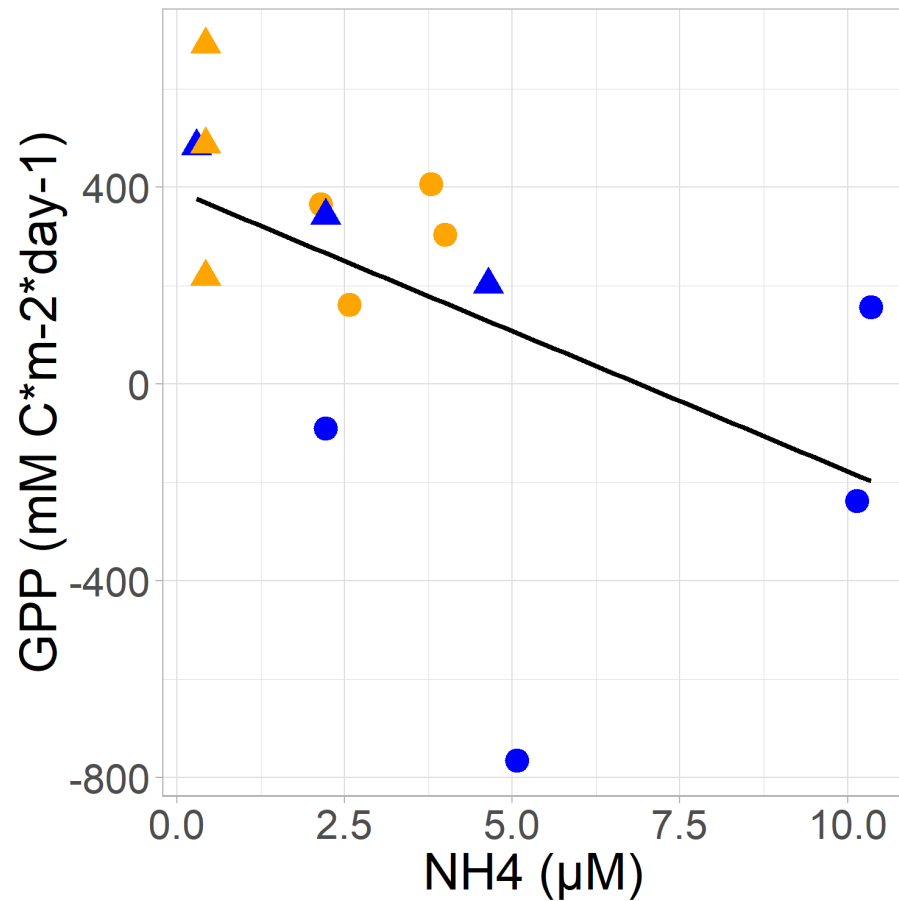|	Estimate	Std. Error	t value	Pr(>|t|)	
(Intercept)	268.46	126.83	2.117	0.0559	.
data$PO4	-44.28	48.35	-0.916	0.3778	

Signif. codes: 0 '***' 0.001 '**' 0.01 '*' 0.05 '.' 0.1 ' ' 1

Residual standard error: 365.3 on 12 degrees of freedom

Multiple R-squared: 0.06533,   Adjusted R-squared: -0.01256

F-statistic: 0.8387 on 1 and 12 DF, p-value: 0.3778

Residuals:

Min	1Q	Median	3Q	Max
-929.51	-66.16	53.74	256.65	449.85

Coefficients:

	Estimate	Std. Error	t value	Pr(>|t|)
(Intercept)	265.85	171.67	1.549	0.147
data$PP	-20.61	40.22	-0.512	0.618

Residual standard error: 373.8 on 12 degrees of freedom

Multiple R-squared: 0.02141, Adjusted R-squared: -0.06014

F-statistic: 0.2626 on 1 and 12 DF, p-value: 0.6177
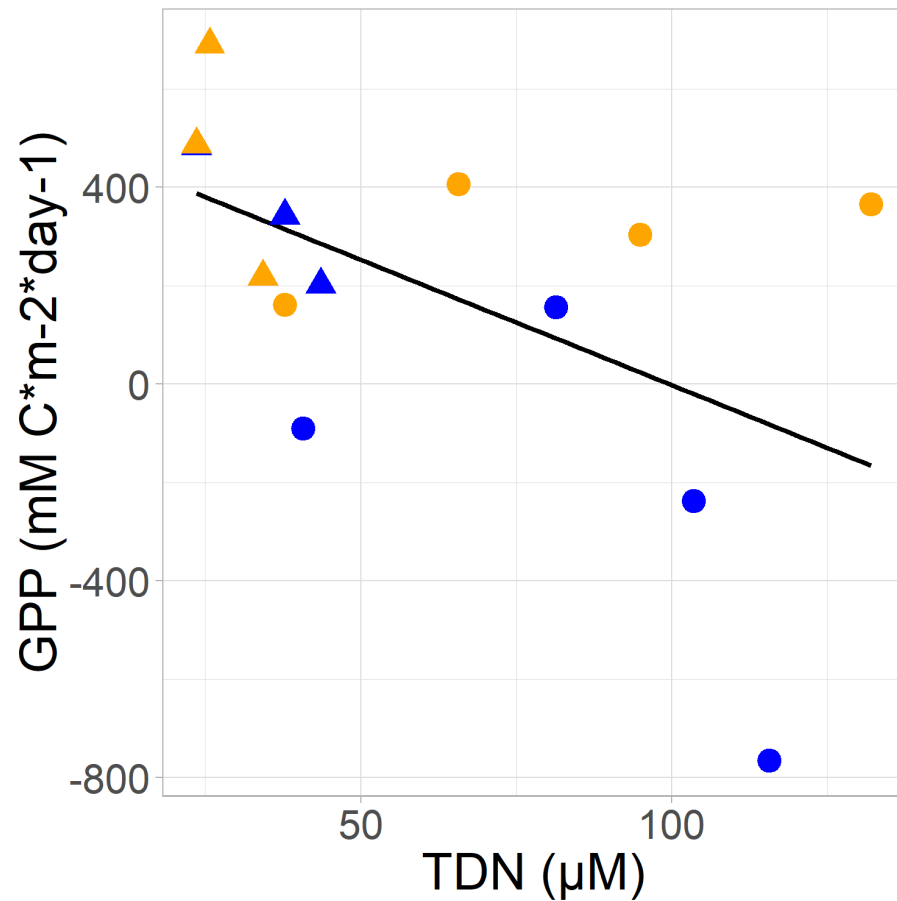
Residuals:

Min	1Q	Median	3Q	Max
-683.0	-143.9	45.5	199.5	530.7

Coefficients:

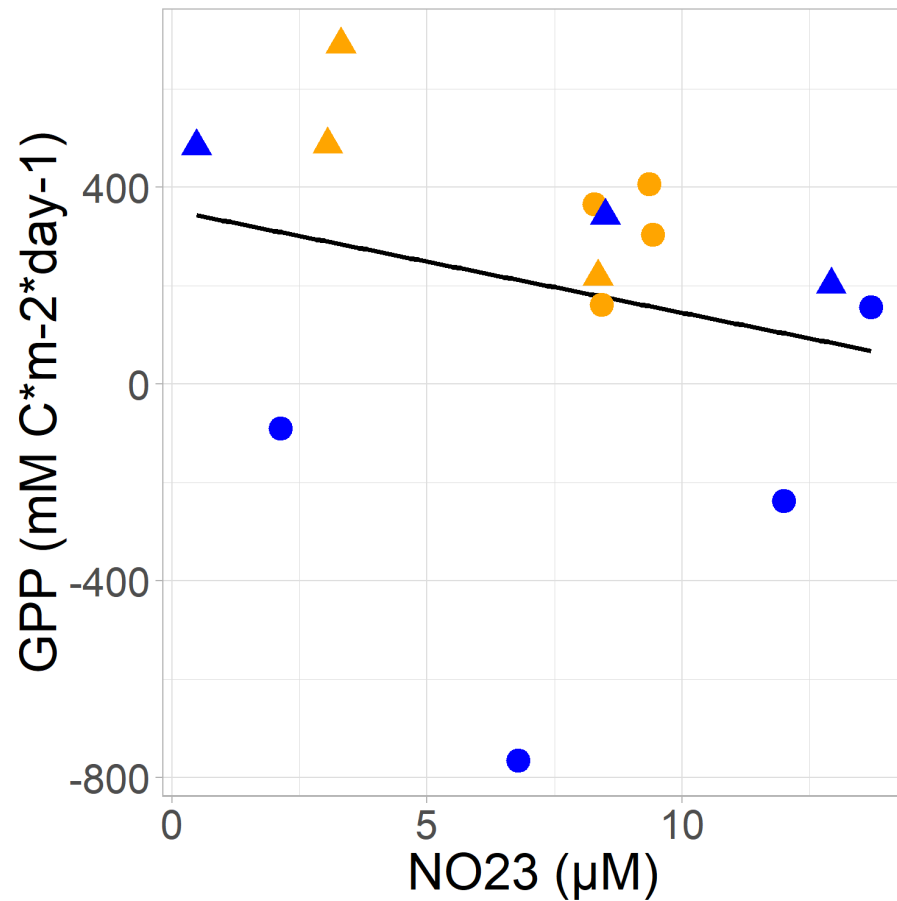|	Estimate	Std. Error	t value	Pr(>|t|)	
(Intercept)	507.273	170.940	2.968	0.0118	*
data$TDN	-5.093	2.403	-2.120	0.0556	.

Signif. codes: 0 '***' 0.001 '**' 0.01 '*' 0.05 '.' 0.1 ' ' 1

Residual standard error: 322.3 on 12 degrees of freedom

Multiple R-squared: 0.2724,   Adjusted R-squared: 0.2118

F-statistic: 4.493 on 1 and 12 DF, p-value: 0.05558
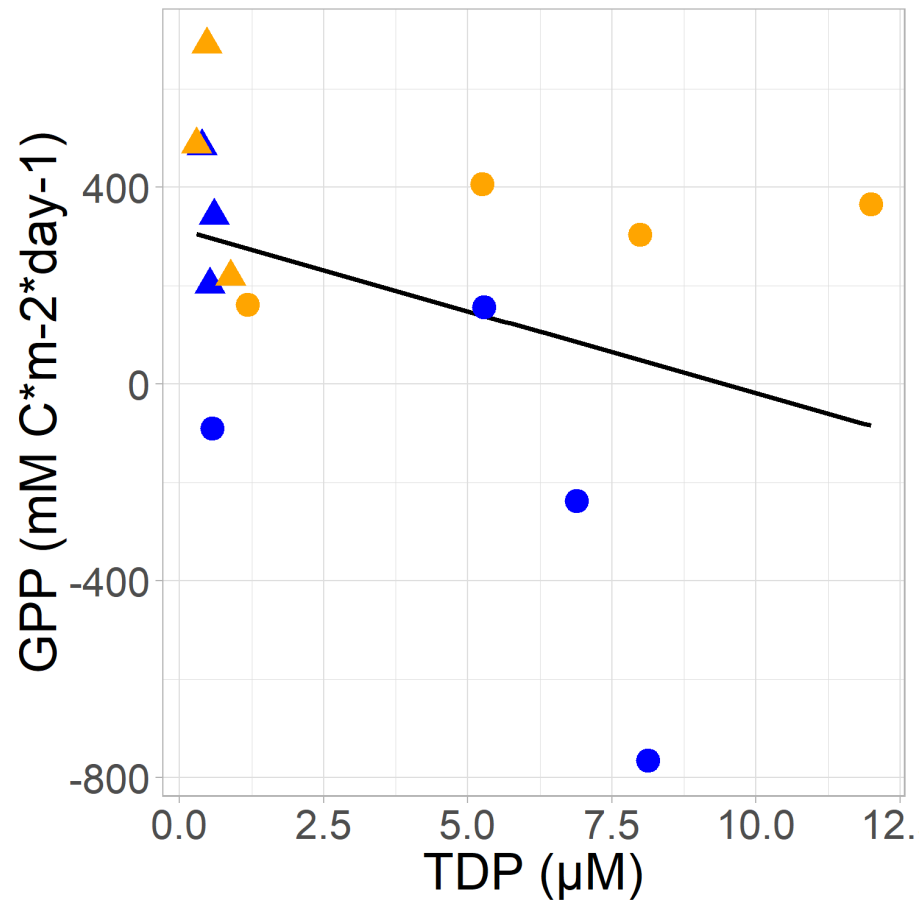
Residuals:

Min	1Q	Median	3Q	Max
-808.86	-109.08	32.92	236.55	449.73

Coefficients:

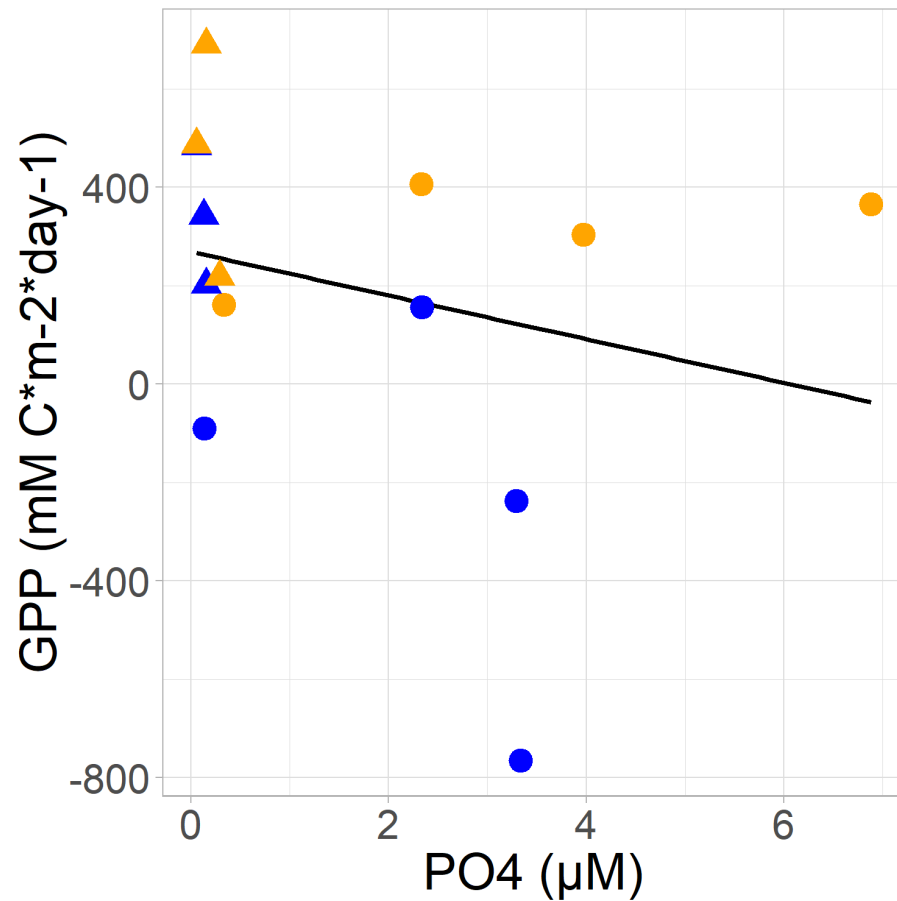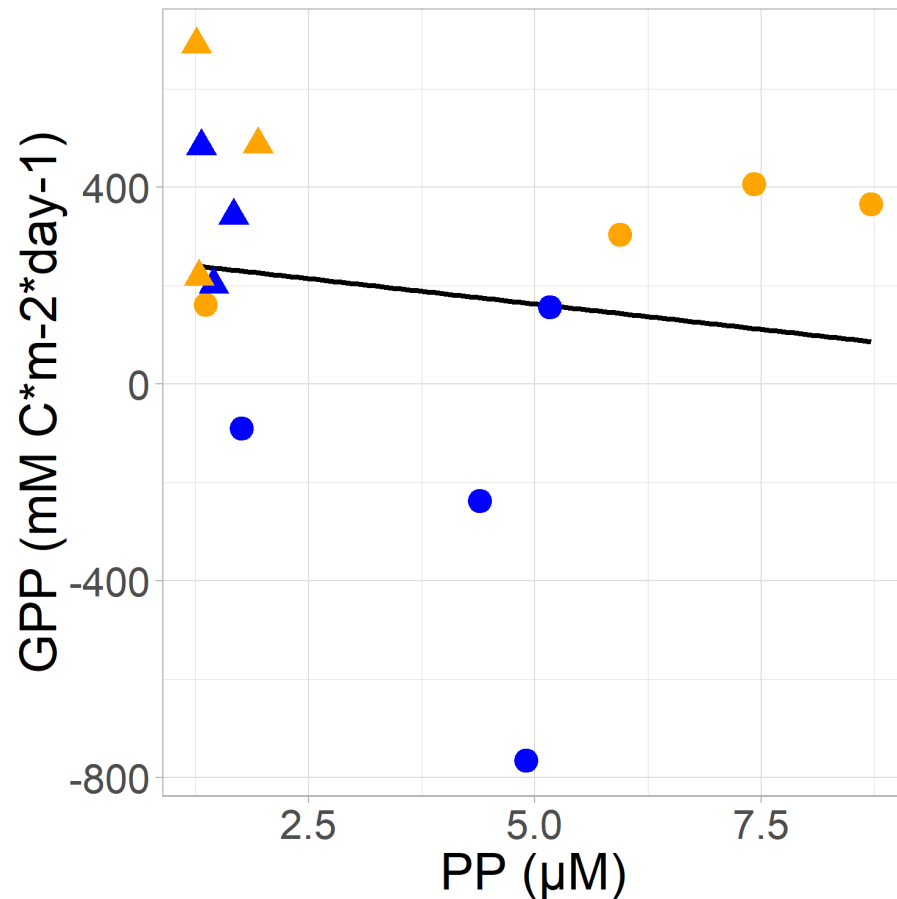|	Estimate	Std. Error	t value	Pr(>|t|)
(Intercept)	313.89	130.48	2.406	0.0332 *
data$TDP	-33.20	25.04	-1.326	0.2095

Signif. codes: 0 '***' 0.001 '**' 0.01 '*' 0.05 '.' 0.1 ' ' 1

Residual standard error: 352.9 on 12 degrees of freedom

Multiple R-squared: 0.1278,   Adjusted R-squared: 0.05513

F-statistic: 1.758 on 1 and 12 DF, p-value: 0.2095
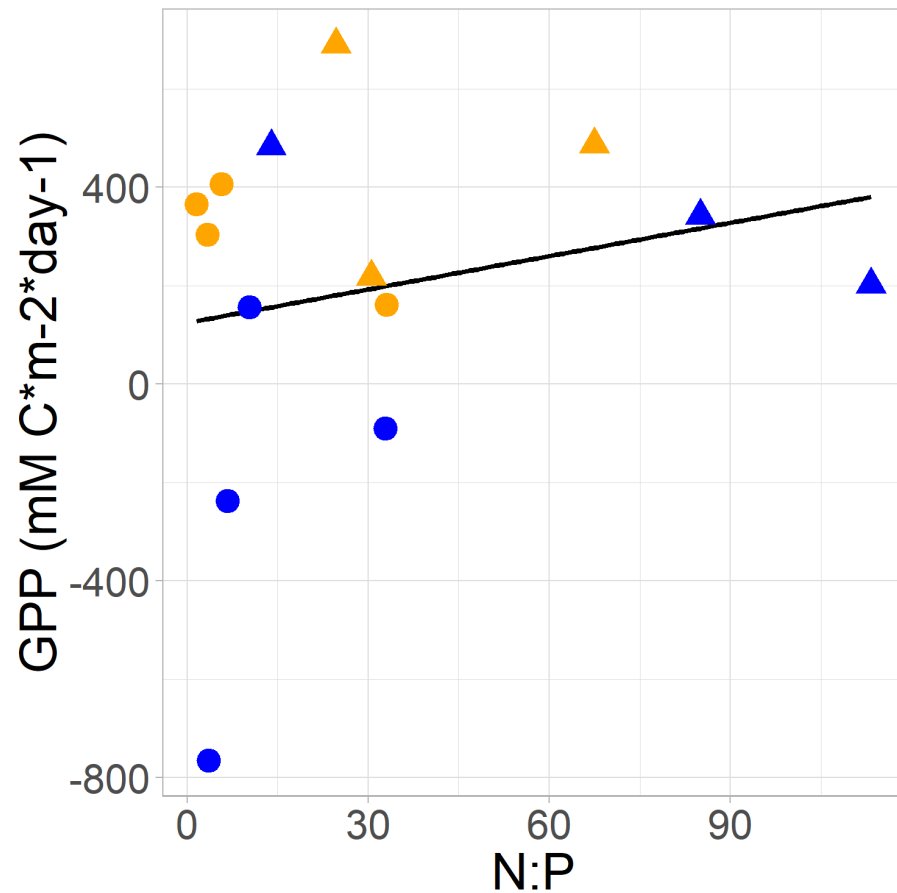
Residuals:

Min	1Q	Median	3Q	Max
-897.5	-143.3	24.9	230.2	509.4

Coefficients:

	Estimate	Std. Error	t value	Pr(>|t|)
(Intercept)	124.722	134.686	0.926	0.373
data$N.P	2.255	2.973	0.759	0.463

Residual standard error: 369.1 on 12 degrees of freedom

Multiple R-squared: 0.04578,   Adjusted R-squared: -0.03374

F-statistic: 0.5757 on 1 and 12 DF, p-value: 0.4626
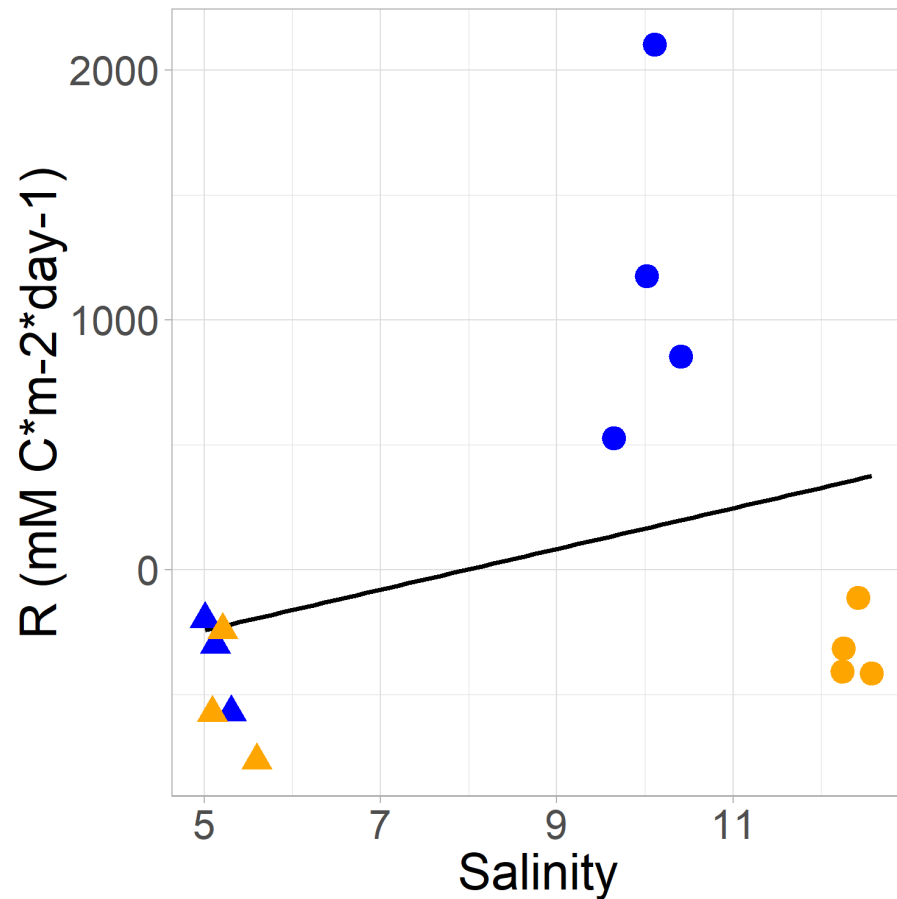
Residuals:

Min	1Q	Median	3Q	Max
-789.1	-548.8	-194.0	302.5	1927.0

Coefficients:

	Estimate	Std. Error	t value	Pr(>|t|)
(Intercept)	-643.27	636.30	-1.011	0.332
data$Salinity	80.86	69.30	1.167	0.266

Residual standard error: 802.6 on 12 degrees of freedom

Multiple R-squared: 0.1019, Adjusted R-squared: 0.02706

F-statistic: 1.362 on 1 and 12 DF, p-value: 0.2659
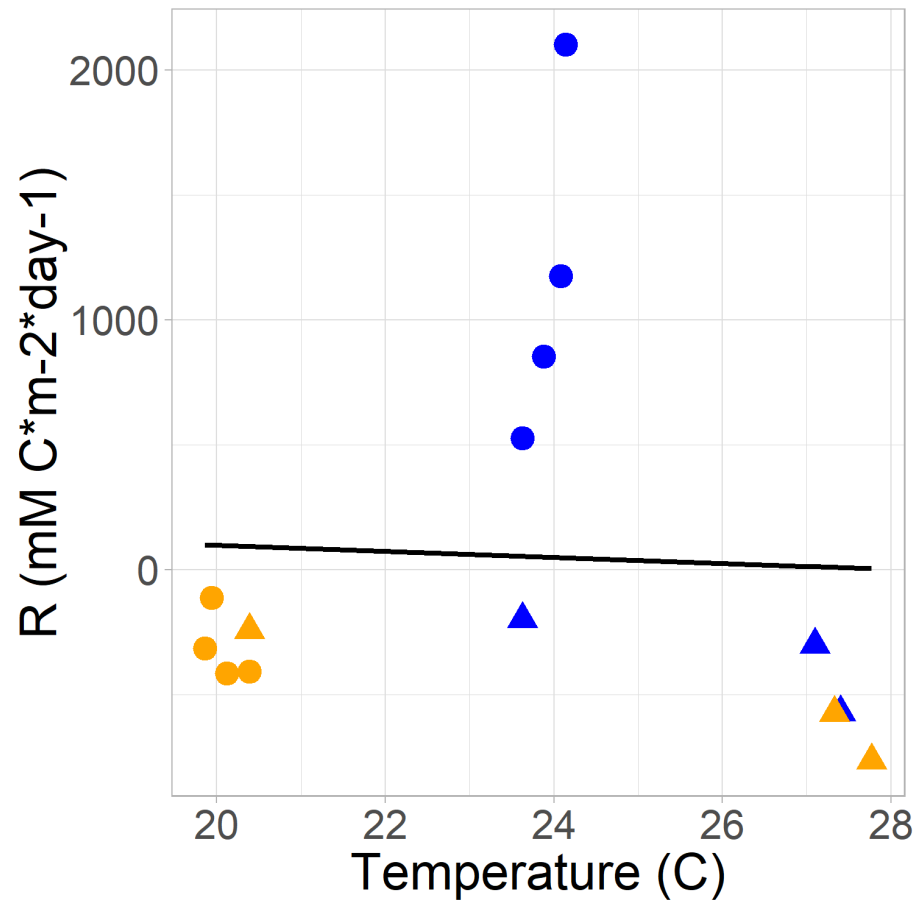
Residuals:

  Min   1Q Median   3Q   Max

-772.6 -507.3 -325.0 301.8 2052.1

Coefficients:

              Estimate Std. Error t value Pr(>|t|)

(Intercept)   319.00   1843.15 0.173 0.865

data$Temperature..C. -11.18   77.68 -0.144 0.888

Residual standard error: 846.2 on 12 degrees of freedom

Multiple R-squared: 0.001723,   Adjusted R-squared: -0.08147

F-statistic: 0.02072 on 1 and 12 DF, p-value: 0.8879
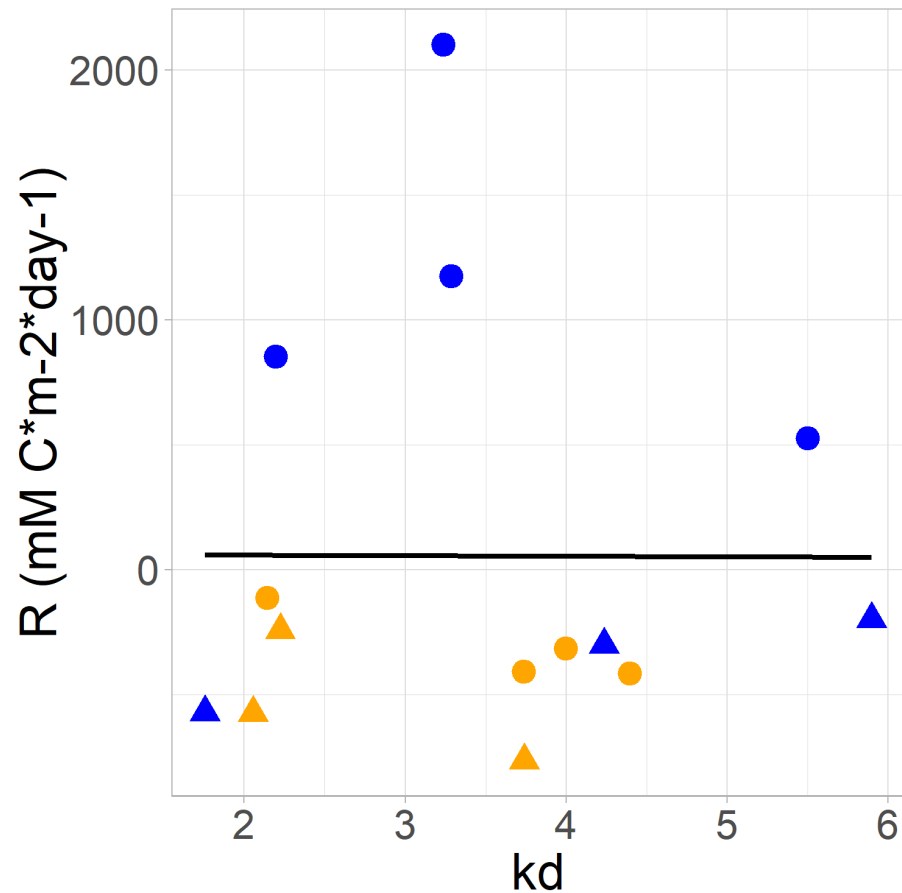
Residuals:

Min	1Q	Median	3Q	Max
-818.7	-466.7	-328.1	316.0	2044.6

Coefficients:

	Estimate	Std. Error	t value	Pr(>|t|)
(Intercept)	69.334	666.255	0.104	0.919
data$kd	-3.938	181.277	-0.022	0.983

Residual standard error: 846.9 on 12 degrees of freedom

Multiple R-squared: 3.933e-05,   Adjusted R-squared: -0.08329

F-statistic: 0.000472 on 1 and 12 DF, p-value: 0.983
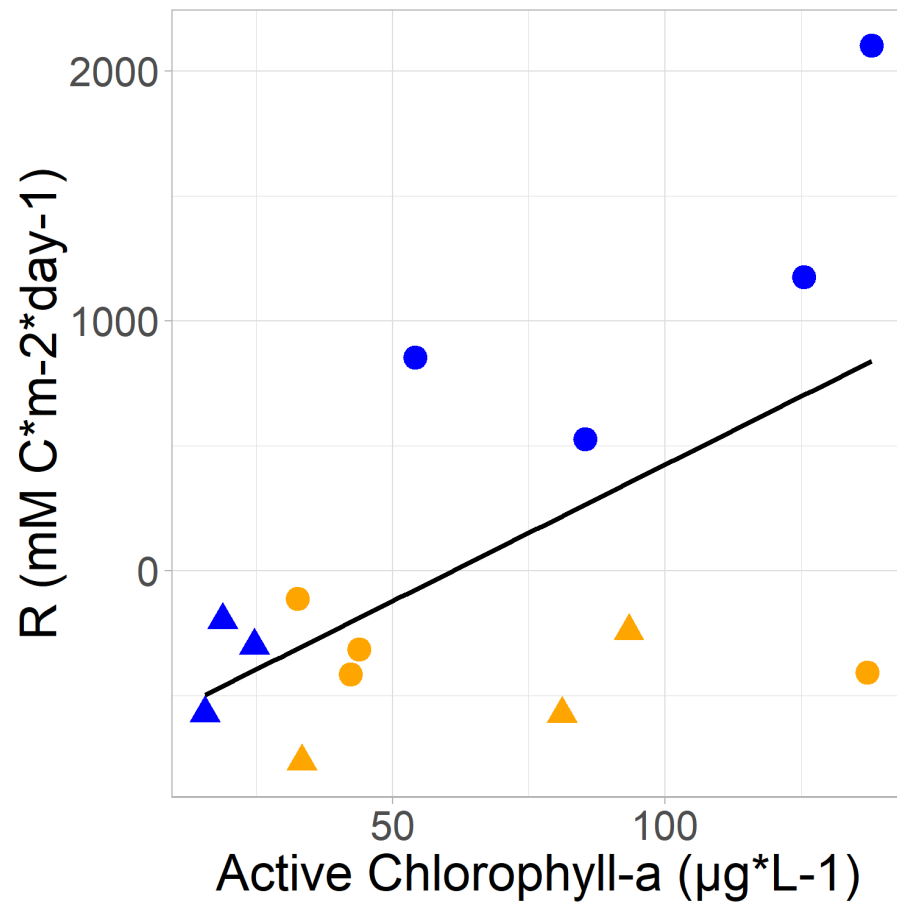
Residuals:

Min	1Q	Median	3Q	Max
-1240.56	-398.76	12.21	263.20	1259.95

Coefficients:

	Estimate	Std. Error	t value
(Intercept)	-668.186	339.849	-1.966
data$Active.Chlorophyll.a..ug.L.	10.948	4.332	2.527

|	Pr(>|t|)
(Intercept)	0.0728 .
data$Active.Chlorophyll.a..ug.L.	0.0266 *

Signif. codes: 0 '***' 0.001 '**' 0.01 '*' 0.05 '.' 0.1 ' ' 1

Residual standard error: 684.2 on 12 degrees of freedom

Multiple R-squared: 0.3473,   Adjusted R-squared: 0.2929

F-statistic: 6.386 on 1 and 12 DF, p-value: 0.02656

223

Residuals:

Min	1Q	Median	3Q	Max
-1433.25	-301.66	-57.81	267.94	1193.95

Coefficients:

	Estimate	Std. Error	t value	Pr(>|t|)
(Intercept)	-628.533	303.636	-2.070	0.0607 .
data$Pheophytin..ug.L.	22.168	7.999	2.771	0.0169 *

Signif. codes: 0 '***' 0.001 '**' 0.01 '*' 0.05 '.' 0.1 ' ' 1

Residual standard error: 661.3 on 12 degrees of freedom

Multiple R-squared: 0.3903,   Adjusted R-squared: 0.3395

F-statistic: 7.681 on 1 and 12 DF, p-value: 0.01692
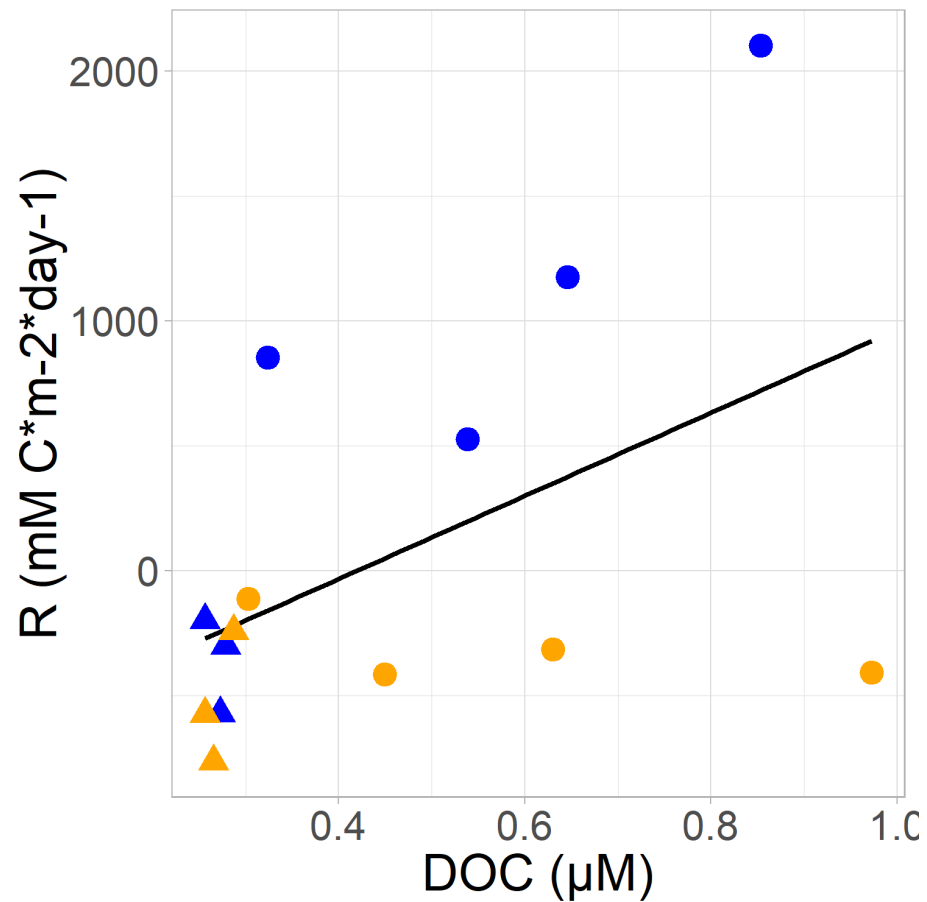
Residuals:

Min	1Q	Median	3Q	Max
-1325.04	-432.33	-46.62	266.06	1381.62

Coefficients:

	Estimate	Std. Error	t value	Pr(>|t|)
(Intercept)	-693.7	434.3	-1.597	0.1362
data$DOC	1656.0	854.7	1.938	0.0766 .

Signif. codes: 0 '***' 0.001 '**' 0.01 '*' 0.05 '.' 0.1 ' ' 1

Residual standard error: 739.2 on 12 degrees of freedom

Multiple R-squared: 0.2383,   Adjusted R-squared: 0.1748

F-statistic: 3.754 on 1 and 12 DF, p-value: 0.07657

Residuals:

Min   1Q Median   3Q   Max

-550.49 -411.61 -160.00 88.05 1809.00

Coefficients:

Estimate Std. Error t value Pr(>|t|)

(Intercept) -461.26   269.56 -1.711 0.1128
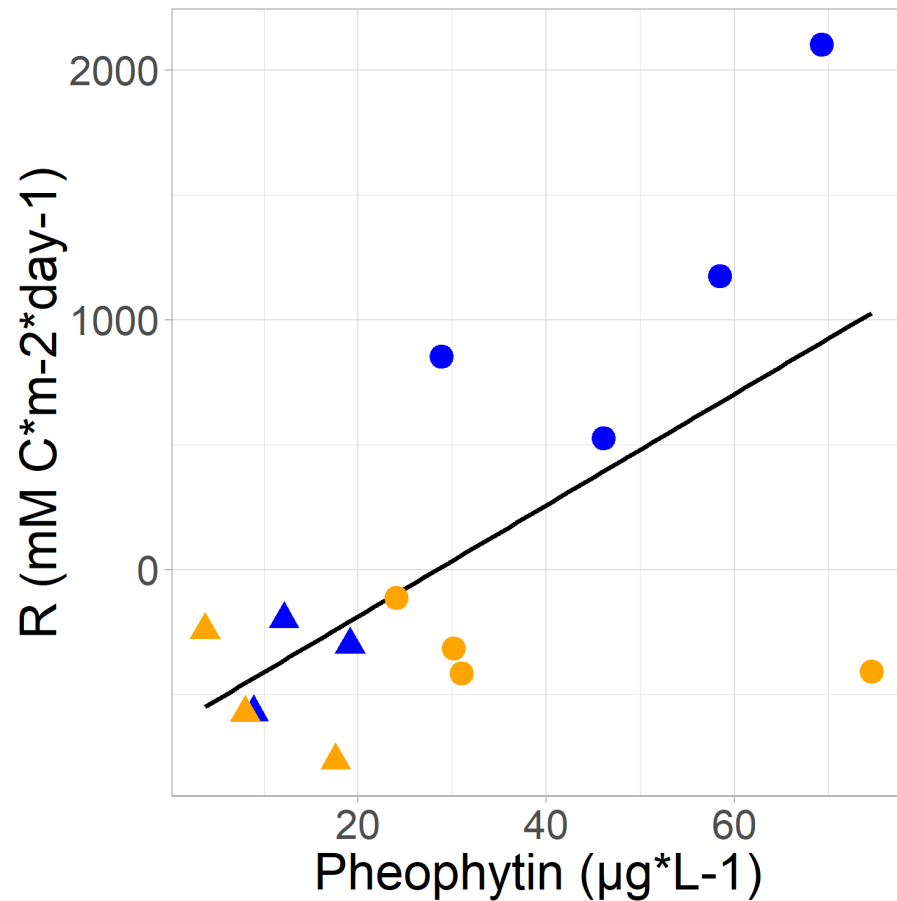
data$NH4   148.65   57.37 2.591 0.0236 *

Signif. codes: 0 '***' 0.001 '**' 0.01 '*' 0.05 '.' 0.1 ' ' 1

Residual standard error: 678.2 on 12 degrees of freedom

Multiple R-squared: 0.3588,   Adjusted R-squared: 0.3053

F-statistic: 6.714 on 1 and 12 DF, p-value: 0.02361
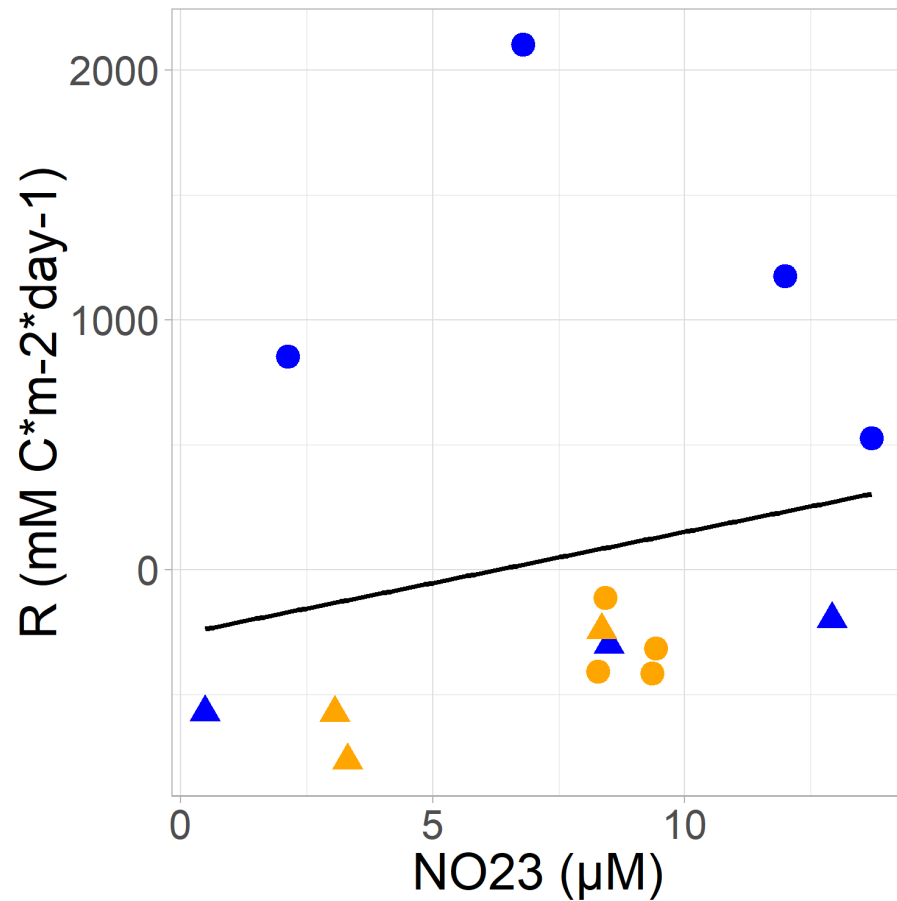
Residuals:

Min	1Q	Median	3Q	Max
-646.1	-461.6	-364.9	119.3	2079.1

Coefficients:

	Estimate	Std. Error	t value	Pr(>|t|)
(Intercept)	-251.35	485.69	-0.518	0.614
data$NO23	40.28	56.69	0.711	0.491

Residual standard error: 829.7 on 12 degrees of freedom

Multiple R-squared: 0.04038,   Adjusted R-squared: -0.03959

F-statistic: 0.505 on 1 and 12 DF, p-value: 0.4909
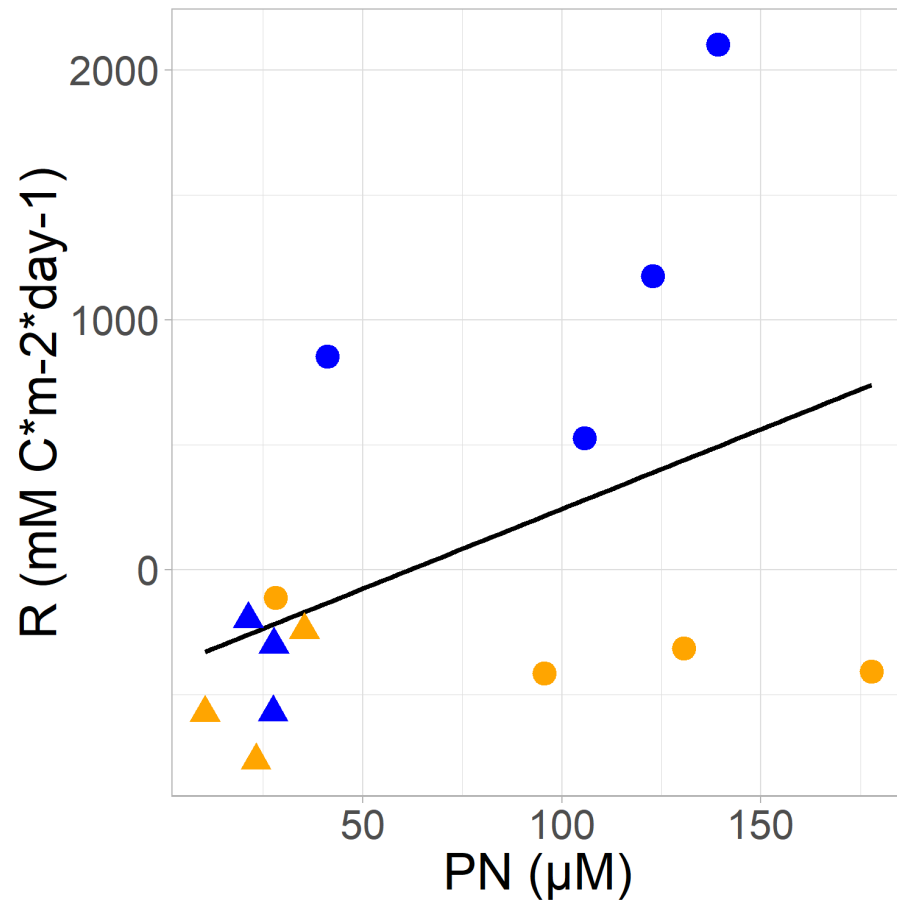
Residuals:

Min	1Q	Median	3Q	Max
-1144.61	-478.25	-80.54	210.97	1609.44

Coefficients:

	Estimate	Std. Error	t value	Pr(>|t|)
(Intercept)	-391.349	336.710	-1.162	0.268
data$PN	6.344	3.802	1.669	0.121

Residual standard error: 763 on 12 degrees of freedom

Multiple R-squared: 0.1883, Adjusted R-squared: 0.1207

F-statistic: 2.784 on 1 and 12 DF, p-value: 0.1211
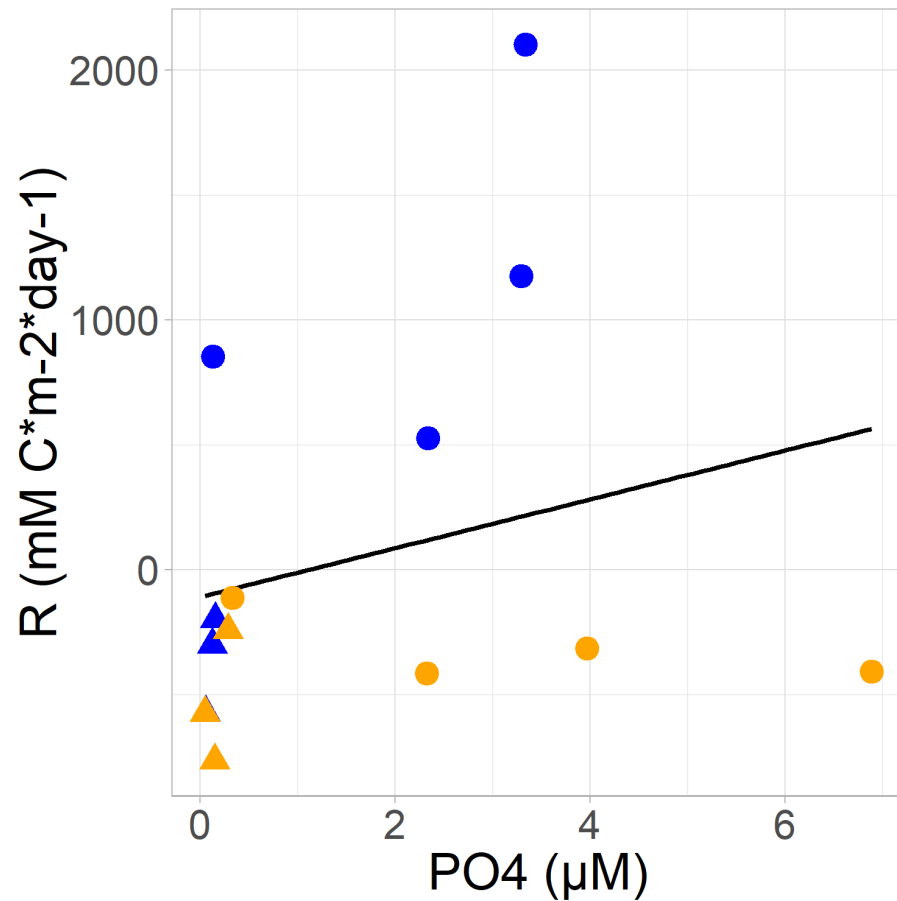
Residuals:

Min	1Q	Median	3Q	Max
-969.4	-518.5	-184.8	295.6	1884.2

Coefficients:

	Estimate	Std. Error	t value	Pr(>|t|)
(Intercept)	-106.67	284.76	-0.375	0.715
data$PO4	96.97	108.55	0.893	0.389

Residual standard error: 820.1 on 12 degrees of freedom

Multiple R-squared: 0.06235, Adjusted R-squared: -0.01579

F-statistic: 0.798 on 1 and 12 DF, p-value: 0.3893
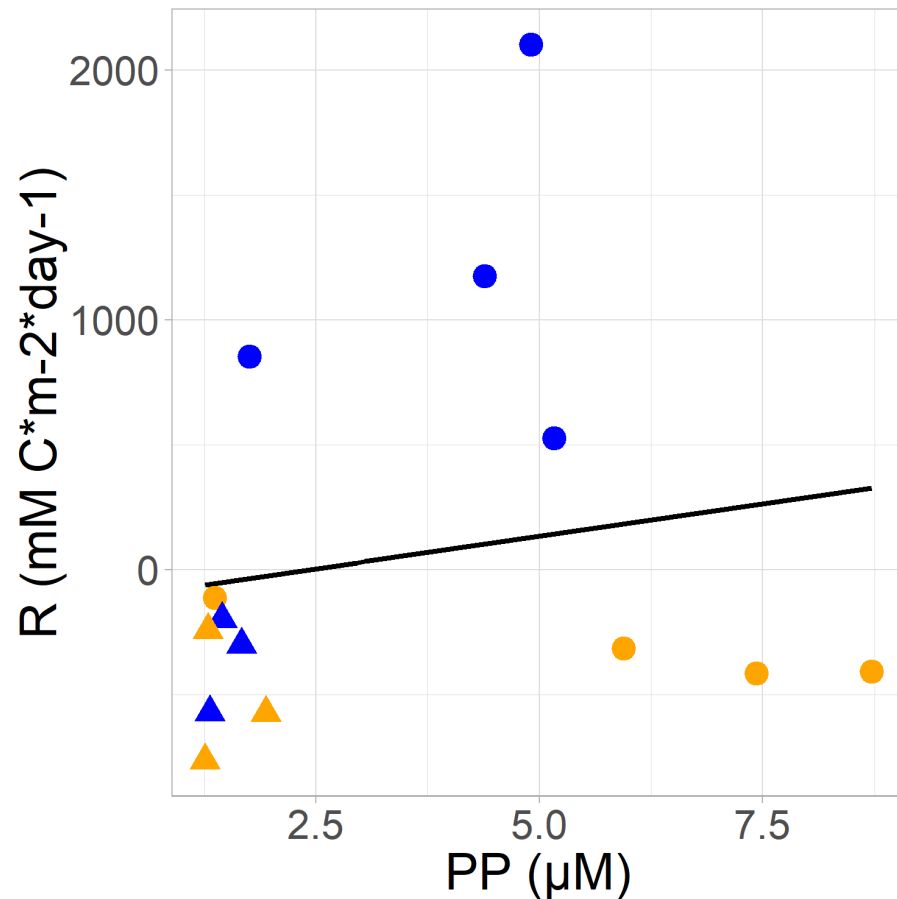
Residuals:

Min	1Q	Median	3Q	Max
-733.0	-522.3	-225.1	273.0	1971.8

Coefficients:

	Estimate	Std. Error	t value	Pr(>|t|)
(Intercept)	-122.33	383.84	-0.319	0.755
data$PP	51.29	89.93	0.570	0.579

Residual standard error: 835.7 on 12 degrees of freedom

Multiple R-squared: 0.0264, Adjusted R-squared: -0.05474

F-statistic: 0.3253 on 1 and 12 DF, p-value: 0.5789
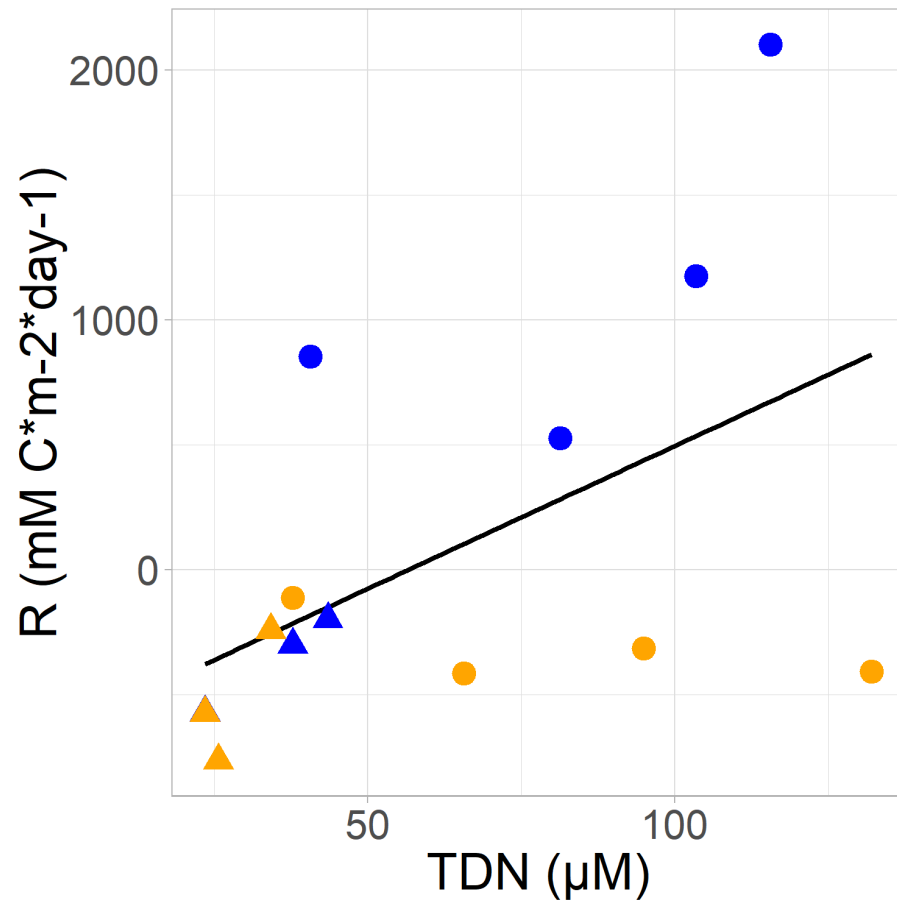
Residuals:

Min	1Q	Median	3Q	Max
-1266.87	-358.88	-69.21	208.32	1429.29

Coefficients:

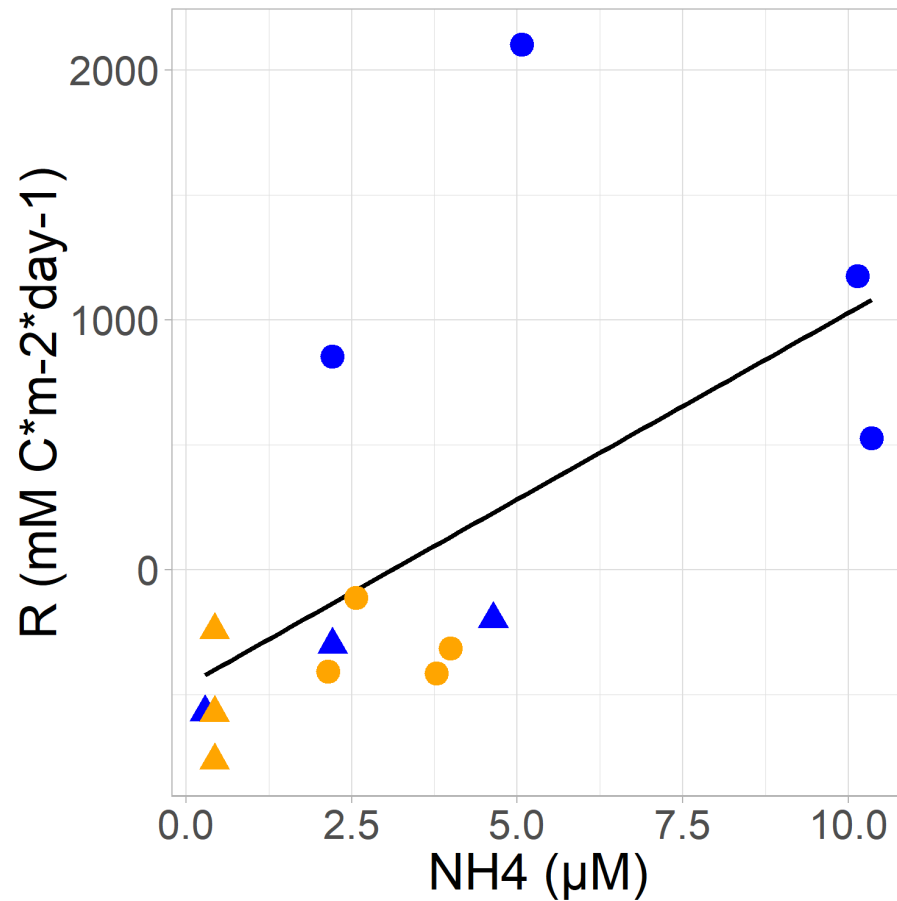|	Estimate	Std. Error	t value	Pr(>|t|)
(Intercept)	-642.818	383.799	-1.675	0.1198
data$TDN	11.368	5.395	2.107	0.0568 .


Signif. codes: 0 '***' 0.001 '**' 0.01 '*' 0.05 '.' 0.1 ' ' 1

Residual standard error: 723.6 on 12 degrees of freedom

Multiple R-squared: 0.2701,   Adjusted R-squared: 0.2092

F-statistic: 4.44 on 1 and 12 DF, p-value: 0.05682

231
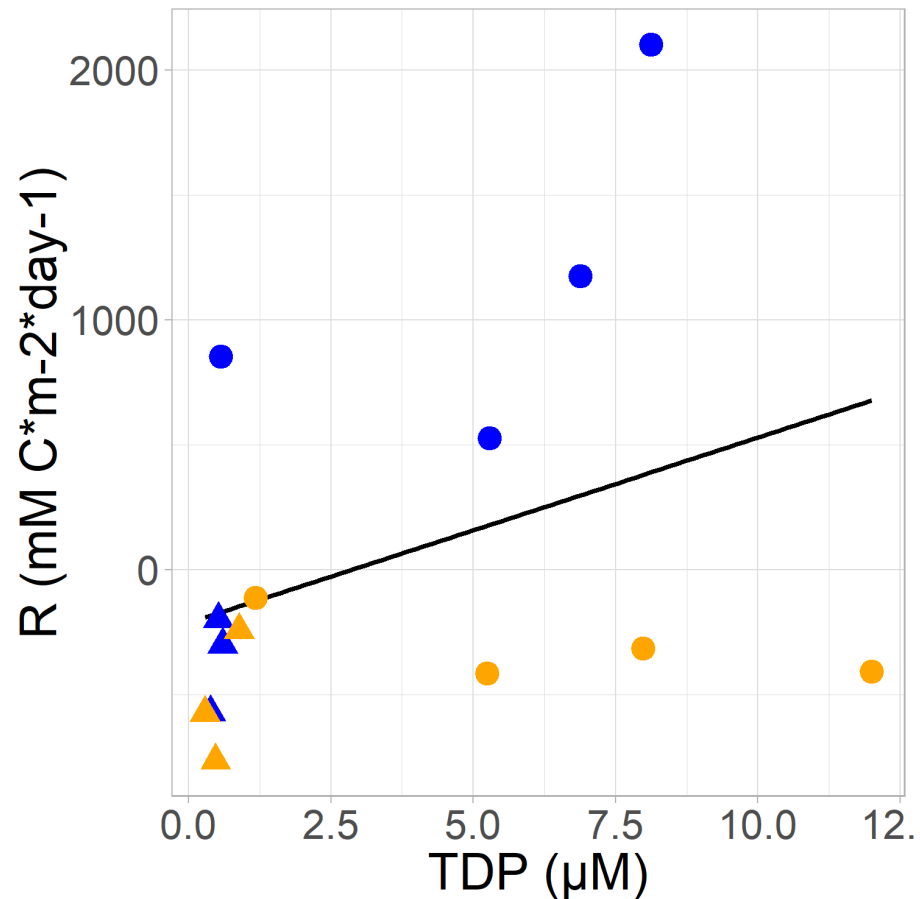
Residuals:

Min	1Q	Median	3Q	Max
-1082.9	-539.2	-116.5	263.0	1712.0

Coefficients:

	Estimate	Std. Error	t value	Pr(>|t|)
(Intercept)	-209.76	292.91	-0.716	0.488
data$TDP	73.71	56.21	1.311	0.214

Residual standard error: 792.1 on 12 degrees of freedom

Multiple R-squared: 0.1254, Adjusted R-squared: 0.05247

F-statistic: 1.72 on 1 and 12 DF, p-value: 0.2143
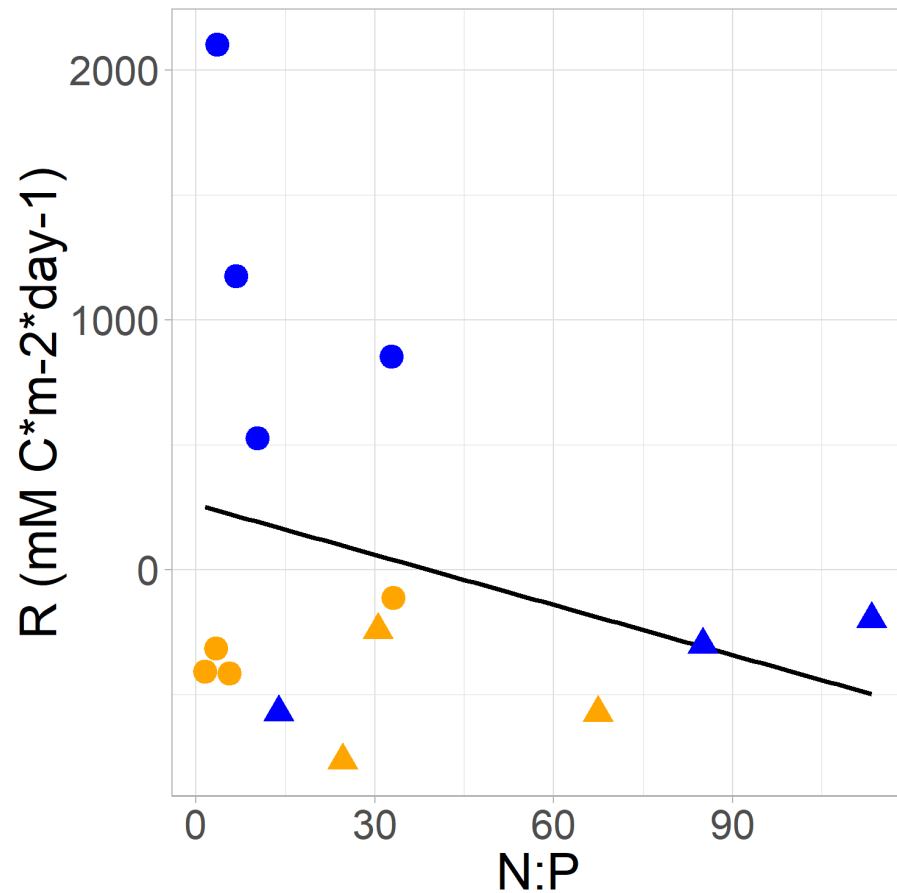
Residuals:

Min	1Q	Median	3Q	Max
-860.9	-617.5	-227.2	324.5	1864.5

Coefficients:

	Estimate	Std. Error	t value	Pr(>|t|)
(Intercept)	260.264	296.660	0.877	0.398
data$N.P	-6.630	6.548	-1.013	0.331

Residual standard error: 812.9 on 12 degrees of freedom

Multiple R-squared: 0.07872, Adjusted R-squared: 0.001944

F-statistic: 1.025 on 1 and 12 DF, p-value: 0.3312

In Situ DO Plots

Residuals:

Min	1Q	Median	3Q	Max
-640.1	-155.5	40.2	160.6	435.4

Coefficients:

	Estimate	Std. Error	t value	Pr(>|t|)
(Intercept)	-17.42	237.92	-0.073	0.943
data$Salinity	-10.71	25.91	-0.413	0.687

Residual standard error: 300.1 on 12 degrees of freedom

Multiple R-squared: 0.01404,   Adjusted R-squared: -0.06813

F-statistic: 0.1709 on 1 and 12 DF, p-value: 0.6866
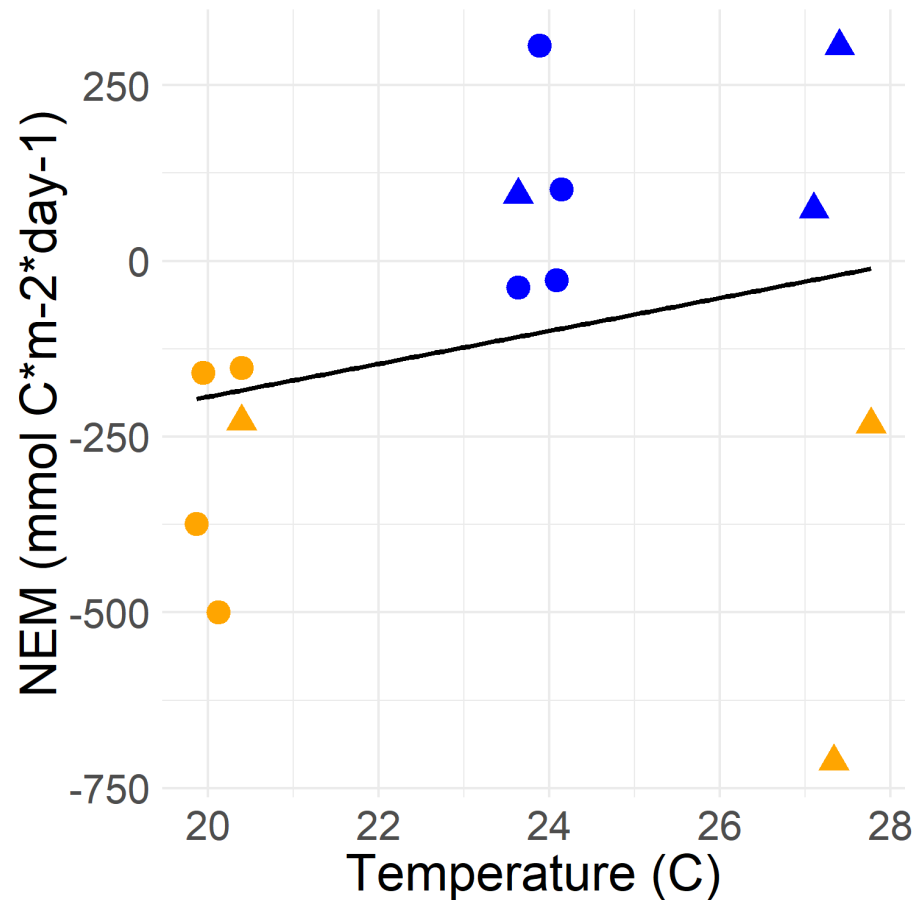
Residuals:

Min	1Q	Median	3Q	Max
-690.63	-144.61	52.83	173.71	408.66

Coefficients:

	Estimate	Std. Error	t value	Pr(>|t|)
(Intercept)	-661.60	638.47	-1.036	0.321
data$Temperature..C.	23.43	26.91	0.871	0.401

Residual standard error: 293.1 on 12 degrees of freedom

Multiple R-squared: 0.0594, Adjusted R-squared: -0.01898

F-statistic: 0.7578 on 1 and 12 DF, p-value: 0.4011
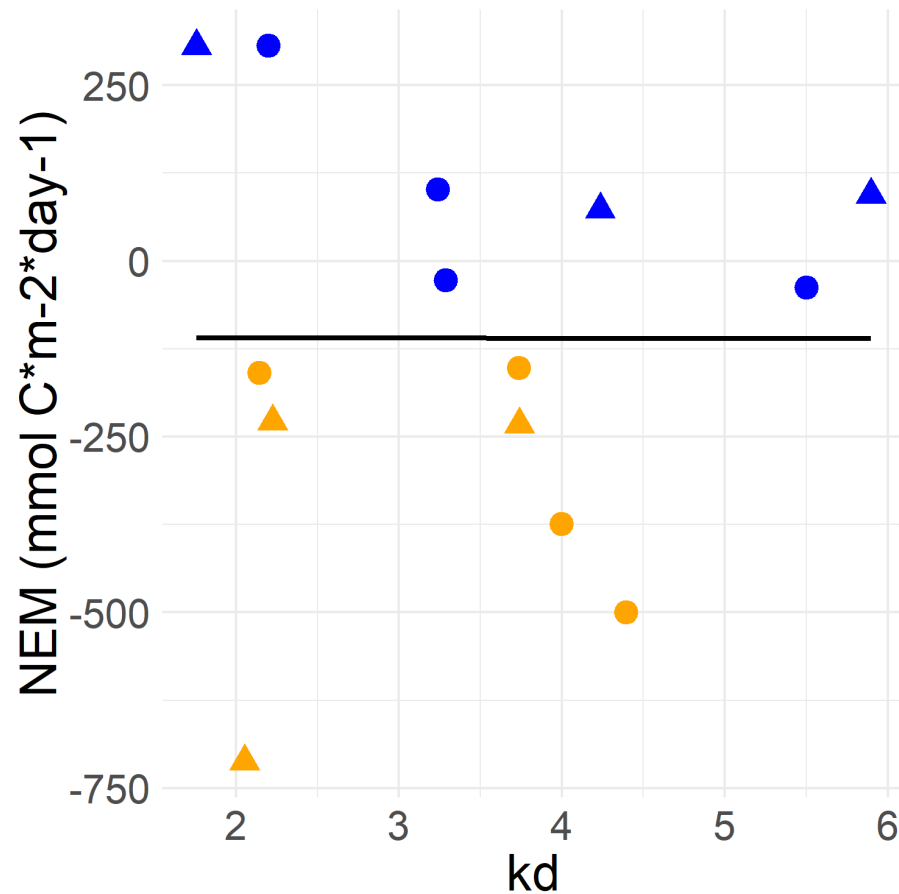
Residuals:

Min	1Q	Median	3Q	Max
-602.14	-121.85	15.66	199.40	416.34

Coefficients:

	Estimate	Std. Error	t value	Pr(>|t|)
(Intercept)	-109.70576	237.76552	-0.461	0.653
data$kd	-0.08692	64.69202	-0.001	0.999

Residual standard error: 302.2 on 12 degrees of freedom

Multiple R-squared: 1.505e-07, Adjusted R-squared: -0.08333

F-statistic: 1.805e-06 on 1 and 12 DF, p-value: 0.9989
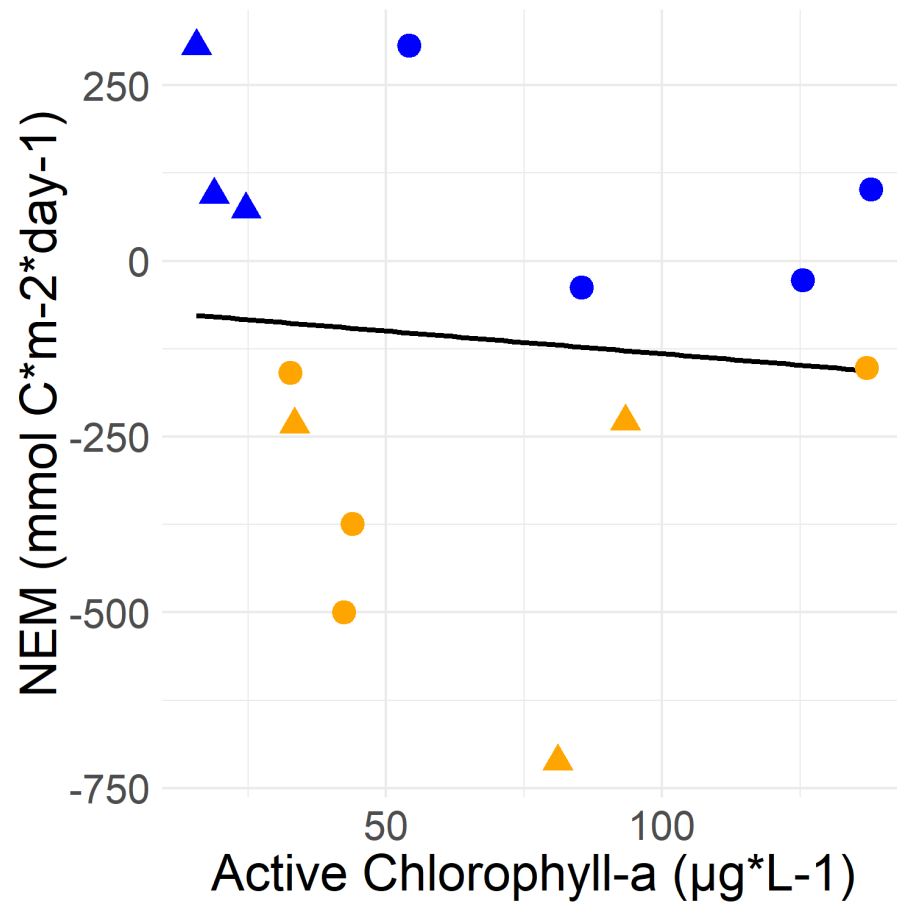
Residuals:

Min	1Q	Median	3Q	Max
-592.3	-133.3	44.7	169.6	408.8

Coefficients:

	Estimate	Std. Error	t value	Pr(>|t|)
(Intercept)	-67.2678	149.4059	-0.450	0.661
data$Active.Chlorophyll.a..ug.L.	-0.6463	1.9045	-0.339	0.740

Residual standard error: 300.8 on 12 degrees of freedom

Multiple R-squared: 0.009507,   Adjusted R-squared: -0.07303

F-statistic: 0.1152 on 1 and 12 DF, p-value: 0.7402
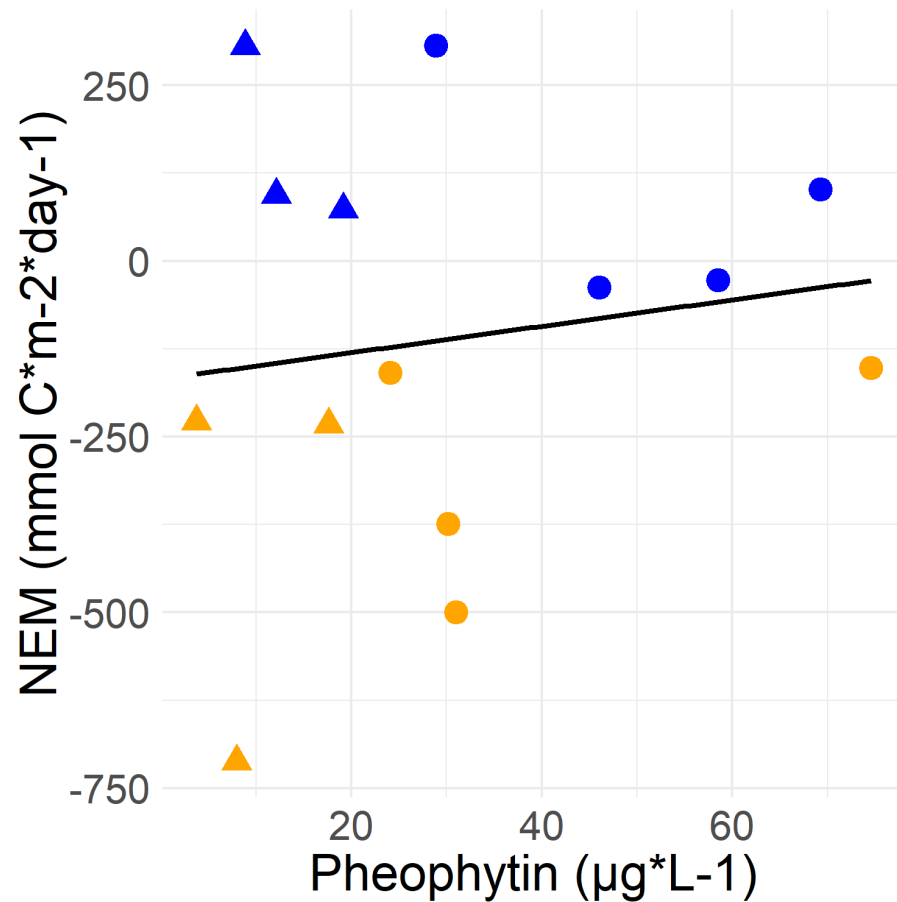
Residuals:

Min	1Q	Median	3Q	Max
-559.06	-117.41	-2.78	188.99	457.25

Coefficients:

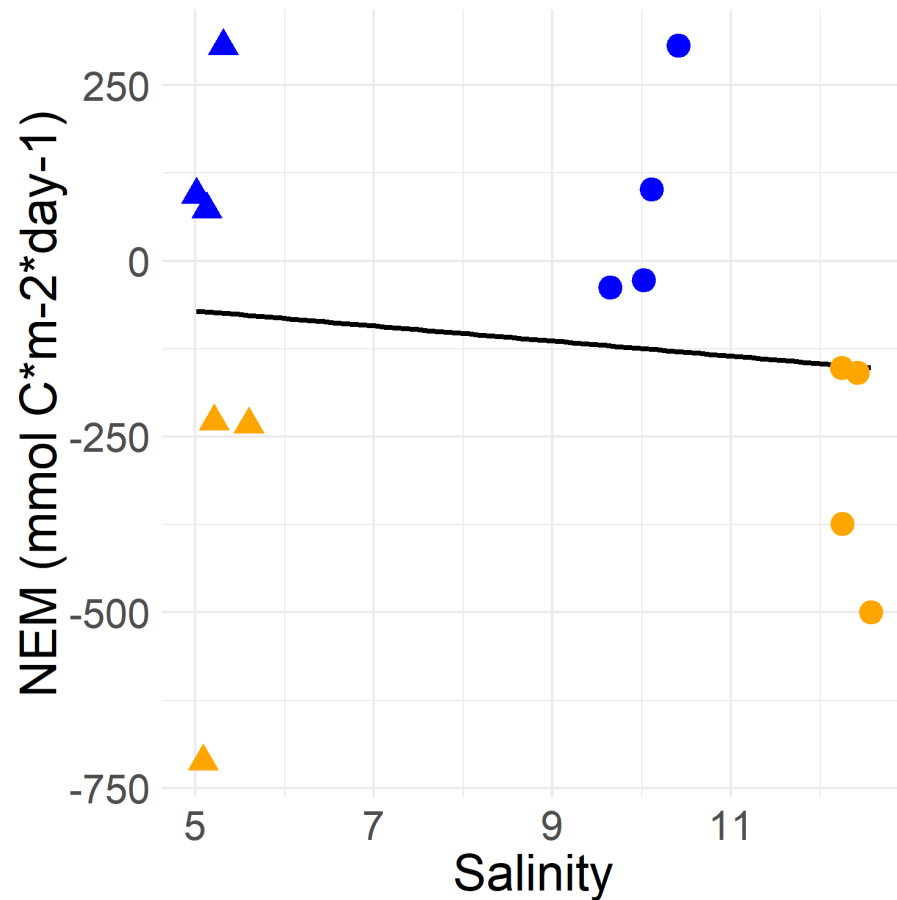|	Estimate	Std. Error	t value	Pr(>|t|)
(Intercept)	-168.017	137.230	-1.224	0.244
data$Pheophytin..ug.L.	1.879	3.615	0.520	0.613

Residual standard error: 298.9 on 12 degrees of freedom

Multiple R-squared: 0.02203,   Adjusted R-squared: -0.05947

F-statistic: 0.2703 on 1 and 12 DF, p-value: 0.6126
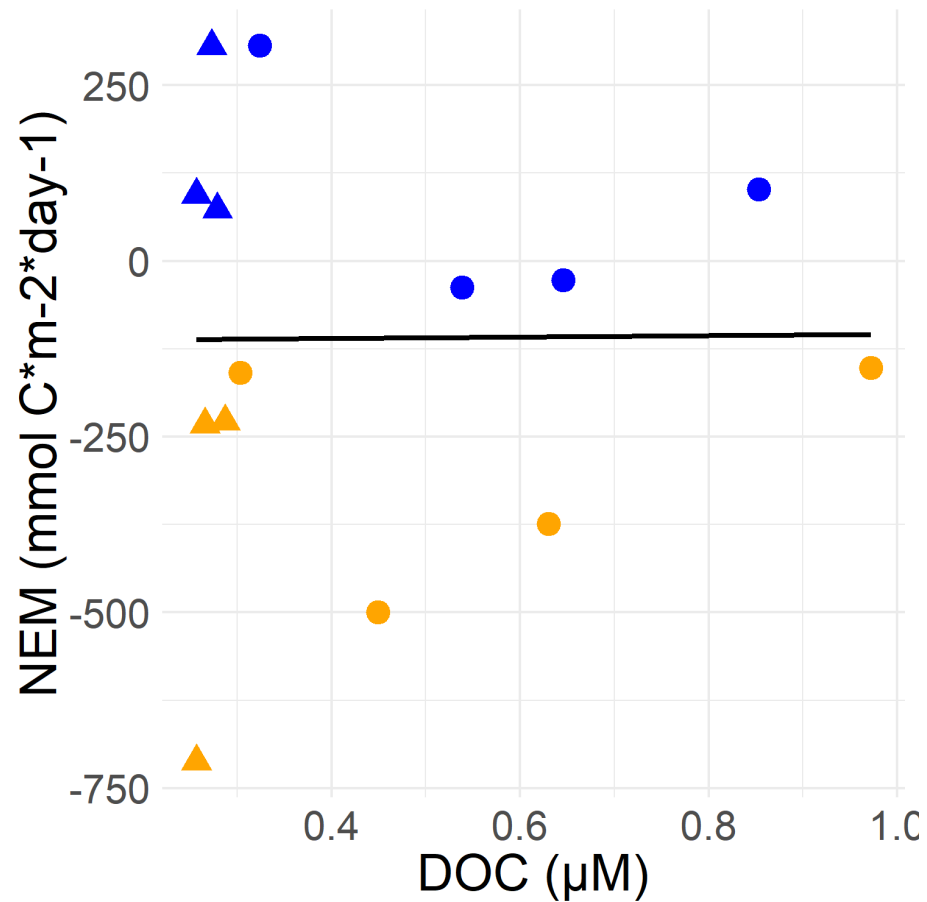
Residuals:

Min	1Q	Median	3Q	Max
-600.05	-120.02	12.51	201.13	417.74

Coefficients:

	Estimate	Std. Error	t value	Pr(>|t|)
(Intercept)	-114.55	177.57	-0.645	0.531
data$DOC	10.03	349.47	0.029	0.978

Residual standard error: 302.2 on 12 degrees of freedom

Multiple R-squared: 6.866e-05,   Adjusted R-squared: -0.08326

F-statistic: 0.000824 on 1 and 12 DF, p-value: 0.9776
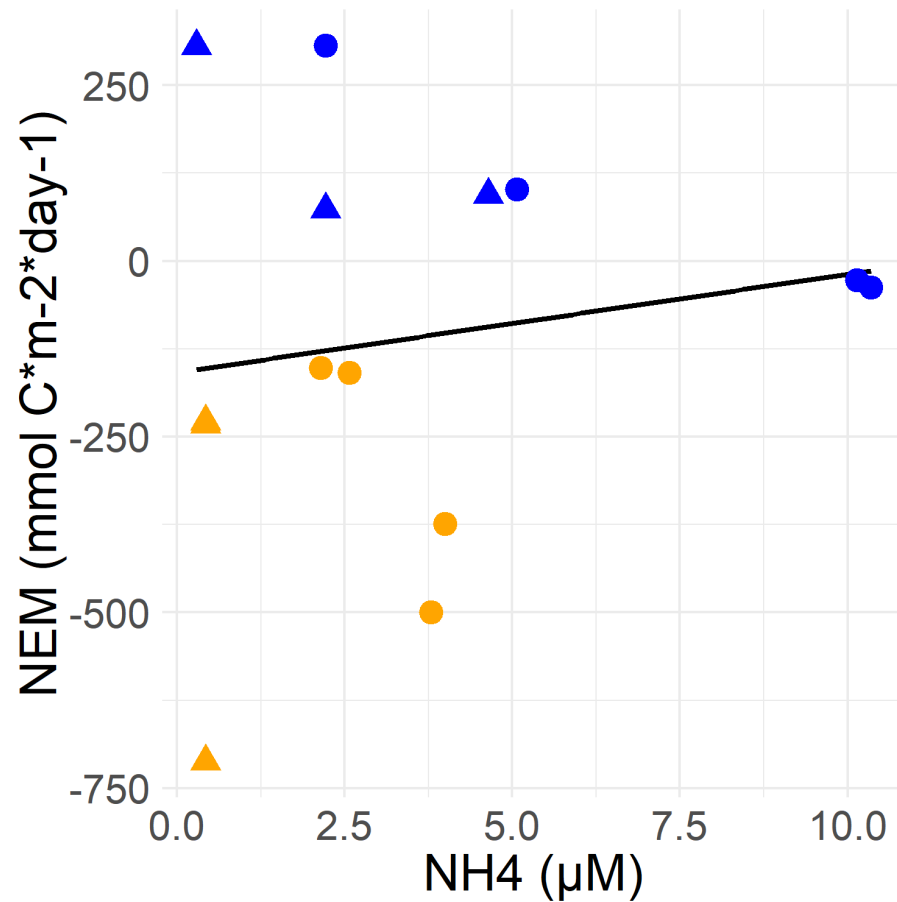
Residuals:

Min	1Q	Median	3Q	Max
-559.39	-79.21	-23.16	189.47	460.57

Coefficients:

	Estimate	Std. Error	t value	Pr(>|t|)
(Intercept)	-158.63	118.62	-1.337	0.206
data$NH4	13.98	25.25	0.554	0.590

Residual standard error: 298.4 on 12 degrees of freedom

Multiple R-squared: 0.02492,   Adjusted R-squared: -0.05634

F-statistic: 0.3066 on 1 and 12 DF, p-value: 0.5899
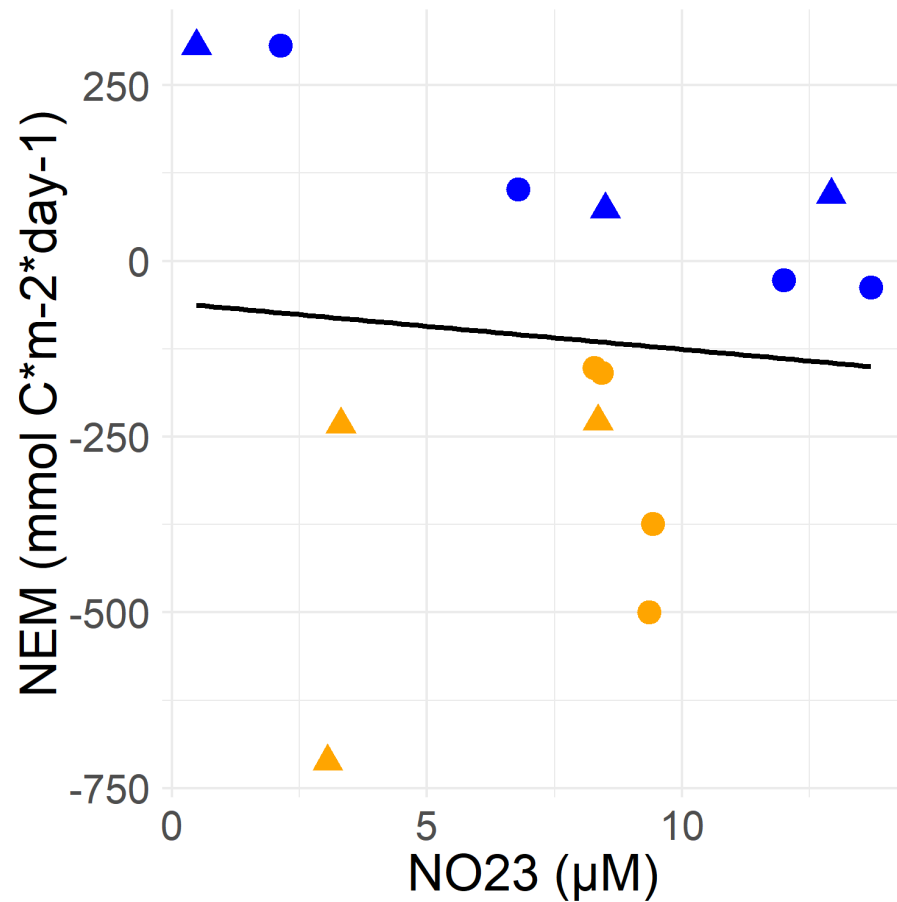
Residuals:

Min	1Q	Median	3Q	Max
-632.15	-141.96	36.98	202.25	380.20

Coefficients:

	Estimate	Std. Error	t value	Pr(>|t|)
(Intercept)	-59.720	176.180	-0.339	0.740
data$NO23	-6.597	20.563	-0.321	0.754

Residual standard error: 301 on 12 degrees of freedom

Multiple R-squared: 0.008504, Adjusted R-squared: -0.07412

F-statistic: 0.1029 on 1 and 12 DF, p-value: 0.7539
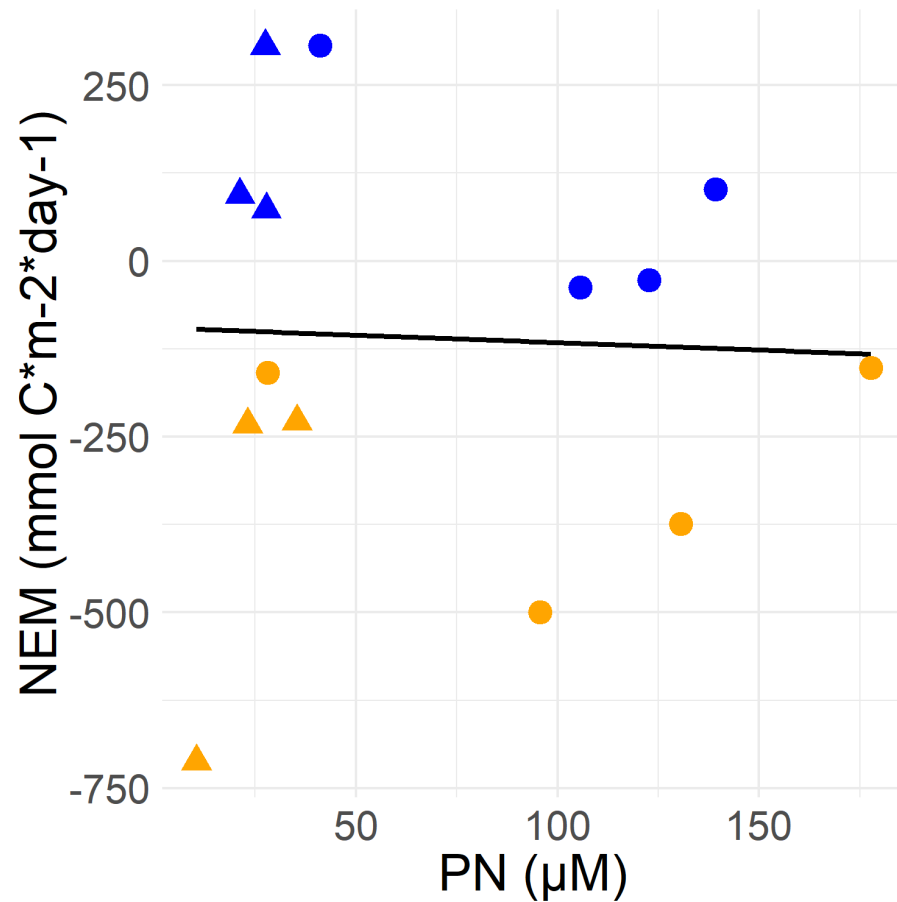
Residuals:

Min	1Q	Median	3Q	Max
-614.71	-131.19	30.61	189.17	410.26

Coefficients:

	Estimate	Std. Error	t value	Pr(>|t|)
(Intercept)	-95.1098	133.2624	-0.714	0.489
data$PN	-0.2114	1.5046	-0.140	0.891

Residual standard error: 302 on 12 degrees of freedom

Multiple R-squared: 0.001642, Adjusted R-squared: -0.08155

F-statistic: 0.01973 on 1 and 12 DF, p-value: 0.8906

243
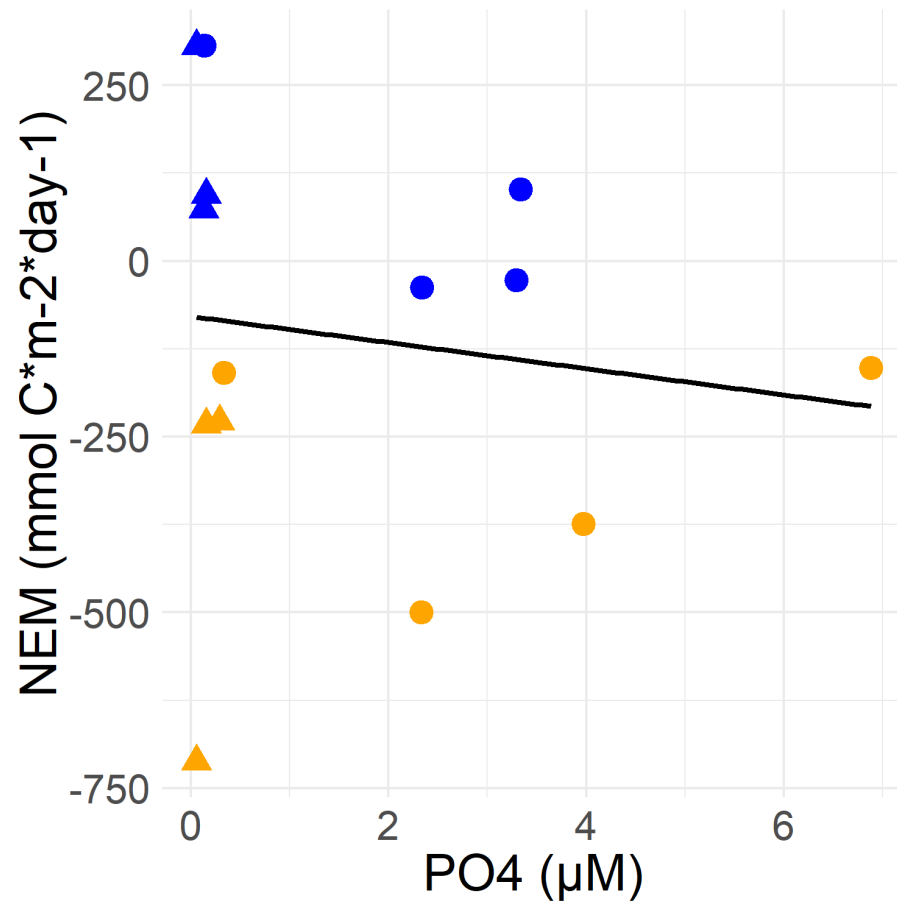
Residuals:

Min	1Q	Median	3Q	Max
-632.18	-149.51	70.14	170.85	387.79

Coefficients:

	Estimate	Std. Error	t value	Pr(>|t|)
(Intercept)	-78.89	104.00	-0.759	0.463
data$PO4	-18.58	39.64	-0.469	0.648

Residual standard error: 299.5 on 12 degrees of freedom

Multiple R-squared: 0.01798, Adjusted R-squared: -0.06385

F-statistic: 0.2197 on 1 and 12 DF, p-value: 0.6476
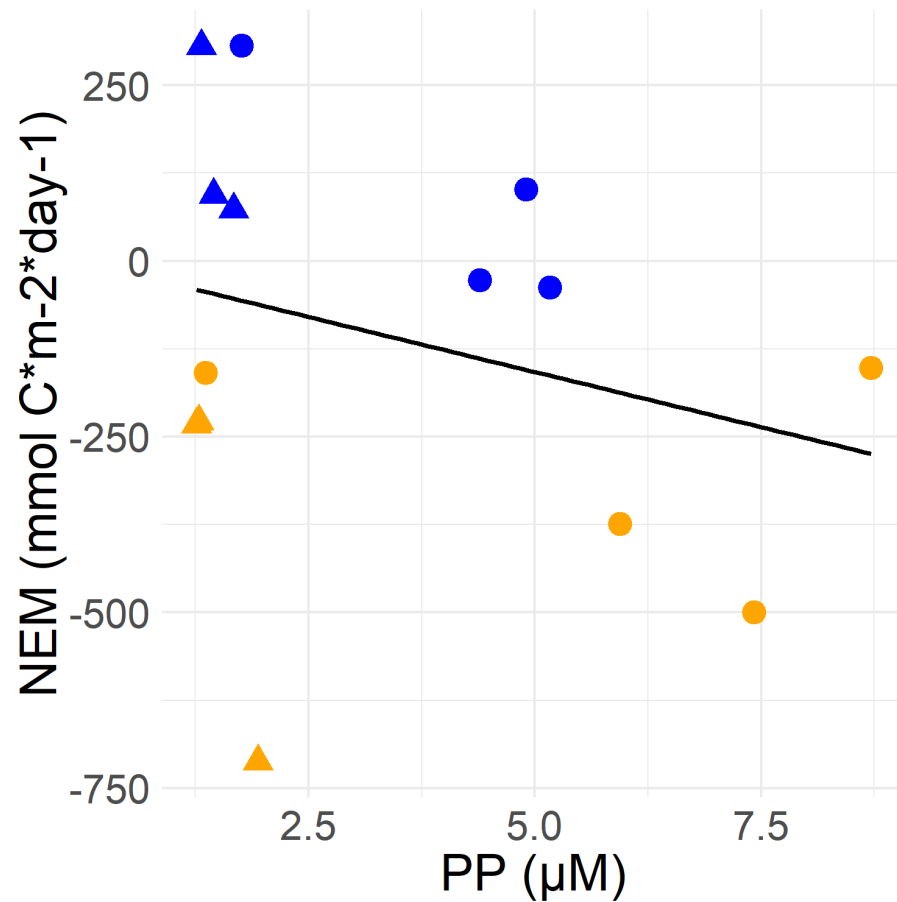
Residuals:

Min	1Q	Median	3Q	Max
-650.0	-186.9	117.0	137.7	362.8

Coefficients:

	Estimate	Std. Error	t value	Pr(>|t|)
(Intercept)	-1.23	133.34	-0.009	0.993
data$PP	-31.34	31.24	-1.003	0.336

Residual standard error: 290.3 on 12 degrees of freedom

Multiple R-squared: 0.07736, Adjusted R-squared: 0.0004693

F-statistic: 1.006 on 1 and 12 DF, p-value: 0.3356
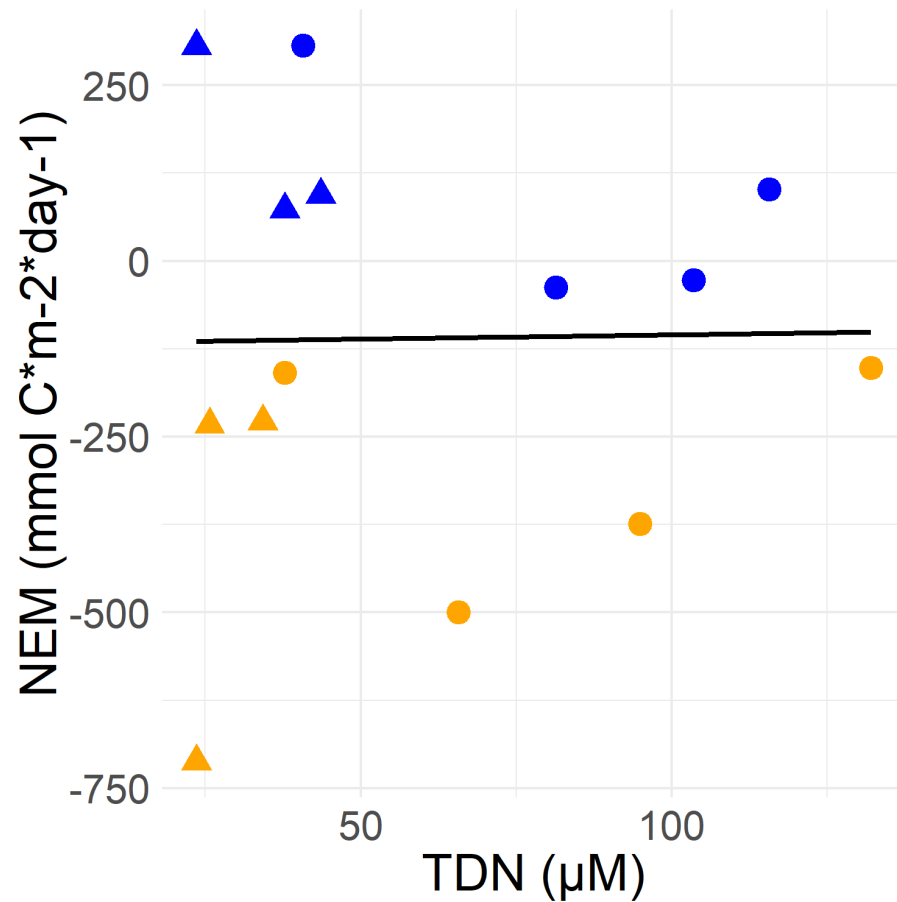
Residuals:

Min	1Q	Median	3Q	Max
-597.48	-117.81	12.21	200.77	420.48

Coefficients:

	Estimate	Std. Error	t value	Pr(>|t|)
(Intercept)	-117.3639	160.2919	-0.732	0.478
data$TDN	0.1197	2.2531	0.053	0.958

Residual standard error: 302.2 on 12 degrees of freedom

Multiple R-squared: 0.0002353,   Adjusted R-squared: -0.08308

F-statistic: 0.002824 on 1 and 12 DF, p-value: 0.9585
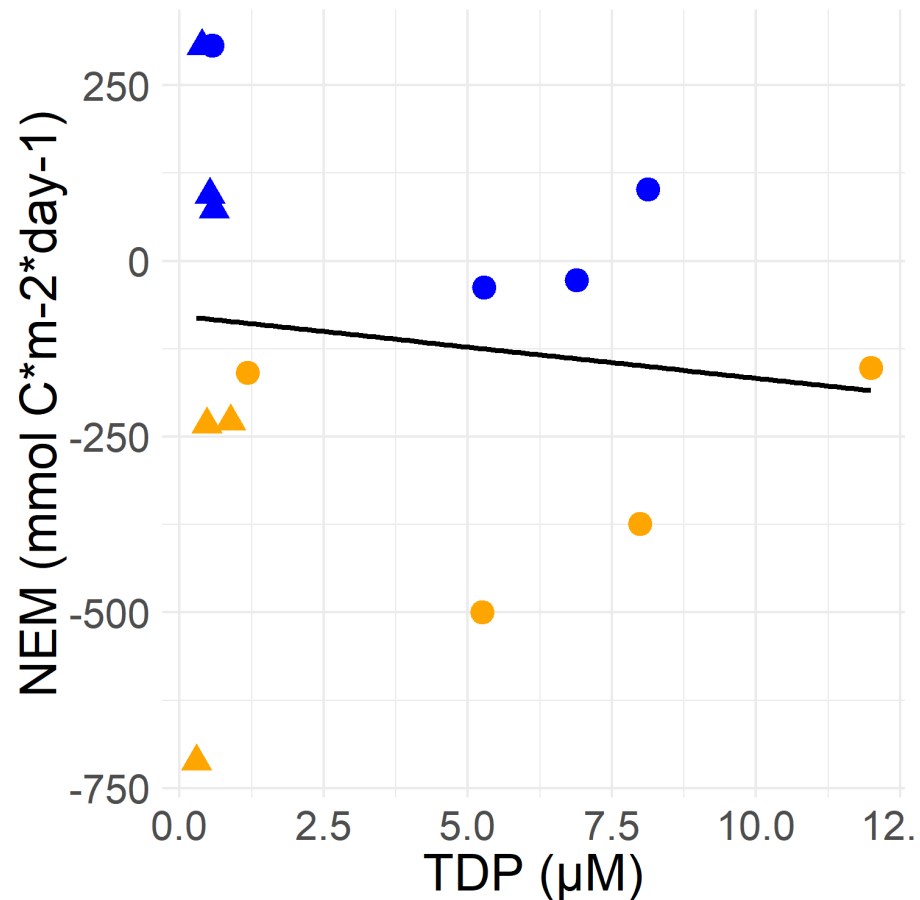
Residuals:

Min	1Q	Median	3Q	Max
-631.41	-148.66	60.23	172.12	389.50

Coefficients:

	Estimate	Std. Error	t value	Pr(>|t|)
(Intercept)	-78.071	110.967	-0.704	0.495
data$TDP	-8.867	21.295	-0.416	0.684

Residual standard error: 300.1 on 12 degrees of freedom

Multiple R-squared: 0.01424,　　　　Adjusted R-squared: -0.0679

F-statistic: 0.1734 on 1 and 12 DF, p-value: 0.6845
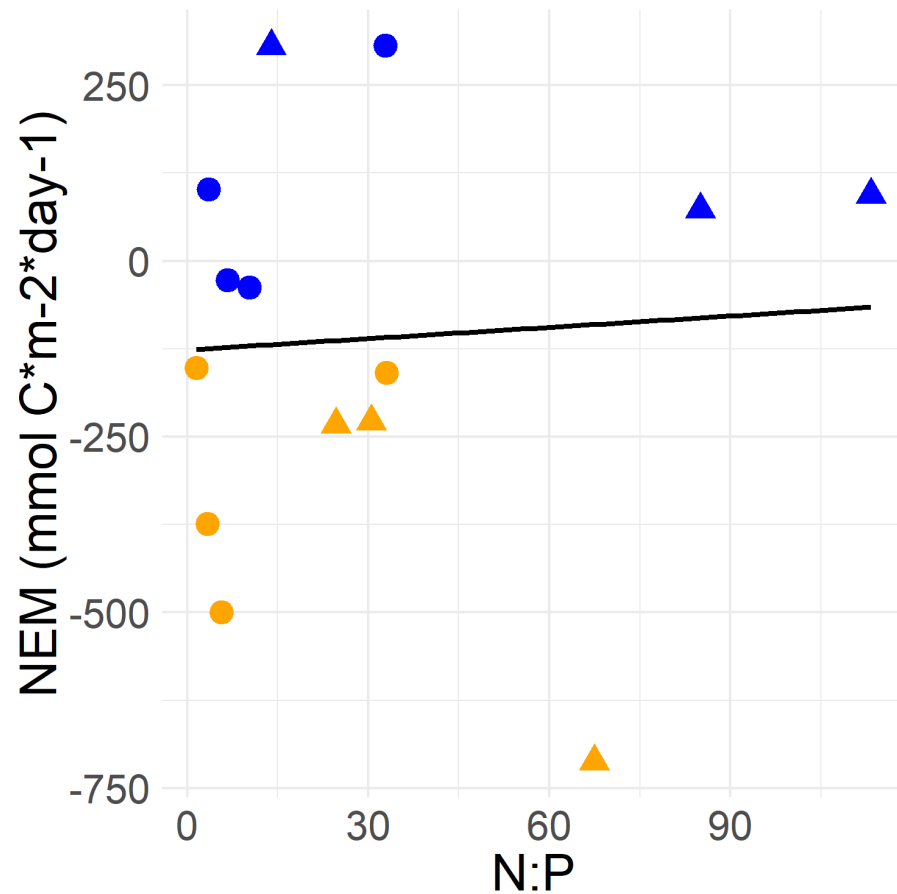
Residuals:

Min	1Q	Median	3Q	Max
-621.61	-119.31	28.91	158.85	425.01

Coefficients:

	Estimate	Std. Error	t value	Pr(>|t|)
(Intercept)	-126.5260	110.0740	-1.149	0.273
data$N.P	0.5355	2.4294	0.220	0.829

Residual standard error: 301.6 on 12 degrees of freedom

Multiple R-squared: 0.004032,   Adjusted R-squared: -0.07897

F-statistic: 0.04858 on 1 and 12 DF, p-value: 0.8293
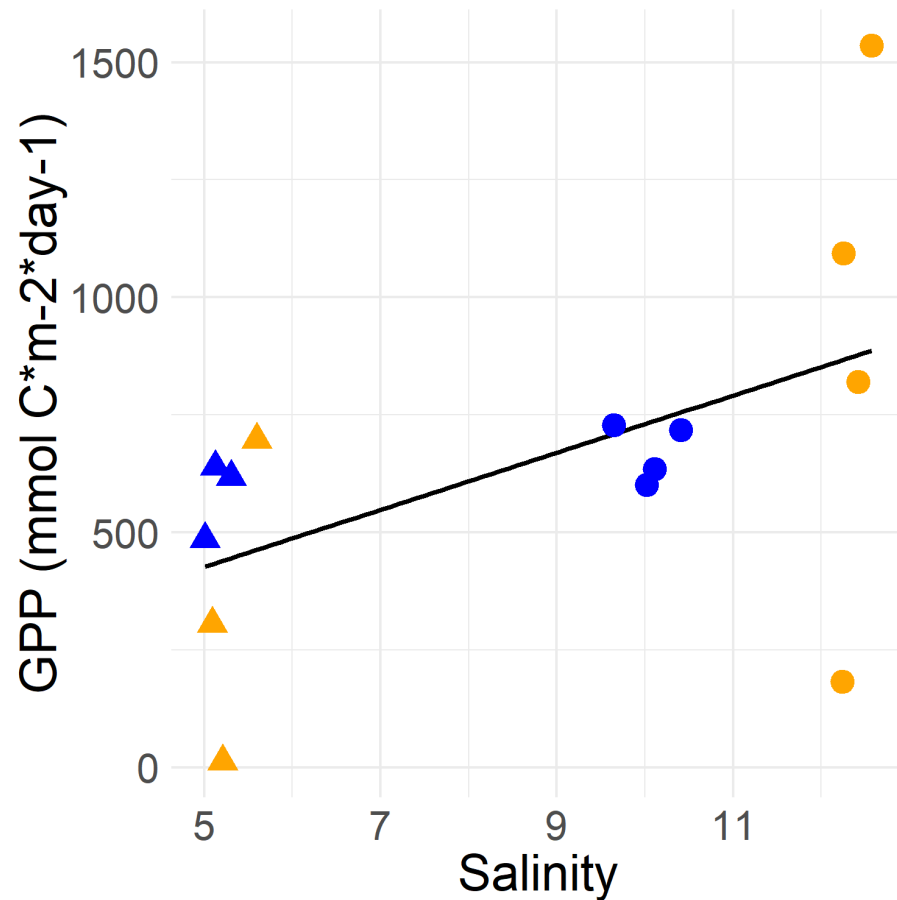
Residuals:

Min	1Q	Median	3Q	Max
-683.88	-119.87	-9.28	196.92	649.03

Coefficients:

	Estimate	Std. Error	t value	Pr(>|t|)	
(Intercept)	122.56	261.03	0.470	0.6471	
data$Salinity	60.79	28.43	2.138	0.0538	.

Signif. codes: 0 '***' 0.001 '**' 0.01 '*' 0.05 '.' 0.1 ' ' 1

Residual standard error: 329.3 on 12 degrees of freedom

Multiple R-squared: 0.2759,   Adjusted R-squared: 0.2156

F-statistic: 4.572 on 1 and 12 DF, p-value: 0.05376

Residuals:

Min	1Q	Median	3Q	Max
-717.23	-128.64	73.78	83.44	798.75

Coefficients:

	Estimate	Std. Error	t value	Pr(>|t|)
(Intercept)	1259.01	823.85	1.528	0.152
data$Temperature..C.	-25.95	34.72	-0.747	0.469

Residual standard error: 378.2 on 12 degrees of freedom

Multiple R-squared: 0.04446,   Adjusted R-squared: -0.03516

F-statistic: 0.5584 on 1 and 12 DF, p-value: 0.4693
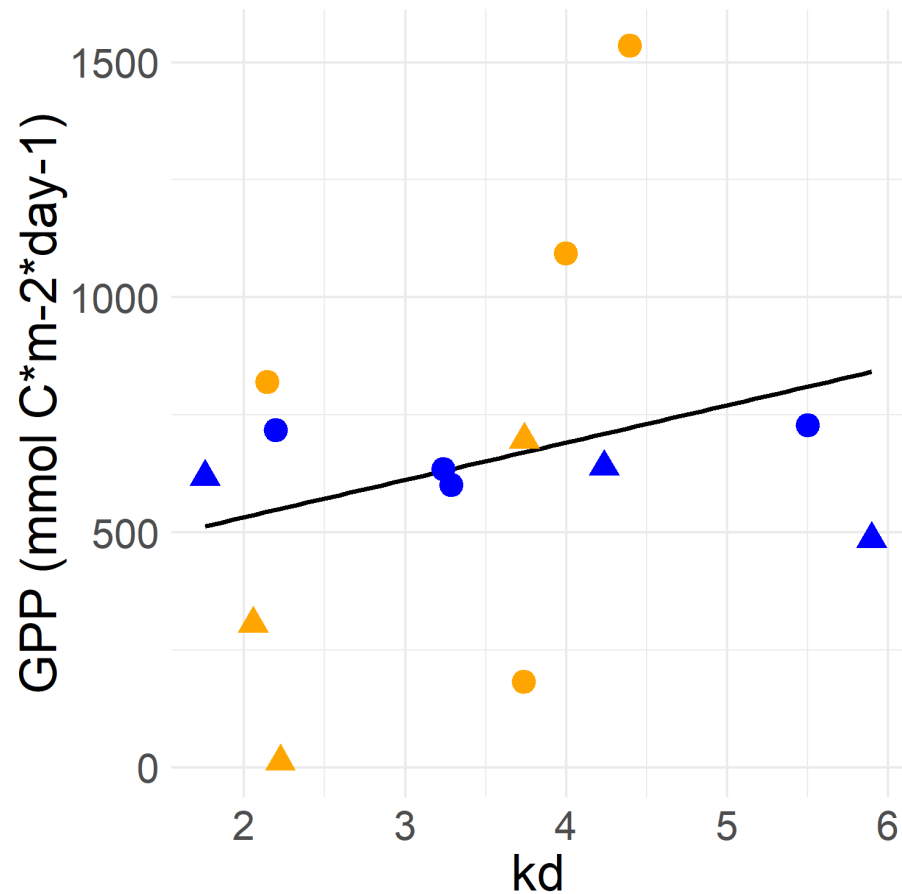
Residuals:

Min	1Q	Median	3Q	Max
-537.52	-193.29	-14.69	153.02	813.34

Coefficients:

	Estimate	Std. Error	t value	Pr(>|t|)
(Intercept)	373.82	292.53	1.278	0.225
data$kd	79.33	79.59	0.997	0.339

Residual standard error: 371.9 on 12 degrees of freedom

Multiple R-squared: 0.07645,   Adjusted R-squared: -0.0005089

F-statistic: 0.9934 on 1 and 12 DF, p-value: 0.3386

251
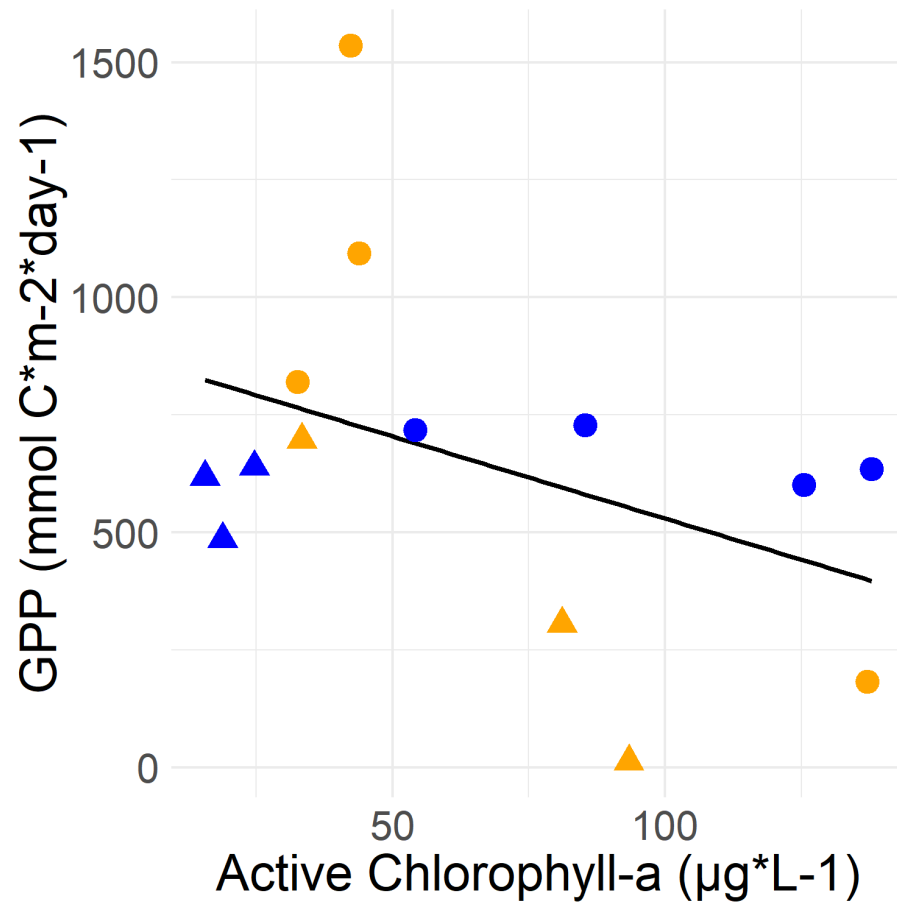
Residuals:

Min	1Q	Median	3Q	Max
-540.04	-214.56	-18.86	157.14	804.41

Coefficients:

	Estimate	Std. Error	t value	Pr(>|t|)
(Intercept)	879.426	175.093	5.023	0.000298 ***
data$Active.Chlorophyll.a..ug.L.	-3.499	2.232	-1.568	0.142905

Signif. codes: 0 '***' 0.001 '**' 0.01 '*' 0.05 '.' 0.1 ' ' 1

Residual standard error: 352.5 on 12 degrees of freedom

Multiple R-squared: 0.17,   Adjusted R-squared: 0.1008

F-statistic: 2.458 on 1 and 12 DF, p-value: 0.1429

252

Residuals:

Min	1Q	Median	3Q	Max
-612.45	-127.68	-5.22	70.14	887.58

Coefficients:

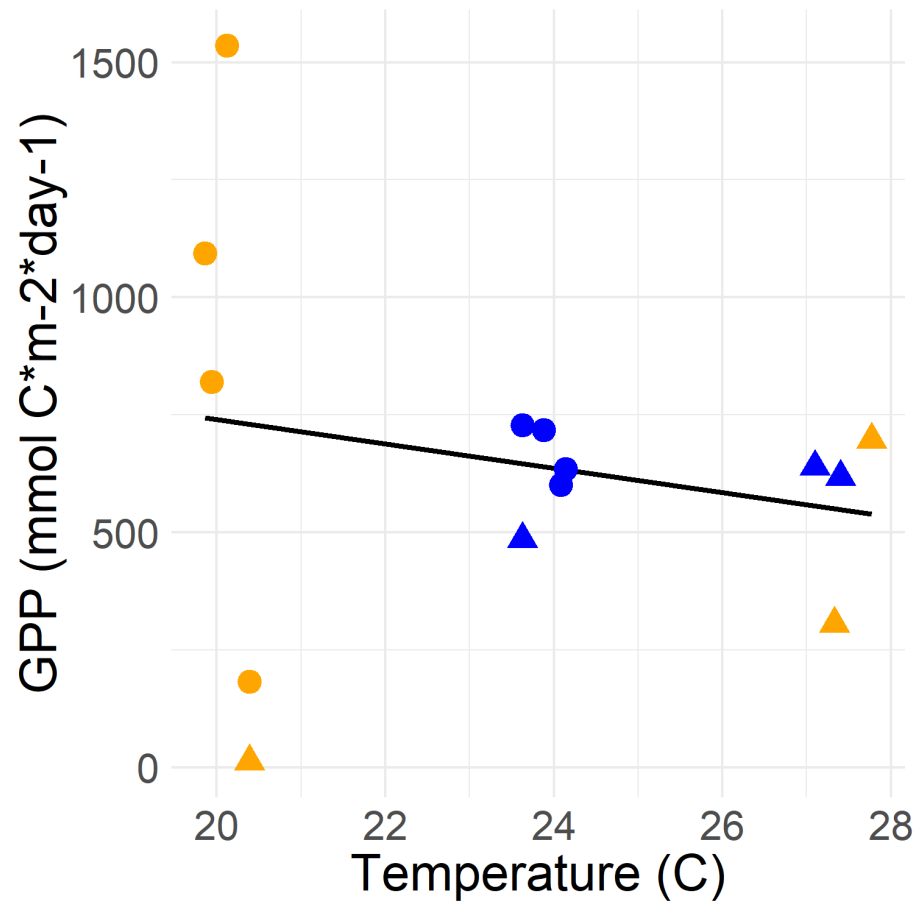|	Estimate	Std. Error	t value	Pr(>|t|)	
(Intercept)	622.0319	177.4146	3.506	0.00433	**
data$Pheophytin..ug.L.	0.8426	4.6736	0.180	0.85993	

Signif. codes: 0 '***' 0.001 '**' 0.01 '*' 0.05 '.' 0.1 ' ' 1

Residual standard error: 386.4 on 12 degrees of freedom

Multiple R-squared: 0.002702,	Adjusted R-squared: -0.08041

F-statistic: 0.03251 on 1 and 12 DF, p-value: 0.8599

253

Residuals:

Min	1Q	Median	3Q	Max
-636.57	-134.46	-9.90	78.07	887.65

Coefficients:

	Estimate	Std. Error	t value	Pr(>|t|)	
(Intercept)	651.479	227.340	2.866	0.0142	*
data$DOC	-7.597	447.409	-0.017	0.9867	

Signif. codes: 0 '***' 0.001 '**' 0.01 '*' 0.05 '.' 0.1 ' ' 1

Residual standard error: 386.9 on 12 degrees of freedom

Multiple R-squared: 2.403e-05,   Adjusted R-squared: -0.08331

F-statistic: 0.0002883 on 1 and 12 DF, p-value: 0.9867

Residuals:

Min	1Q	Median	3Q	Max
-551.35	-221.75	-15.26	125.93	879.25

Coefficients:

	Estimate	Std. Error	t value	Pr(>|t|)	
(Intercept)	552.28	149.19	3.702	0.00303	**
data$NH4	27.53	31.75	0.867	0.40284	

Signif. codes: 0 '***' 0.001 '**' 0.01 '*' 0.05 '.' 0.1 ' ' 1

Residual standard error: 375.4 on 12 degrees of freedom

Multiple R-squared: 0.05897,   Adjusted R-squared: -0.01945

F-statistic: 0.752 on 1 and 12 DF, p-value: 0.4028

Residuals:

Min	1Q	Median	3Q	Max
-643.21	-188.50	5.46	120.45	868.97

Coefficients:

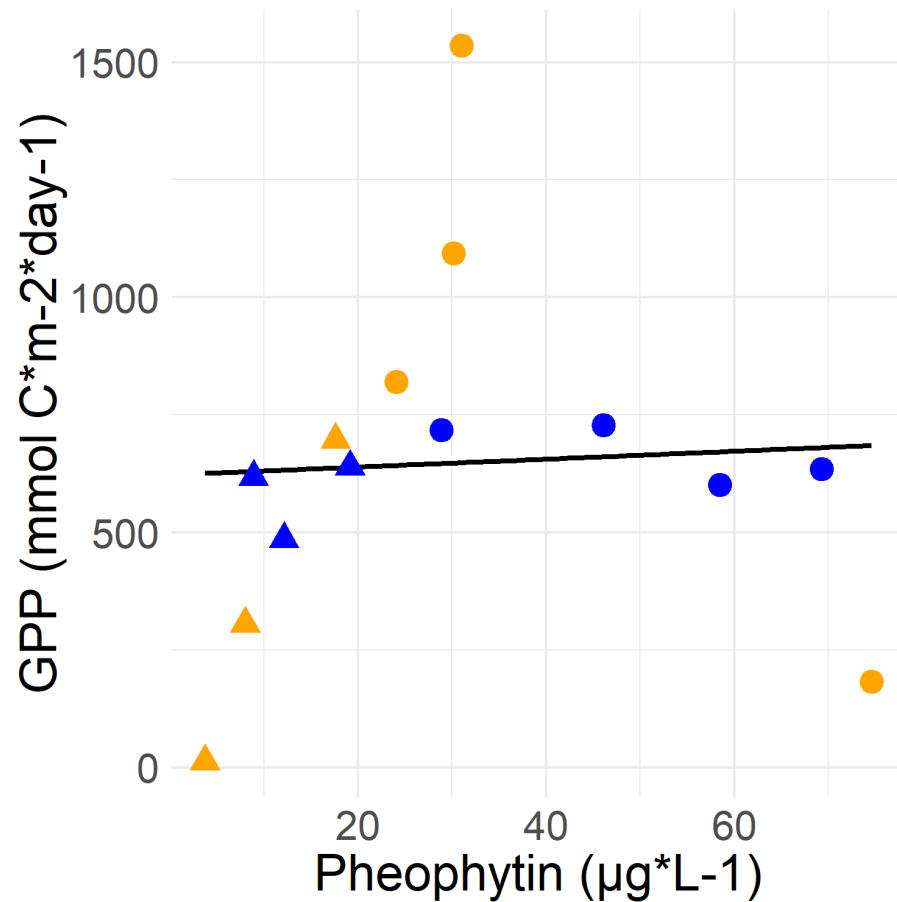|	Estimate	Std. Error	t value	Pr(>|t|)
(Intercept)	565.61	224.93	2.515	0.0272 *
data$NO23	10.81	26.25	0.412	0.6877

Signif. codes: 0 '***' 0.001 '**' 0.01 '*' 0.05 '.' 0.1 ' ' 1

Residual standard error: 384.2 on 12 degrees of freedom

Multiple R-squared: 0.01394,   Adjusted R-squared: -0.06823

F-statistic: 0.1697 on 1 and 12 DF, p-value: 0.6877

Residuals:

Min	1Q	Median	3Q	Max
-600.87	-110.31	22.68	97.41	862.93

Coefficients:

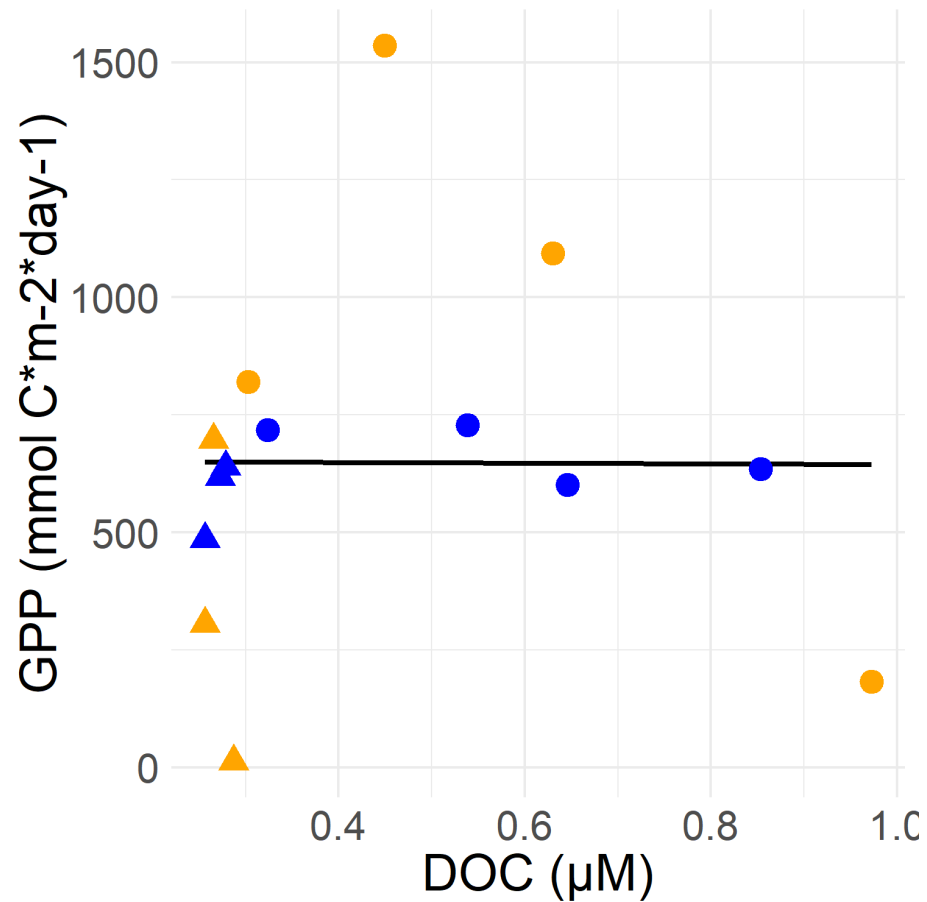|	Estimate	Std. Error	t value	Pr(>|t|)	
(Intercept)	578.8137	168.8904	3.427	0.00501	**
data$PN	0.9823	1.9069	0.515	0.61583	

Signif. codes: 0 '***' 0.001 '**' 0.01 '*' 0.05 '.' 0.1 ' ' 1

Residual standard error: 382.7 on 12 degrees of freedom

Multiple R-squared: 0.02163,   Adjusted R-squared: -0.0599

F-statistic: 0.2653 on 1 and 12 DF, p-value: 0.6158

257

Residuals:

   Min   1Q Median   3Q   Max
-623.97 -127.70   -6.45   80.19 882.33

Coefficients:

            Estimate Std. Error t value Pr(>|t|)
(Intercept) 634.348   134.210   4.727 0.000491 ***
data$PO4   8.177   51.161   0.160 0.875679
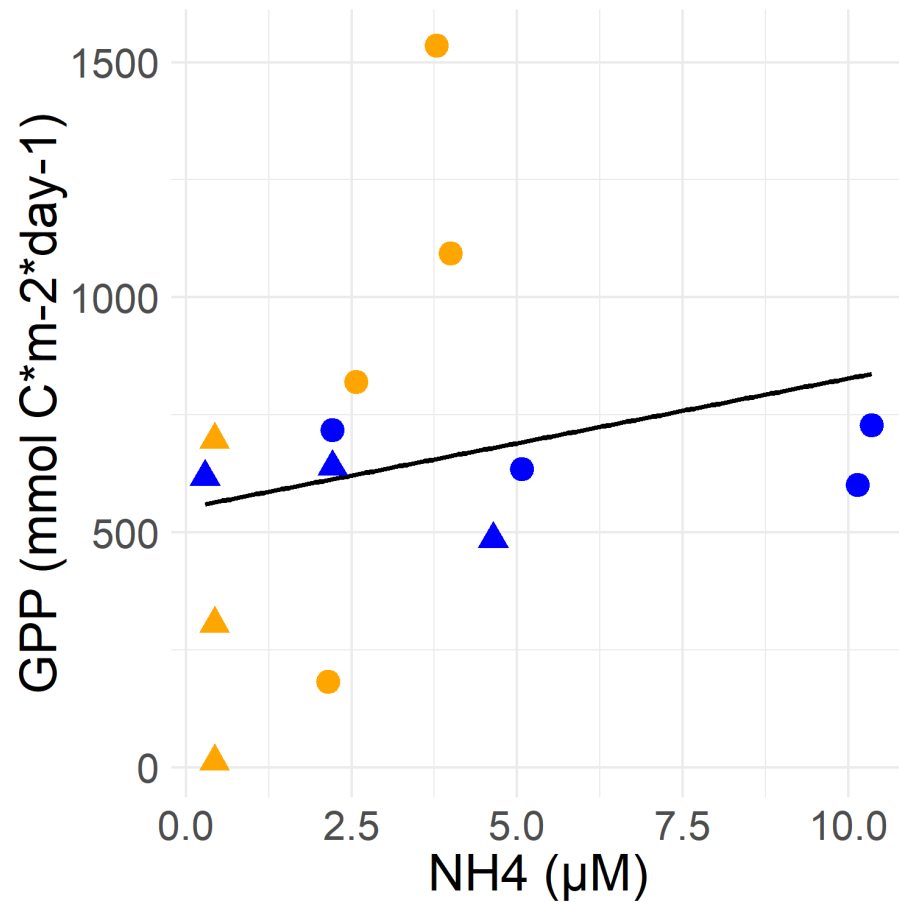---

Signif. codes: 0 '***' 0.001 '**' 0.01 '*' 0.05 '.' 0.1 ' ' 1

Residual standard error: 386.5 on 12 degrees of freedom

Multiple R-squared: 0.002124,   Adjusted R-squared: -0.08103

F-statistic: 0.02554 on 1 and 12 DF, p-value: 0.8757

Residuals:

Min	1Q	Median	3Q	Max
-706.61	-87.08	35.87	150.26	705.78

Coefficients:

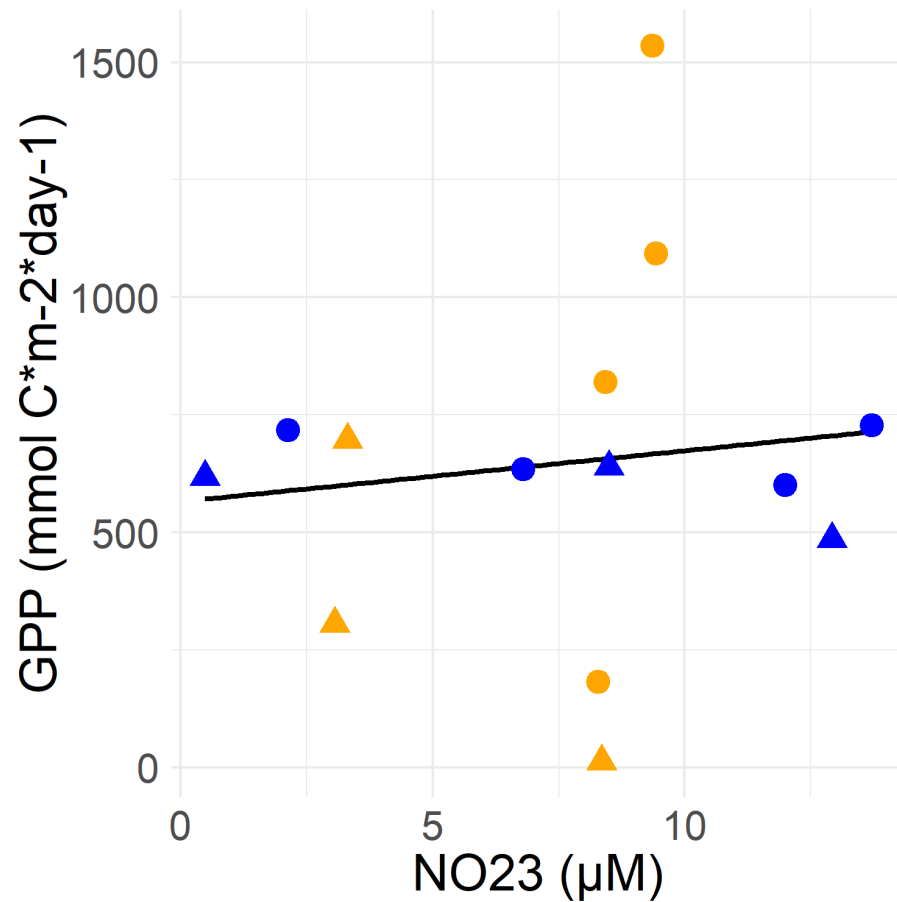|	Estimate	Std. Error	t value	Pr(>|t|)
(Intercept)	488.36	168.44	2.899	0.0133 *
data$PP	46.00	39.46	1.166	0.2664

Signif. codes: 0 '***' 0.001 '**' 0.01 '*' 0.05 '.' 0.1 ' ' 1

Residual standard error: 366.7 on 12 degrees of freedom

Multiple R-squared: 0.1017,   Adjusted R-squared: 0.02686

F-statistic: 1.359 on 1 and 12 DF, p-value: 0.2664

Residuals:

   Min   1Q Median   3Q   Max

-617.23 -131.77   1.05 80.53 884.86

Coefficients:

        Estimate Std. Error t value Pr(>|t|)

(Intercept) 607.1680 204.7804 2.965 0.0118 *
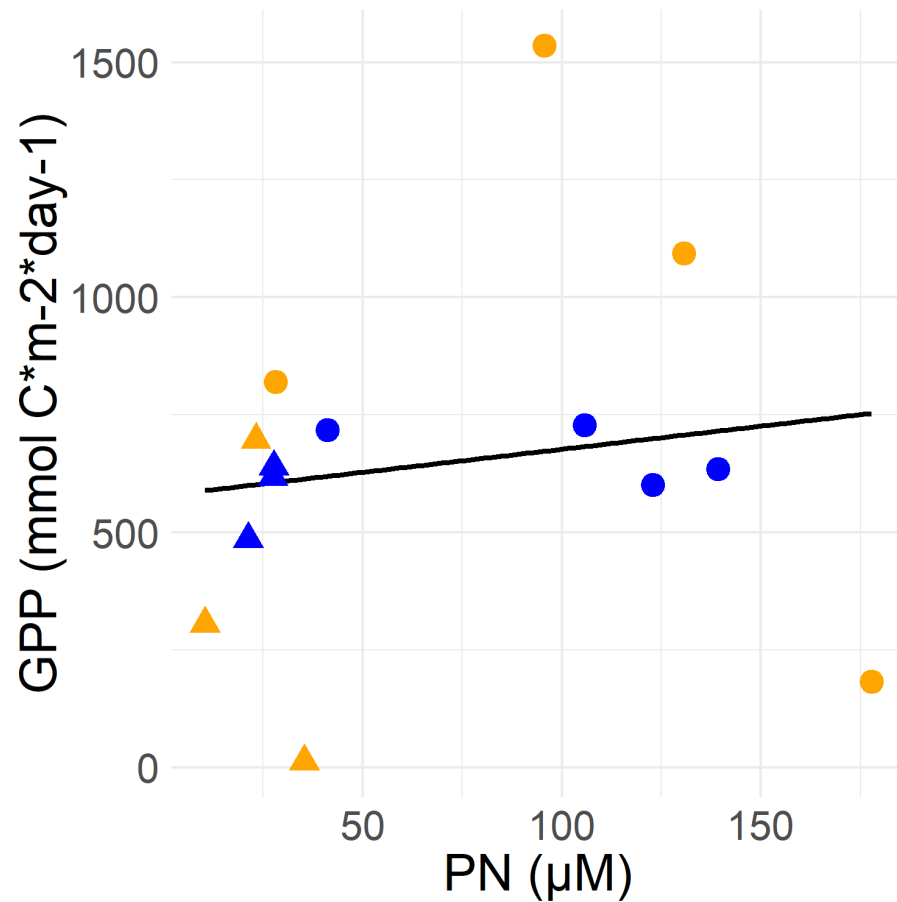
data$TDN   0.6651   2.8785 0.231 0.8212

Signif. codes: 0 '***' 0.001 '**' 0.01 '*' 0.05 '.' 0.1 ' ' 1

Residual standard error: 386.1 on 12 degrees of freedom

Multiple R-squared: 0.00443,   Adjusted R-squared: -0.07853

F-statistic: 0.0534 on 1 and 12 DF, p-value: 0.8212
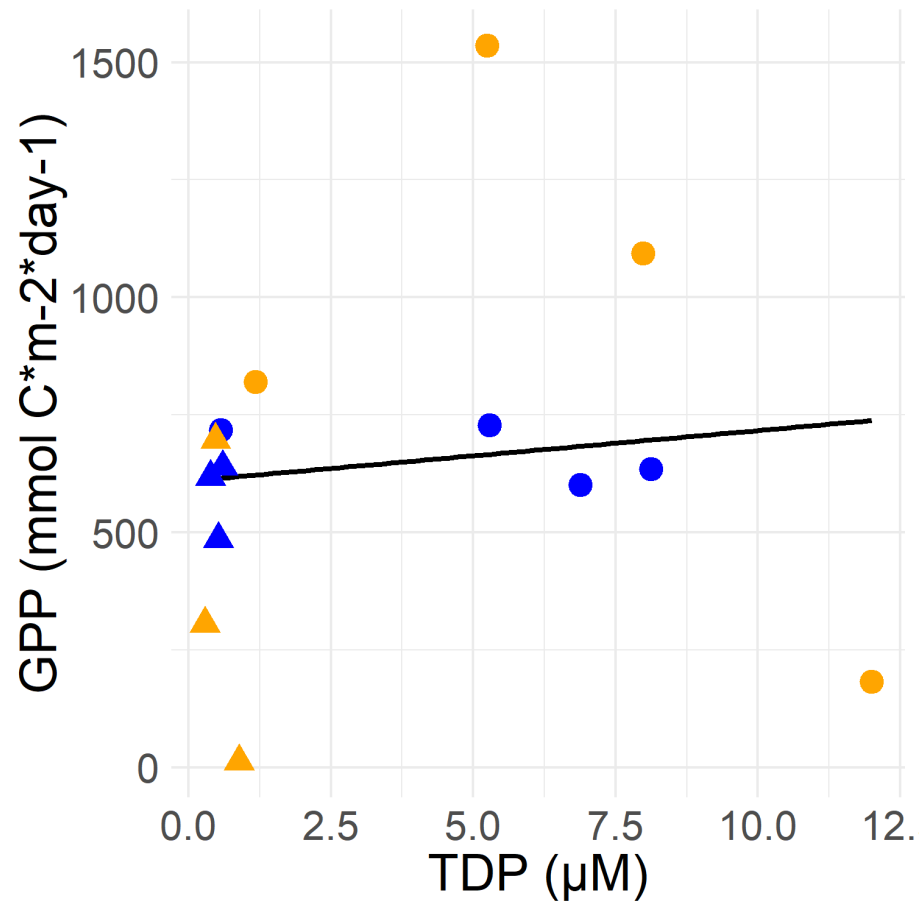
Residuals:

Min	1Q	Median	3Q	Max
-606.15	-117.76	13.96	97.09	870.02

Coefficients:

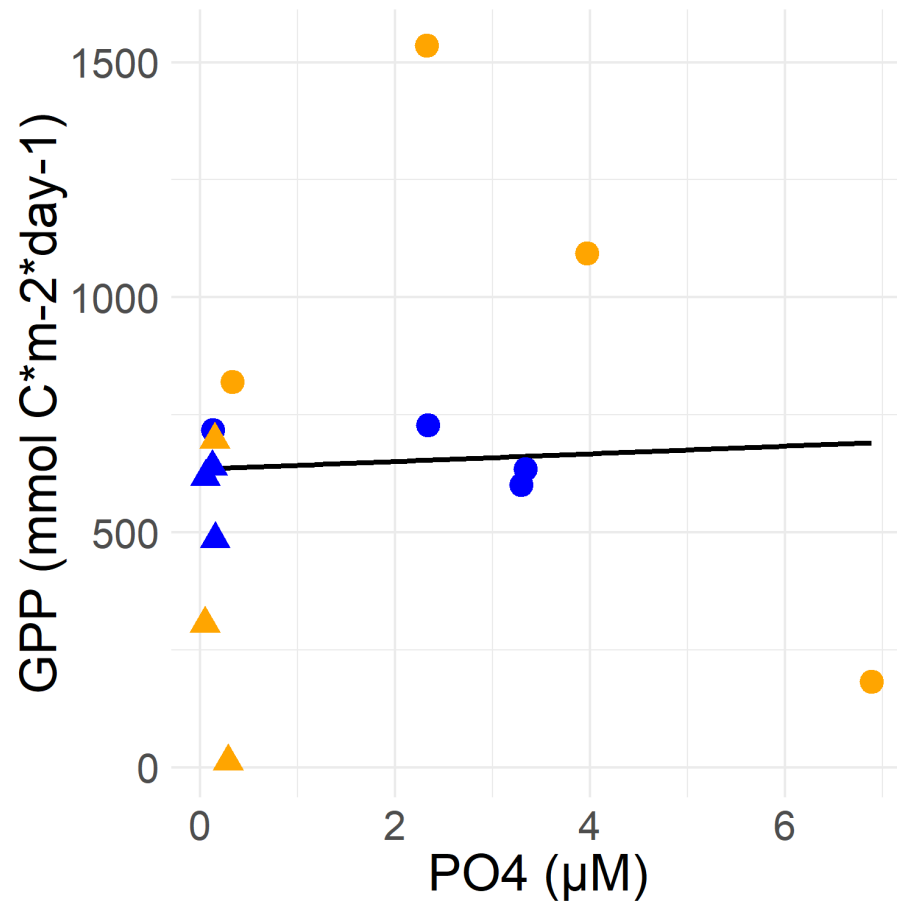|	Estimate	Std. Error	t value	Pr(>|t|)	
(Intercept)	609.39	142.17	4.286	0.00106	**
data$TDP	10.73	27.28	0.393	0.70094	

Signif. codes: 0 '***' 0.001 '**' 0.01 '*' 0.05 '.' 0.1 ' ' 1

Residual standard error: 384.5 on 12 degrees of freedom

Multiple R-squared: 0.01273,   Adjusted R-squared: -0.06954

F-statistic: 0.1547 on 1 and 12 DF, p-value: 0.7009

Residuals:

Min   1Q Median   3Q   Max

-636.19 -114.18   24.53 138.19 811.47

Coefficients:

         Estimate Std. Error t value Pr(>|t|)

(Intercept) 741.304   135.557   5.469 0.000143 ***

data$N.P   -3.023   2.992 -1.010 0.332246

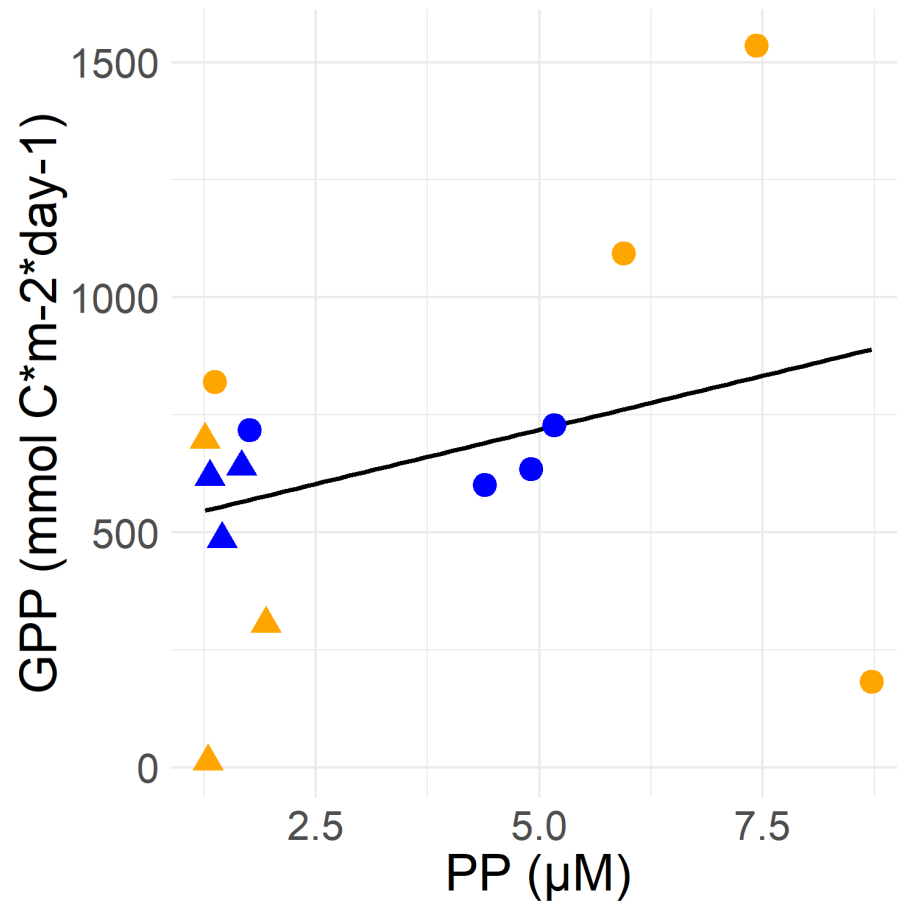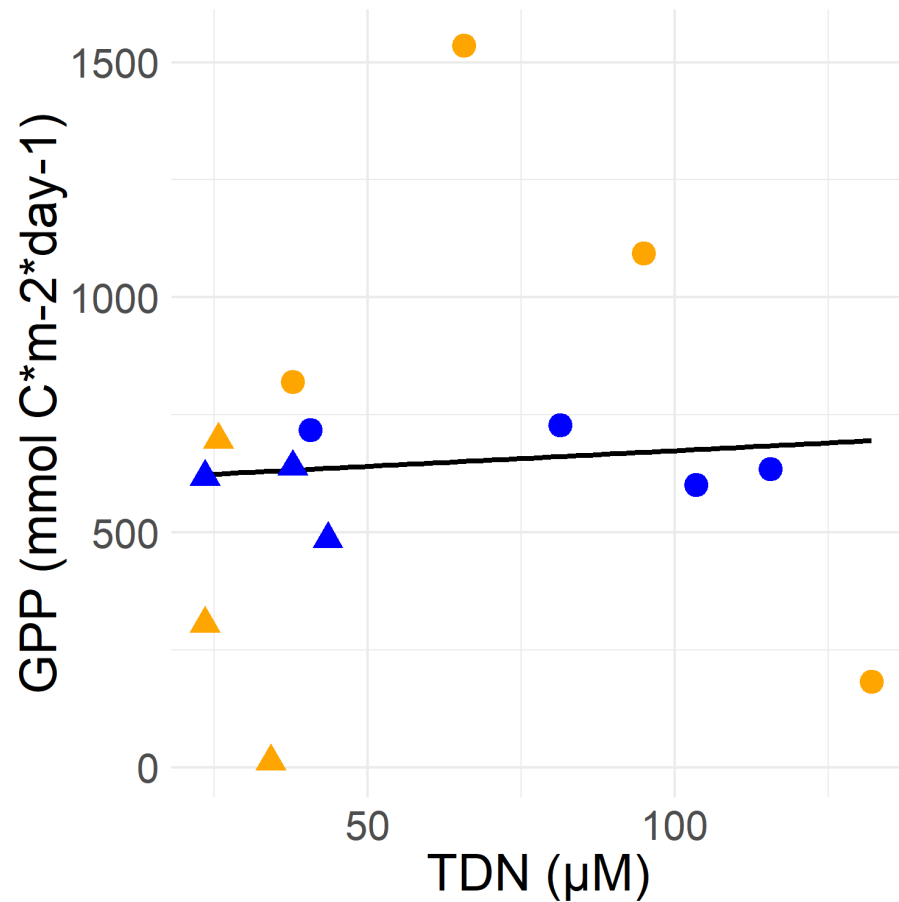
Signif. codes: 0 '***' 0.001 '**' 0.01 '*' 0.05 '.' 0.1 ' ' 1

Residual standard error: 371.5 on 12 degrees of freedom

Multiple R-squared: 0.0784,   Adjusted R-squared: 0.001605

F-statistic: 1.021 on 1 and 12 DF, p-value: 0.3322

Residuals:

Min	1Q	Median	3Q	Max
-996.35	-307.25	85.55	260.55	680.72

Coefficients:

	Estimate	Std. Error	t value	Pr(>|t|)
(Intercept)	-140.0	369.1	-0.379	0.711
data$Salinity	-71.5	40.2	-1.779	0.101

Residual standard error: 465.5 on 12 degrees of freedom

Multiple R-squared: 0.2087, Adjusted R-squared: 0.1427

F-statistic: 3.164 on 1 and 12 DF, p-value: 0.1006
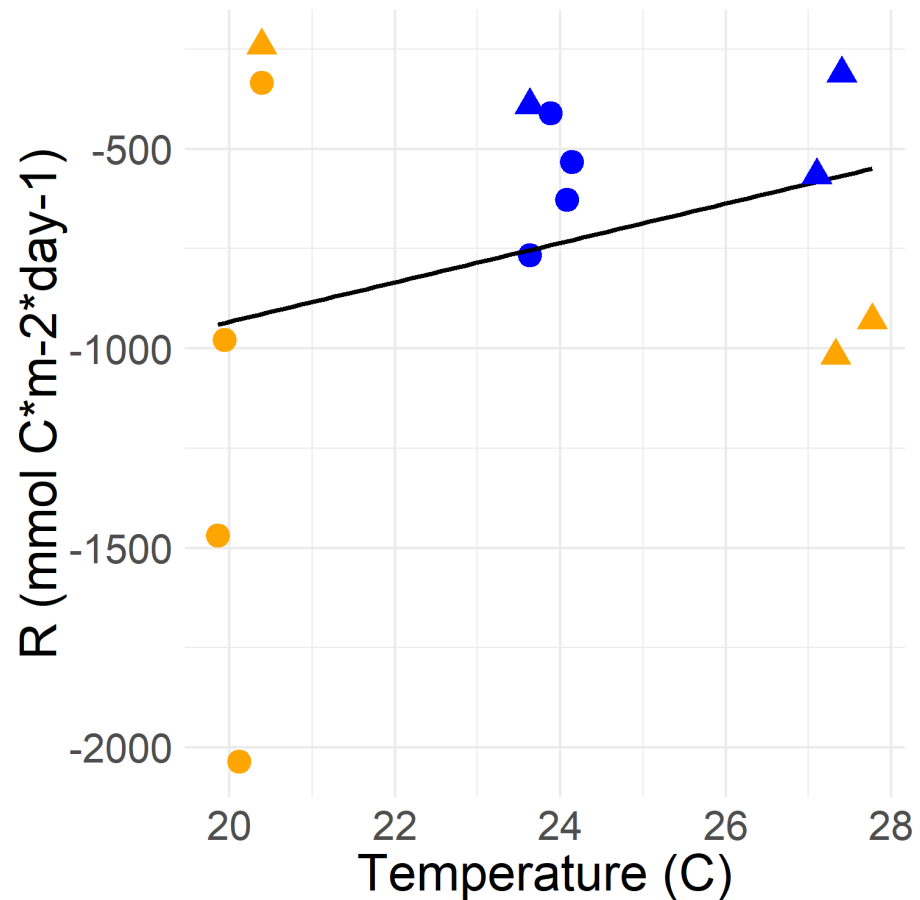
Residuals:

Min	1Q	Median	3Q	Max
-1107.83	-296.11	60.07	312.10	672.73

Coefficients:

	Estimate	Std. Error	t value	Pr(>|t|)
(Intercept)	-1920.62	1088.55	-1.764	0.103
data$Temperature..C.	49.37	45.88	1.076	0.303

Residual standard error: 499.8 on 12 degrees of freedom

Multiple R-squared: 0.08801, Adjusted R-squared: 0.01201

F-statistic: 1.158 on 1 and 12 DF, p-value: 0.303
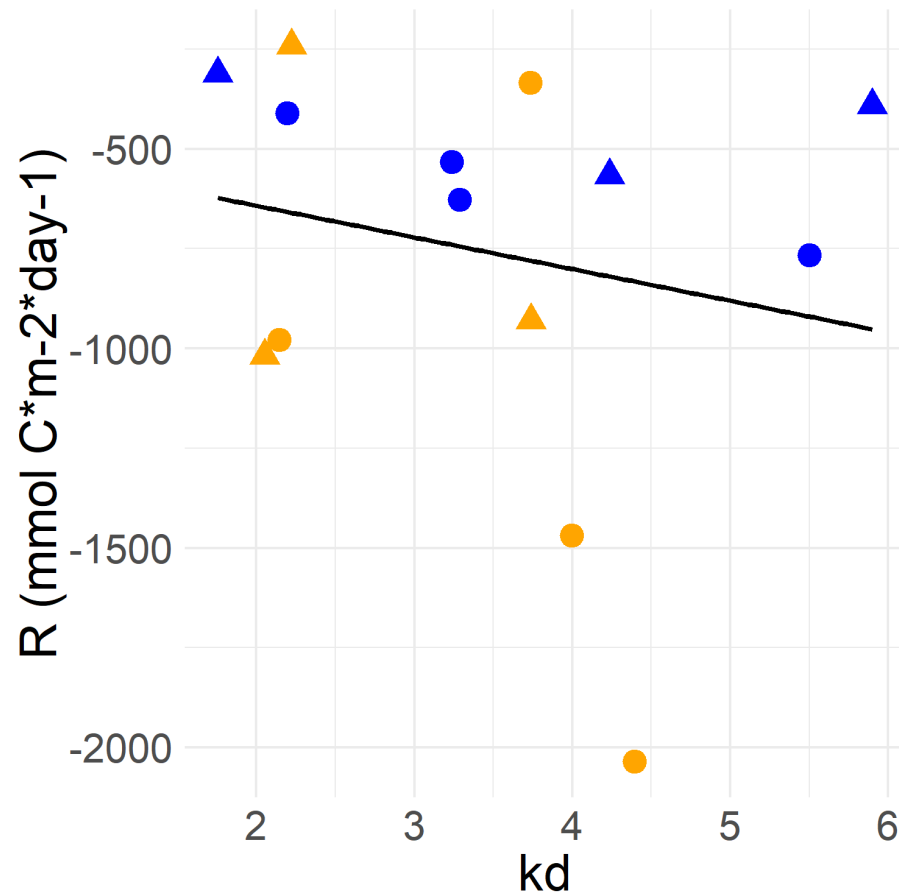
Residuals:

	Min	1Q	Median	3Q	Max
	-1202.6	-280.9	180.9	296.8	560.8

Coefficients:

	Estimate	Std. Error	t value	Pr(>|t|)
(Intercept)	-483.53	402.97	-1.200	0.253
data$kd	-79.42	109.64	-0.724	0.483

Residual standard error: 512.2 on 12 degrees of freedom

Multiple R-squared: 0.04189,   Adjusted R-squared: -0.03795

F-statistic: 0.5246 on 1 and 12 DF, p-value: 0.4828
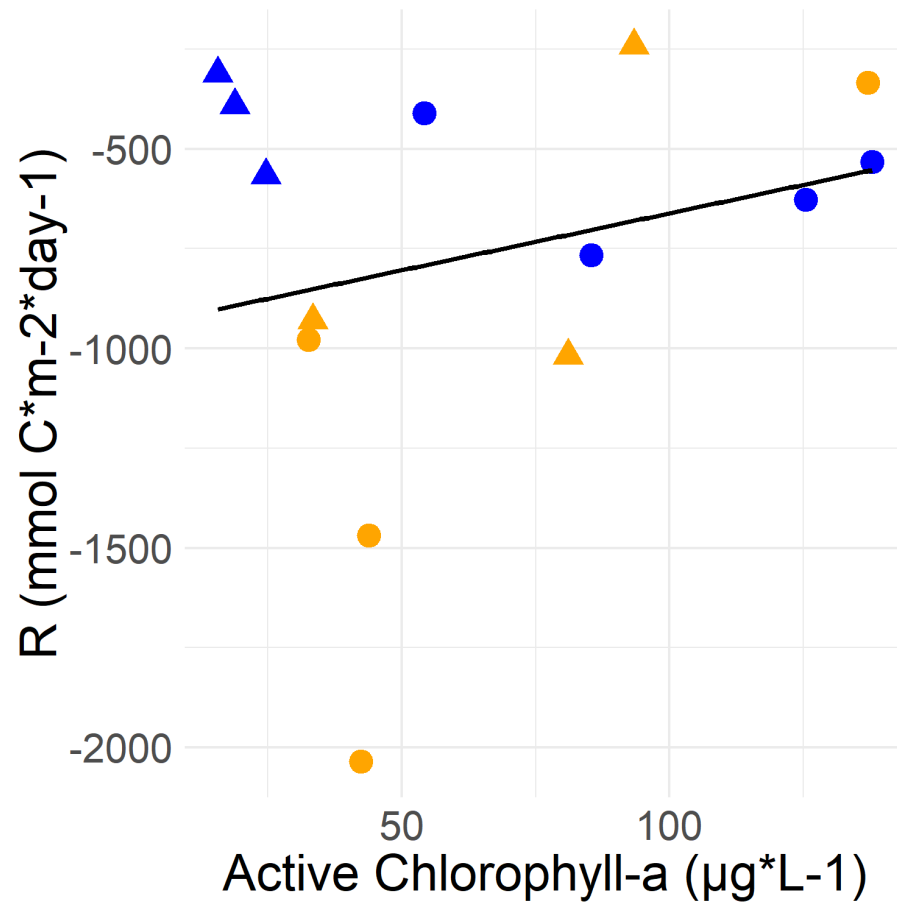
Residuals:

Min	1Q	Median	3Q	Max
-1209.16	-113.28	-9.49	363.44	590.29

Coefficients:

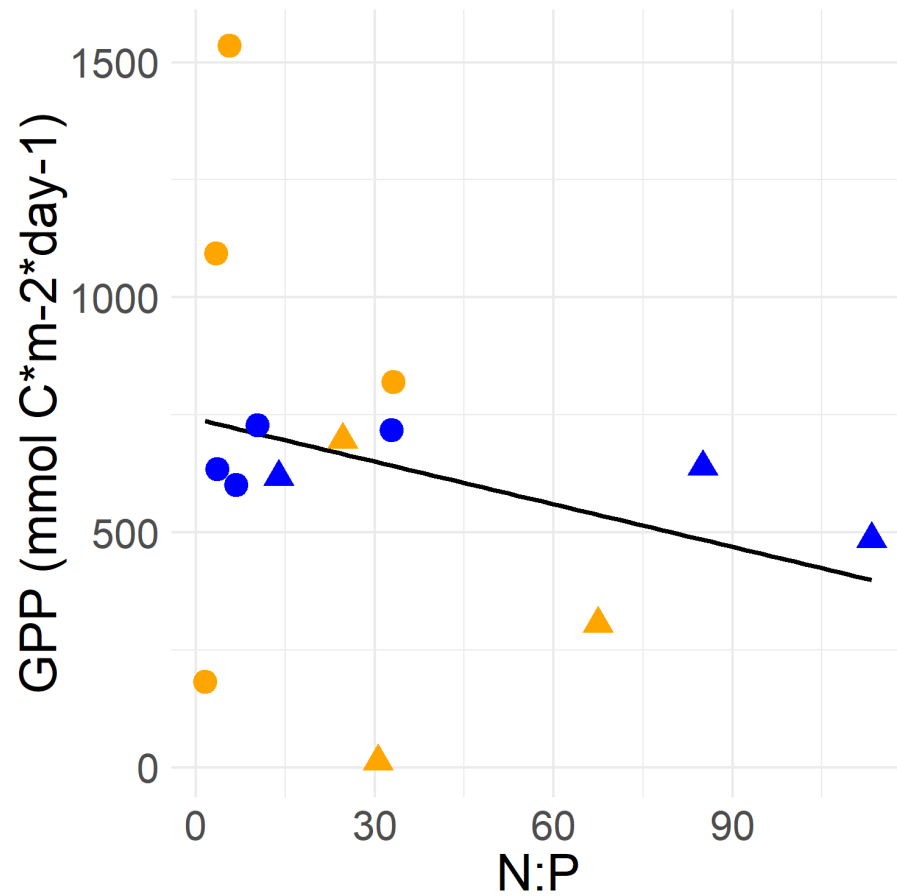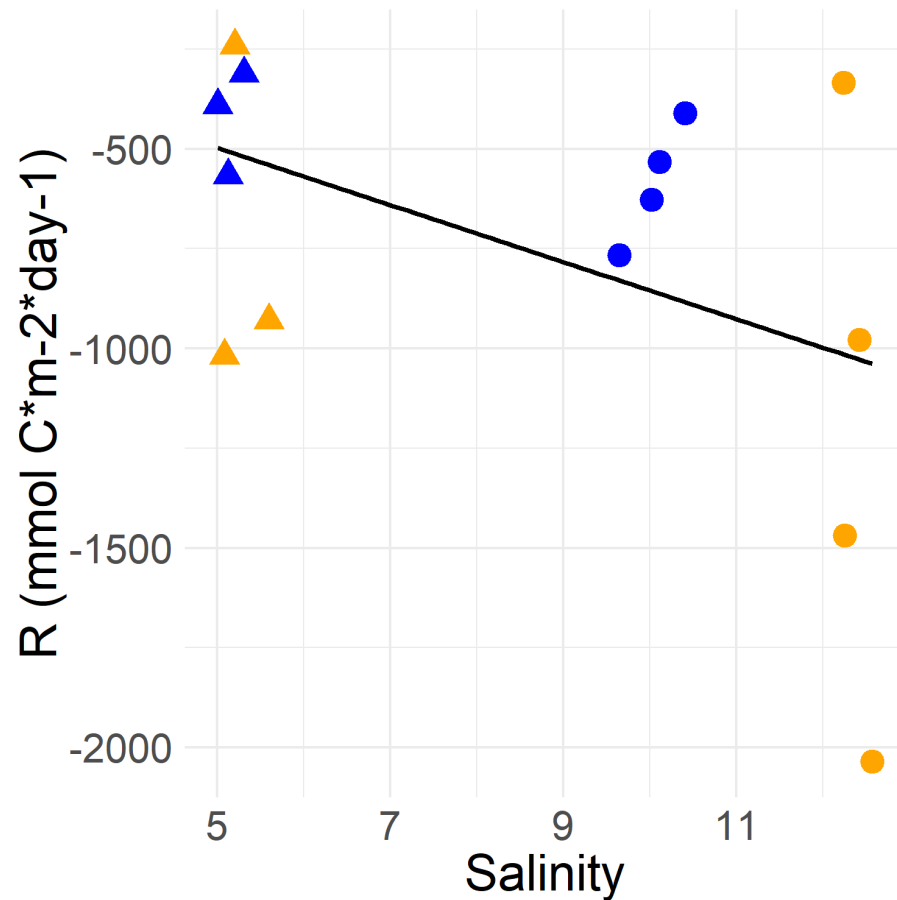|	Estimate	Std. Error	t value	Pr(>|t|)
(Intercept)	-946.694	251.776	-3.760	0.00272 **
data$Active.Chlorophyll.a..ug.L.	2.853	3.209	0.889	0.39152

Signif. codes: 0 '***' 0.001 '**' 0.01 '*' 0.05 '.' 0.1 ' ' 1

Residual standard error: 506.9 on 12 degrees of freedom

Multiple R-squared: 0.06178,   Adjusted R-squared: -0.01641

F-statistic: 0.7902 on 1 and 12 DF, p-value: 0.3915

Residuals:

    Min   1Q Median   3Q   Max

-1277.2 -199.7   143.3   371.0 545.0

Coefficients:

                    Estimate Std. Error t value Pr(>|t|)

(Intercept)   -790.049   240.005 -3.292 0.00644 **

data$Pheophytin..ug.L.   1.037   6.322   0.164 0.87247

Signif. codes: 0 '***' 0.001 '**' 0.01 '*' 0.05 '.' 0.1 ' ' 1

Residual standard error: 522.7 on 12 degrees of freedom

Multiple R-squared: 0.002236,   Adjusted R-squared: -0.08091

F-statistic: 0.02689 on 1 and 12 DF, p-value: 0.8725

Residuals:

Min	1Q	Median	3Q	Max
-1277.0	-205.5	160.8	365.2	519.8

Coefficients:

	Estimate	Std. Error	t value	Pr(>|t|)	
(Intercept)	-766.02	307.47	-2.491	0.0284	*
data$DOC	17.63	605.10	0.029	0.9772	

Signif. codes: 0 '***' 0.001 '**' 0.01 '*' 0.05 '.' 0.1 ' ' 1

Residual standard error: 523.3 on 12 degrees of freedom

Multiple R-squared: 7.073e-05,   Adjusted R-squared: -0.08326

F-statistic: 0.0008488 on 1 and 12 DF, p-value: 0.9772

Residuals:

Min	1Q	Median	3Q	Max
-1272.9	-227.9	197.5	369.6	475.5

Coefficients:

	Estimate	Std. Error	t value	Pr(>|t|)
(Intercept)	-710.91	207.19	-3.431	0.00497 **
data$NH4	-13.55	44.09	-0.307	0.76381

Signif. codes: 0 '***' 0.001 '**' 0.01 '*' 0.05 '.' 0.1 ' ' 1

Residual standard error: 521.3 on 12 degrees of freedom

Multiple R-squared: 0.007813,   Adjusted R-squared: -0.07487

F-statistic: 0.09449 on 1 and 12 DF, p-value: 0.7638

Residuals:

Min	1Q	Median	3Q	Max
-1246.9	-237.1	206.6	304.2	529.6

Coefficients:

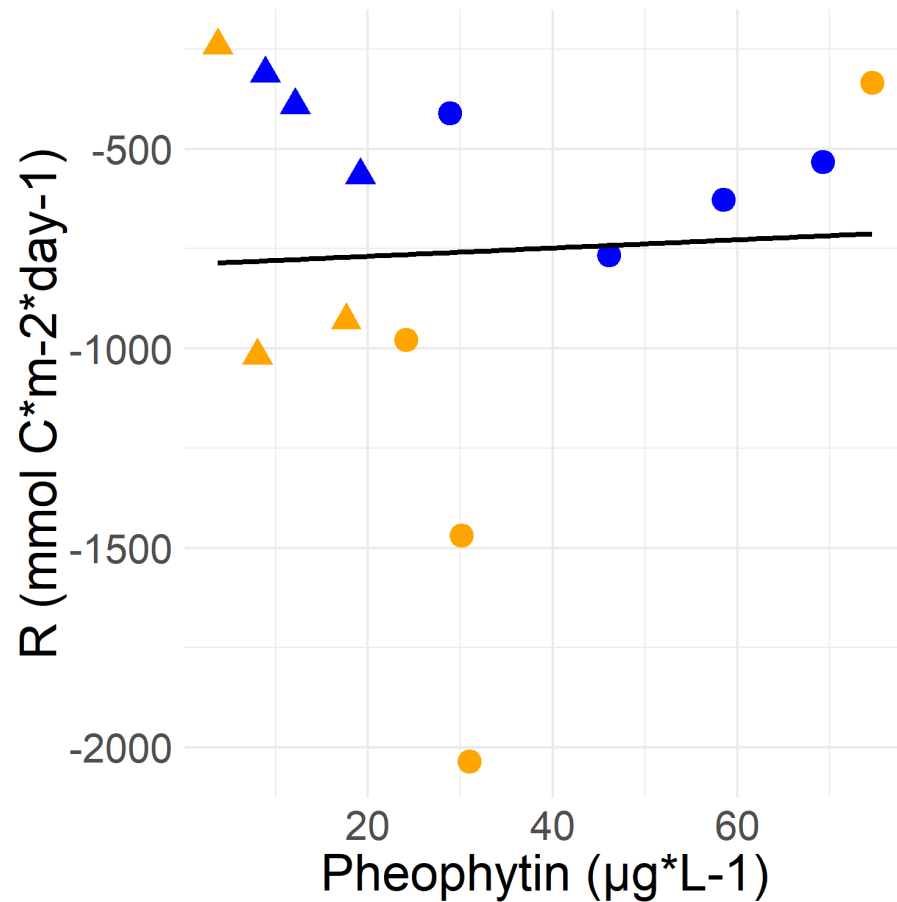|	Estimate	Std. Error	t value	Pr(>|t|)
(Intercept)	-625.33	303.32	-2.062	0.0616 .
data$NO23	-17.41	35.40	-0.492	0.6317

Signif. codes: 0 '***' 0.001 '**' 0.01 '*' 0.05 '.' 0.1 ' ' 1

Residual standard error: 518.1 on 12 degrees of freedom

Multiple R-squared: 0.01976,   Adjusted R-squared: -0.06193

F-statistic: 0.2419 on 1 and 12 DF, p-value: 0.6317

Residuals:

Min	1Q	Median	3Q	Max
-1247.0	-260.4	166.7	311.3	551.7

Coefficients:

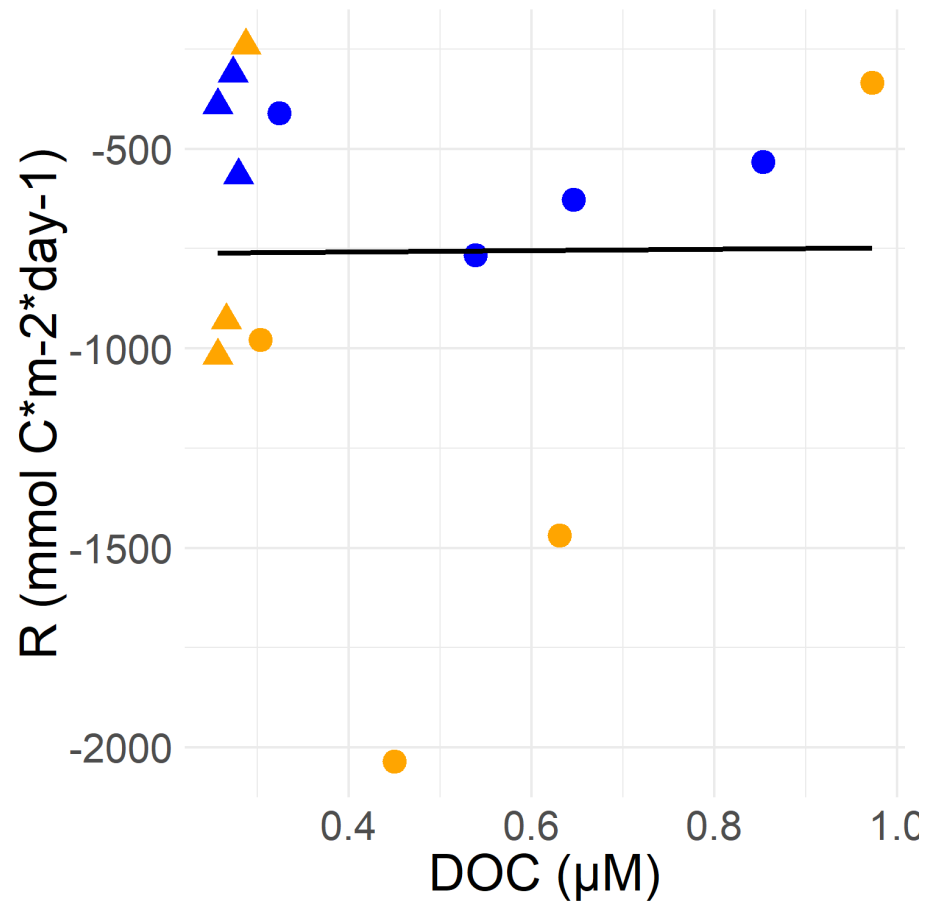|	Estimate	Std. Error	t value	Pr(>|t|)
(Intercept)	-673.923	228.907	-2.944	0.0123 *
data$PN	-1.194	2.585	-0.462	0.6525

Signif. codes: 0 '***' 0.001 '**' 0.01 '*' 0.05 '.' 0.1 ' ' 1

Residual standard error: 518.7 on 12 degrees of freedom

Multiple R-squared: 0.01746,   Adjusted R-squared: -0.06441

F-statistic: 0.2133 on 1 and 12 DF, p-value: 0.6525

271

Residuals:

Min	1Q	Median	3Q	Max
-1259.6	-245.5	161.9	321.2	563.1

Coefficients:

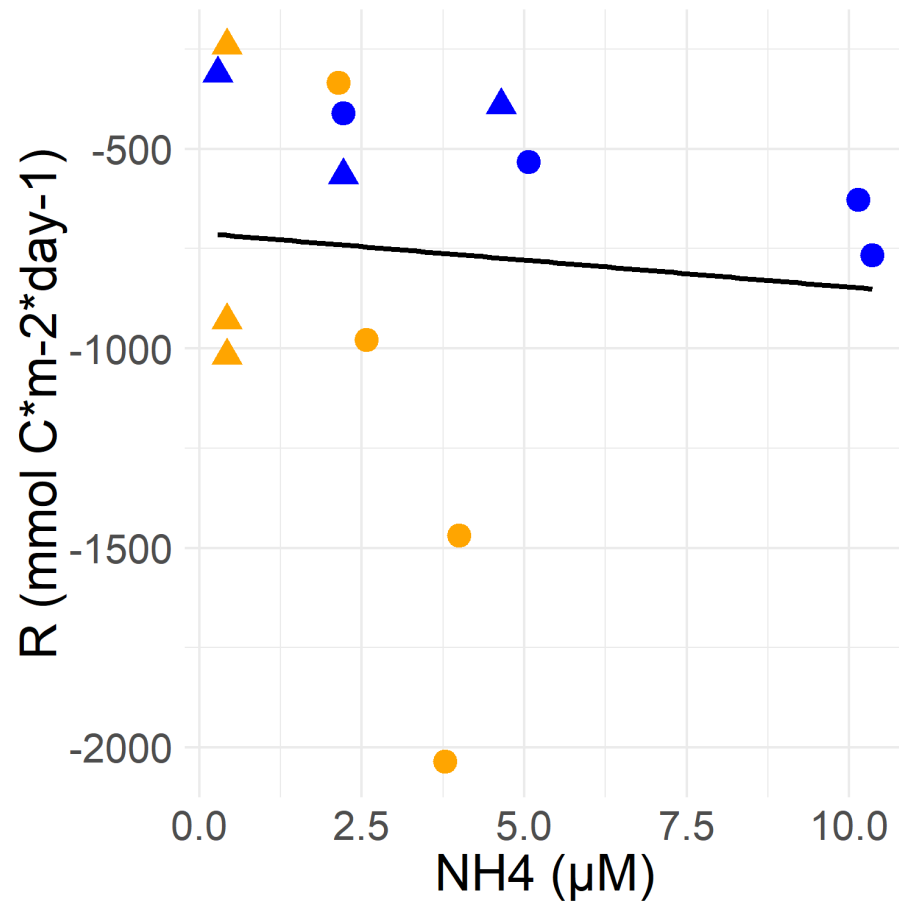|	Estimate	Std. Error	t value	Pr(>|t|)	
(Intercept)	-713.23	180.58	-3.950	0.00193	**
data$PO4	-26.76	68.84	-0.389	0.70427	

Signif. codes: 0 '***' 0.001 '**' 0.01 '*' 0.05 '.' 0.1 ' ' 1

Residual standard error: 520.1 on 12 degrees of freedom

Multiple R-squared: 0.01244,   Adjusted R-squared: -0.06986

F-statistic: 0.1511 on 1 and 12 DF, p-value: 0.7043

Residuals:

  Min   1Q Median   3Q   Max

-971.2 -369.8 162.1 263.2 829.3

Coefficients:

        Estimate Std. Error t value Pr(>|t|)

(Intercept) -489.59   220.67 -2.219 0.0466 *
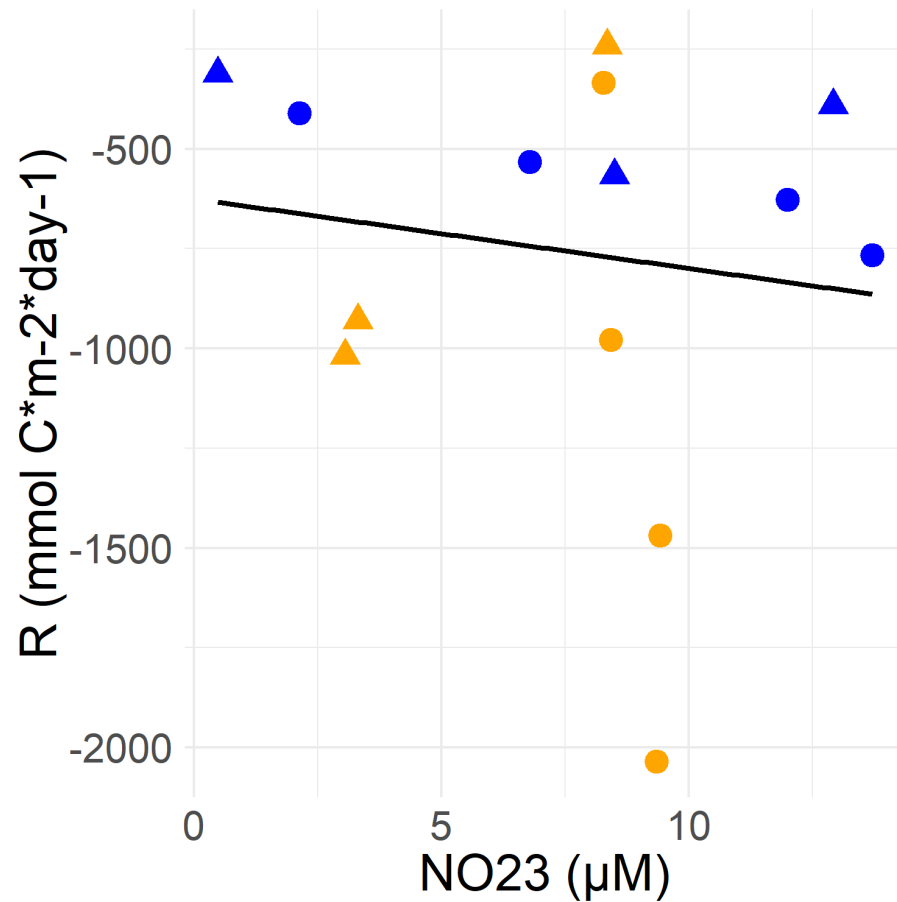
data$PP   -77.34   51.70 -1.496 0.1605

Signif. codes: 0 '***' 0.001 '**' 0.01 '*' 0.05 '.' 0.1 ' ' 1

Residual standard error: 480.4 on 12 degrees of freedom

Multiple R-squared: 0.1572,   Adjusted R-squared: 0.08693

F-statistic: 2.238 on 1 and 12 DF, p-value: 0.1605

273

Residuals:

Min	1Q	Median	3Q	Max
-1274.7	-222.9	166.0	351.9	502.0

Coefficients:

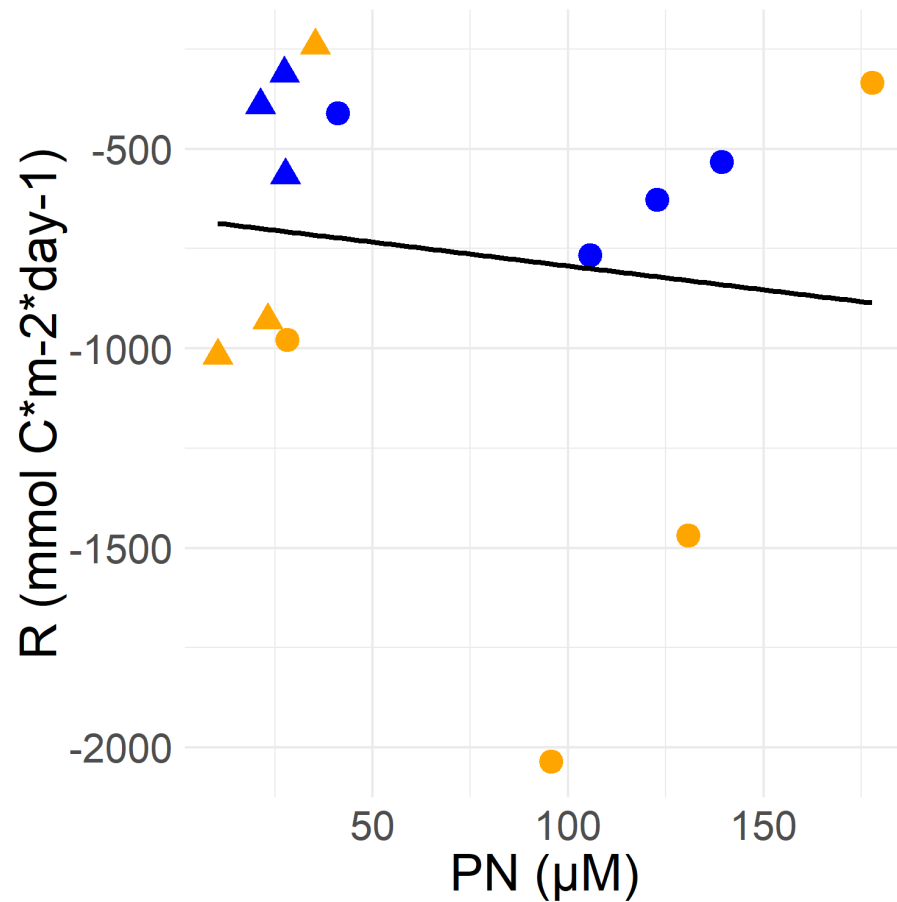|	Estimate	Std. Error	t value	Pr(>|t|)
(Intercept)	-724.5319	277.3504	-2.612	0.0227 *
data$TDN	-0.5454	3.8986	-0.140	0.8911

Signif. codes: 0 '***' 0.001 '**' 0.01 '*' 0.05 '.' 0.1 ' ' 1

Residual standard error: 522.9 on 12 degrees of freedom

Multiple R-squared: 0.001628,   Adjusted R-squared: -0.08157

F-statistic: 0.01957 on 1 and 12 DF, p-value: 0.8911

274
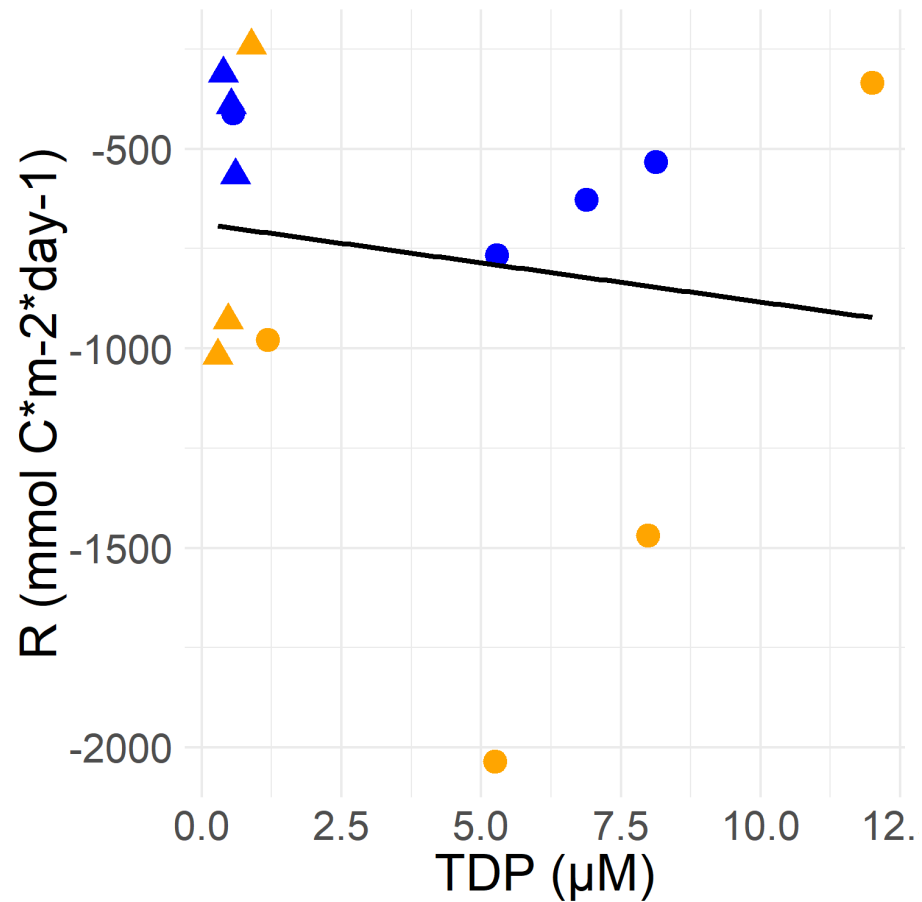
Residuals:

Min	1Q	Median	3Q	Max
-1244.8	-259.3	163.7	312.0	588.2

Coefficients:

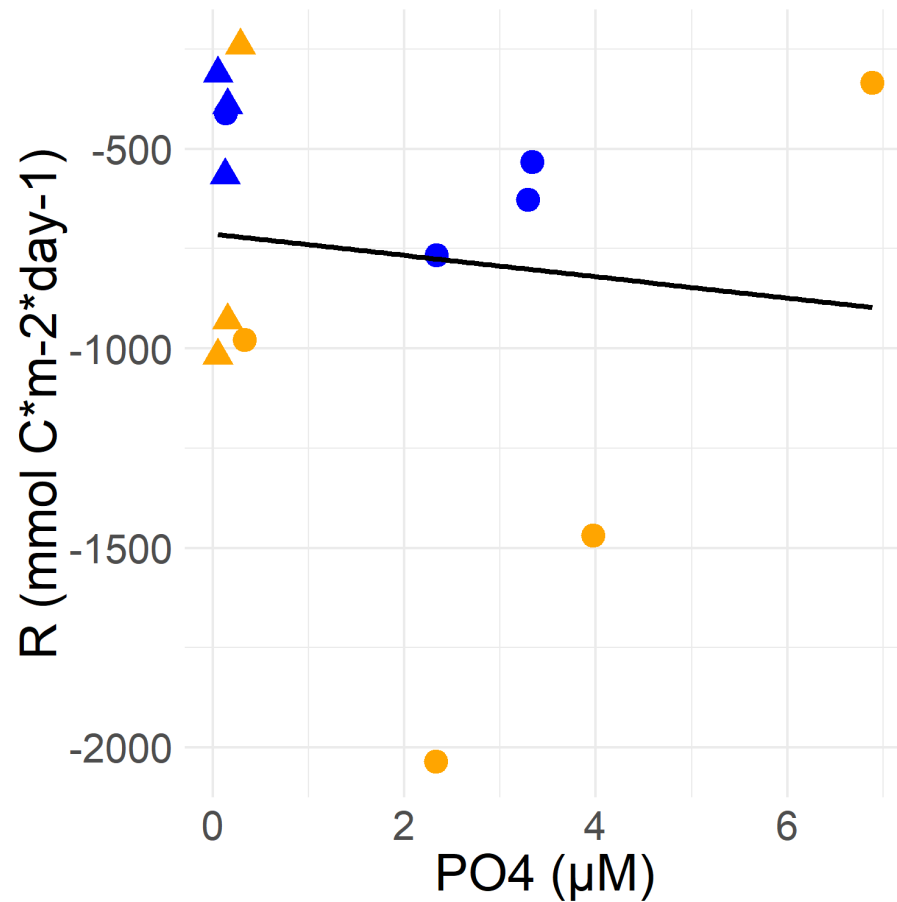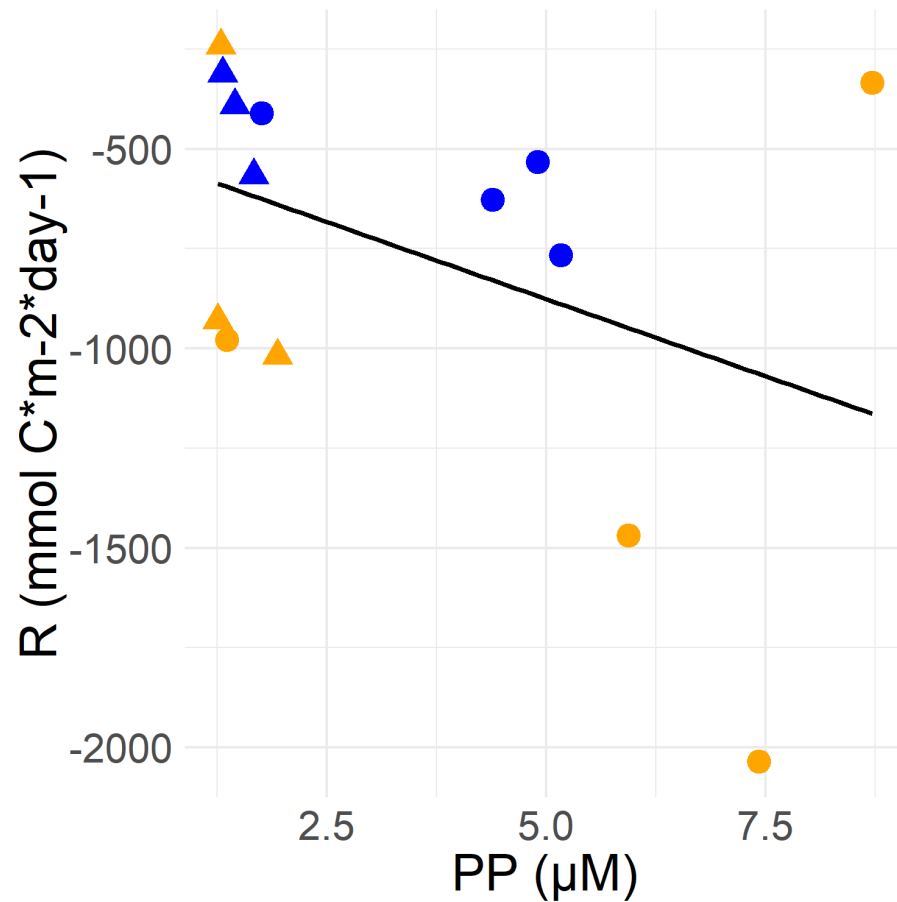|	Estimate	Std. Error	t value	Pr(>|t|)	
(Intercept)	-687.5	191.3	-3.594	0.00368	**
data$TDP	-19.6	36.7	-0.534	0.60309	

Signif. codes: 0 '***' 0.001 '**' 0.01 '*' 0.05 '.' 0.1 ' ' 1

Residual standard error: 517.2 on 12 degrees of freedom

Multiple R-squared: 0.02321,   Adjusted R-squared: -0.05819

F-statistic: 0.2852 on 1 and 12 DF, p-value: 0.6031
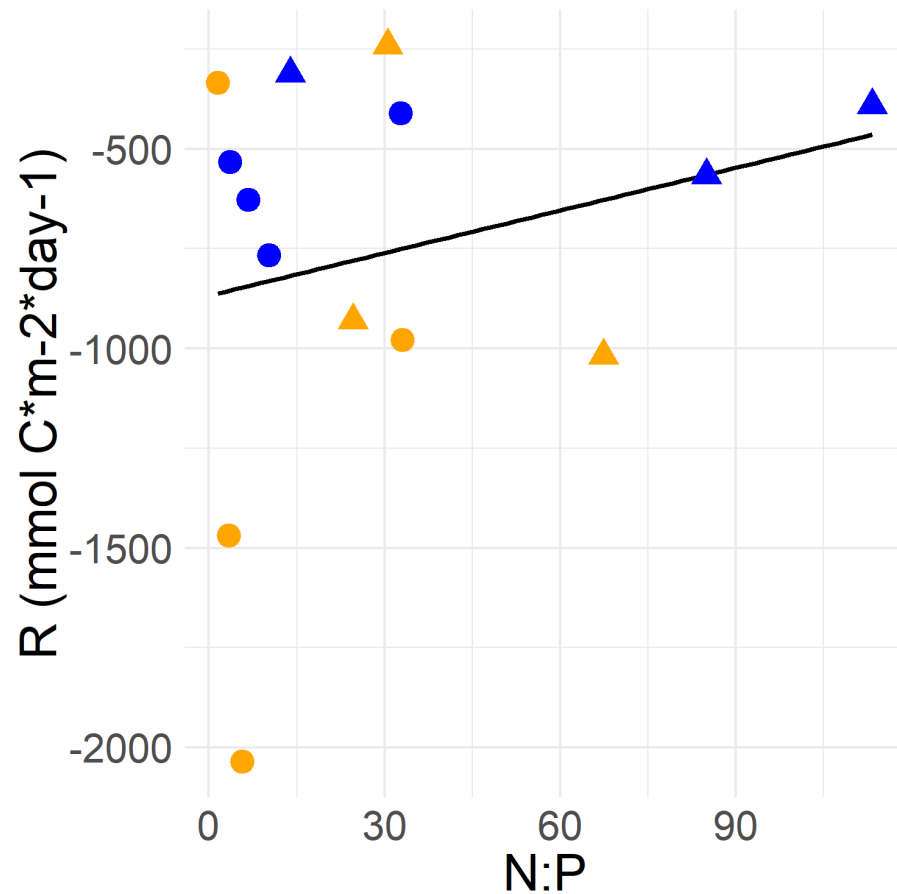
Residuals:

Min	1Q	Median	3Q	Max
-1187.34	-208.73	69.35	335.81	528.02

Coefficients:

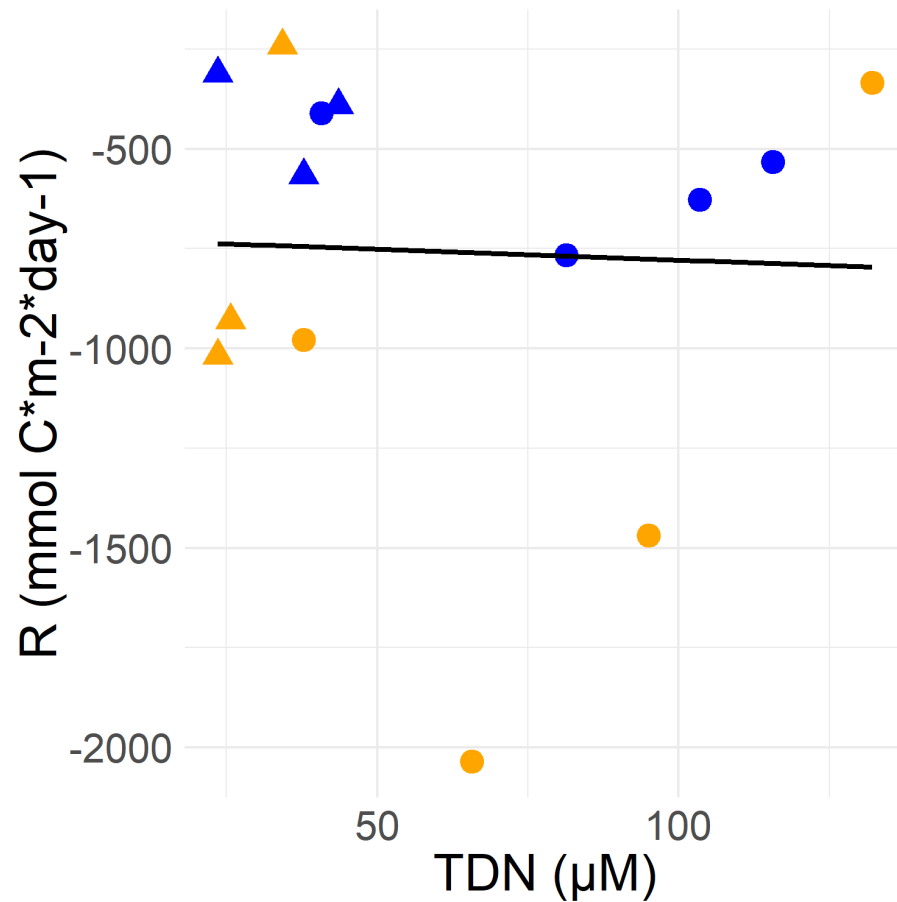|	Estimate	Std. Error	t value	Pr(>|t|)
(Intercept)	-867.830	185.219	-4.685	0.000527 ***
data$N.P	3.558	4.088	0.870	0.401124

Signif. codes: 0 '***' 0.001 '**' 0.01 '*' 0.05 '.' 0.1 ' ' 1

Residual standard error: 507.5 on 12 degrees of freedom

Multiple R-squared: 0.05939,   Adjusted R-squared: -0.01899

F-statistic: 0.7577 on 1 and 12 DF, p-value: 0.4011

Photosynthetron Metabolism
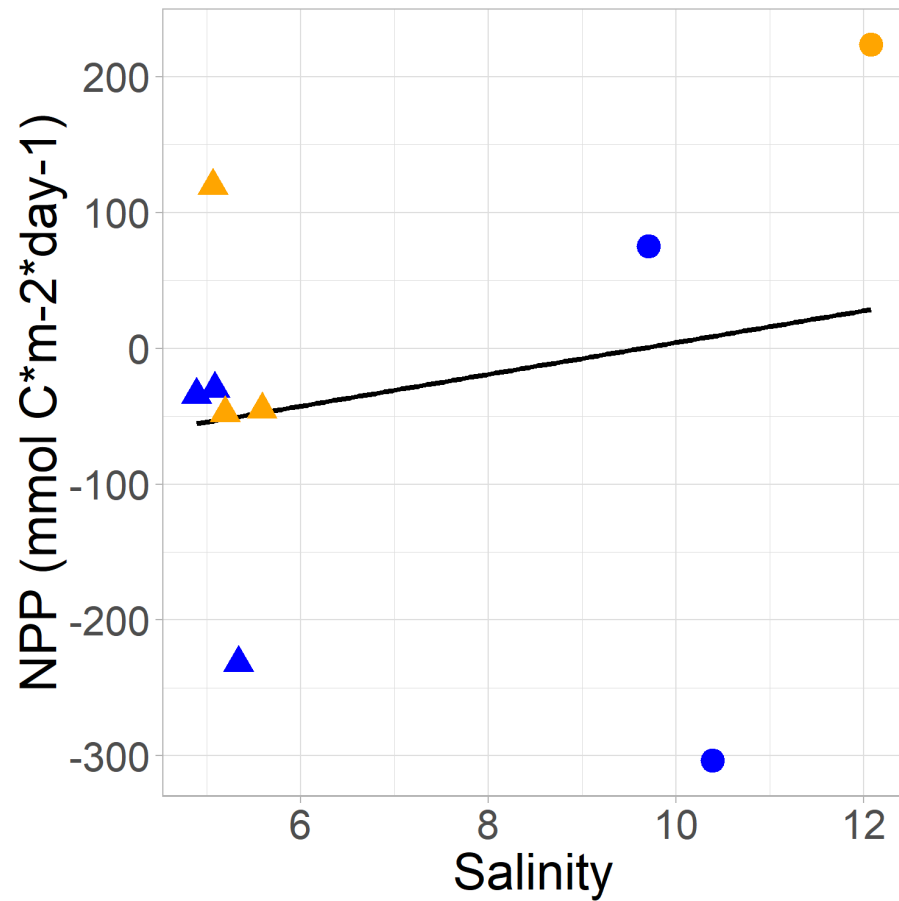
Residuals:

    Min   1Q   Median   3Q   Max
-314.410   4.098   22.171   73.625   187.486

Coefficients:

            Estimate Std. Error t value Pr(>|t|)
(Intercept)   -118.89   158.11 -0.752   0.477
data$Salinity   12.48   20.81   0.600   0.568

Residual standard error: 170.4 on 7 degrees of freedom

  (1 observation deleted due to missingness)

Multiple R-squared: 0.04889,   Adjusted R-squared: -0.08698

F-statistic: 0.3598 on 1 and 7 DF, p-value: 0.5675
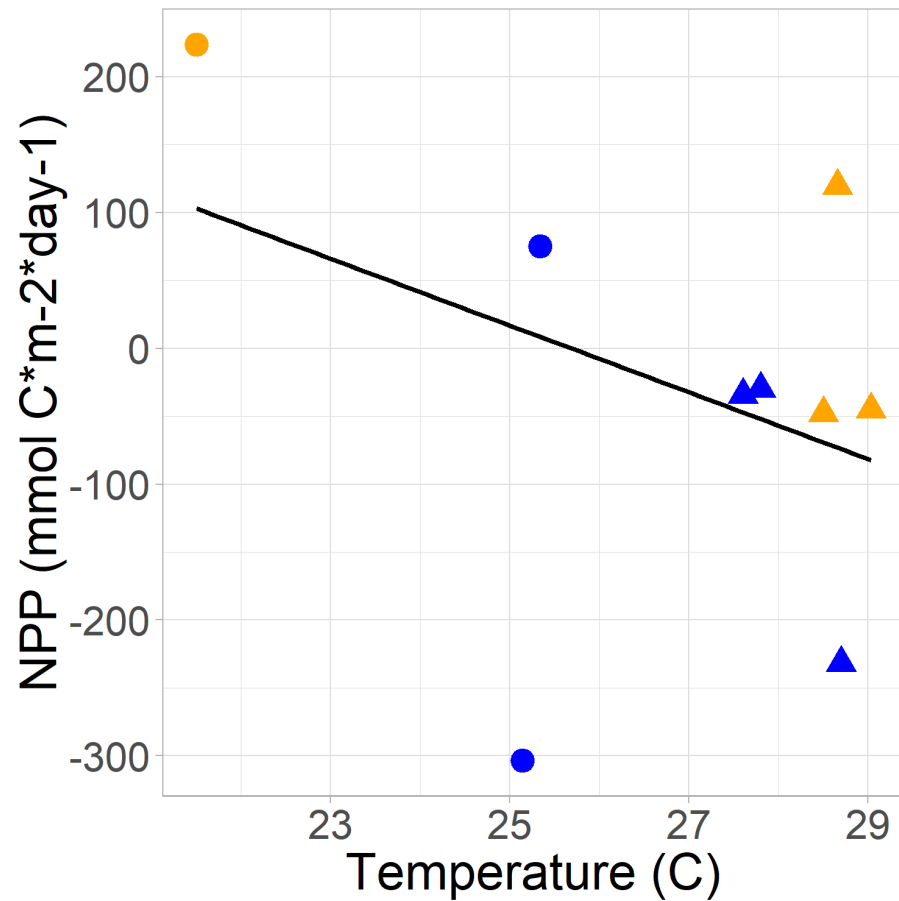
Residuals:

Min	1Q	Median	3Q	Max
-284.29	-86.17	38.42	90.14	195.49

Coefficients:

	Estimate	Std. Error	t value	Pr(>|t|)
(Intercept)	375.19	480.05	0.782	0.460
data$Temperature	-16.51	19.41	-0.851	0.423

Residual standard error: 166.3 on 7 degrees of freedom

 (1 observation deleted due to missingness)

Multiple R-squared: 0.09367,   Adjusted R-squared: -0.03581

F-statistic: 0.7234 on 1 and 7 DF, p-value: 0.4232
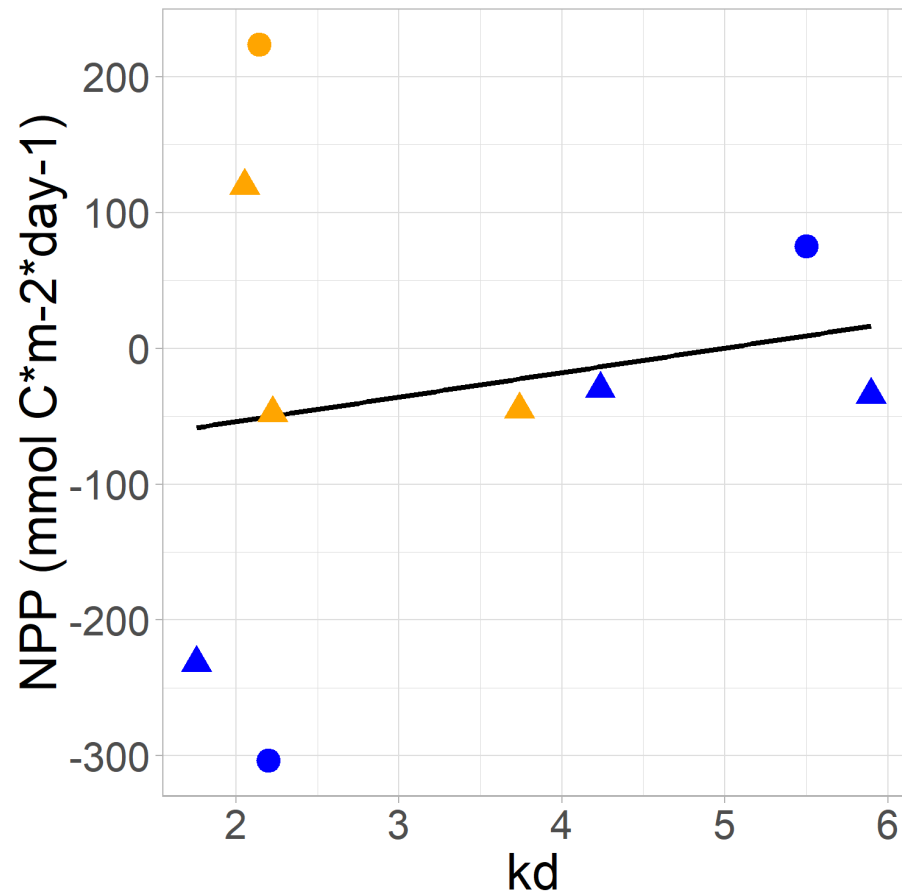
Residuals:

Min	1Q	Median	3Q	Max
-252.98	-50.66	-16.15	65.91	274.96

Coefficients:

	Estimate	Std. Error	t value	Pr(>|t|)
(Intercept)	-90.10	138.60	-0.650	0.536
data$kd	18.07	38.18	0.473	0.650

Residual standard error: 172 on 7 degrees of freedom

 (1 observation deleted due to missingness)

Multiple R-squared: 0.03101,　　　　Adjusted R-squared: -0.1074

F-statistic: 0.224 on 1 and 7 DF, p-value: 0.6504

Residuals:

Min	1Q	Median	3Q	Max
-279.79	-72.92	30.80	59.86	274.19

Coefficients:

	Estimate	Std. Error	t value	Pr(>|t|)
(Intercept)	-91.326	111.329	-0.820	0.439
data$Active.Chlorophyll.a..ug.L.	1.249	1.964	0.636	0.545

Residual standard error: 169.9 on 7 degrees of freedom

(1 observation deleted due to missingness)

Multiple R-squared: 0.05461,	Adjusted R-squared: -0.08045

F-statistic: 0.4043 on 1 and 7 DF, p-value: 0.5451

Residuals:

Min	1Q	Median	3Q	Max
-289.054	-12.773	6.445	62.337	245.499

Coefficients:

	Estimate	Std. Error	t value	Pr(>|t|)
(Intercept)	-59.997	105.299	-0.570	0.587
data$Pheophytin..ug.L.	1.581	4.698	0.336	0.746

Residual standard error: 173.3 on 7 degrees of freedom
 (1 observation deleted due to missingness)

Multiple R-squared: 0.01592,   Adjusted R-squared: -0.1247

F-statistic: 0.1132 on 1 and 7 DF, p-value: 0.7464

282

Residuals:

Min	1Q	Median	3Q	Max
-277.457	-10.558	9.888	35.663	255.864

Coefficients:

	Estimate	Std. Error	t value	Pr(>|t|)
(Intercept)	-124.6	219.8	-0.567	0.589
data$DOC	304.6	686.0	0.444	0.670

Residual standard error: 172.3 on 7 degrees of freedom
 (1 observation deleted due to missingness)
Multiple R-squared: 0.02739,   Adjusted R-squared: -0.1116
F-statistic: 0.1971 on 1 and 7 DF, p-value: 0.6704
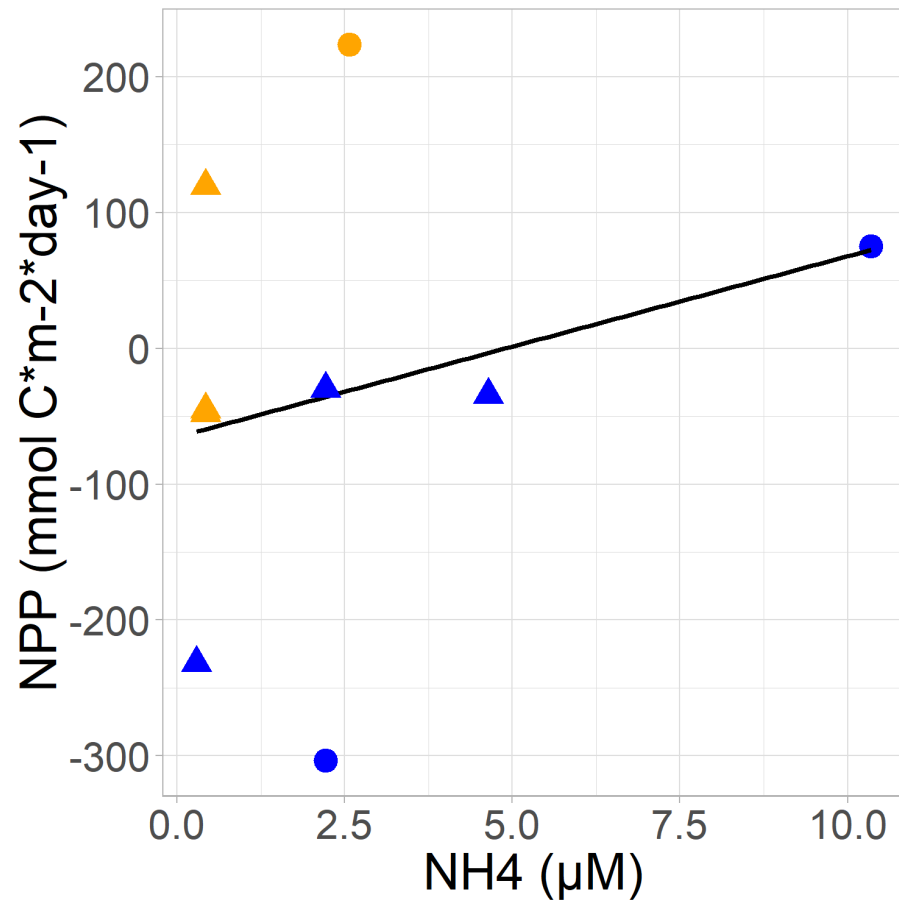
Residuals:

Min	1Q	Median	3Q	Max
-267.624	-30.716	6.026	14.593	254.609

Coefficients:

	Estimate	Std. Error	t value	Pr(>|t|)
(Intercept)	-65.19	73.97	-0.881	0.407
data$NH4	13.30	18.38	0.724	0.493

Residual standard error: 168.5 on 7 degrees of freedom

 (1 observation deleted due to missingness)

Multiple R-squared: 0.06958,   Adjusted R-squared: -0.06334

F-statistic: 0.5235 on 1 and 7 DF, p-value: 0.4928

284
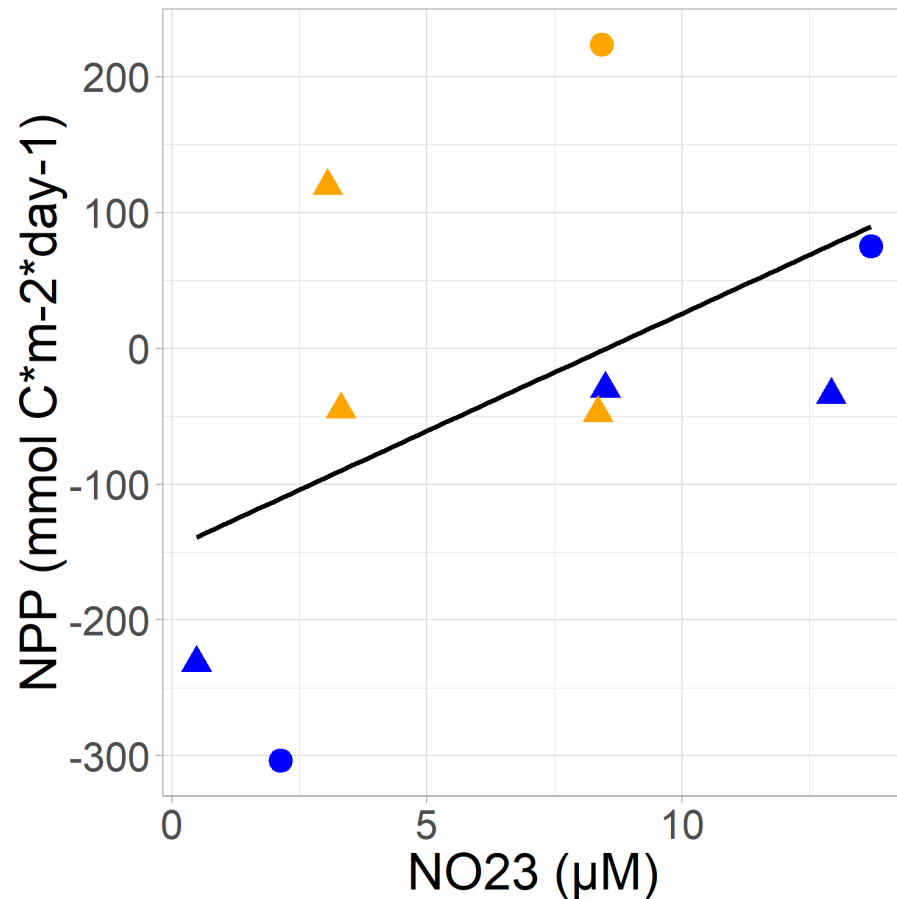
Residuals:

Min	1Q	Median	3Q	Max
-192.84	-92.69	-29.29	45.15	225.27

Coefficients:

	Estimate	Std. Error	t value	Pr(>|t|)
(Intercept)	-147.32	91.06	-1.618	0.150
data$NO23	17.29	11.22	1.541	0.167

Residual standard error: 151 on 7 degrees of freedom

 (1 observation deleted due to missingness)

Multiple R-squared: 0.2533, Adjusted R-squared: 0.1466

F-statistic: 2.375 on 1 and 7 DF, p-value: 0.1672
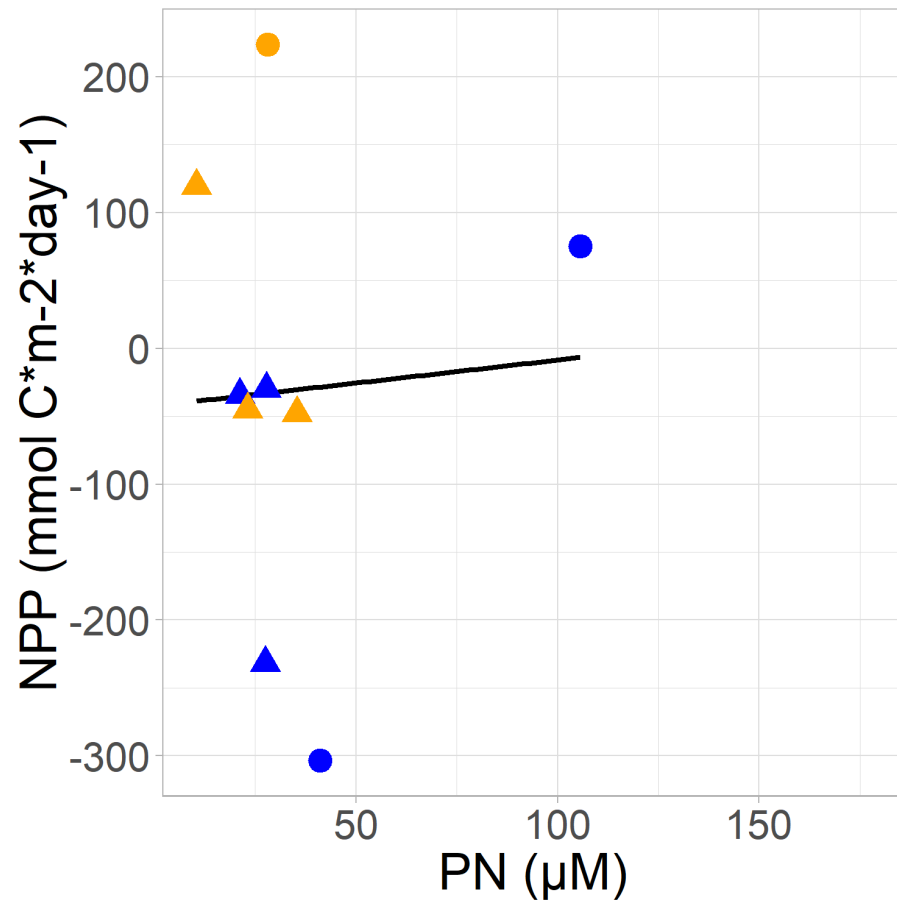
Residuals:

Min	1Q	Median	3Q	Max
-274.888	-17.195	1.029	81.892	256.504

Coefficients:

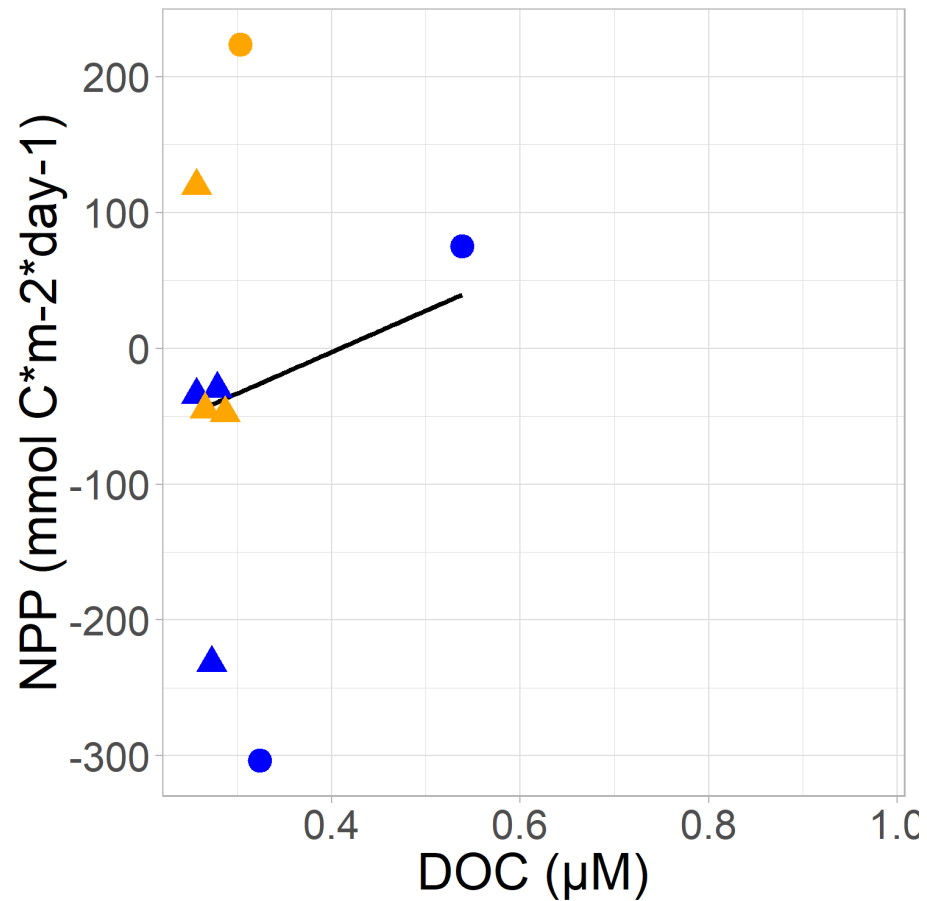|	Estimate	Std. Error	t value	Pr(>|t|)
(Intercept)	-42.4032	98.4500	-0.431	0.680
data$PN	0.3377	2.2305	0.151	0.884

Residual standard error: 174.4 on 7 degrees of freedom
 (1 observation deleted due to missingness)
Multiple R-squared: 0.003264,   Adjusted R-squared: -0.1391
F-statistic: 0.02292 on 1 and 7 DF, p-value: 0.8839
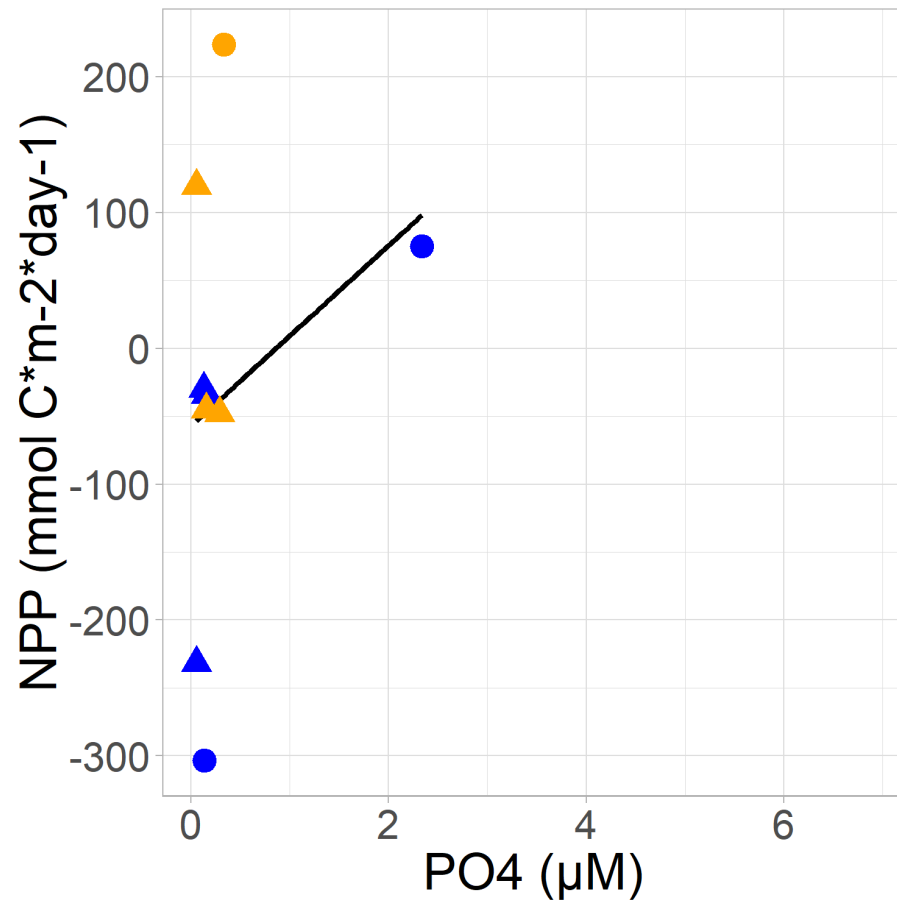
Residuals:

Min	1Q	Median	3Q	Max
-255.029	-22.829	2.166	19.050	258.666

Coefficients:

	Estimate	Std. Error	t value	Pr(>|t|)
(Intercept)	-57.14	64.42	-0.887	0.405
data$PO4	66.37	80.64	0.823	0.438

Residual standard error: 166.8 on 7 degrees of freedom

 (1 observation deleted due to missingness)

Multiple R-squared: 0.08822,   Adjusted R-squared: -0.04203

F-statistic: 0.6773 on 1 and 7 DF, p-value: 0.4377
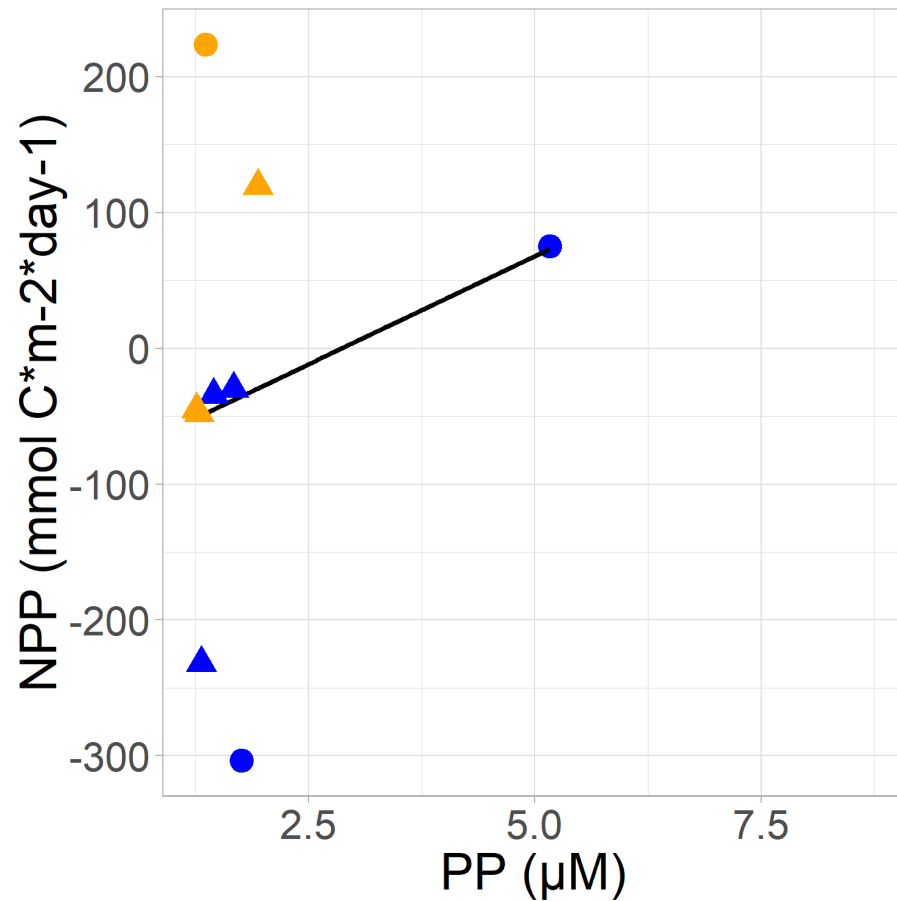
Residuals:

Min	1Q	Median	3Q	Max
-268.121	2.095	6.275	10.824	271.387

Coefficients:

	Estimate	Std. Error	t value	Pr(>|t|)
(Intercept)	-91.22	108.23	-0.843	0.427
data$PP	31.81	48.25	0.659	0.531

Residual standard error: 169.5 on 7 degrees of freedom

 (1 observation deleted due to missingness)

Multiple R-squared: 0.05845,   Adjusted R-squared: -0.07605

F-statistic: 0.4346 on 1 and 7 DF, p-value: 0.5308
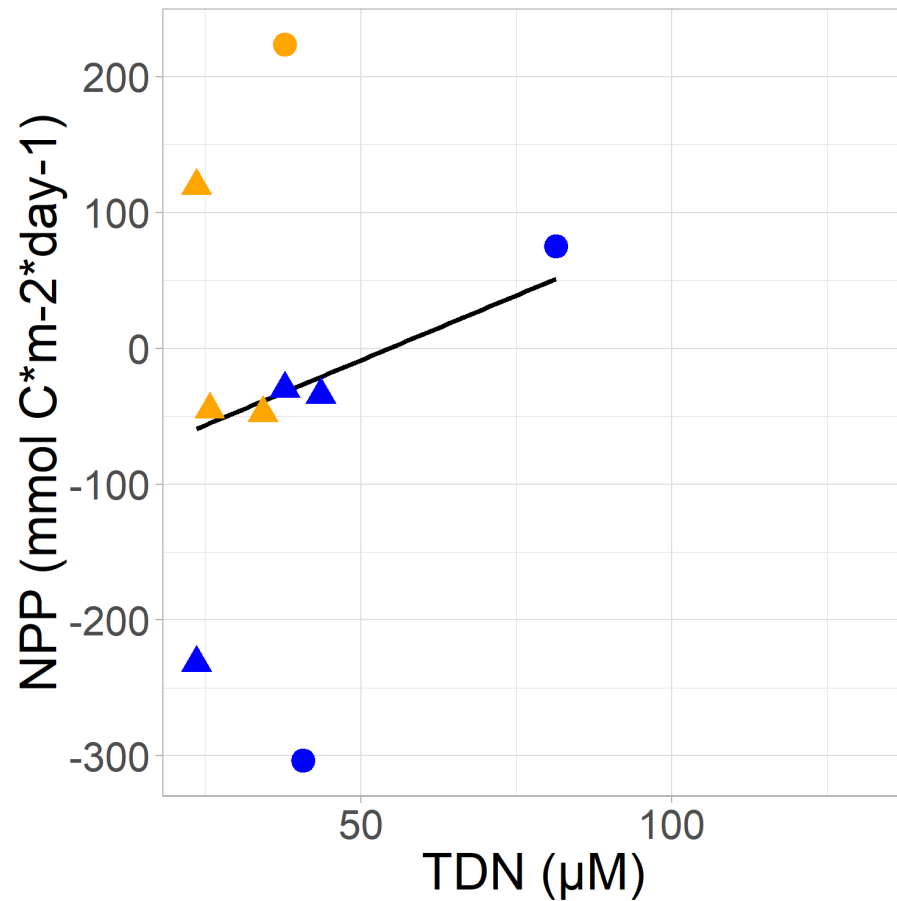
Residuals:

Min	1Q	Median	3Q	Max
-276.790	-13.052	2.311	24.076	255.641

Coefficients:

	Estimate	Std. Error	t value	Pr(>|t|)
(Intercept)	-104.273	144.145	-0.723	0.493
data$TDN	1.909	3.420	0.558	0.594

Residual standard error: 171 on 7 degrees of freedom

 (1 observation deleted due to missingness)

Multiple R-squared: 0.0426, Adjusted R-squared: -0.09417

F-statistic: 0.3115 on 1 and 7 DF, p-value: 0.5942
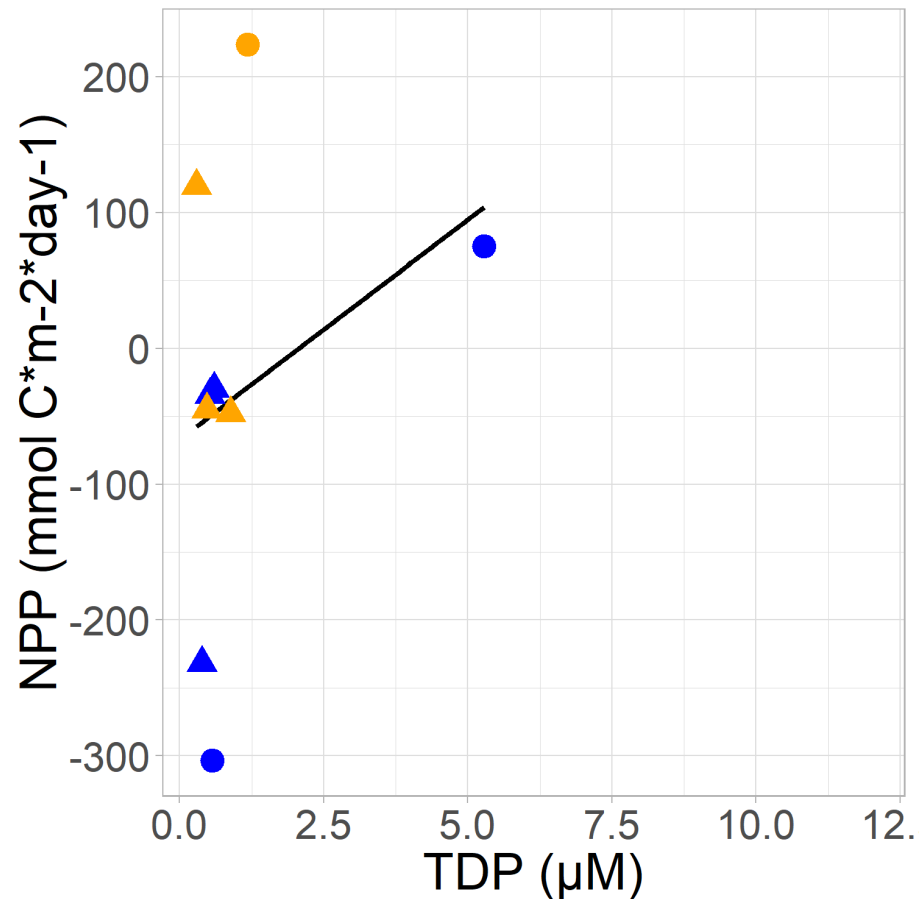
Residuals:

Min	1Q	Median	3Q	Max
-254.603	-28.620	6.694	17.795	252.445

Coefficients:

	Estimate	Std. Error	t value	Pr(>|t|)
(Intercept)	-66.93	69.47	-0.964	0.367
data$TDP	32.32	37.15	0.870	0.413

Residual standard error: 166 on 7 degrees of freedom

 (1 observation deleted due to missingness)

Multiple R-squared: 0.09761,   Adjusted R-squared: -0.0313

F-statistic: 0.7572 on 1 and 7 DF, p-value: 0.4131
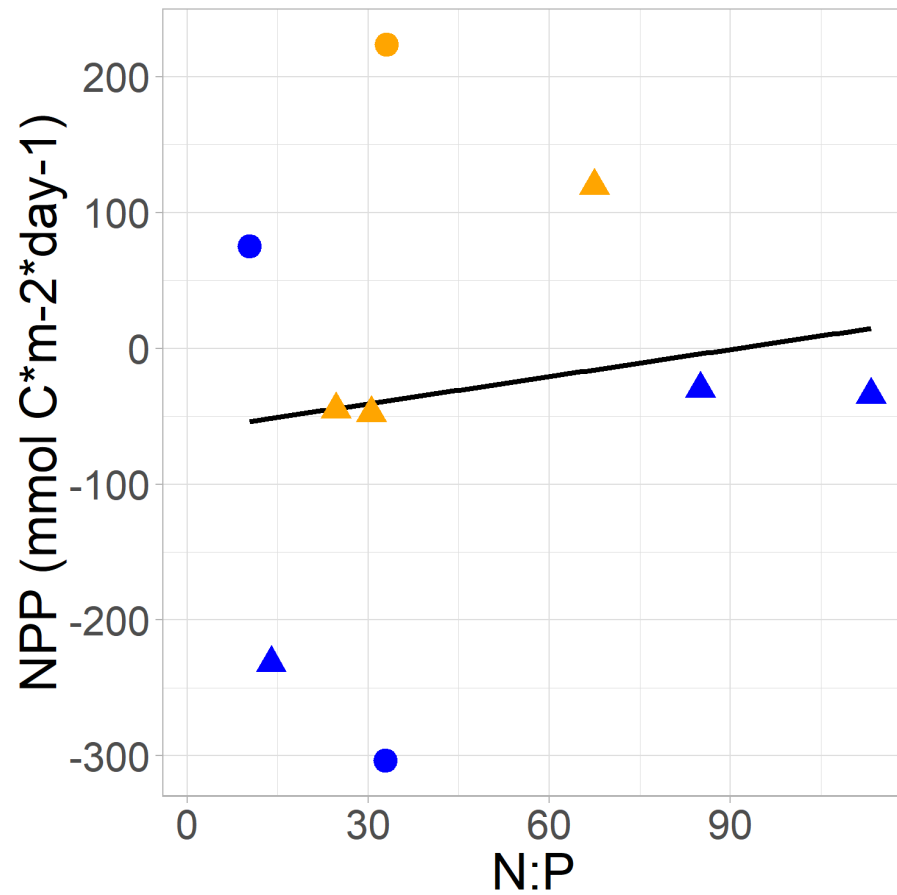
Residuals:

Min	1Q	Median	3Q	Max
-264.42	-48.90	-7.19	129.13	262.38

Coefficients:

	Estimate	Std. Error	t value	Pr(>|t|)
(Intercept)	-60.8156	98.2431	-0.619	0.555
data$N.P	0.6664	1.7416	0.383	0.713

Residual standard error: 172.9 on 7 degrees of freedom
 (1 observation deleted due to missingness)
Multiple R-squared: 0.02049,   Adjusted R-squared: -0.1194
F-statistic: 0.1464 on 1 and 7 DF, p-value: 0.7134
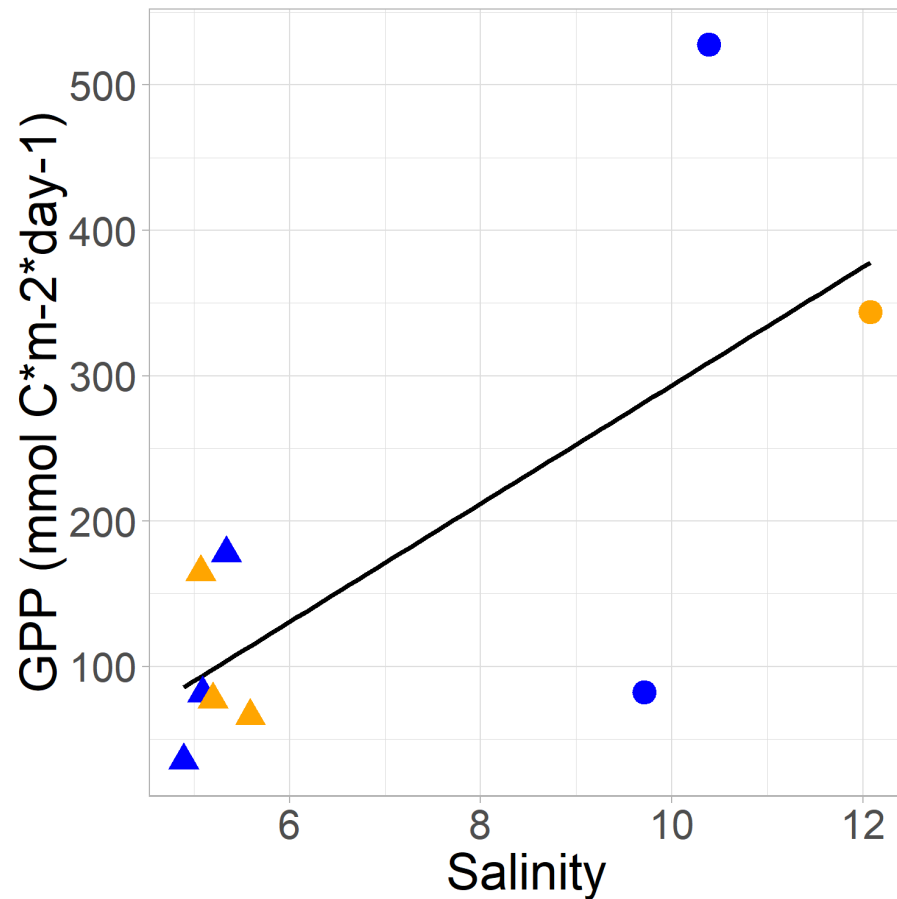
Residuals:

Min	1Q	Median	3Q	Max
-192.50	-47.65	-20.65	71.54	222.87

Coefficients:

	Estimate	Std. Error	t value	Pr(>|t|)
(Intercept)	-109.26	113.74	-0.961	0.3688
data$Salinity	39.79	14.97	2.659	0.0325 *

Signif. codes: 0 '***' 0.001 '**' 0.01 '*' 0.05 '.' 0.1 ' ' 1

Residual standard error: 122.6 on 7 degrees of freedom

 (1 observation deleted due to missingness)

Multiple R-squared: 0.5024,   Adjusted R-squared: 0.4313

F-statistic: 7.068 on 1 and 7 DF, p-value: 0.03253

292

Residuals:

Min	1Q	Median	3Q	Max
-152.65	-103.50	-56.91	43.77	345.53

Coefficients:

	Estimate	Std. Error	t value	Pr(>|t|)
(Intercept)	509.02	484.93	1.050	0.329
data$Temperature	-13.68	19.61	-0.698	0.508

Residual standard error: 168 on 7 degrees of freedom

 (1 observation deleted due to missingness)

Multiple R-squared: 0.06502,   Adjusted R-squared: -0.06855

F-statistic: 0.4868 on 1 and 7 DF, p-value: 0.5079
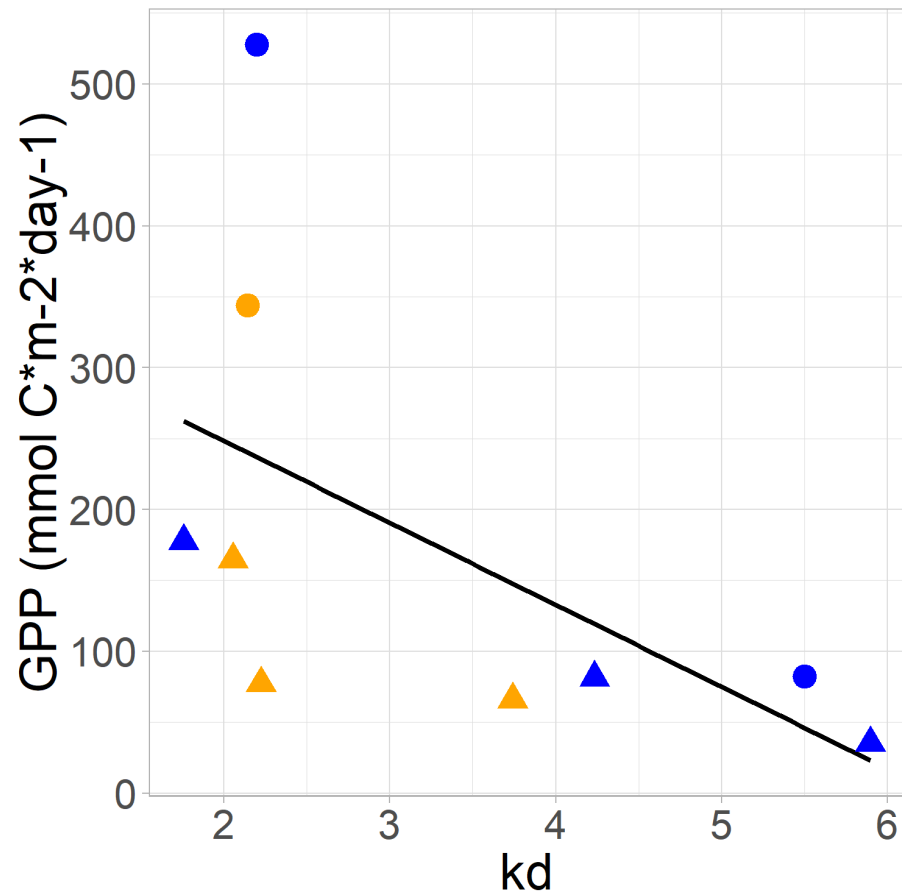
Residuals:

Min	1Q	Median	3Q	Max
-158.06	-81.90	-37.88	36.11	290.81

Coefficients:

	Estimate	Std. Error	t value	Pr(>|t|)	
(Intercept)	364.04	115.39	3.155	0.016	*
data$kd	-57.82	31.79	-1.819	0.112	

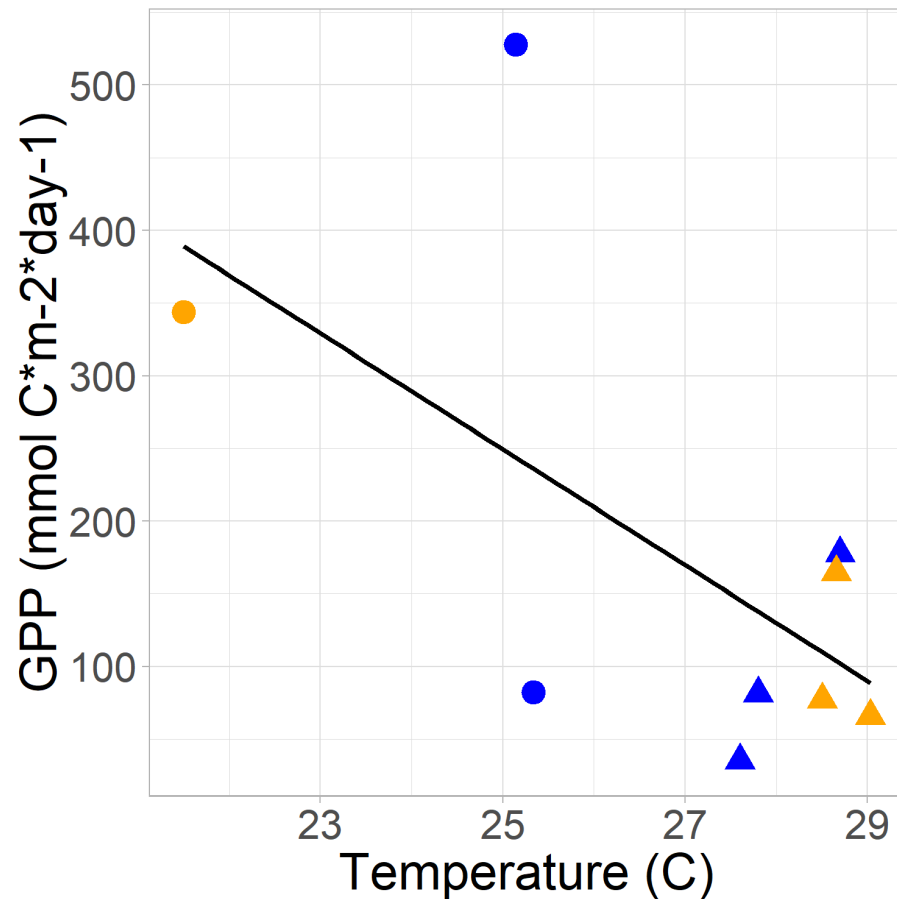Signif. codes: 0 '***' 0.001 '**' 0.01 '*' 0.05 '.' 0.1 ' ' 1

Residual standard error: 143.2 on 7 degrees of freedom
 (1 observation deleted due to missingness)
Multiple R-squared: 0.321,   Adjusted R-squared: 0.2239
F-statistic: 3.309 on 1 and 7 DF, p-value: 0.1117

294

Residuals:

Min	1Q	Median	3Q	Max
-279.79	-72.92	30.80	59.86	274.19

Coefficients:

	Estimate	Std. Error	t value	Pr(>|t|)
(Intercept)	-91.326	111.329	-0.820	0.439
data$Active.Chlorophyll.a..ug.L.	1.249	1.964	0.636	0.545

Residual standard error: 169.9 on 7 degrees of freedom

 (1 observation deleted due to missingness)

Multiple R-squared: 0.05461,   Adjusted R-squared: -0.08045

F-statistic: 0.4043 on 1 and 7 DF, p-value: 0.5451

Residuals:

Min	1Q	Median	3Q	Max
-181.06	-103.37	-45.98	37.51	321.33

Coefficients:

	Estimate	Std. Error	t value	Pr(>|t|)
(Intercept)	111.017	101.792	1.091	0.312
data$Pheophytin..ug.L.	3.305	4.542	0.728	0.490

Residual standard error: 167.6 on 7 degrees of freedom

 (1 observation deleted due to missingness)

Multiple R-squared: 0.07033,   Adjusted R-squared: -0.06248

F-statistic: 0.5296 on 1 and 7 DF, p-value: 0.4904
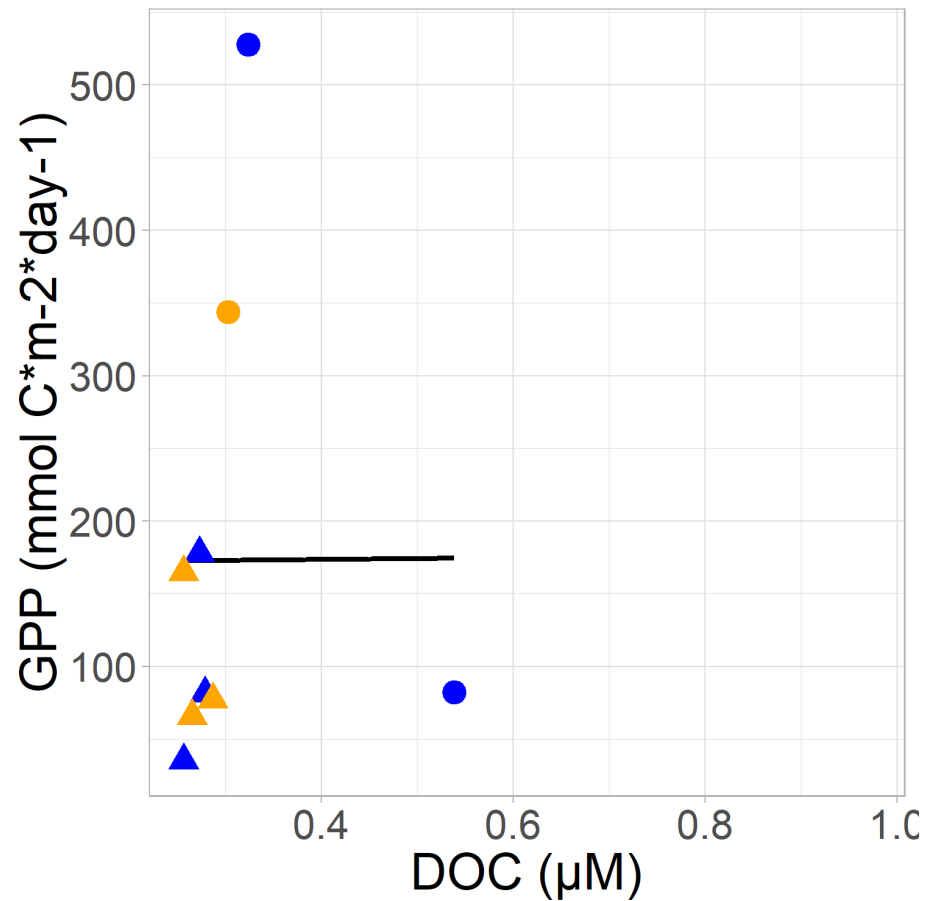
Residuals:

Min	1Q	Median	3Q	Max
-137.32	-95.41	-91.43	5.19	354.79

Coefficients:

	Estimate	Std. Error	t value	Pr(>|t|)
(Intercept)	171.032	221.660	0.772	0.466
data$DOC	6.195	691.835	0.009	0.993

Residual standard error: 173.8 on 7 degrees of freedom
 (1 observation deleted due to missingness)
Multiple R-squared: 1.146e-05,   Adjusted R-squared: -0.1428
F-statistic: 8.019e-05 on 1 and 7 DF, p-value: 0.9931
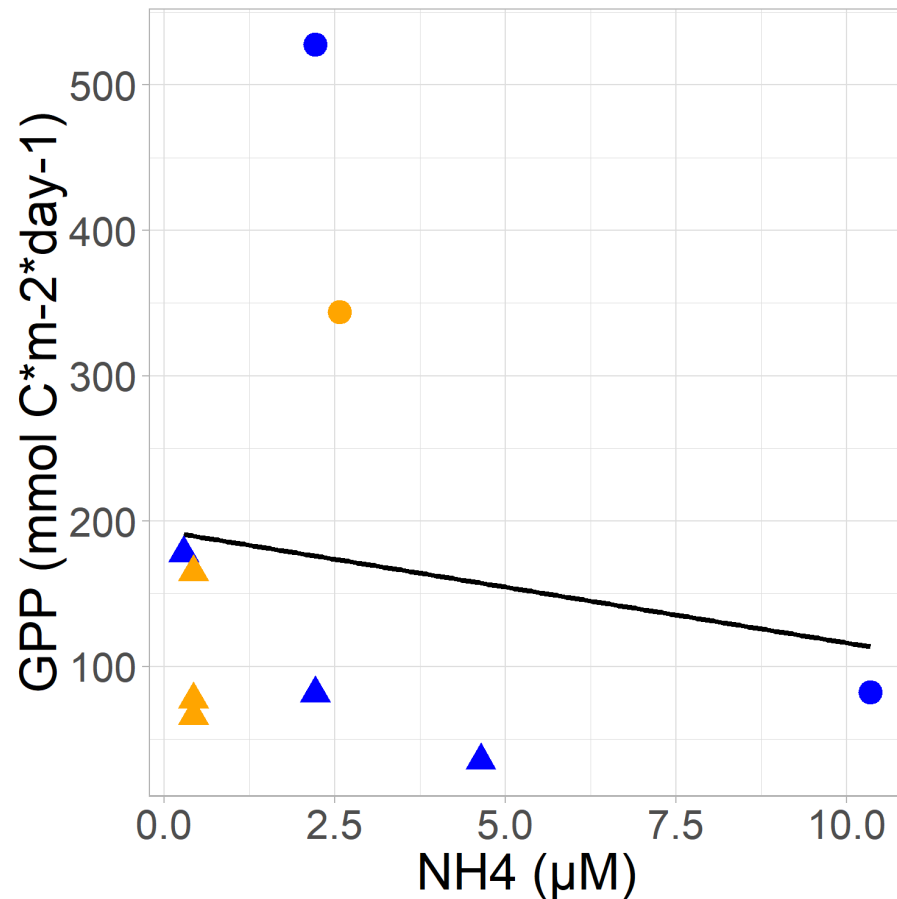
Residuals:

Min	1Q	Median	3Q	Max
-123.83	-112.35	-31.38	-12.93	351.78

Coefficients:

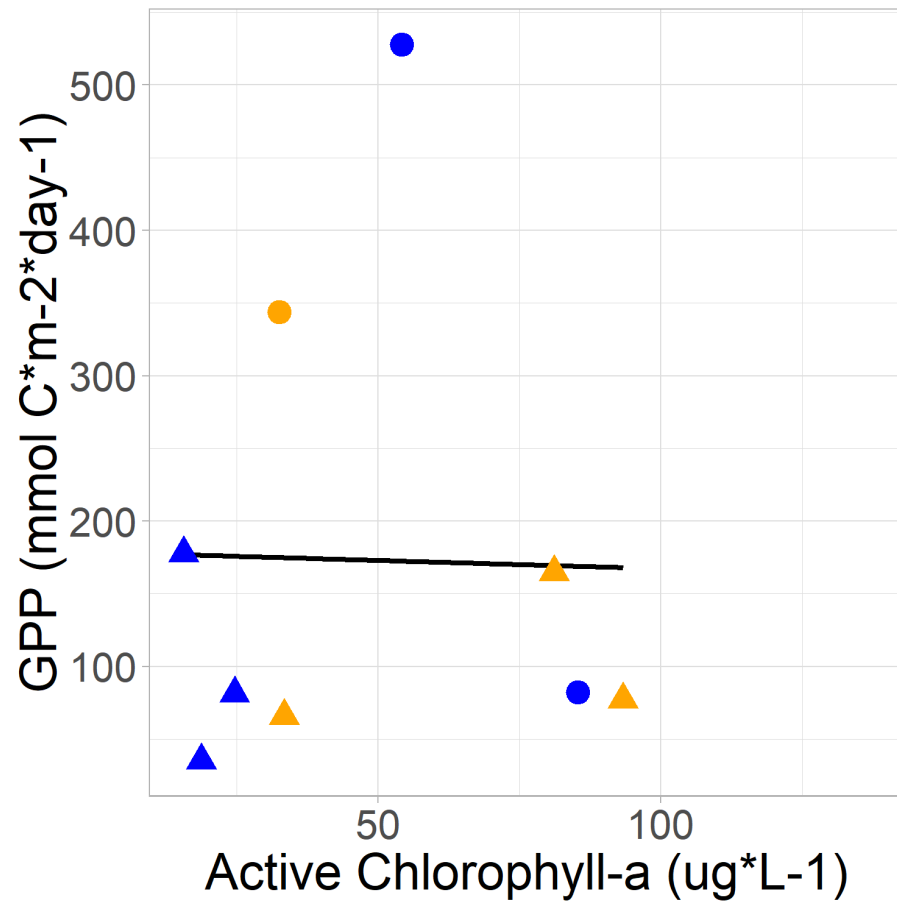|	Estimate	Std. Error	t value	Pr(>|t|)
(Intercept)	193.036	75.370	2.561	0.0375 *
data$NH4	-7.674	18.730	-0.410	0.6943

Signif. codes: 0 '***' 0.001 '**' 0.01 '*' 0.05 '.' 0.1 ' ' 1

Residual standard error: 171.7 on 7 degrees of freedom

 (1 observation deleted due to missingness)

Multiple R-squared: 0.02342,   Adjusted R-squared: -0.1161

F-statistic: 0.1679 on 1 and 7 DF, p-value: 0.6943

Residuals:

Min	1Q	Median	3Q	Max
-160.04	-71.14	-65.02	15.92	283.66

Coefficients:

	Estimate	Std. Error	t value	Pr(>|t|)	
(Intercept)	276.84	93.62	2.957	0.0212	*
data$NO23	-15.36	11.53	-1.332	0.2247	

Signif. codes: 0 '***' 0.001 '**' 0.01 '*' 0.05 '.' 0.1 ' ' 1

Residual standard error: 155.2 on 7 degrees of freedom

 (1 observation deleted due to missingness)

Multiple R-squared: 0.2021,   Adjusted R-squared: 0.08814

F-statistic: 1.773 on 1 and 7 DF, p-value: 0.2247

299

Residuals:

Min	1Q	Median	3Q	Max
-141.05	-95.60	-74.12	3.03	356.20

Coefficients:

	Estimate	Std. Error	t value	Pr(>|t|)
(Intercept)	181.390	97.997	1.851	0.107
data$PN	-0.237	2.220	-0.107	0.918

Residual standard error: 173.6 on 7 degrees of freedom
 (1 observation deleted due to missingness)
Multiple R-squared: 0.001626,   Adjusted R-squared: -0.141
F-statistic: 0.0114 on 1 and 7 DF, p-value: 0.918
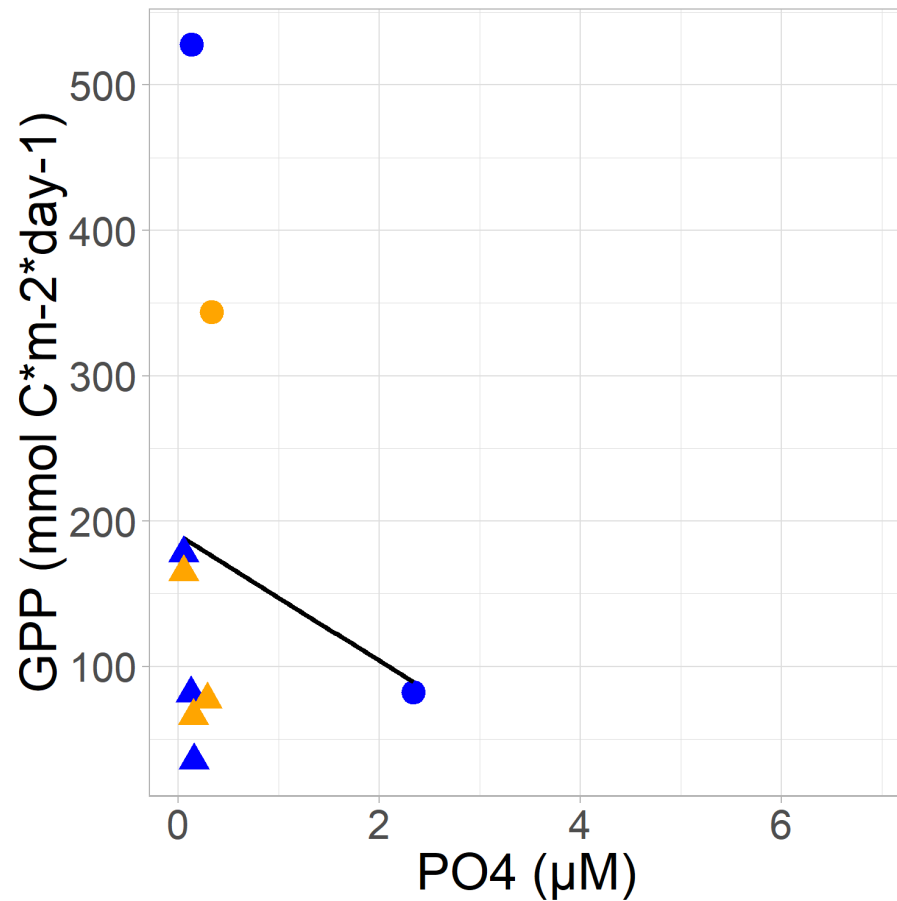
Residuals:

Min	1Q	Median	3Q	Max
-148.38	-103.60	-23.32	-7.12	343.17

Coefficients:

	Estimate	Std. Error	t value	Pr(>|t|)	
(Intercept)	190.38	65.82	2.892	0.0232	*
data$PO4	-43.23	82.39	-0.525	0.6161	

Signif. codes: 0 '***' 0.001 '**' 0.01 '*' 0.05 '.' 0.1 ' ' 1
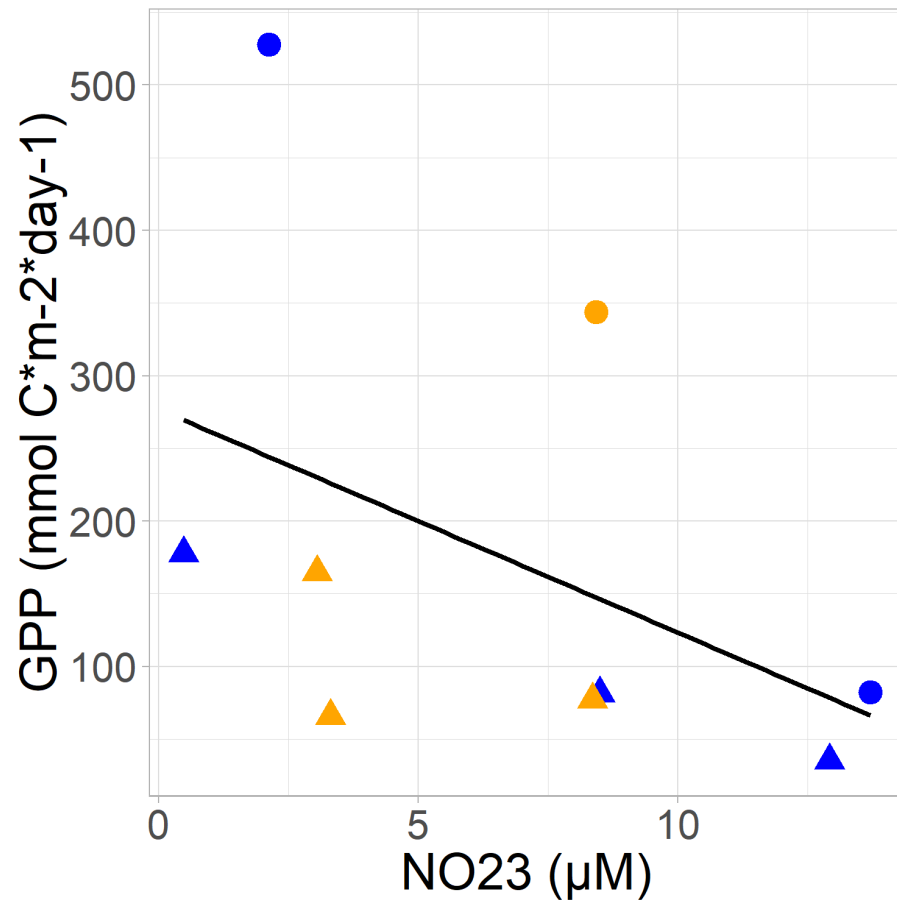
Residual standard error: 170.5 on 7 degrees of freedom

 (1 observation deleted due to missingness)

Multiple R-squared: 0.03783,   Adjusted R-squared: -0.09962

F-statistic: 0.2752 on 1 and 7 DF, p-value: 0.6161

Residuals:

     Min   1Q Median   3Q   Max
-146.27 -107.19 -29.82 -6.26 352.01

Coefficients:

            Estimate Std. Error t value Pr(>|t|)
(Intercept)   208.77   109.79   1.902   0.099 .
data$PP   -18.73   48.94 -0.383   0.713

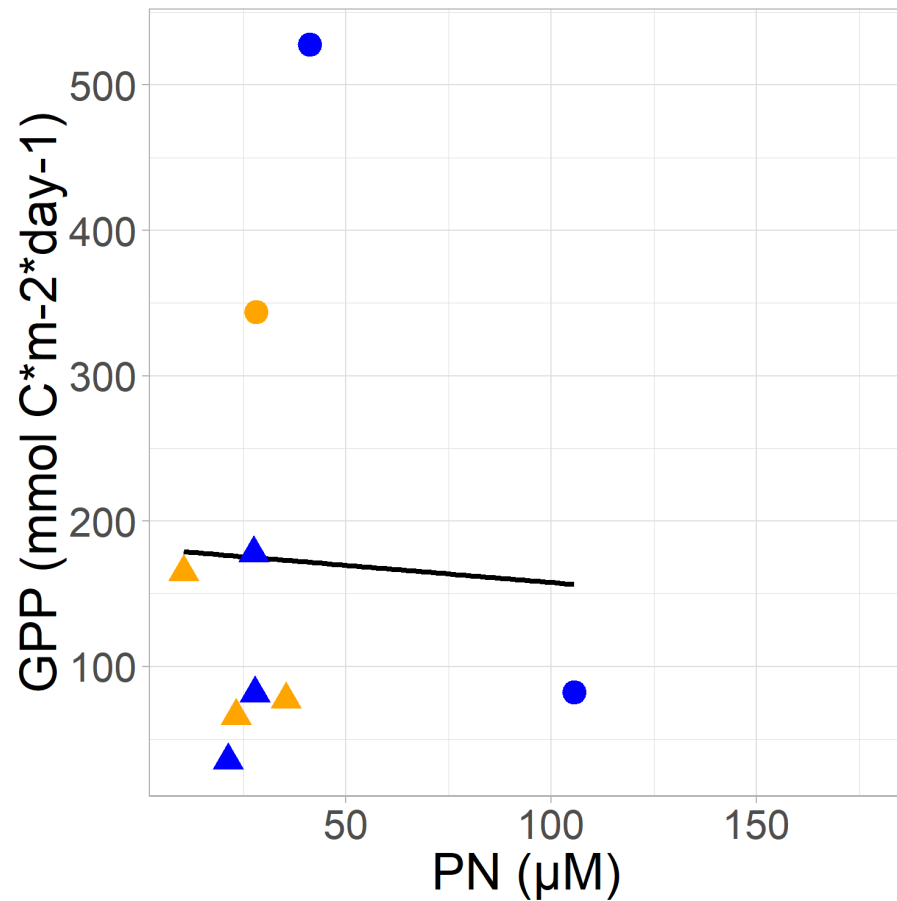Signif. codes: 0 '***' 0.001 '**' 0.01 '*' 0.05 '.' 0.1 ' ' 1

Residual standard error: 172 on 7 degrees of freedom
 (1 observation deleted due to missingness)
Multiple R-squared: 0.02048,	Adjusted R-squared: -0.1194
F-statistic: 0.1464 on 1 and 7 DF, p-value: 0.7134

Residuals:

Min	1Q	Median	3Q	Max
-133.70	-99.17	-55.90	-7.40	356.50

Coefficients:

	Estimate	Std. Error	t value	Pr(>|t|)
(Intercept)	204.536	145.942	1.401	0.204
data$TDN	-0.816	3.463	-0.236	0.820

Residual standard error: 173.1 on 7 degrees of freedom
 (1 observation deleted due to missingness)
Multiple R-squared: 0.00787,   Adjusted R-squared: -0.1339
F-statistic: 0.05553 on 1 and 7 DF, p-value: 0.8205
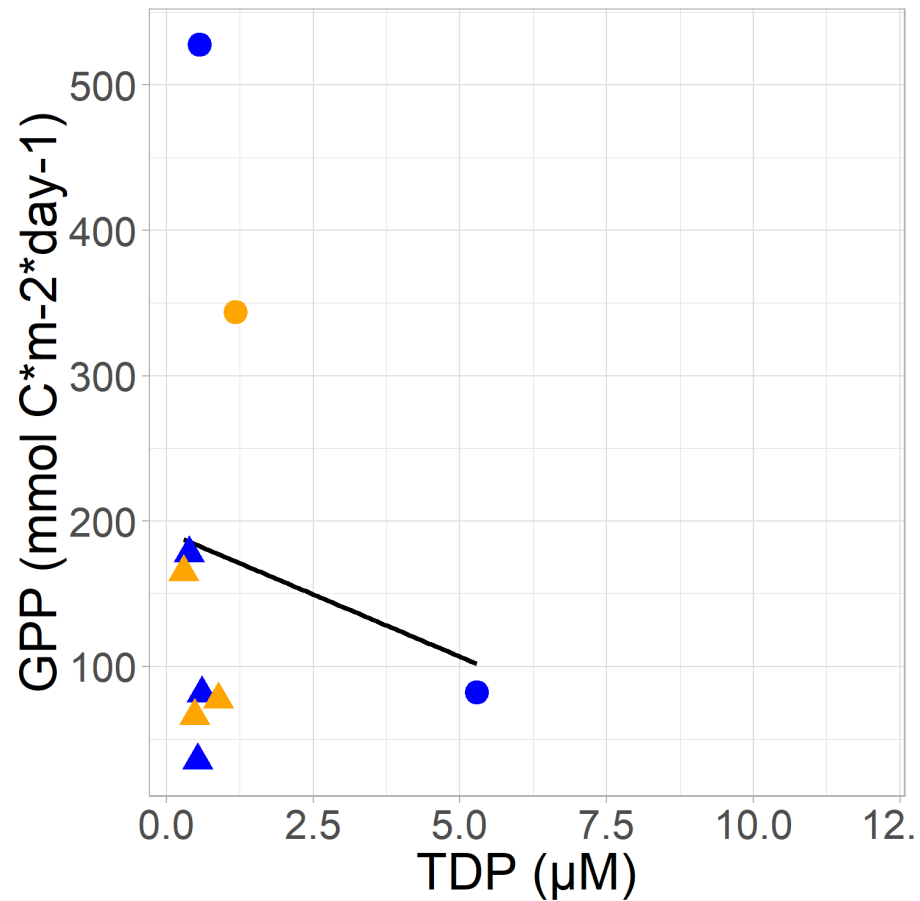
Residuals:

Min	1Q	Median	3Q	Max
-148.00	-100.70	-22.57	-7.82	345.14

Coefficients:

	Estimate	Std. Error	t value	Pr(>|t|)	
(Intercept)	192.31	71.72	2.681	0.0315	*
data$TDP	-17.12	38.35	-0.446	0.6688	

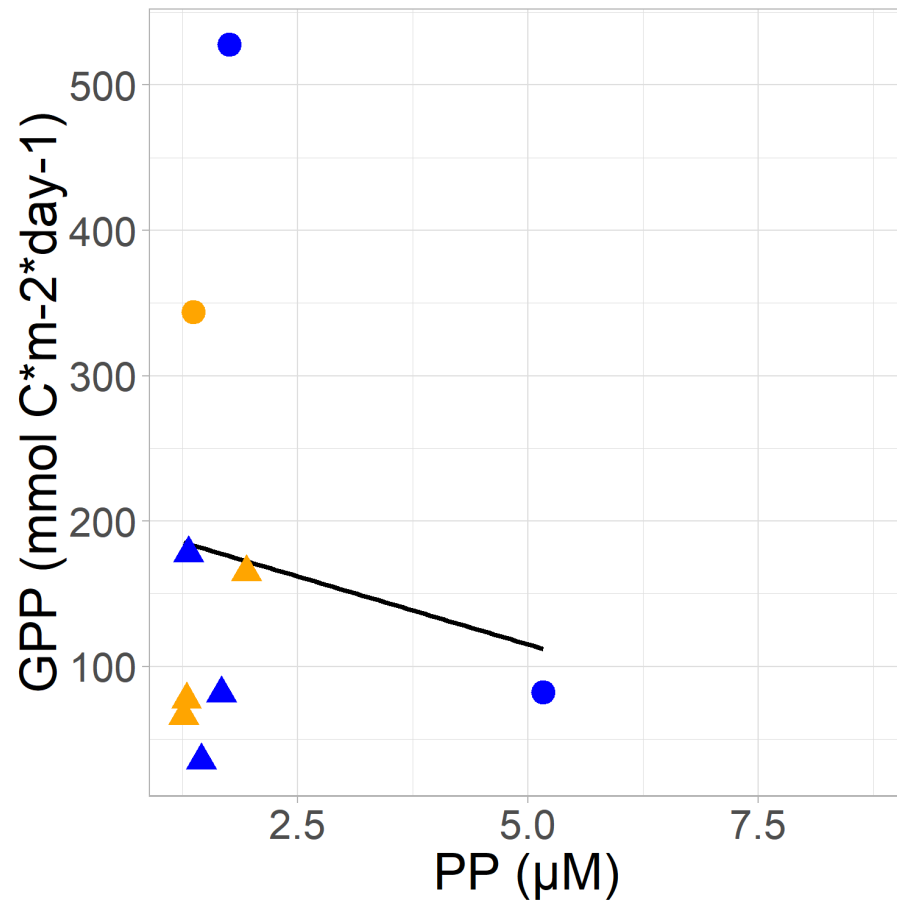
Signif. codes: 0 '***' 0.001 '**' 0.01 '*' 0.05 '.' 0.1 ' ' 1

Residual standard error: 171.4 on 7 degrees of freedom

 (1 observation deleted due to missingness)

Multiple R-squared: 0.02767,   Adjusted R-squared: -0.1112

F-statistic: 0.1992 on 1 and 7 DF, p-value: 0.6688

Residuals:

   Min   1Q Median   3Q   Max

-137.67 -115.60 -39.38 20.75 337.79

Coefficients:

         Estimate Std. Error t value Pr(>|t|)

(Intercept) 233.547   94.589 2.469 0.0429 *
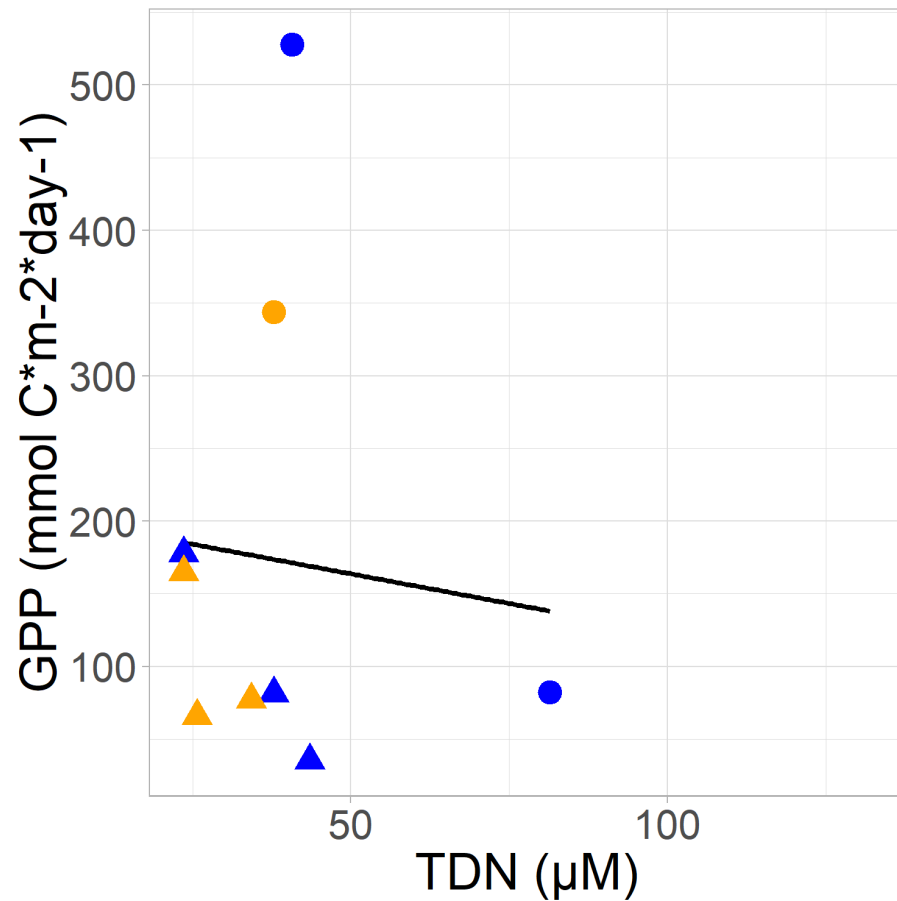
data$N.P   -1.327   1.677 -0.791 0.4548

Signif. codes: 0 '***' 0.001 '**' 0.01 '*' 0.05 '.' 0.1 ' ' 1

Residual standard error: 166.5 on 7 degrees of freedom

 (1 observation deleted due to missingness)

Multiple R-squared: 0.08207,   Adjusted R-squared: -0.04906

F-statistic: 0.6259 on 1 and 7 DF, p-value: 0.4548

Residuals:

	Min	1Q	Median	3Q	Max
	-731.60	41.94	79.09	129.67	318.12

Coefficients:

	Estimate	Std. Error	t value	Pr(>|t|)
(Intercept)	-51.77	280.45	-0.185	0.858
data$Salinity	-28.55	34.27	-0.833	0.429

Residual standard error: 326.8 on 8 degrees of freedom

Multiple R-squared: 0.07982, Adjusted R-squared: -0.0352

F-statistic: 0.6939 on 1 and 8 DF, p-value: 0.429
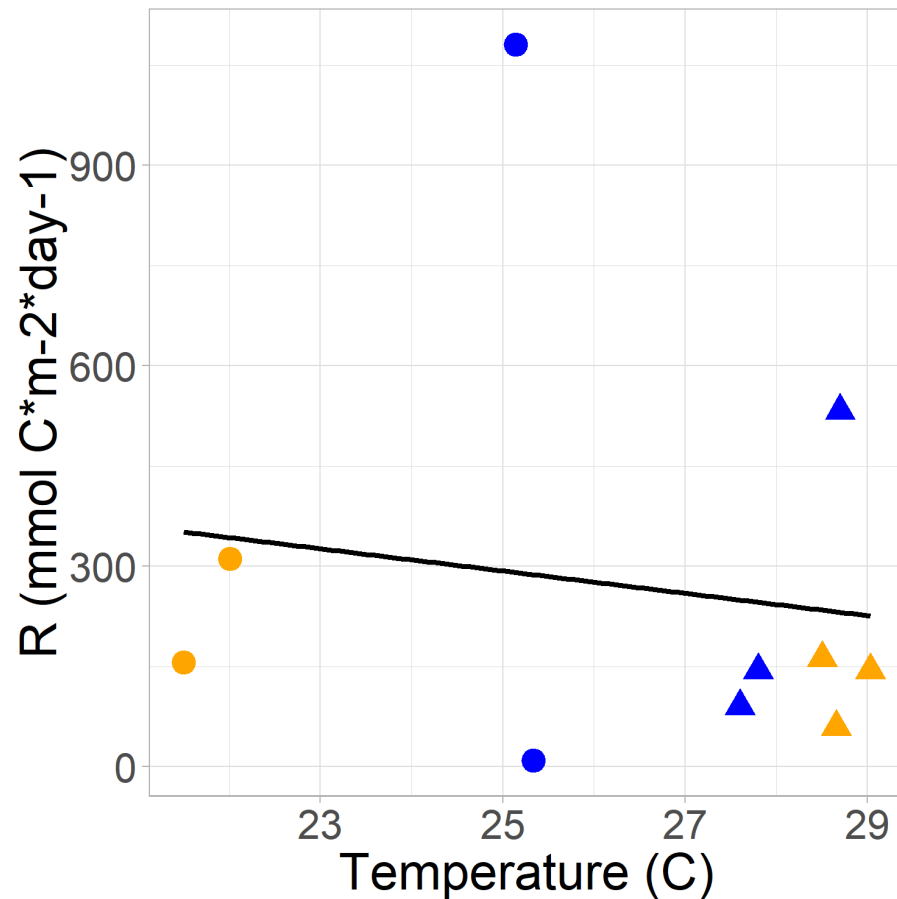
Residuals:

Min	1Q	Median	3Q	Max
-811.91	-8.71	117.96	165.73	259.23

Coefficients:

	Estimate	Std. Error	t value	Pr(>|t|)
(Intercept)	-242.88	878.10	-0.277	0.789
data$Temperature	-1.08	36.09	-0.030	0.977

Residual standard error: 340.7 on 8 degrees of freedom

Multiple R-squared: 0.0001119, Adjusted R-squared: -0.1249

F-statistic: 0.000895 on 1 and 8 DF, p-value: 0.9769
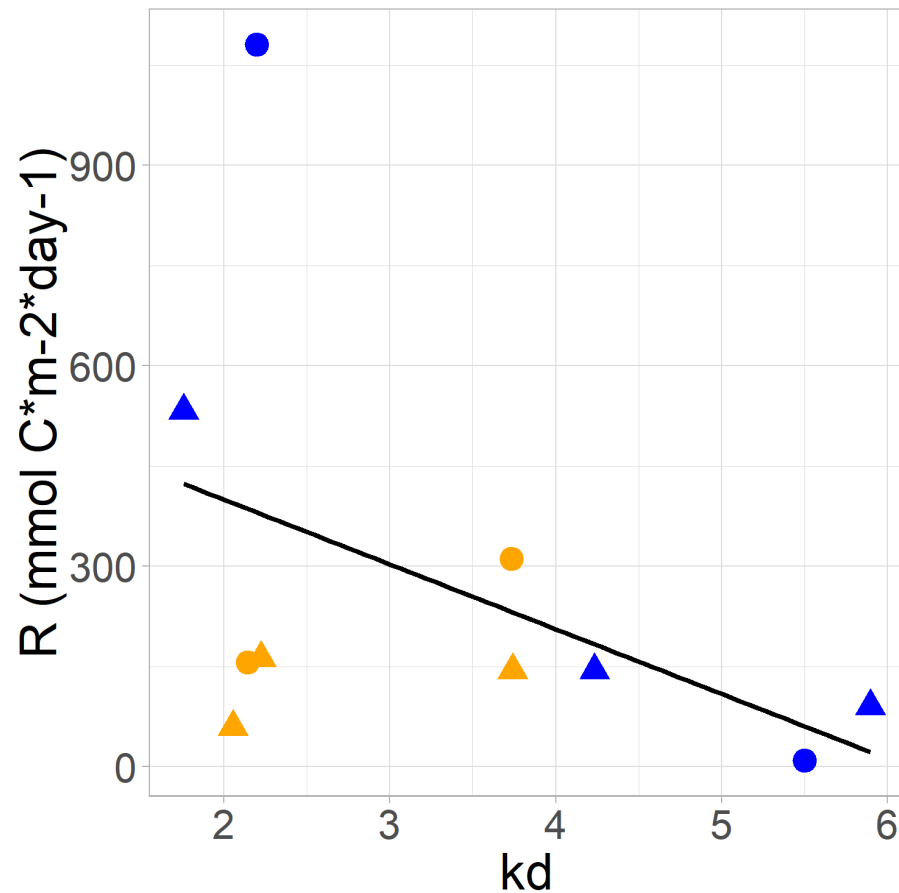
Residuals:

Min	1Q	Median	3Q	Max
-700.00	-76.51	44.90	183.29	335.40

Coefficients:

	Estimate	Std. Error	t value	Pr(>|t|)	
(Intercept)	-593.64	244.16	-2.431	0.0411	*
data$kd	96.98	67.06	1.446	0.1862	

Signif. codes: 0 '***' 0.001 '**' 0.01 '*' 0.05 '.' 0.1 ' ' 1

Residual standard error: 303.3 on 8 degrees of freedom

Multiple R-squared: 0.2072,   Adjusted R-squared: 0.1081

F-statistic: 2.091 on 1 and 8 DF, p-value: 0.1862

Residuals:

Min	1Q	Median	3Q	Max
-809.38	-49.92	135.06	182.40	241.45

Coefficients:

	Estimate	Std. Error	t value	Pr(>|t|)
(Intercept)	-307.0149	194.7835	-1.576	0.154
data$Active.Chlorophyll.a..ug.L.	0.6607	2.8205	0.234	0.821

Residual standard error: 339.5 on 8 degrees of freedom

Multiple R-squared: 0.006812,   Adjusted R-squared: -0.1173

F-statistic: 0.05487 on 1 and 8 DF, p-value: 0.8207
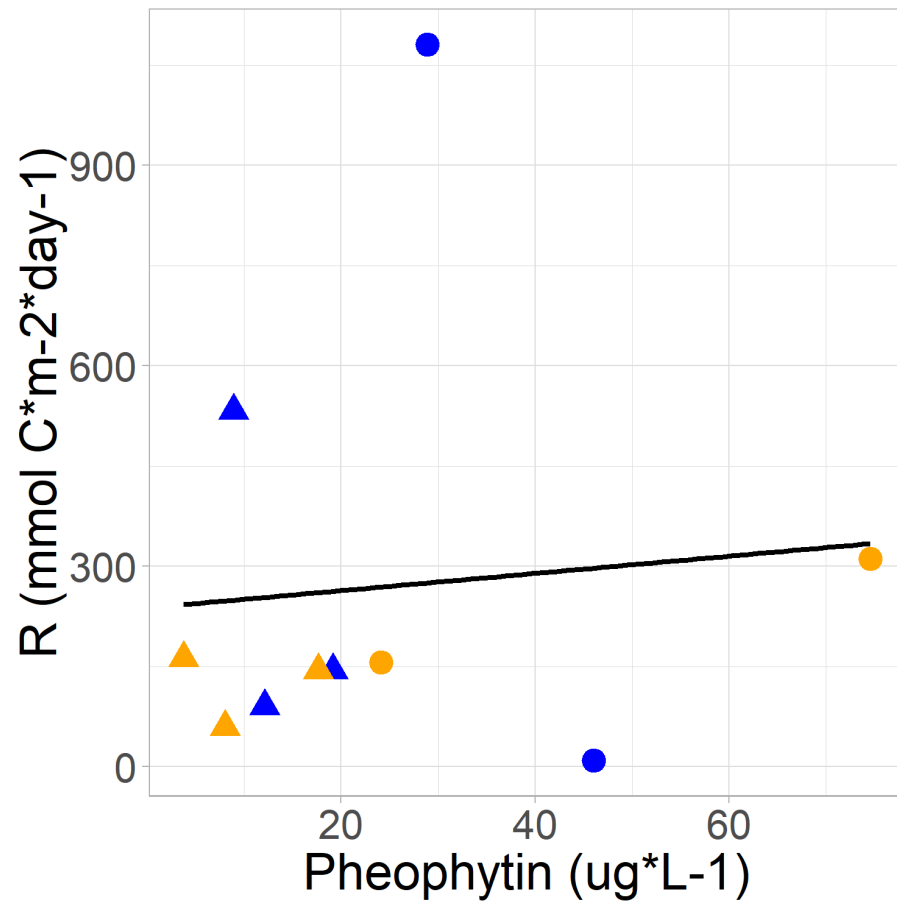
Residuals:

Min	1Q	Median	3Q	Max
-805.73	37.35	114.33	151.64	287.85

Coefficients:

	Estimate	Std. Error	t value	Pr(>|t|)
(Intercept)	-237.565	166.942	-1.423	0.193
data$Pheophytin..ug.L.	-1.290	5.257	-0.245	0.812

Residual standard error: 339.4 on 8 degrees of freedom

Multiple R-squared: 0.007473,   Adjusted R-squared: -0.1166

F-statistic: 0.06023 on 1 and 8 DF, p-value: 0.8123
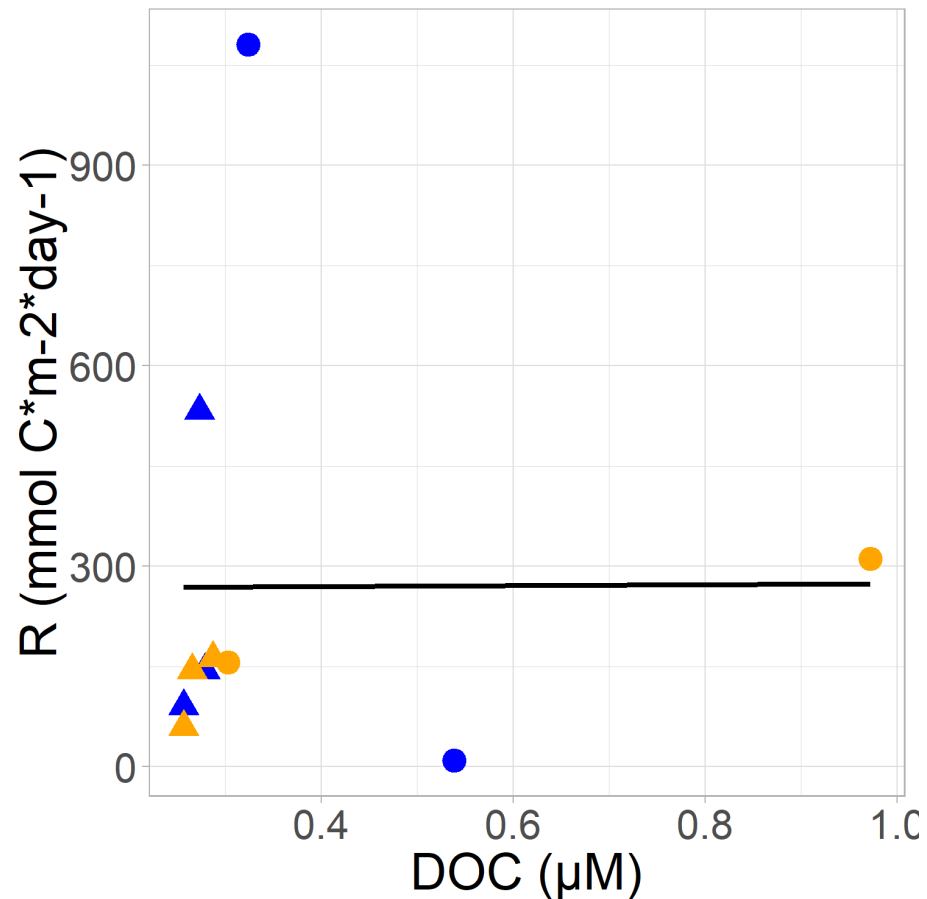
Residuals:

Min	1Q	Median	3Q	Max
-811.98	-1.72	118.05	164.37	260.91

Coefficients:

	Estimate	Std. Error	t value	Pr(>|t|)
(Intercept)	-266.358	217.440	-1.225	0.255
data$DOC	-6.892	502.887	-0.014	0.989

Residual standard error: 340.7 on 8 degrees of freedom

Multiple R-squared: 2.348e-05, Adjusted R-squared: -0.125

F-statistic: 0.0001878 on 1 and 8 DF, p-value: 0.9894
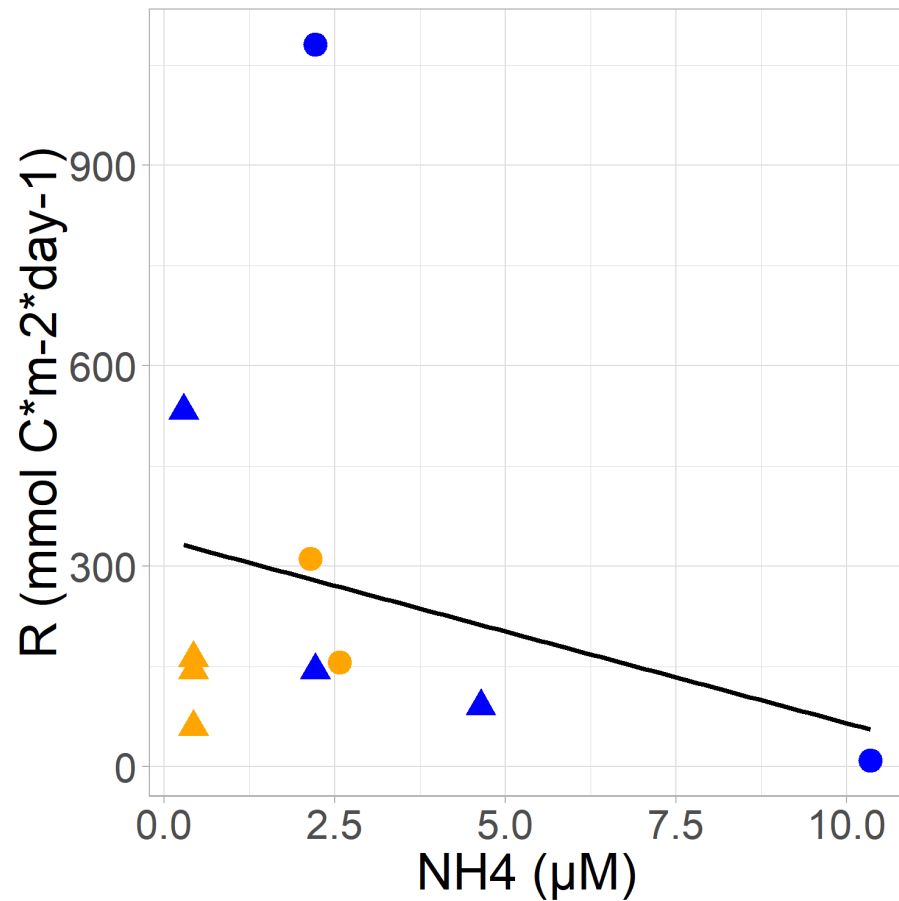
Residuals:

Min	1Q	Median	3Q	Max
-801.83	-10.87	117.25	157.46	268.70

Coefficients:

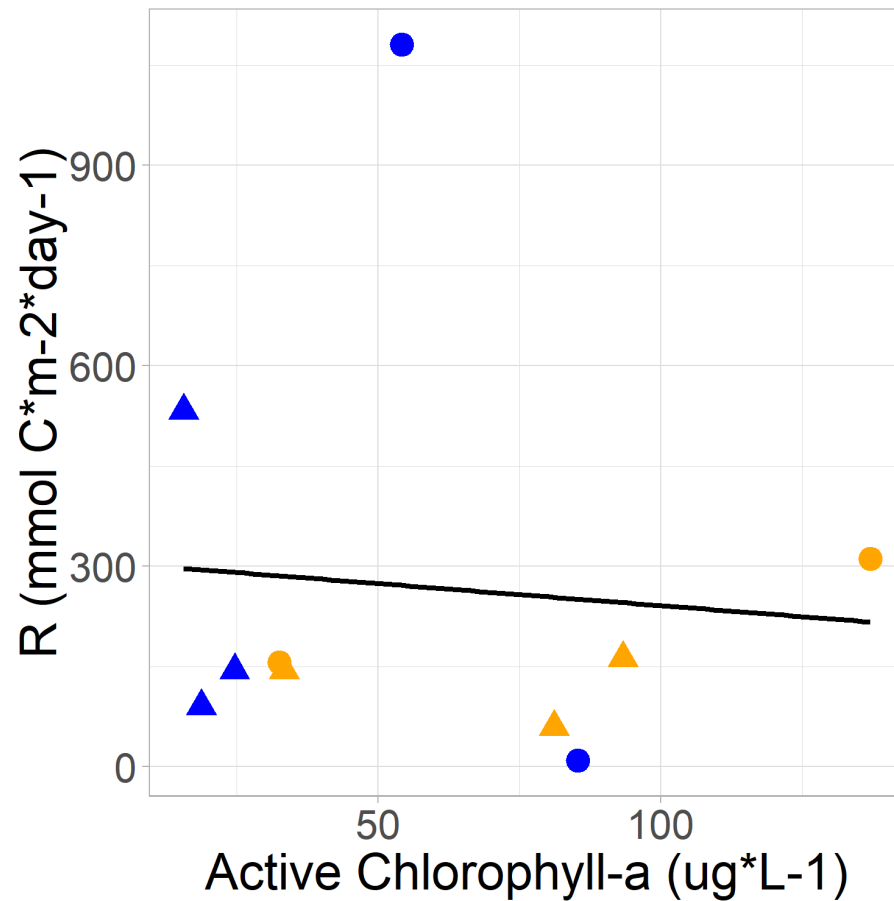|	Estimate	Std. Error	t value	Pr(>|t|)	
(Intercept)	-339.46	138.89	-2.444	0.0403	*
data$NH4	27.43	35.82	0.766	0.4658	

Signif. codes: 0 '***' 0.001 '**' 0.01 '*' 0.05 '.' 0.1 ' ' 1

Residual standard error: 328.8 on 8 degrees of freedom

Multiple R-squared: 0.0683,   Adjusted R-squared: -0.04816

F-statistic: 0.5865 on 1 and 8 DF, p-value: 0.4658

Residuals:

    Min   1Q Median   3Q   Max
-612.34 -59.24   25.47   56.59 370.59

Coefficients:

            Estimate Std. Error t value Pr(>|t|)
(Intercept) -556.77   166.12 -3.352   0.0101 *
data$NO23   41.62   20.42   2.038   0.0760 .

Signif. codes: 0 '***' 0.001 '**' 0.01 '*' 0.05 '.' 0.1 ' ' 1

Residual standard error: 276.4 on 8 degrees of freedom

Multiple R-squared: 0.3417,   Adjusted R-squared: 0.2594

F-statistic: 4.152 on 1 and 8 DF, p-value: 0.07596
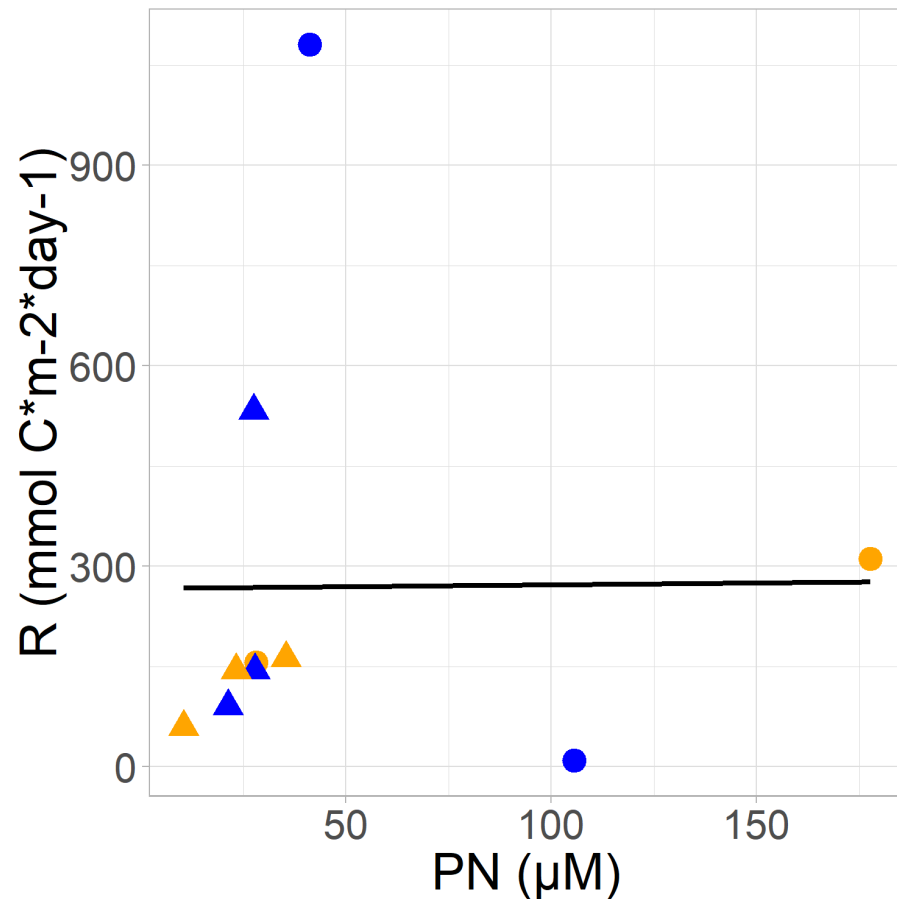
Residuals:

Min	1Q	Median	3Q	Max
-812.10	0.49	117.41	163.61	262.90

Coefficients:

	Estimate	Std. Error	t value	Pr(>|t|)
(Intercept)	-266.17001	153.18316	-1.738	0.12
data$PN	-0.05573	2.18529	-0.026	0.98

Residual standard error: 340.7 on 8 degrees of freedom

Multiple R-squared: 8.128e-05,   Adjusted R-squared: -0.1249

F-statistic: 0.0006503 on 1 and 8 DF, p-value: 0.9803
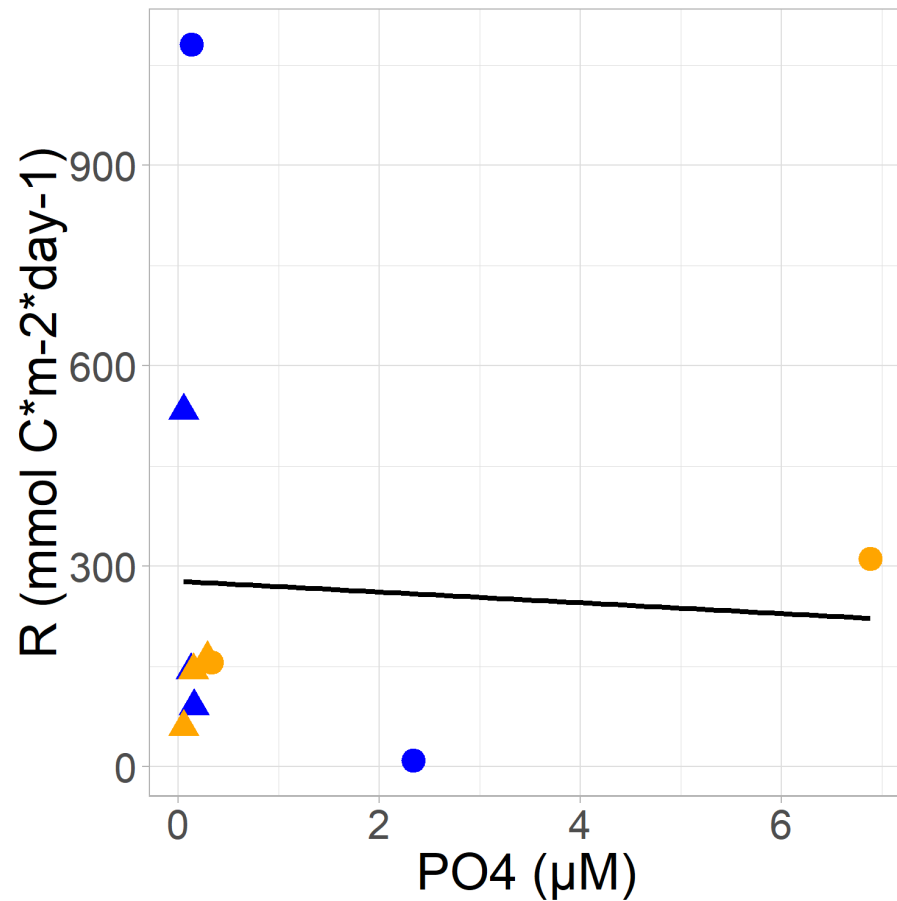
Residuals:

  Min   1Q Median   3Q   Max
-804.2 -38.4 125.3 172.4 249.4

Coefficients:

        Estimate Std. Error t value Pr(>|t|)
(Intercept) -277.427   120.877 -2.295   0.0509 .
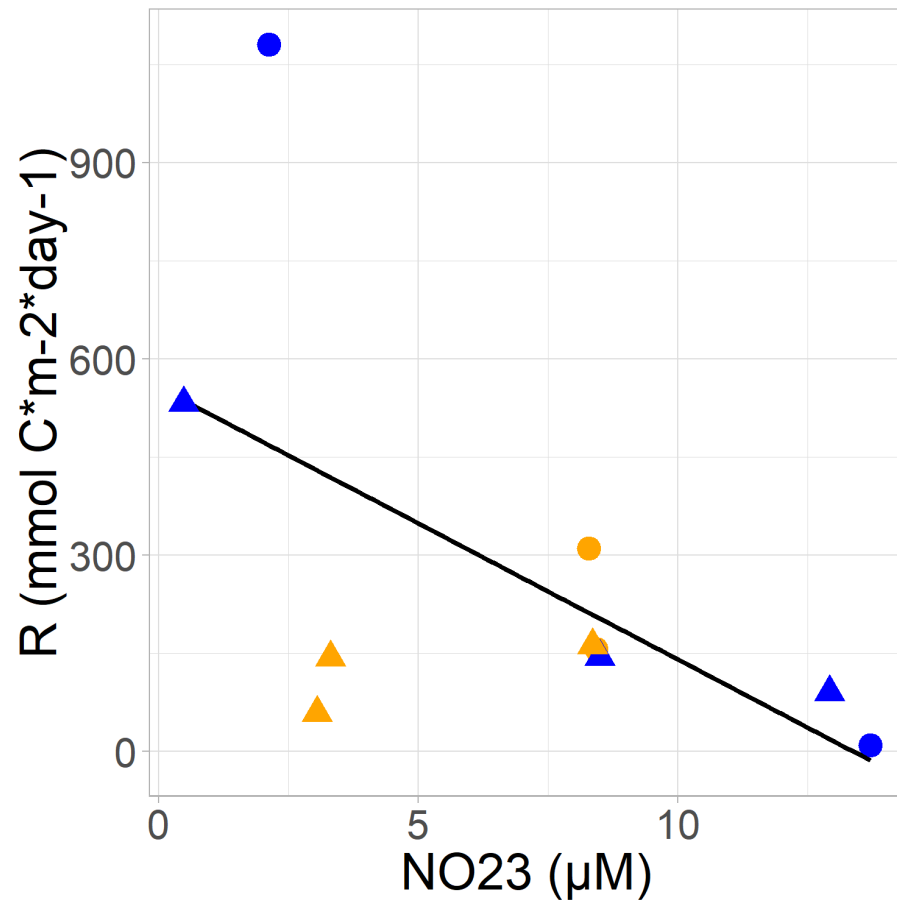data$PO4   8.064   52.423   0.154   0.8816

Signif. codes: 0 '***' 0.001 '**' 0.01 '*' 0.05 '.' 0.1 ' ' 1

Residual standard error: 340.2 on 8 degrees of freedom

Multiple R-squared: 0.002949,   Adjusted R-squared: -0.1217

F-statistic: 0.02366 on 1 and 8 DF, p-value: 0.8816
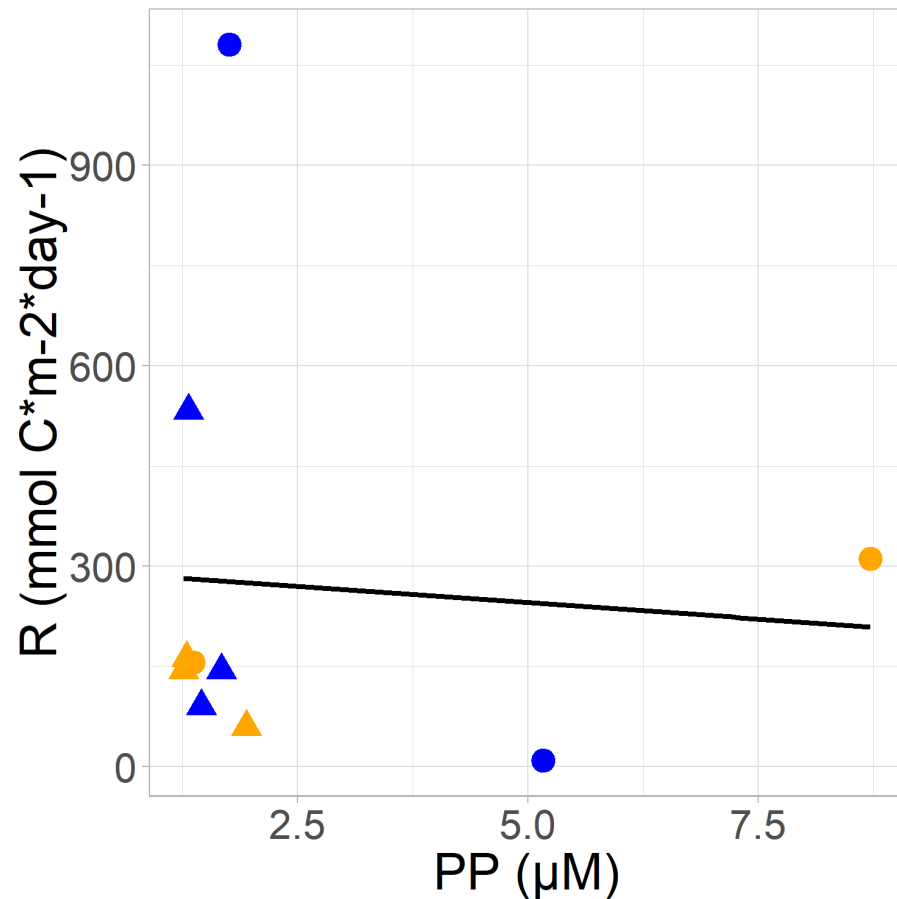
Residuals:

Min	1Q	Median	3Q	Max
-803.48	-46.33	129.14	176.79	234.66

Coefficients:

	Estimate	Std. Error	t value	Pr(>|t|)
(Intercept)	-294.280	160.985	-1.828	0.105
data$PP	9.768	46.228	0.211	0.838

Residual standard error: 339.7 on 8 degrees of freedom

Multiple R-squared: 0.00555, Adjusted R-squared: -0.1188

F-statistic: 0.04465 on 1 and 8 DF, p-value: 0.8379
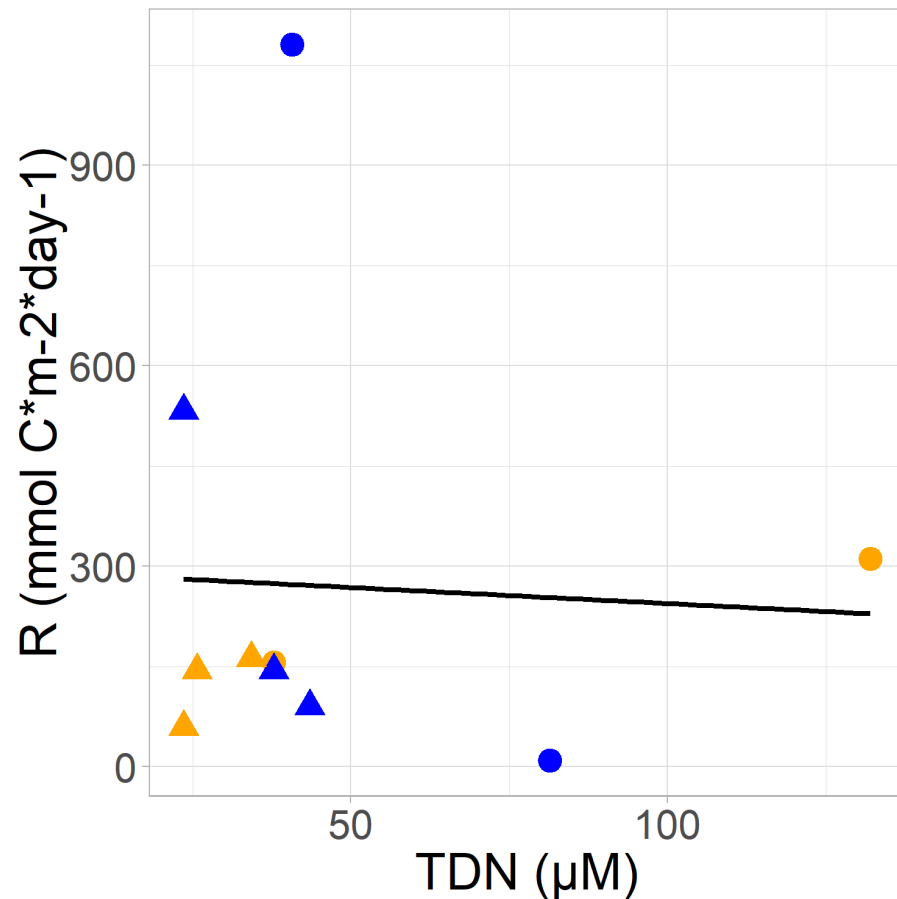
Residuals:

Min	1Q	Median	3Q	Max
-808.10	-33.22	123.53	169.47	243.80

Coefficients:

	Estimate	Std. Error	t value	Pr(>|t|)
(Intercept)	-291.9833	193.4296	-1.510	0.17
data$TDN	0.4794	3.3454	0.143	0.89

Residual standard error: 340.3 on 8 degrees of freedom

Multiple R-squared: 0.002561, Adjusted R-squared: -0.1221

F-statistic: 0.02054 on 1 and 8 DF, p-value: 0.8896
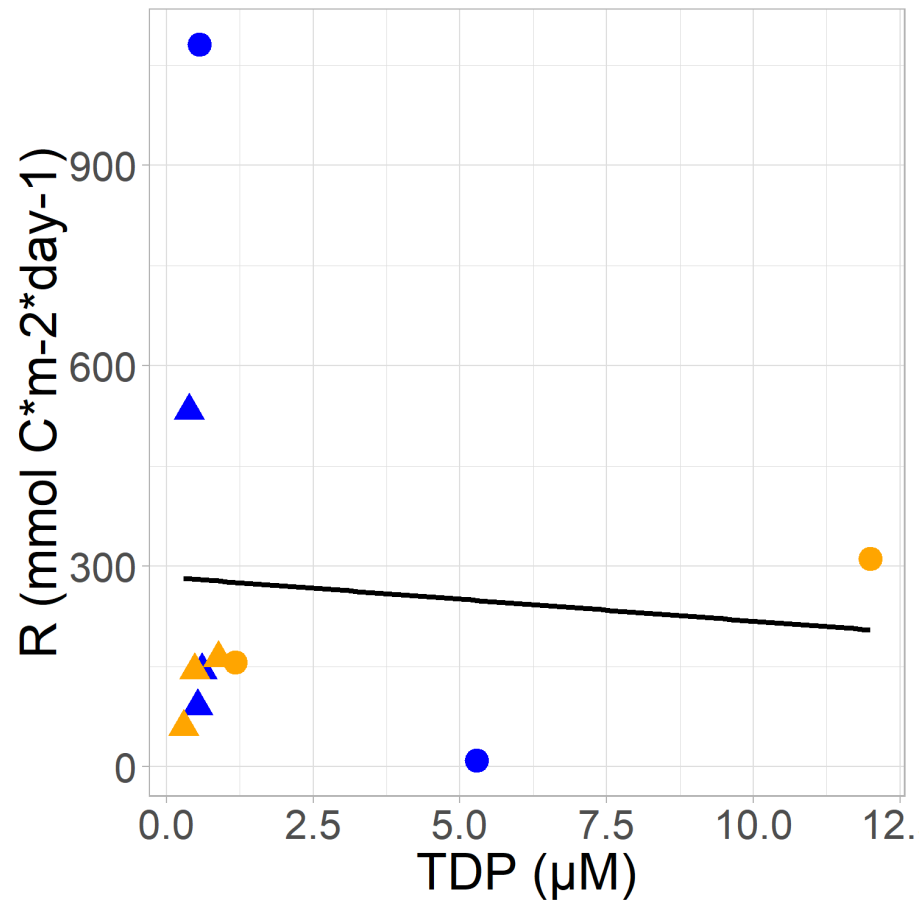
Residuals:

     Min   1Q Median   3Q   Max
-800.73 -50.71 127.37 176.39 239.63

Coefficients:

             Estimate Std. Error t value Pr(>|t|)
(Intercept) -283.534   126.626 -2.239   0.0555 .
data$TDP   6.578   30.234   0.218   0.8332

Signif. codes: 0 '***' 0.001 '**' 0.01 '*' 0.05 '.' 0.1 ' ' 1

Residual standard error: 339.7 on 8 degrees of freedom

Multiple R-squared: 0.005882,   Adjusted R-squared: -0.1184

F-statistic: 0.04733 on 1 and 8 DF, p-value: 0.8332

Residuals:

Min	1Q	Median	3Q	Max
-137.67	-115.60	-39.38	20.75	337.79

Coefficients:

	Estimate	Std. Error	t value	Pr(>|t|)	
(Intercept)	233.547	94.589	2.469	0.0429	*
data$N.P	-1.327	1.677	-0.791	0.4548	

Signif. codes: 0 '***' 0.001 '**' 0.01 '*' 0.05 '.' 0.1 ' ' 1

Residual standard error: 166.5 on 7 degrees of freedom
 (1 observation deleted due to missingness)
Multiple R-squared: 0.08207,   Adjusted R-squared: -0.04906
F-statistic: 0.6259 on 1 and 7 DF, p-value: 0.4548

319

REFERENCES

Benson, Bruce B., and Daniel Krause Jr. "The concentration and isotopic fractionation of oxygen dissolved in freshwater and seawater in equilibrium with the atmosphere 1." *Limnology and oceanography* 29.3 (1984): 620-632.

Borges, A., & Abril, G. (2011). 5.04-Carbon dioxide and methane dynamics in estuaries. *Treatise on Estuarine and Coastal Science, Volume 5: Biogeochemistry*, 119-161.
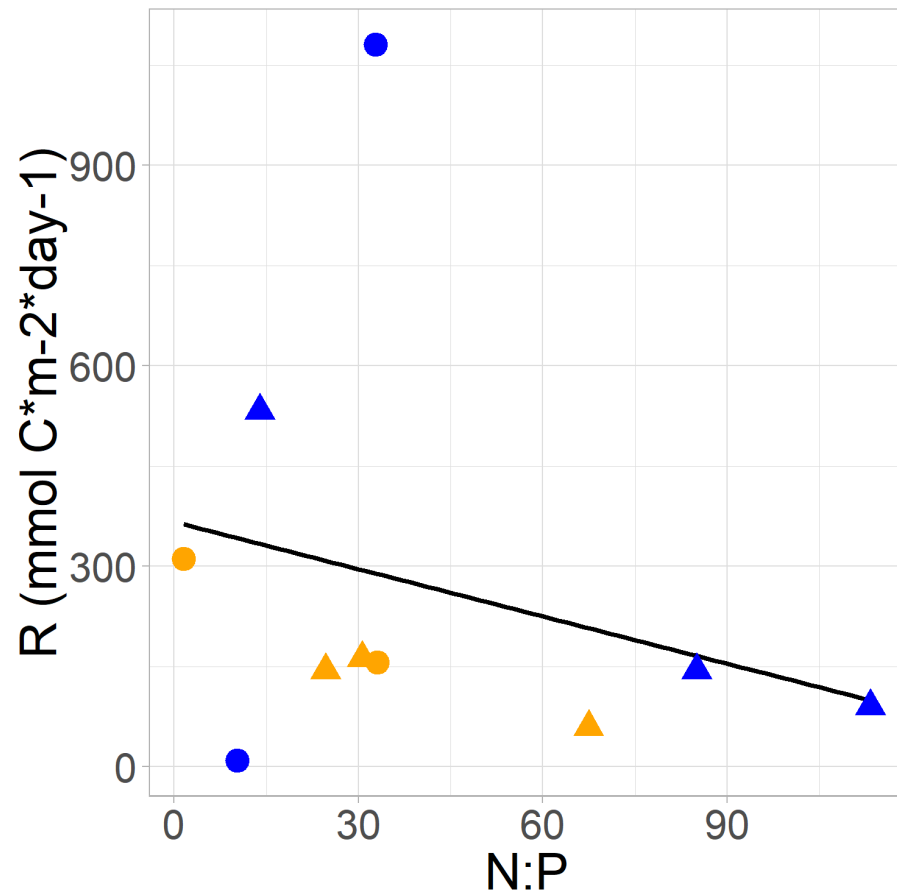
Boynton, W. R., Kemp, W. M., & Keefe, C. W. (1982). A comparative analysis of nutrients and other factors influencing estuarine phytoplankton production. In *Estuarine comparisons* (pp. 69-90). Academic Press.

Boynton, W. R., Murray, L., Hagy, J. D., Stokes, C., & Kemp, W. M. "A comparative analysis of eutrophication patterns in a temperate coastal lagoon." *Estuaries* 19.2 (1996): 408-421.

Bricker, S. B., Longstaff, B., Dennison, W., Jones, A., Boicourt, K., Wicks, C., & Woerner, J. (2008). Effects of nutrient enrichment in the nation's estuaries: a decade of change. *Harmful Algae*, *8*(1), 21-32.

Caffrey, J. M., Murrell, M. C., Amacker, K. S., Harper, J. W., Phipps, S., & Woodrey, M. S. "Seasonal and inter-annual patterns in primary production, respiration, and net ecosystem metabolism in three estuaries in the northeast Gulf of Mexico." *Estuaries and coasts* 37.1 (2014): 222-241.

Caffrey, Jane M. "Factors controlling net ecosystem metabolism in US estuaries." *Estuaries* 27.1 (2004): 90-101.

Cai, Wei-Jun, and Yongchen Wang. "The chemistry, fluxes, and sources of carbon dioxide in the estuarine waters of the Satilla and Altamaha Rivers, Georgia." *Limnology and Oceanography* 43.4 (1998): 657-668.

Cai, W. J., Huang, W. J., Luther, G. W., Pierrot, D., Li, M., Testa, J., ... & Xu, Y. Y. (2017). Redox reactions and weak buffering capacity lead to acidification in the Chesapeake Bay. *Nature communications*, *8*(1), 369.

Cai, W. J. (2011). Estuarine and coastal ocean carbon paradox: CO2 sinks or sites of terrestrial carbon incineration?. *Annual review of marine science*, *3*, 123-145.

Carignan, Richard, Anne-Marie Blais, and Chantal Vis. "Measurement of primary production and community respiration in oligotrophic lakes using the Winkler method." *Canadian Journal of Fisheries and Aquatic Sciences* 55.5 (1998): 1078-1084.

Casamayor, E. O., García-Cantizano, J., Mas, J., & Pedrós-Alió, C. "Primary production in estuarine oxic/anoxic interfaces: contribution of microbial dark CO2 fixation in the Ebro River Salt Wedge Estuary." *Marine Ecology Progress Series* 215 (2001): 49-56.

Casamayor, E. O., Llirós, M., Picazo, A., Barberán, A., Borrego, C. M., & Camacho, A. "Contribution of deep dark fixation processes to overall CO 2 incorporation and large vertical changes of microbial populations in stratified karstic lakes." *Aquatic Sciences* 74.1 (2012): 61-75..

Casamayor, E. O. (2010). Vertical distribution of planktonic autotrophic thiobacilli and dark CO2 fixation rates in lakes with oxygen–sulfide interfaces. *Aquatic Microbial Ecology*, *59*(3), 217-228.

CH2M HILL, 2011a. Task 3-Waterway and Estuary Characterization, Rock Creek Aerator and Water Quality Study Report to Anne Arundel County Maryland Department of Public Works.

CH2M HILL, 2011b. Task4-Aeration Evaluation Technical Memorandum to Anne Arundel County Maryland Department of Public Works.

Conley, D. J. (1999). Biogeochemical nutrient cycles and nutrient management strategies. In *Man and River Systems*(pp. 87-96). Springer, Dordrecht.

Conley, D. J., Carstensen, J., Ærtebjerg, G., Christensen, P. B., Dalsgaard, T., Hansen, J. L., & Josefson, A. B. "Long-term changes and impacts of hypoxia in Danish coastal waters." *Ecological Applications*17.sp5 (2007): S165-S184.

Corrales, R. A., & Maclean, J. L. (1995). Impacts of harmful algae on seafarming in the Asia-Pacific areas. *Journal of Applied Phycology*, *7*(2), 151-162.

Cronin, W. B., & Pritchard, D. W. (1975). *Additional statistics on the dimensions of the Chesapeake Bay and its tributaries: Cross-section widths and segment volumes per meter depth*. Johns Hopkins University.

Crosson, E. (2008). A cavity ring-down analyzer for measuring atmospheric levels of methane, carbon dioxide, and water vapor. *Applied Physics B*, *92*(3), 403-408.

Crosswell, Joseph R., Iris C. Anderson, Jennifer W. Stanhope, Bryce Van Dam, Mark J. Brush, Scott Ensign, Michael F. Piehler, Brent McKee, Molly Bost, and Hans W. Paerl. "Carbon budget of a shallow, lagoonal estuary: Transformations and source-sink dynamics along the river-estuary-ocean continuum." *Limnology and Oceanography*62.S1 (2017).

Dagenais-Bellefeuille, S., & Morse, D. (2013). Putting the N in dinoflagellates. *Frontiers in microbiology*, *4*, 369.

D'Elia, Christopher F., Paul A. Steudler, and Nathaniel Corwin. "Determination of total nitrogen in aqueous samples using persulfate digestion 1." *Limnology and oceanography* 22.4 (1977): 760-764.

Diaz, Robert J., and Rutger Rosenberg. "Spreading dead zones and consequences for marine ecosystems." *science* 321.5891 (2008): 926-929.

Diaz, R. J., Selman, M., & Chique-Canache, C. (2017). Global Eutrophic and Hypoxic Coastal Systems: Eutrophication and Hypoxia–Nutrient Pollution in Coastal Waters.

Dickson, A.G., Sabine, C.L. and Christian, J.R. (Eds.) 2007. *Guide to best practices for ocean CO$_2$ measurements*. PICES Special Publication 3, 191 pp.

Dickson, A.G. "An exact definition of total alkalinity and a procedure for the estimation of alkalinity and total inorganic carbon from titration data." Deep-Sea Res. 28A: (1981). 609–623.

Dickson, A.G., Afghan, J.D. and Anderson, G.C. "Reference materials for oceanic CO2 analysis: a method for the certification of total alkalinity." Mar. Chem. (2003). 80: 185– 197.

Dortch, Q., & Whitledge, T. E. (1992). Does nitrogen or silicon limit phytoplankton production in the Mississippi River plume and nearby regions?. *Continental Shelf Research*, *12*(11), 1293-1309.

Duarte, C. M., Conley, D. J., Carstensen, J., & Sánchez-Camacho, M. (2009). "Return to Neverland: shifting baselines affect eutrophication restoration targets." *Estuaries and Coasts*, *32*(1), (2009) 29-36.

Eilers, P. H. C., and J. C. H. Peeters. "A model for the relationship between light intensity and the rate of photosynthesis in phytoplankton." *Ecological modelling* 42.3-4 (1988): 199-215.

Eyre, B. D., Ferguson, A. J., Webb, A., Maher, D., & Oakes, J. M. "Metabolism of different benthic habitats and their contribution to the carbon budget of a shallow oligotrophic sub-tropical coastal system (southern Moreton Bay, Australia)". *Biogeochemistry*, *102*(1-3), (2011) 87-110.

Fisher, S. G., & Likens, G. E. (1973). Energy flow in Bear Brook, New Hampshire: an integrative approach to stream ecosystem metabolism. *Ecological monographs*, *43*(4), 421-439.

Gazeau, F., Borges, A. V., Barrón, C., Duarte, C. M., Iversen, N., Middelburg, J. J., ... & Gattuso, J. P. (2005). Net ecosystem metabolism in a micro-tidal estuary (Randers Fjord, Denmark): evaluation of methods. *Marine Ecology Progress Series*, *301*, 23-41.

Gilbert, N. (2009). Environment: the disappearing nutrient. *Nature News*, *461*(7265), 716-718.

Giordano, Juliette CP, Mark J. Brush, and Iris C. Anderson. "Ecosystem metabolism in shallow coastal lagoons: patterns and partitioning of planktonic, benthic, and integrated community rates." *Marine Ecology Progress Series* 458 (2012): 21-38.

Gran, G. 1952. Determination of the equivalence point in potentiometric titrations. Part II. Analyst 77: 661–670.

Grasshoff, K. "Procedures for the automatic determination of seawater constituents." *Methods of Seawater Analysis*(1976): 276-279.

Hagy, J. D., Boynton, W. R., Keefe, C. W., & Wood, K. V. "Hypoxia in Chesapeake Bay, 1950–2001: long-term change in relation to nutrient loading and river flow." *Estuaries*, *27*(4), (2004). 634-658.

Harris, L. A., C. L. S. Hodgkins, M. C. Day, D. Austin, J. M. Testa, W. Boynton, L. Van Der Tak, and N. W. Chen. (2015). "Optimizing recovery of eutrophic estuaries: impact of destratification and re-aeration on nutrient and dissolved oxygen dynamics." *Ecological Engineering*, *75*, (2015). 470-483.

Holling, C. S. "Resilience and stability of ecological systems." *Annual review of ecology and systematics*, *4*(1), (1973) 1-23.

Hopkinson, C. S., & Smith, E. M. (2005). Estuarine respiration: an overview of benthic, pelagic, and whole system respiration. *Respiration in aquatic ecosystems*, 122-146.

Howarth, R., Chan, F., Conley, D. J., Garnier, J., Doney, S. C., Marino, R., & Billen, G. "Coupled biogeochemical cycles: eutrophication and hypoxia in temperate estuaries and coastal marine ecosystems." *Frontiers in Ecology and the Environment*, *9*(1), (2011). 18-26.

Howarth, R. W., & Marino, R. (2006). Nitrogen as the limiting nutrient for eutrophication in coastal marine ecosystems: evolving views over three decades. *Limnology and Oceanography*, *51*(1part2), 364-376.

Howarth, R., Ramakrishna, K., Choi, E., Elmgren, R., Martinelli, L., Mendoza, A., ... & Zhao-Liang, Z. (2005). Nutrient management. *Ecosystems and human wellbeing: policy responses*, *3*, 295-2311.

Jassby, Alan D., and Trevor Platt. "Mathematical formulation of the relationship between photosynthesis and light for phytoplankton." *Limnology and oceanography* 21.4 (1976): 540-547.

Jones, F.E. and Harris, G.L. "ITS-90 density of water formulation for volumetric standards calibration". J. Res. Natl. Inst. Stand. Technol. 97, (1992). 335–340.

Jordan, T. E., Cornwell, J. C., Boynton, W. R., & Anderson, J. T. (2008). Changes in phosphorus biogeochemistry along an estuarine salinity gradient: The iron conveyer belt. *Limnology and Oceanography*, *53*(1), 172-184.

Kemp, W.M., Boynton, W.R., Adolf, J.E., Boesch, D.F., Boicourt, W.C., Brush, G., Cornwell, J.C., Fisher, T.R., Glibert, P.M., Hagy, J.D. and Harding, L.W., (2005). Eutrophication of Chesapeake Bay: historical trends and ecological interactions. *Marine Ecology Progress Series*, *303*, pp.1-29.

Kemp, W. M., Sampou, P., Caffrey, J., Mayer, M., Henriksen, K., & Boynton, W. R. (1990). Ammonium recycling versus denitrification in Chesapeake Bay sediments. *Limnology and Oceanography*, *35*(7), 1545-1563.

Kemp, W. M., Testa, J. M., Conley, D. J., Gilbert, D., & Hagy, J. D. "Temporal responses of coastal hypoxia to nutrient loading and physical controls." *Biogeosciences*, *6*(12), (2009). 2985-3008.

Kremer, James N., Alyssa Reischauer, and Charlene D'Avanzo. "Estuary-specific variation in the air-water gas exchange coefficient for oxygen." *Estuaries* 26.4 (2003): 829-836.

Lee, Dong Y., et al. "Elevated microbial CO_2 production and fixation in the oxic/anoxic interface of estuarine water columns during seasonal anoxia." *Estuarine, Coastal and Shelf Science*164 (2015): 65-76.

Lewis, Ernie & Wallace, D.W.R. & J. Allison, L. (1998). CO2SYS-Program developed for CO2 system calculations. Carbon Dioxide Inf. Anal. Centre. 10.2172/639712.

Jiang, Li-Qing, Wei-Jun Cai, and Yongchen Wang. "A comparative study of carbon dioxide degassing in river-and marine-dominated estuaries." *Limnology and Oceanography*53.6 (2008): 2603-2615.

Malone, T. C., Conley, D. J., Fisher, T. R., Glibert, P. M., Harding, L. W., & Sellner, K. G. (1996). Scales of nutrient-limited phytoplankton productivity in Chesapeake Bay. *Estuaries*, *19*(2), 371-385.

Marino, R., & Howarth, R. W. (1993). Atmospheric oxygen exchange in the Hudson River: Dome measurements and comparison with other natural waters. *Estuaries*, *16*(3), 433-445.

Maryland Department of Natural Resources. 2005. Standard Operatind Procedure #SC-04: Pycnocline Calculation.

Middelburg, J. J., and L. A. Levin. "Coastal hypoxia and sediment iogeochemistry." *Biogeosciences* 6.7 (2009): 1273-1293.

Mosier, A. C., & Francis, C. A. (2008). Relative abundance and diversity of ammonia-oxidizing archaea and bacteria in the San Francisco Bay estuary. *Environmental microbiology*, *10*(11), 3002-3016.

Nixon, Scott W. "Coastal marine eutrophication: a definition, social causes, and future concerns." *Ophelia* 41.1 (1995): 199-219.

Nixon, S. W. (1998). Enriching the sea to death. *Scientific American*, *9*(3), 48-53.

Nixon, S. W., Ammerman, J. W., Atkinson, L. P., Berounsky, V. M., Billen, G., Boicourt, W. C., ... & Garber, J. H. (1996). The fate of nitrogen and phosphorus at the land-sea margin of the North Atlantic Ocean. *Biogeochemistry*, *35*(1), 141-180.

Nixon, S. W., Oviatt, C. A., Frithsen, J., & Sullivan, B. (1986). Nutrients and the productivity of estuarine and coastal marine ecosystems. *Journal of the Limnological Society of Southern Africa*, *12*(1-2), 43-71.

Odum, Howard T. "Primary production in flowing waters1." *Limnology and oceanography* 1.2 (1956): 102-117.

Paerl, Hans W. "Controlling eutrophication along the freshwater–marine continuum: dual nutrient (N and P) reductions are essential." *Estuaries and Coasts* 32.4 (2009): 593-601.

Paerl, H. W., Valdes, L. M., Joyner, A. R., Piehler, M. F., & Lebo, M. E. (2004). Solving problems resulting from solutions: evolution of a dual nutrient management strategy for the eutrophying Neuse River Estuary, North Carolina. *Environmental Science & Technology*, *38*(11), 3068-3073.

Paerl, H. W., Willey, J. D., Go, M., Peierls, B. L., Pinckney, J. L., & Fogel, M. L. (1999). Rainfall stimulation of primary production in western Atlantic Ocean waters: roles of different nitrogen sources and co-limiting nutrients. *Marine Ecology Progress Series*, *176*, 205-214.

Redfield, A. C. (1963). The influence of organisms on the composition of seawater. *The sea*, *2*, 26-77.

Santoro, A. E., Casciotti, K. L., & Francis, C. A. (2010). Activity, abundance and diversity of nitrifying archaea and bacteria in the central California Current. *Environmental Microbiology*, *12*(7), 1989-2006.

Scheffer, M., Carpenter, S., Foley, J. A., Folke, C., & Walker, B. "Catastrophic shifts in ecosystems." *Nature*, *413*(6856), (2001). 591.

Scheffer, M., van den Berg, M., Breukelaar, A., Breukers, C., Coops, H., Doef, R., & Meijer, M. L. (1994). Vegetated areas with clear water in turbid shallow lakes. *Aquatic Botany*, *49*(2-3), 193-196.

Schlesinger, W.H., 1997. Biochemistry: An Analysis of Global Change, second ed. Academic Press, New York.

Shammas, N. K. (2007). Fine pore aeration of water and wastewater. In *Advanced Physicochemical Treatment Technologies* (pp. 391-448). Humana Press.

Silsbe, G.M., and Sairah Y. Malkin (2015). phytotools: Phytoplankton Production Tools. R package version 1.0. https://CRAN.R-project.org/package=phytotools.

Smith, S. V., & Hollibaugh, J. T. "Coastal metabolism and the oceanic organic carbon balance." *Reviews of Geophysics*, *31*(1), (1993). 75-89.

Smith, S. V., Hollibaugh, J. T., Dollar, S. J., & Vink, S. (1991). Tomales bay metabolism: C꞉N꞉P stoichiometry and ecosystem heterotrophy at the land-sea interface. *Estuarine, Coastal and Shelf Science*, *33*(3), 223-257.

Smith, E. M., & Kemp, M. W. (2001). Size structure and the production/respiration balance in a coastal plankton community. *Limnology and Oceanography*, *46*(3), 473-485.

Sorokin, Y. I., Sorokin, P. Y., Avdeev, V. A., Sorokin, D. Y., & Ilchenko, S. V. (1995). Biomass, production and activity of bacteria in the Black Sea, with special reference to chemosynthesis and the sulfur cycle. *Hydrobiologia*, *308*(1), 61-76.

Spokes, Lucinda J., and Tim D. Jickells. "Is the atmosphere really an important source of reactive nitrogen to coastal waters?." *Continental Shelf Research* 25.16 (2005): 2022-2035.

Staehr, P. A., Testa, J. M., Kemp, W. M., Cole, J. J., Sand-Jensen, K., & Smith, S. V. "The metabolism of aquatic ecosystems: history, applications, and future challenges." *Aquatic Sciences*, *74*(1), (2012). 15-29.

Stokes, C. *Influences of environmental variables on photosynthetic and respiratory quotients in Chesapeake Bay*. Diss. MSc thesis, University of Maryland, College Park, (1996).

Sverdrup, H. U. (1953). On conditions for the vernal blooming of phytoplankton. *J. Cons. Int. Explor. Mer*, *18*(3), 287-295.

Sylvan, J. B., Dortch, Q., Nelson, D. M., Maier Brown, A. F., Morrison, W., & Ammerman, J. W. (2006). Phosphorus limits phytoplankton growth on the Louisiana shelf during the period of hypoxia formation. *Environmental science & technology*, *40*(24), 7548-7553.

Testa, Jeremy Mark, and W. Michael Kemp. "Hypoxia-induced shifts in nitrogen and phosphorus cycling in Chesapeake Bay." *Limnology and Oceanography* 57.3 (2012): 835-850.

United States Environmental Protection Agency. 1972. Federal Water Pollution Control Amendments of 1972.

Vahtera, E., D.J. Conley, B.G. Gustafsson, H. Kuosa, H. Pitka¨nen, O.P. Savchuk, T. Tamminen, M. Viitasalo, et al. 2007. Internal ecosystem feedbacks enhance nitrogen-fixing cyanobacteria blooms and complicate management in the Baltic Sea. Ambio 36: 186–194.

Wanninkhof, Rik. "Relationship between wind speed and gas exchange over the ocean." *Journal of Geophysical Research: Oceans* 97.C5 (1992): 7373-7382.

Weiss, R.F. "Carbon dioxide in water and seawater: the solubility of a non-ideal gas." *Marine chemistry* 2.3 (1974): 203-215.